GROUND SURFACE MOTIONS IN THE FRASER DELTA DUE TO EARTHQUAKES

BY

DOUGLAS MONTAGUE WALLIS

B.A. SC., UNIVERSITY OF BRITISH COLUMBIA, 1975

A THESIS SUBMITTED IN PARTIAL FULFILLMENT OF
THE REQUIREMENTS FOR THE DEGREE OF
MASTER OF APPLIED SCIENCE

IN

THE FACULTY OF GRADUATE STUDIES

(Department of Civil Engineering)

We accept this thesis as conforming

to the required standard

THE UNIVERSITY OF BRITISH COLUMBIA

April, 1979

In presenting this thesis in partial fulfilment of the requirements for an advanced degree at the University of British Columbia, I agree that the Library shall make it freely available for reference and study. I further agree that permission for extensive copying of this thesis for scholarly purposes may be granted by the Head of my Department or by his representatives. It is understood that copying or publication of this thesis for financial gain shall not be allowed without my written permission.

Department of Civil Engineering

The University of British Columbia
2075 Wesbrook Place
Vancouver, Canada
V6T 1W5

Date Oct 1 1979

ABSTRACT

The purpose of this thesis is to investigate the potential ground surface motions in the Fraser Delta due to earthquakes. The geological history of the area is reviewed and information concerning the nature of the thick soil deposits that form the Delta is presented. The dynamic properties of the Delta soils are calculated and a model of the deposit is developed for use with existing computer analysis based on wave propagation theory. The computer analysis method involves the computation of the ground motions as a vertically propagating shear wave passes from bedrock, through soil layers, to the surface. The accuracy of the model was checked at three sites by comparison of the surface motions computed using a recorded bedrock object motion with the ground surface motion recorded during the same earthquake. The close correlation between the computed and recorded motions confirms the validity of the analysis method and the soil model.

The surface motions resulting from larger, maximum probable, earthquakes are computed. It was found that the thick soil deposits of the Delta affect both the ground accelerations and the period of the peak structural accelerations. Under the influence of low magnitude earthquakes the maximum acceleration is larger on the surface of the deep soil deposits than it is on nearby bedrock outcrops, while for large magnitude earthquakes the reverse is true. During large magnitude earthquakes, short buildings with periods of 0.25 sec. will experience greater accelerations if they are founded on bedrock than they will if

founded on the thick soil deposits of the Delta. Taller buildings with periods of about one second will experience far greater accelerations if they are founded on deep soil deposits than they would if founded on bedrock.

Comparison of Standard Penetration Test data in the Fraser Delta with empirical relations indicates that under large magnitude earthquakes liquefaction is likely in the upper few meters of the Delta sand deposits, but is unlikely below the 6 or 9 meter depth.

TABLE OF CONTENTS

LIST OF TABLES

LIST OF FIGURES

ACKNOWLEDGEMENTS

The Writer wishes to express his thanks to his research supervisor Dr. P.M. Byrne for his guidance during this research. He further wishes to express his appreciation to Dr. R.G. Campanella for his valuable suggestions.

Data on the soil properties in the Fraser Delta were kindly made available by Cook, Pickering and Doyle Limited, MacLeod Geotechnical Limited, British Columbia Hydro, and the Vancouver office of the Geological Survey of Canada. Time histories of local earthquake motions were provided by Dr. W.G. Milne of the Pacific Geoscience Centre, Department of Energy, Mines and Resources.

The Writer would also like to express his appreciation to the National Research Council of Canada and Golder Brawner and Associates who provided financial support for this investigation.

PURPOSE AND SCOPE

The Fraser River Delta is an area that is growing rapidly to meet industrial and residential demands. It is a populated region in the most seismicly active zone in Canada. Design of engineering structures should incorporate the effects of possible earthquakes. An earthquake can produce additional forces which must be resisted by the structural members and foundation. It can also reduce the strength of the foundation soil by processes such as liquefaction.

To assess the effects of the earthquake induced forces on the structure, the characteristics of the earthquake must be known. These characteristics can be expressed in terms of a response spectra. It is well documented that the ground surface motions in areas of deep soil deposits are greatly affected by the type and extent of the soils present. Mathematical methods are in existance which allow the ground motion characteristics in deep soil deposits to be modelled under the influence of an earthquake. These modelling techniques require knowledge of the dynamic properties of the soil.

This study is developed in three stages. In the first stage, available data describing the extent of the soil deposits and their engineering properties were collected and analyzed to produce soil profiles describing the dynamic soil properties of three sites in the Fraser Delta. The second stage involved using existing methods of dynamic analysis to find the degree of accuracy with which the analysis method, using the properties determined in stage one, agreed with the observed behaviour in situations where

the surface response was known. In the third stage the model was used to predict the ground response to larger, maximum probable, earthquakes.

CHAPTER 1

INTRODUCTION TO THE AREA OF STUDY

1-1 Physical Setting

The Fraser River Delta occupies an area in the southwest corner of mainland British Columbia that stretches eastward from the Strait of Georgia a distance of 23 kilometers, and northward from Boundary Bay a distance of 16 kilometers (figure 1-1-1). The most dominant geomorphological feature of the delta area is the Fraser River, which emerges onto the delta at New Westminster through a narrow gap in Pleistocene sediments, and splits into two major channels. On the eastern delta front, gently sloping tidal flats extend westward 6 kilometers into the Strait of Georgia, to the delta fore-slope, where the slopes are steeper. On the southern front, to the east of the Point Roberts upland, the tidal flats extend southward into Boundary Bay.

The Fraser Delta forms the western part of the Fraser Lowland, which stretches eastward from Vancouver, and north-eastward from Bellingham, Washington to define a triangular area with its apex 105 kilometers east of the Strait of Georgia. The Fraser Lowland is bounded on the north by the Coast Mountains and on the east by the Cascade Mountains (figure 1-1-2). It forms the eastern part of a major physiographic region, the Georgia Depression. The Georgia Depression is part of a linear structural depression which runs from Alaska through Hecate Strait, Georgia Strait, and the Willamette-Puget Lowland to the Great Valley of California.

The surficial deposits of the Fraser Lowland consist of late glacial and post-glacial deposits, overlying older rock formations of irregular topography. These older formations outcrop at several locations in the lowland. The delta is an area of low relief and low elevation where post-glacial sands, silts, and clays, to depths of up to 210 meters overlie Pleistocene deposits existing to depths of over 800 meters (700 meters at Boundary Bay).

Figure 1-1-3 shows the location of the surficial silt, sand and gravel deposits in the western Fraser Lowland. Areas of peat deposits have not been marked since these are generally less than 8 meters thick. A more detailed breakdown of the surficial deposits can be seen on maps by Johnston (1923), Armstrong (1956,1957,1960). Figure 1-1-4 shows areas of till outcrop, and approximate contours of the buried contact between the upper till surface and the over-lying , more recent deposits. The bedrock outcrops and the approximate bedrock contours are shown in figure 1-1-5. Figures 1-1-3, 1-1-4, and 1-1-5 have been adapted from unpublished maps compiled by A. Jerkevics.

The remainder of the lowland consists of low, flat-topped hills or uplands separated by wide, flat-bottomed valleys, Most of these uplands are composed of Pleistocene deposits of glacial or Glaciomarine origin; though some, such as Capitol Hill and Burnaby Mountain have bedrock cores and a few are raised marine delta (Armstrong 1957).

The recent and Pleistocene deposits overlie Tertiary and Cretaceous rocks which extend to depths of up to 4600 meters (Holland 1976). To the east of the lowland the Tertiary and Cretaceous rocks are reduced in thickness and overlie Pre-Tertiary metamorphics with ultrabasic intrusions,and paleocene formations. In the south, the contact between the older and younger rocks is obscure and probably involves a fault relationship (Hopkins 1966). The western boundary of the basin is open to the Strait of Georgia. To the north the Tertiary and Cretaceous rocks reduce in thickness and overlie Crystalline Complex. The Coast Crystalline Complex is the granitic unit which forms the mountains that rise abruptly north of Vancouver to between 1500 and 2100 meters. It has been described extensively by Roddick (1965). This same unit underlies the Paleozoic and Mesozoic strata that bound the Fraser Lowland to the south and east (McTaggert 1977).

The Fraser Delta is presently growing due to the accumulation of river sediments on the delta front. The Fraser River is the largest river in British Columbia, with an outflow varying from 800 m^3/s to 10,000 m^3/s (Hoos and Packman 1974), drawn from a drainage area of 270,000 square kilometers. The river carries 20 million cubic meters of sediment per year. These sediments are deposited to form tidal flats having slopes varying from 1 to 3.5 degrees (Mathews and Shepard 1962). A critical examination of the growth patterns of the present delta is important, since it may reveal patterns of sediment distribution that will

aid the interpretation of the soil types and the variability in the buried delta deposits.

Infilling of abandoned channels, gulley formation by active channels and slumping are three mechanisms that disrupt the uniform deposition of the sediments. The Strait of Georgia is relatively protected from the waters of the Pacific Ocean, but its restricted passages and the tidal nature result in currents which contribute to the shaping of the delta. The irregularity of these shaping forces and the possible non-uniformity of isostatic rebound within the Fraser Lowland area (Mathews, Fyles and Nasmith 1970)., indicate the probability of a complex growth pattern. Scotton (1977) suggests that this is quite likely, even though he found no difference in the engineering properties of samples of a particular soil type but of possible age difference. This suggests that once classified by type, the properties of the delta soil deposits will be well bounded.

1-2 Pre Pleistocene History

In Lower Cretaceous times (see appendix 1 for geologic time scale) the area which is now the Fraser Lowland was a marine basin having volcanic islands (figure 1-2-5). This resulted in the formation of bedrock which was both volcanic and sedimentary in nature. Magma rose from depths within the earth and solidified to form coarse crystalline, igeneous rocks, composed mainly of quartz diorite and granodiorite. The older volcanic and sedimentary strata were incorporated into the magma as roof pendants and inclusions. During this process some recrystalization occurred,

forming metamorphic rocks. As cooling took place, cracking of the rock mass allowed the underlying magma to rise into the crystalized rocks to form dykes and sills. This complex structure is called the Coast Crystalline Complex (Formerly known as the Coast Range Batholyth).

In Upper Cretaceous and Lower Tertiary times the Coast Crystalline Complex was elevated above sea level and an erosional period started. The eroded material was washed towards the Pacific Ocean. By Lower Tertiary times these sediments had become cemented by groundwater, and compressed to form conglomerate, sandstone, siltstone and shale. During this period, volcanic activity resulted in the formation of dykes and sills. The Burrard and Kitsilano Formations, which outcrop on the Burrard Peninsula, north of the present Fraser Delta, are two such sedimentary formations. Johnston (1923), who first defined these two formations, was not convinced that there was a prolonged time break between the two formations, and Roddick (1965) now considers them a single unit. Similar formations, with thicknesses of over a thousand meters, underly the present delta.

In Late Tertiary times, uplift of the basin occurred and the sedimentary sheets were eroded in the north to form a broad peneplain sloping down to what is now the delta area.

1-3 Pleistocene History

The Fraser Lowland has undergone at least three major and one minor ice advance (figure 6). These advances can be distinguished by the sequence of soil deposits layed down during and after each glacial advance. In the Pre-Olympia period, the Semour and Semiamu Groups are the only recognizable Pleistocene deposits. They may

overlie glacial and interglacial sequences (Danner 1968), or non-glacial Pliocene deposits. The Semour and the Semiamu advances produced two of the three till layers that are found underlying the present Fraser Delta, and which can be seen on exposed river banks and sea cliffs in the Fraser Lowland. Throughout this work the term 'till' is used as a shorter version of 'glacial till', which is a very compact, unsorted mixture of sand, silt, clay and stones, deposited directly beneath the glacier ice. This excludes from the 'till' classification as used herein, material of the same composition which has been deposited through water from floating ice, and which is sometimes called glacio-marine till.

The Olympia Interglaciation, which started about 50,000 years ago, and followed the Semour and Semaimu advances is the period when the major part of the presently existing non-glacial Quadra sediments were layed down. The Point Grey cliffs date to this time (Armstrong 1956), and are part of a flood plain that may have extended to Vancouver Island. The later phases of the Olympia Interglaciation were periods of erosion for many areas. Much of the topography of the Burrard Peninsula and of other areas of the Fraser Lowland were then shaped close to their present configuration.

The Olympia Interglaciation was followed by the Fraser Glaciation, which started about 18,000 years ago. The first advance of the glacier, the Vashon Stade, was the third of the major ice advances that shaped the topography of the Fraser Lowland. It distributed outwash, till and glacio-marine drift over the Quadra sediments. Surrey Till and Newton Stoney Clay are two such deposits that are present in Surrey to depths of 9 meters (Armstrong 1956). The retreat of the ice occurred predominantly through wasting. The

ice thinned and floated, laying down the glacio-marine deposits. As in the Semour glaciation, the land was depressed by the weight of the 2100 meters of ice.

The Vashon Stade was followed by the Everson Interstade, which started about 13,000 years ago, and subdued the topography by infilling. Mathews et al (1970), subdivided the Everson Interstade into Post Vashon Emergence and the Pre-Sumas Subsidence. During the Post-Vashon Emergence, which marked the removal of the weight of ice, the sand and gravel deposits of the Capillano Group were layed down. During the Pre-Sumas Subsidence the glacio-marine Watcom deposits were layed down.

The Everson Interstade was followed by the Sumas Stade, which was a minor advance in which the ice approached to within 40 kilometers of Vancouver. It started about 11,500 years ago, and lasted for about 1,500 years. It has been estimated that at this time , the land under present day Richmond was depressed by about 210 meters (Blunden 1973), so that Sumas deposits were layed down as glacio-marine layers of sand, silt, clay and unsorted material. It should be noted that estimates both of the times of the glacial periods and of the position of the land surface relative to the ocean, will depend on the methods by which these values were obtained.

1-4 Post Glacial (Recent) History

After the Sumas Glaciation, which ended between 10,000 and 8,000 years ago, came a period of isostatic adjustment: the Sumas Emergence. This uplift of about 150 meters produced the terraces

and beaches on the present day Vancouver North Shore, and subjected the former deep-water deposits of the Fraser River to wave erosion. By 7000 BP (Before Present) the mouth of the Fraser advanced from its end-of-Pleistocene position at present-day New Westminster to the position now occupied by Twigg Island. By this time, the southward flow of the Fraser to Boundary Bay had stopped (Blunden 1973). At 2500 BP the land rose about 3 meters relative to the ocean, uplifting the salt marshes off Lulu Island to form Sea Island.

The surface of the present delta is composed of sand and silt deposits with some clay, and large areas of peat, the latter up to 8 meters deep. Due to the method of growth of the delta there exist abandoned river channels which have become infilled with sand and silt and covered with more recent deposits. The present channels are being kept stable by dredging, dyking and using jetties to control the currents.

The present delta front is growing due to the deposition of the river sediments. Johnston (1923) estimated the rate of delta extension to be 3 meters per year, while Mathews and Shepard, (1962) in a more extensive survey off Main Channel, found the rate there to vary on average from 2.3 meters per year at the 6-meter depth to 8.5 meters per year at the 90-meter depth. This increased growth rate at depth means that the slope of the delta front is more shallow now than it was 30 years ago. Mathews and Shepard indicate that this may be due to the reduced amount of sand-size sediment deposited, as a result of man's dredging activities in the

river channels. Luternaúer (1975) has pointed out that the underwater topography and rate of growth at any particular spot on the delta front is highly variable. Some parts are advancing at various rates while other parts are stable.

CHAPTER 2

SOIL CHARACTERISTICS OF THE FRASER DELTA

2-1 Soil Type and Extent

The present delta consists predominantly of loose sand silt and clay deposits resting in a deep basin formed of Pleistodene deposits overlying bedrock. Surficial deposits can be identified by careful mapping, however the variation of the soils with depth is more difficult to determine. By mentally picturing the delta as being composed of an infinite number of elements in three dimensional space, one can see that extensive surficial mapping will only reveal the nature of the elements on one plane in this space. Knowledge of the third dimension can only be obtained by probing vertically. This can be done using direct drilling and sampling methods, or indirect geophysical methods.

If undisturbed samples could be recovered from the total length of the drill hole, the nature of a single line of elements in this three dimensional space would be known. This is an expensive procedure for a relatively small amount of information. For reasons of cost, most drilling will be done with the aim of recovering relatively undisturbed samples every 1.5 or 3 meters, and noting intermediate changes in the soils by watching the cuttings being brought to the surface with the drilling fluid. This method obviously cannot identify all the elements on a particular line.

Geophysical surveys generally involve making traverses along the ground surface: hence the examination is of soil elements defining part of a vertical plane. Unfortunately these geophysical methods are capable only of recognizing major changes in specific soil properties, and then only if the surveys are related to borehole data. In terms of the model of elements in space, this means that we know something about the elements on the top plane, but very little about elements on other planes, particularly those near the bottom of the space. Knowledge of the processes by which these delta deposits were layed down and the processes which have since shaped them will prove invaluable when trying to deduce the nature of the delta deposits from the small amount of data available.

The depth of bedrock is not well known. Figure 1-1-5 indicates that bedrock lies at depths generally over 300 meters throughout most of the delta. In the northern part of the delta, where the sedimentary rocks slope up to form the Burrard Peninsula, the depths are slightly less, probably in the 210 or 240 meter depth range. A remarkable feature is the irregularity of the buried contact between the bedrock and the Pleistocene deposits. This can be seen both from the individual points that were obtained from bore holes, ranging from 250 to 700 meters, and from the more detailed contours to the east of the delta. These contours were obtained by consultants who correlated detailed geophysical work with borehole data. The irregular bedrock topography would be the result of erosion that took place during the uplift in

Oliogocene and Miocene ages, and the glaciation in the Pleistocene Age.

Above the bedrock lie the Pleistocene deposits. Figure 1-4 shows that the depth to the top of these deposits is likely to be over 120 meters, and is probably about 210 meters throughout most of the delta. The contact between the Pleistocene and the recent deposits slopes upward in the north, until the Pleistocene deposits reach the surface on the southern part of the Burrard Peninsula. They also reach the surface to the east in Surrey and White Rock, and the south on the Point Roberts Upland, which must have been án island in early Pleistocene times. Despite the fact that Annacis Island is close to both the high New Westminster and Surrey areas of Pleistocene deposits, the top of the Pleistocene deposits is several hundred feet below ground surface there. This is because a channel had been eroded by the Fraser River.

It is evident from the discussion of glacial history that these Pleistocene deposits could consist of up to three layers of glacial till, possibly separated by interglacial deposits of sands, silts, and clays. At any particular location, the existence of a complete profile with layers of each deposit type is unlikely, because of the effects of erosion.

Above the Pleistocene sediments lie the recent deposits. To obtain an understanding of the sequencing of the beds it is important to consider the stages in the growth of the delta. At the end of Pleistocene times, the waters of the Fraser River

emerging from their narrow channel at New Westminster, slowed as they spread out into what was then a part of the Strait of Georgia. The heavy sand-size particles would quickly be dropped to form the near-horizontal top-set beds as the velocity and sediment carrying capacity were reduced. As the velocity was further reduced with distance from the river mouth, silt-size particles were layed down with the smaller sand sizes. At some distance from the mouth, an increase in slope would occur as increasingly finer grained soils were deposited in the relatively still waters to form the near-horizontal bottom-set beds. This method of development would lead one to expect a soil profile in the delta that consists of sands near the surface, grading down to silts in the middle layers, and clays at depth.

This generalized profile would be affected by any perturbations to such a uniform, idealized system. The flow velocity and volume of the Fraser was not constant, so the amount of sediment available to be added to the delta and the distance from the mouth to the spot where a particular particle-size drop would vary with time. Seasonal variations of this type result in the varves that have been observed in drill holes on the delta. Variations in bottom topography and ocean currents would modify the shape of the advancing delta. Isotatic rebound and eustatic shifts would change the flow patterns of the river, and result in alteration in the model patterns by erosion. Abandoned river channels would fill with material that was of a different nature than that found in the surrounding lands. An example of this is the old channel that exists on LuluIsland to the north-west of

Annacis Island and the present southern channel.(Armstrong 1956) It is from 0.8 to 1.6 kilometers wide and about 6 kilometers long. It can be seen on maps of the surficial deposits because the channel was active recently enough to be covered by a small thickness of floodplain silt instead of peat.

The major part of the recent delta deposits conform generally to the basic profile described, and is thus explicable on the basis of the delta's growth mechanism. There are surficial floodplain and swamp deposits to shallow depths, usually less than 8 meters, underlain generally by sands to depths of about 30 meters. Under the sand there is silt, which is underlain by clays at depth. In the Point Roberts area the till layers rise up to the surface. The surrounding deposits consist of sands and silts, presumably because the clays settled in the deep water that surrounded this one-time island.

The surficial deposits of the delta area have been described by Armstrong (1956), and those of Richmond have been described in more detail by Blunden (1973). Since the description of surficial deposits is peripheral to the central purpose of this paper, only brief and generalized reference will be made to their distribution. The western half of the delta has surficial deposits which consist of material ranging from clays to sandy silts, to depths of up to 4.5 meters, overlying sand or silty sand. Generally this top layer is graded, with the finer material being found further inland. The western half of the delta is covered to a large degree by surficial peat layers. These peat layers may be up to 8 meters deep and generally overlie sand silty sand. Some

of the thinner peat layers overly a thin clayey-silt layer which rests on the thick sand or silty sand layer. Peat seams are often found in layers of other material within 4.5 meters of the surface. Blunden (1973) indicated that in some areas the variable surficial layer overlies clay rather than the sand or silty sand usually found. Figures 2-1-1 and 1-1-2 shows generalized soil profiles of the surficial deposits, and their distribution within the delta.

2-2 Soil Data Requirements

To model the behaviour of a soil deposit under the influence of dynamic excitation the stress-strain behaviour of the soil under the prevailing field conditions must be known. Cyclic testing in the laboratory has provided an understanding of the general type of behaviour that can be expected over a range of conditions for various soil types. The mathematical analysis must incorporate a model of these stress-strain characteristics that successfully duplicates the behaviour of the soil over the stress range anticipated, to a degree of accuracy consistent with the type of analysis.

The possession of a realistic stress-stain law, and a method of analysis with which it can be used does not in itself allow analysis of a field problem. The characteristics of the soil profile must be known well enough that the soil stress-strain law can be determined. This could be done by direct laboratory testing of the soil, or empirically, through a knowledge of more easily obtainable properties. Unless the problem involves a critical

installation in a specific area, direct laboratory testing for stress-strain relations is not practical because of the difficulty in obtaining representative undisturbed samples and the extensive and costly testing procedure. The calculation of the stress-strain characteristics, generally expressed in terms of shear modulus and damping at various strain levels from other more easily obtainable properties, is the method that was used in this study. This method is particularly suited becasue of the large areal extent of the delta, and the existence of soil data from engineering projects.

2-3 Soil Data Source and Accuracy

The development of soil profiles, which presented the characteristics of the soil layers adequately for a dynamic analysis, was undertaken in three stages. The first stage involved the collection of existing data. These data consisted mainly of the borehole logs and the results of laboratory tests which had been undertaken by local geotechnical consultants as part of site investigations for engineering projects, and were made available through the generosity of these firms. Where data was not available, either because the engineering property was not one which was commonly tested for, or because the tests were not performed in the particular area where the information was needed, a realistic estimate of the desired property had to be obtained. This operation constituted the second stage. These properties were estimated through an interpretation of the available data and a knowledge of the origins of the deposits. The third stage

involved the use of the standard engineering properties that had been obtained in the first two stages to develop profiles of the soil which characterized their dynamic behaviour. Essentially, this entailed determining the shear modulus and damping ratio of the soil layers when subjected to a range of shear strains. These two functions describe the stress-strain behaviour of the soil in a way that enables mathematical modelling of the soil when subject to earthquake-induced ground motions.

The engineering properties which are presented here range from fundamental soil properties such as friction angle, to index properties such as Atterberg limits or blow count from the Standard Penetration test which have been correlated empirically with the more fundamental properties.

The data that is portrayed on the borehole logs has been subjected to several potential sources of error before being developed into this presentable form. The lateral variability of the soil should be considered. The log obtained from one drill hole is assumed to be representative of the immediately surrounding area. While this is likely to be true when considering the general form and properties of the soil, it may not be true when looking at details of the profile because of the soil variation resulting from the irregular delta growth.

Normal drilling procedures do not provide the observer with a complete representation of the soil, even at the particular site being tested. Samples of the soil are usually taken at intervals greater than one meter. The variation of the soil between the points

of sampling is interpreted by the driller by qualitatively noting the rate of advance of the bit and the type of material being returned as cuttings. Samples may not be representative of the layer within which they lie, and are disturbed to varying degrees, depending on the sampling procedure and the degree of care exercised by the driller.

In the testing of the samples there is opportunity to introduce error through improper handling or the use of non-standard procedure. In situ testing eliminates the problems of trying to procure an undisturbed sample, but adverse field conditions make it difficult to obtain high quality results. Even if credible results are obtained there may be doubt as to whether the test itself is meaningful. Having the drillers logs, the laboratory classification of the samples, and the results of any field or laboratory tests performed, the engineer must use his experience and knowledge of the area to prepare his interpretation of the soil profile. Similarly, the available data had to be interpreted for the research purposes of this project.

2-4 Water Content

Water content data is relatively easy to obtain for plastic soils since it involves measuring the wet and dry weight of a sample, which may be disturbed so long as it is not allowed to drain. Water content is a useful parameter to check in the classification procedure. In fine-grained samples procured below the water table where 100% saturation can be assumed it gives the void ratio of the

soil, when multiplied by the specific gravity of the solids. In cases where the consolidation characteristics of the soil can be determined, comparison with the actual change in void ratio determined from the field water content will indicate whether the soil type and the method of deposition are constant with depth.

The variation of water content with depth for the clay soils is shown in Figure 2-4-1. The water content varies linearly from 45% at the surface to 29% at a depth of 30 meters. Samples with organic content have water contents greater than the mean. This, and the possibility that water table fluctuation has produced an over-consolidated desiccated layer, accounts for the larger variation of the moisture content at the surface of the deposit. The water content profile in the silt soils has the same form as the clay profile, varying from an average of 41% at the surface to 26% at a depth of 60 meters as shown in figure 2-4-2. The presence of organic material and clays near the ground surface, results in the larger scattering of the near surface samples towards higher water contents. The water content of the peat soils is highly variable, as shown in figure 2-4-3. Generally, seams less than 0.3 meters thick have water contents varying from 100 to 250%. Seams from 0.3 to 1.0 meters thick have water contents varying from 250% to 600%. The larger layers have moisture contents varying from 600% to 1150%.

2-5 Atterberg Limits

The liquid limit and plastic limit are useful parameters in the classification of fine-grained soils, particularly clays. As

part of the test procedure the samples are remolded, so the disturbed samples recovered during the Standard Penetration Test are suitable for analysis. The tests do not yield results directly in terms of fundamental soil properties, but experience has led to relations which indicate the general characteristics of the soil.

Figure 2-5-1 shows the liquid and plastic limits for the clay soils under study plotted against depth. Both are constant with depth, the liquid limit having a mean value of 34% and the plastic limit a mean value of 22%. A plot of the liquid and plastic limits with depth for the silt soils is shown in figure 2-5-2. A close examination of the plot reveals that the points are better characterized by discontinuous vertical lines rather than by a continuous sloping line. This feature points to the existence of at least two distinct silt types. The data plotted above the discontinuity in the mean line were obtained in general from a different location in the delta than the data plotted below the discontinuity so this phenomina is unlikely to be the result of a sudden change in the composition of the Fraser River sediments. The mean liquid limit is about 40% in the upper silt and 33% in the lower silt. The mean plastic limit is 30% in the upper silt and 23% in the lower silt.

The plasticity index is defined as the difference between the liquid limit and the plastic limit, and is indicative of the range in water contents over which the soil retains its plasticity. Figure 2-5-3 shows a plot of the plasticity index in the silt soils, it is constant with depth, varying from 5% to 15%, with a mean of 9%.

Figure 2-5-4 presents a plot of the plasticity index in the clay soils. It varies from 8% to 17% and has a mean of 11%. The plasticity index can be plotted against the liquid limit of the soils on the plasticity chart, as shown in figure 2-5-5. According to their plotted position on the plasticity chart, the clay would be classified as an inorganic clay of medium plasticity, and the silts as inorganic silts of medium compressibility. These soils, classified principally on the basis of grain size, retain their classification when examined in terms of plasticity. Though the mean values for the soils plot quite distinctly on the plasticity chart, when the range of values is considered, the areas defined overlap substantially. This is particularly true in the case of the lower silt, which can almost be classified in these terms as a clay.

The liquidity index is defined as the difference between the natural water content and the plastic limit, divided by the plasticity index. It provides a measure of the softness of the soil in its remolded state by showing how close the moisture content of the soil in its natural state is to the liquid limit. Using the straight line mean relationships developed for the limits and indices, the liquidity index of the clay is calculated to range from a projected average of 2.0 at surface to 0.64 at a depth of 50 meters. The liquidity index of the upper silt varies from 1.3 at the surface to 0.55 at a depth of 25 meters and the liquidity index of the lower silt varies from 1.3 at 25 meters to 0.33 at 60 meters. Each deposit shows the same trend, changing from a very soft consistency in the upper regions to a stiffer one with depth.

2-6 Compression Index

The compression index is the slope of the plot of void ratio versus the logerithum of confining pressure obtained from a consolidation test. As such it is indicative of the amount of settlement that can be expected to occur as the result of a known increase in effective normal pressure. Figure 2-6-1 is a plot of compression index against depth for the silts. The presence of two distinct silt types is again revealed by a discontinuity in the compression index values with depth. The upper silt has constant compression index with depth, varying from 0.20 to 0.40 about a mean of 0.31. The plot shows the compression index of the lower silt to be constant with depth at a mean value of 0.21, with data points in the range from 0.15 to 0.26. The data points from the sandy silts plot generally in the lower end of the this range, while those from the clayey silts plot in the upper end. The limited data obtained indicates the compression index of the sand to be almost an order of magnitude less than that of the silt, with a value of about 0.06.

The compression index of the clay is constant with depth, varying from 0.33 to 0.48 with a mean value of 0.42 as shown in figure 2-6-2. The compression index of clays can also be estimated from the liquid limit using Skempton's equation $C_c = 0.009$ (liquid limit - 10). Using the mean liquid limit of 34%, this equation predicts a value of compression index of 0.22. This predicated value is less than the measured values. The reason may be that this clay is more sensitive than those used by

Skempton to define his relationship between the compression index of remolded and undisturbed clays.

The change in void ratio that would result from the consolidation of a homogenous soil deposit was calculated and compared to the actual void ratio change with depth, based on the water content. The void ratio in clay calculated at 50 meters below the surface from the consolidation characteristics differs only 3% from that deduced from the measured water content. This good correlation confirms the hypothesis that the clay deposits are normally consolidated and uniform in structure and constitutive components with depth. A similar analysis gives a variation of 11% in the void ratios at the 30 meter depth in the upper silt, and an variation of 20% at the 50 meter depth in the lower silt. This larger variation may be in part the result of having used a single straight line to characterize the water content with depth instead of fitting separate lines for the upper and lower silts. An examination of the lower silt data reveals that the water content may change less with depth than is indicated by the single straight line fit.

2-7 Undrained Shear Strength

The undrained shear strength of soils may be determined by performing a vane shear test or an unconfined compression test on an undisturbed sample. The torvane and pocket penetrometer can also be used to give quick results on small specimens, but are not as accurate. Figure 2-7-1 is a plot of the undrained shear strength of clay with depth as determined by these methods. Below the 6

meter depth the data can be characterized by a straight line passing through the origin. By assuming a value for the unit weight of the soil, the slope of this line can be expressed in terms of a ratio of the undrained shear strength (C) to the effective overburden pressure (P). This clay has a C/P ratio of 0.19. The C/P ratio can also be estimated from Skempton's equation, C/P = 0.10 + 0.004 (plasticity index), which gives a value of 0.14. These two estimates of the C/P ratio are in good agreement considering the small number of data points at depth and that Skempton's equation is generalized for all clays. Samples obtained in the top 6 meters of the deposit deviate substantially from the straight line C/P relationship due to the overconsolidation effect of surface dessication. The shear strengths in this upper layer range up to 105 kPa.

The undrained shear strength data for the silts are shown plotted against depth in figure 2-7-2. As with the clay, a distinct dessicated layer is present above the 6 meter depth. Below the 6 meter depth, the data are widely scattered. The shallowly sloping line having a C/P ratio of 0.30 is fitted to data determined in one area using a pocket penetrometer, while the steeply sloping line having a C/P ratio of 0.11 is fitted to data gathered over a slightly larger area using various techniques. The larger variation in the results of the tests could be due both to the fact that the samples were from different areas of the delta and to the different tests and test techniques used.

The handling of the sample and the rate of testing will affect the results because completely undrained conditions may not exist in the silt-size sample. Though Skempton's equation was developed for clays, it may be applicable to a certain extent to these silts because, as can be seen from the plasticity chart (figures 2-5-5), the silts can have a high clay content. The C/P ratio determined from Skempton's equation is 0.14, which lies between those defined by the two straight lines.

2-8 Dry Density of Sand

To measure the density of a soil a representative sample must be obtained in such a way that the original volume of the sample can be measured or calculated. The volume of a fine grained soil sample can be measured as it is extracted from the ground by the sampling tool, or it can be calculated in the laboratory by measuring the water content if the specific gravity is known, and the soil is saturated. The water content of sand and therefore the volume cannot be determined from field samples handled using normal methods because the pore spaces are too large to prevent drainage of the sample before the wet weight can be determined. This means that the volume of sample must be measured directly in the field during the sampling procedure. These measurements are difficult to obtain accurately. Figure 2-8-1 shows the dry density of sand samples taken from various locations in the delta. There is no discernable trend with depth, the values ranging from 14 kN/m^3 to 16.5 kN/m^3, around a mean value of 15 kN/m^3.

The void ratio is related to the dry density by the equation:

$$e = \frac{\gamma_w Gs}{\gamma_d} - 1$$

Here e is the void ratio, γ_w is the unit weight of water, γ_d is the dry density of the soil, and Gs is the specific gravity. Using a specific gravity of 2.8, and the dry density values shown in figure 2-8-1, the void ratio of the sand was calculated to range from 0.68 to 0.96 about a mean of 0.84 for those sands sampled.

2-9 Standard Penetration Test

The standard penetration test involves counting the number of blows of a standard weight that are required to drive a standard sampler into the bottom of a drill hole. It gives results in terms of blow counts, which are dependent on more fundamental properties of the soil. Unfortunately, because of the many variables and sources of error involved in the testing procedure and the absence of complete theoretical understanding of the mechanism of soil-sampler interaction, the relationship between the blow counts and these more fundamental properties is not well developed. Existing correlations were developed using particular soils and procedures and often under laboratory rather than field conditions, so that even if the relation is accurate under those particular conditions, it is unlikely to be universally representative. This means that the trends shown in these correlations should be representative but that the actual

magnitudes cannot be found without specific site testing to adjust the criteria for specific soils.

Despite these disadvantages, the Standard Penetration Test (SPT) is widely used for site investigation of deep soil deposits because it can be easily be performed using a standard drill rig and it allows recovery of samples. These samples are disturbed but are suitable for use in some tests and for classification. This laboratory information, obtained from from the SPT sample, when used with the blow count information, allows indentification of the soil layers and indicates the variation within each layer of those properties which influence the blow count.

Soil properties determined from the blow counts of two standard penetration tests can differ because of the difference in the state of the soil between the two tests, because of a variation in procedure between the two tests, or because of inaccuracies in the function used to correlate the blow count with those properties. The first is the difference that we wish to observe, while the second and third must be regarded as errors, to be minimized.

The state of the soil, as it influences the SPT can be thought of in terms of the stress regime, the strength characteristics and the failure mechanism. In its undisturbed form, the stress state of the soil can be described in terms of an overburden pressure and a lateral pressure. This indicates the importance of the over consolidation ratio, which influences the lateral pressure and is effected by the method of deposition of the soil and its stress

history. This stress state will be altered locally by the presence of the bore hole, but the magnitude and extent of this local variation is difficult to determine. The soil strength is generally expressed in terms of a cohesion and a friction angle, the values of which will depend on the void ratio of the soil. The failure mechanism which must occur if the sampler is to penetrate into the soil, will vary to some degree with soil properties. Particle size, shape, gradation and orientation are important. In silt-size soils below the water table the small pore spaces inhibit the flow of pore fluid, resulting in partial liquefaction of the soil surrounding the sampler with each blow, so that the penetration resistance is greatly reduced from that observed in the more free draining sand samples. This reduction became significant in the data reviewed for this work when the soil was composed of more than 20 percent silt.

In a test such as the SPT, entailing an arbitrary procedure, variations in the prescribed procedure can be considered errors only in the sense that they will prevent data obtained in a non-standard way from being compared with the standard data. Modifications to the test procedure may well result in data which are more meaningful in the particular sense for which that data is required. In order to assess the accuracy with which any two data sets may be compared, it is important to have an understanding of those elements of procedure which can affect the results of the test.

Kovacs, Evans, and Griffith (1977) undertook a study to assess the effect of some of these variables on the measured blow counts. They found that the number of turns of rope around the cathead changed

the friction between rope and cathead, which in turn affected the speed at which the weight could fall, and so influenced the amount of energy imparted to the top of the drill string. A larger number of wraps of the rope around the cathead reduces the energy imparted and increases the blow count for one foot of penetration. They found that new, stiffer ropes, when released from the cathead, formed loops with a larger radius of curvature than older ropes, reducing friction and increasing the energy imparted. The cathead speed and the mechanism by which the operator released the rope were also found to have an effect on the energy imparted. These are only some of the sources of variation in the amount of energy imparted to the top of the drill string. Though the effects of these variations could be limited by callibrating each drill rig to a standard impact energy, this does not help when comparing old test results, and will not aid in solution of some of the other problems which have their origin below the ground.

Rod length will influence blow count. Gibbs and Holtz (1957) found that the blow count was increased when using a long rod in a deep hole through loose sands because of the weight of the rod, but was decreased when using a long rod in dense sands because of the energy lost due to the flexure and whipping of the rods. The types of rods used and their physical condition will also influence the blow count because of the variation in weight, and the differences in stiffness and size of eccentricities.

The blow count in the STP is generally recorded over three increments of 0.15 meters, making the total penetration of the sampler 0.45 meters. If the driller does not exercise care in

cleaning out the bottom of the hole, the loose disturbed soil found there will result in low initial blow counts which do not characterize the soil. Uncharacteristically high blow counts may occur near the end of the 0.45 meter penetration if the sampler is over-driven or if operation becomes obstructed by soil within the tube or casing. The ASTM designation D1586-67 describing the penetration test indicates that the first 0.15 meter increment should be considered as a seating drive, and the number of blows required for the second and third increments of 0.15 meters should be considered the penetration resistance. Not all firms use this procedure. Schnable (1971) suggests that a more logical procedure would be to seat the sampler with a few light taps, and then to record the blow count on the first 0.3 meters of penetration. He points out that this method requires a skillful driller, however the whole method is such that the results of the test will only be significant if it is performed by a skillful and experienced driller. Schnable must be assuming that the bulb of soil affected by the stress relief in the bottom of the drill hole is small enough in extent and magnitude that the blow count measured there is not affected by this phenomenon any more that it is in the deeper two 0.15 meter increments. This assumption seems to be supported by the data shown by Schmertmann (1971). He used a 'friction cone SPT formula' with data collected from cone penetration tests in the form of the frictional and end bearing components of resistance to predict the blow counts in each of the three 0.15 meter increments that would be expected from a SPT in the same soil. These values were compared with the actual blow count values that

were obtained from a carefully executed SPT in an adjacent hole. The ratio of the blow counts in the first increment to those in the third increment, and those in the second increment to those in the third increment in loose to medium sands was respectively 0.61 and 0.80 for the predicted values, and 0.63 and 0.81 for the observed values. The excellent agreement of both sets of ratios not only indicates the viability of Schmertmann's 'friction cone SPT formula' but also shows that under the controlled testing procedure used, the blow counts in the first 0.15 meter increment were not abnormally low. The increase in the blow count over the three increments is more probably due to the way that the sampler mobilizes the penetration resistance in a combination of side friction and end bearing, rather than due to a change in soil strength with depth.

Much of the SPT data collected for this study included blow counts reported over the first 0.3 meters of penetration. Though data presented in this way is valid it cannot be compared directly with data recorded over the 0.15 to 0.45 meter penetration range. To facilitate data comparison and to permit the use of relationships which have been developed to correlate the blow counts in the 0.15 to 0.45 meter range with more fundamental soil properties, a relationship was developed to allow the blow counts recorded over the first 0.3 meters of penetration to be expressed as equivalent blow counts in the 0.15 to 0.45 meter penetration range.

A typical plot of blow count versus depth for a sand layer is shown in figure 2-9-1. One curve shows the variation of blow count recorded over the first 0.3 meters of penetration while the other is a plot of the blow count recorded from 0.15 to 0.45 meters

on the same sample. These two curves are roughly parallel. To assess the degree of correspondence between the two curves, a method of comparison was needed which would not compare the two curves with an artificial curve of some arbitrary shape, but with each other. The change in blow count between successive tests was used as a method of comparing the curves. It was assumed that the variation of the blow count would be linerally proportional to the magnitude of the blow count, so the change in blow counts between two successive tests was normalized by dividing it by the average of the two values. The ratio of these normalized differences was called the 'coefficient of relative curve smoothness' and was plotted against depth. This coefficient, developed from blow counts recorded from 0 to 0.3 meters and those from 0.15 to 0.45 meters, is shown in figure 2-9-2, and the coefficient from those recorded from 0 to 0.3 meters and those recorded from 0.3 to 0.6 meters is shown on figure 2-9-3. The points are scattered, but evenly distributed around the axis where the coefficient of relative curve smoothness is equal to 1. This suggests the validity of the normalizing procedure. Points plotting to the left of the axis show that the blow count curve for penetration from 0 to 0.3 meters is smoother than that for penetration from 0.15 to 0.45 meters. This could be due to loose soil in the bottom of the drill hole which would give a reduced but constant number of blows in the first few inches which would not show in the 0.15 to 0.45 meter reading. It could also be due to the jamming of the sampler in the last few inches,

which would result in an abnormally high blow count in the 0.15 to 0.45 meter reading. When the points plot to the right of the axis, it indicates that the blow count for curve penetration from 0.15 to 0.45 is smoother than that for penetration from 0 to 0.3 meters. This could be due to irregular or improper cleaning of the drill hole before the sampler was placed, which is indicative of poor drilling technique. Because of the crudeness of the analysis, the variation in the points away from the axis would be significant only when several consecutive points exhibited the same trends. With the exception of one set of data shown in figure 2-9-3 this is not the case. The points lie scattered about the axis, indicating that a simple relationship between the blow count recorded when penetrating from 0 to 0.3 meters and from 0.15 to 0.45 meters should exist.

To reveal this relationship, the difference between the blow count recorded during penetration from 0 to 0.3 meters and that recorded from 0.15 to 0.45 meters was calculated and normalized by dividing it by the blow count from 0 to 0.3 meters. Expressed as a percentage this difference was plotted against depth in figure 2-9-4. Figure 2-9-5 shows the results of the same procedure applied to the difference in blow counts recorded from 0 to 0.3 and 0.3 to 0.6 meters. The best fit straight line characterizing each data set was determined and replotted for convenience in figure 2-9-6. The increase in blow count recorded for penetration from 0.15 to 0.45 meters penetration over that recorded from 0 to 0.3 meters varied from 49% at the surface of the sand deposit to 37% at a depth of 30 meters. The increased blow count measured from 0.3 to 0.6 meters penetration over that measured from 0 to

0.3 meters ranged from 66% at the surface to 53% at a depth of 30 meters.

This decrease in the 'per cent difference' with depth means that the first blow count increment, from 0 to 0.15 meters contributes proportionately more to the total reading, with depth, than does the last increment from 0.3 to 0.45 meters. This phenomenon cannot be due to the presence of an initial disturbed layer at the bottom of the drill hole as this would produce the opposite effect, the uniformly loose layer giving nearly constant blow count and increasing the 'per cent difference' with depth. The trend is more reasonably related to the mechanism by which the penetration resistance is mobilized. Using the 'friction cone SPT formula' developed by Schmertmann (1971), the total penetration resistance developed at a particular depth of sampler embedment can be subdivided into the percentage due to end bearing, and that due to side friction. (appendix 2). For sands, this relation predicts that approximately 72% of the penetration resistance would be provided by end bearing at the 0.15 meter penetration level, while at the 0.45 meter level the end bearing component would be reduced to 46%. Because the resistance developed by end bearing is more dominant in the first 0.15 meter increment of each test, the reduction in the 'percent difference' values with depth below the ground surface could be due to a disproportionate increase in the resistance generated through end bearing. As the sampler is driven, a compacted plug of soil is formed ahead of it. The end bearing resistance is affected by the increased confining pressure at depth and also by the increased energy required to

compact the soil at depth.

To check the usefulness of the relation developed between the blow count recorded from 0 to 0.3 meters and that recorded from 0.15 to 0.45 meters, data from one driller describing the blow count from 0.15 to 0.45 meters was compared to data obtained by another driller and in the same area recorded from 0 to 0.3 meters but modified to give the equivalent 0.15 to 0.45 meter readings using the curve in figure 2-9-6. Figure 2-9-7 shows the curve developed from the blow count recorded by one driller for penetration from 0 to 0.3 meters in each test. The curve describing the blow count data recorded during penetration from 0.15 to 0.45 meters is depicted in figure 2-9-8. Figure 2-9-9 is a comparison of these two curves and the curve modified from the 0 to 0.3 meter penetration curve to give the equivalent blow count for the 0.15 to 0.45 meter penetration. The comparison between the measured and modified curves showing the blow count for the 0.15 to 0.45 meter penetrations is good, particularly considering that the two test sets were performed by different drillers, each using their own technique and equipment, and in view of the fact that the drill holes were not in the same spot, even though close in location.

Additional blow count information from drill holes in the Fraser Delta is shown plotted against depth in figures 2-9-10 to 2-9-21. A curve has been fitted to each data set, and where necessary the conversion shown in figure 2-9-6 has been applied to this curve express the data in terms of the equivalent blow count from 0.15 to 0.45 meters of penetration on each sample.

The data in each figure are widely spread from the mean due to irregularities in the soil itself, and in the testing procedure. In figure 2-9-12 data obtained by two drillers in the same area are plotted together. One data set predicts higher blow counts with depth than does the other, pointing to a variation in the drilling technique and equipment. Figure 2-9-15 is composed of vertical lines indicating average blow counts over the depths defined by each line, rather than points indicating the measured blow count at a specific depth. Because of this presentation of averaged data, the curve fitting gives results which are less indicative of the soils present. Figure 2-9-11 shows a plot of blow count from drill holes in the Sturgeon Bank Sea Island area. Those samples closer to Sea Island generally show higher blow counts than those farther out on the banks, though a single curve is used to characterize all the data.

The curves representing the blow count for penetration from 0.15 to 0.45 meters are summarized in figure 2-9-22. These are the curves that will be used to determine soil properties, since the correlations between soil properties and the SPT have been developed using sampler penetration from 0.15 to 0.45 meters. The curves are grouped together in two major concentrations, with some lone curves indicating lower blow counts. The first group is composed of curves which run roughly in a straight line from a blow count (N) of 14 at 6 meters to an N of 62 at 18 meters. This group is composed of data from bore holes along the northern part of the delta, one site on Sea Island, one south of Sea Island on Number Three Road, one near the head of the delta, and one south of

the Oak Street Bridge. The second group is composed of curves which run in a straight line from an N of 15 at 6 meters to an N of 35 at 18 meters. Below 18 meters the N value remains almost constant to the limit of the data at 40 meters. This group is composed of data from sites throughout the central portion of the delta. There are sites on Annacis Island, on South Eastern Lulu Island, in Ladner, and in the Sturgeon Bank-Sea Island area. The curve characterizing the soil in the Brighouse area of Richmond resembles the curves of group 2 to a depth of 12 meters, where the slope changes and N remains constant, or decreases slightly with depth. The Tilbury Island curve shows a low N until a depth of 27 meters is reached, where it joins the second group of curves. The Roberts Bank curve depicts a very low N, ranging from 11 at a depth of 6 meters to 41 at a depth of 30 meters.

Despite the trends that may seem to be apparent regarding the distribution of the soil profile types, it would be a mistake to make generalizations, other than that the N value appears to be less on the banks than throughout the rest of the delta. This is so because this data was collected for the purpose of understanding the soil profile at three particular locations rather than everywhere in the delta. It may however, on the basis of the wide distribution of data, be reasonable to assume that the sand types shown here are typical and representative of these throughout the delta.

2-10 Relative Density of Sands

The relative density of a soil is a measure of the density

of the soil relative to its most dense and most loose states. It is defined as follows:

$$Dr = \frac{e_{max} - e}{e_{max} - e_{min}}$$

where Dr = Relative Density
e = in-situ void ratio
e_{max} = void ratio of sample in its loosest state
e_{min} = void ratio of sample in its densest state

Accordingly, the larger the value of relative density the more dense the sample. A standard procedure for the test is presented in ASTM Designation D2049-69, however many firms use non-standard techniques.

The errors inherent in the relative density test were investigated by Tavenas, Ladd, and LaRochelle (1972). In addition to the errors introduced by the use of non-standard technique, and the error in determining the in-situ void ratio from field volume measurements, they found that the formulation of the equation for relative density magnified laboratory errors which in themselves were within reasonable bounds. They found that the variability of the relative density was usually 10 times that of the maximum and minimum densities, giving errors in the relative density in the order of plus or minus 30 to 47%.

Because of the difficulty in determining the relative density and the large amount of data available from the SPT, correlations have been developed between the N value and relative density. Although this increases dramatically the amount of relative density information

that is available, it decreases the accuracy of such data. To develop the relationship, the relative density must be determined for soils of known N value, known properties and known state of stress. Such a complete relationship would be difficult to formulate and impractical for field application where the important parameters affecting the relative density are not any better known than the relative density itself. For this reason the relative density and N value are generally correlated with the vertical effective stress only, though Saito (1977) points out that the mean effective principal stress would be better, and de Mello (1971) in his extensive state of the art report on the SPT indicated that important effect of the friction angle. Other errors are incorporated in the relation through the laboratory determination of the relative density for the correlation. The majority of the relations in existence were developed by simulating field conditions in the laboratory. This simulation is not exact, so additional errors are introduced at this point. In addition to this, there are all the errors inherent in the SPT.

Despite the problems involved in the application of such empirical correlations, they continue to be used because they give large volumes of inexpensive information. When using these correlations it must be remembered that they were developed by testing a specific soil in a particular fashion, so they should only be used qualitatively until the criteria can be adjusted by local testing. De Mello (1971) warns of the danger inherent in using these correlations blindly when he says 'if any sand is not

closely similar to the (tested) sands, the chances of adequately representing the behaviour by analogy with the (test) results will be very small.'

Many researchers have developed relationships between the blow count of the SPT and overburden pressure at various values of relative density. In the Fraser River Delta, the water table is generally within a few feet of the ground surface, and the sand deposits quite uniform. The dry density of the sand is shown in figure 2-8-1 to be in the range from 14.3 kN/m^3 to 15.5 kN/m^3, which suggests that a reasonable assumption for the saturated unit weight would be 19.2 kN/m^3. Using this value, the soil profile can be idealized as one having buoyant unit weight of 9.4 kN/m^3, constant with depth. This allows the blow count-relative density information to be plotted against depth as well as overburden pressure. Figures 2-10-1 and 2-10-2 show five such relations. Though the curves are similar in trend there can be a 50% difference between the relative density values predicted for a sample at a particular depth and with a particular N value.

If the SPT data is to be used to advantage, it is important to determine which of these relationships best describes the sands present in the delta. To this end, these relationships can be examined on the basis of various criteria. The experimental methods used to determine the relationships can be examined. The grain size curves of the test soils can be compared to those of samples from the field. Direct measurements of the relative density determined from field samples can be compared to predicted values. The variation of relative density with depth can be checked for conformity with

the relations predicted from a knowledge of the history of the deposit.

The Bazaraa curves (1967) were developed from data obtained in the field, and would therefore be subject to the errors in blow count and relative density measurement outlined previously. The other researchers tried to simulate field conditions in the laboratory. Though this allowed careful measurements to be taken in a controlled environment, it would not eliminate all the sources of error present in the field and could introduce other errors through inaccurate modelling of the field conditions. The laboratory procedures involved driving the sampler into a large container of soil which had been placed at some known relative density, and which could be subjected to a known vertical stress by loading the plate covering the surface of the container. However, the container used to hold the soil could not produce precisely the same boundary conditions as those in the field. Marcuson and Bieganousky (1977) improved an earlier method by using a container formed of alternating steel and rubber rings stacked to the required height, so that the container could deform slightly in the vertical direction when the top plate was loaded, thereby reducing the effects of the side friction. The placement of the soil at uniform density throughout the container is difficult. The method of obtaining a known relative density varied between researchers, but in some cases the density control was not good. In the laboratory, the effects of the friction between the rod and the hole or casing were not reproduced, and the rod length; though varied to a certain extent in the testing

programs, would not correspond exactly to the field situation.

The majority of the tests were performed on air dried samples. Gibbs and Holtz (1957) performed a series of tests on submerged samples, but were unsatisfied with their results, and recommended that the curves developed for the air dried sand be used for the submerged situation. Marcuson and Bieganousky (1977) performed their series of tests on submerged samples, but did not achieve complete saturation. One of the problems encountered in testing the submerged samples is that within the small testing tank, the pore pressure response system resulting from the dynamic loading would not duplicate that found in the field.

The grain size distribution of the sands tested to develop the relative density-blow count relationship are shown in figure 2-10-3 and the grain size distribution of sand samples obtained from the Fraser Delta are shown in figure 2-10-4. The samples were procured from the western part of the delta so these curves may not be representative of the total delta sand deposits. The sands used by Gibbs and Holtz (1957) and Schultze and Melzer (1965) compare poorly with the soils in the delta. They are larger in grain size and more well graded than the delta soils. The sand used by Shultze and Menzenbach (1961) compares more favourably, being more uniform and smaller in grain size. The sands used by Marcuson and Bieganousky (1977) are closest in grain size to the samples from the delta: they are similar in uniformity, though they lie in the upper range of actual grain size.

With knowledge of the soil characteristics and the variability of the depositional environment, the shape of the curves relating

blow count to effective overburden pressure for various values of relative density can be predicted. It was found in section 2-6 that the change in void ratio with depth determined from the water content values in the silt and clay soils could be accounted for by the consolidation of the soil under the weight of the overburden. This indicates that the depositional environment has been constant throughout the time when these deposits were layed down. Accordingly, one would expect the sand deposits to differ in density with depth in a manner prescribed by the consolidation characteristics of the soil. The values of relative density and dry density with depth which are shown in table 2-9-1 were used with an assumed specific gravity in the solution of simultaneous equations to yield average values of maximum and minimum void ratio for the sand deposit. The analysis yielded an average maximum void ratio of 1.2 and an average minimum void ratio of 0.66. These values were used with the compression index of the sand to predict the change in relative density that would occur with depth as a result of the deposits consolidating under its own weight. Over a change in depth of one logarithmic increment, say from 3 to 30 meters, the relative density was found to increase by an increment of 10.1%.

The various relative density relations shown in figures 2-10-1 and 2-10-2 were checked to see whether they satisfied this criterion, by overlaying them on the average blow count curves shown in figure 2-9-22. Recall that there were two general curve shapes, one where the N value increased linearly to a depth of 18 meters and then remained almost constant with depth, and another where the

N value increased linearly to a larger value at a greater depth. The former group of curves was examined first. The Schultze and Menzenback and the Bazaraa curves correspond most closely to the predicted curve shape. These were followed, in order of best fit by the Marcuson and Bieganouski, the Gibbs and Holtz, and the Schultze and Melzer curves. When the theory describing the increase in relative density with depth was applied to the latter group of curves poor correspondence was achieved with the relative density relations. The Schultze and Melzer curves provided a better fit than the others, but one that was not particularly close. This suggests that the latter curve group represents profiles where the soils or the depositional environment were not uniform with depth, so that the relative density increases with depth more than could be expected from the consolidation of the deposit under its own weight. This phenomina could also be explained if the sands in this latter group had a very high silt content so that the consolidation characteristics would resemble those of the more compressable silts, predicting a much larger increase in relative density with depth. However, an examination of the drill logs does not lend support to this hypothesis.

Actual field measurement of relative densities are critical in the selection of the relative density relation which best describes the soils of the delta. The values of relative density from table 2-10-1 are shown at the appropriate depths along with the plot of N against depth for the drill holes in that area,

from figure 2-9-22. The large variability in the relative density measurements is more likely due to errors in the measurement than to actual variability in the soil. The average relative density measurement is 63%, so it was assumed, from the knowledge of the shape of the curve, that the relative density would increase quickly from a value of 58% at a depth of 3 meters, to a value of 68% at a depth of 30 meters. On the basis of these values, and the ratio of the change in relative density to the resulting change in N value at various depths, as observed from the relative density relations in figures 2-10-1 and 2-10-2, the approximate lines showing the change in N value with depth for relative densities of 60% and 80% were constructed in figure 2-10-5. These lines were compared with the relative density curves. The correlation with the Schultze and Menzenbach curves was very good. The Gibbs and Holtz curves gave a reasonable prediction, but the other relations were less satisfactory.

Scotton (1977) performed a series of carefully controlled relative density measurements on the near-surface soils at Sturgeon Bank. Using these and N values from nearby drill holes, he concluded that the Bazaraa relative density relations better described these soils than the Gibbs and Holtz relations. This is consistent with the observation that the Gibbs and Holtz relation over-estimates the relative density calculated on the basis of the curve shape determined from the consolidation characteristics, though the difference could be due in part to the tests being performed on a different soil type.

On the basis of these discussions, the Schultze and Menzenbach relations were selected as best describing the relative density

characteristics of the delta sands. This relation is much closer in form to the Gibbs and Holtz than to the Bazaraa relation. At depths less than 4.5 meters, where the Schultze and Menzenback relation is not defined, the relative density may be better described by the Bazaraa than the Gibbs and Holtz relations. It is important to remember that this choice of a relative density relation was based on a small number of relative density measurements and that the choice of this relation does not mean that it is the result of the most accurate testing program. Rather, it best describes the particular soils in the Fraser Delta.

2-11 Friction Angle of Sands

The angle of internal friction depends primarily on the relative density or void ratio of the soil, the grain size distribution and the grain shape. Its direct dependence on the stress state of the soil is small. The fraction angle is generally determined using the data from triaxial or shear tests to define the failure envelope of the soil. Figure 2-11-1 is a plot of friction angle against dry density for two sand types. One is a fine to medium sand, and the other is a silty sand. Both soil types show the expected trend of increasing friction angle with increasing dry density. The silty sand had a friction angle 5 or 6 degrees greater than the clean sand at the same dry density.

De Mello (1971) suggests that the apparent friction angle may be more fundamental and more significant parameter to use in correlations with the blow count of the SPT than the relative

density. It may be possible to develop a single relationship between the N value and friction angle with confining pressure which is applicable to all sand types. Once the friction angle had been determined, the relation between it and the relative density could be developed for each soil type.

The curves developed by De Mello are shown in figure 2-11-2 in a form relating the N value and the depth below surface for various values of friction angle. This was done using an average value for the specific gravity and assuming the soil to be saturated. De Mello's curves describing the fine sand, and the average of the fine and coarse sands are shown. The relations are in the form of straight lines because of the form of statistical analysis used. Shown with these relations are the plots of N value against depth for the sites where the samples used to determine the friction angles shown in figure 2-11-1.

Using the mean dry density from figure 2-8-1 of 14.9 kN/m^3, figure 2-11-1 indicates that the fine to medium sand has a friction angle of 38.5 degrees. Using De Mello's relation with the mean of the fine and medium curves in figure 2-11-2 results in a predicted friction angle of 41 degrees for the penetration profile shown. This is a reasonable correlation. The silty sand samples were taken from Roberts Bank, where no separate measurements of dry density were obtained, so the average dry density achieved in the tests was used to give an anticipated friction angle of 37 degrees, from figure 2-11-1. Using the set of curves describing the fine sand in figure 2-11-2 and the N profile for the Roberts Bank area, a friction angle of 36 degrees was predicted. This is a good correlation, which tends to confirm that the N value can be related

more successfully to the friction angle than to the relative density for a large range of soil types.

CHAPTER 3

DYNAMIC ANALYSIS

3-1 Type of Analysis

In areas of seismic activity, the design of engineering structures should incorporate some method of considering the effects of possible earthquakes. The method used to assess these effects will depend on the type and the purpose of the structure and the problems associated with its potential failure. Various criteria are considered when attempting to characterize the effects of an earthquake on a particular structure. The maximum acceleration and the frequency content of the motion are important.

The frequency content is of particular interest as structures having a predominant period close to that of the earthquake will expeience large deflections. Most buildings are designed to absorb the energy of the earthquake through the ductility of their members. For such designs, the duration of the strong motion and the duration of any large acceleration pulses are important, as the energy-absorbing capacity of the structure is finite.

To analyze the effects of an earthquake on a structure, whether it be a building, an earth structure, or a buried structure; the changing characteristics of the motion and their effects,can be followed from the source to the bedrock at the site, through the soil layers to the surface, and through the building as a whole,

to individual members. This procedure involves a modelling process, which becomes increasingly difficult and costly as more stages are included. At some stage, a break is made from consideration of the earthquake's dynamic effects to consideration of the structural behavior in terms of standard design methods.

The National Building Code of Canada has divided the country into zones of varying seismic risk and defines the ground acceleration on rock or deep soil deposits that may be used to calculate equivalent horizontal inertial loading. These loads are included with other loads in the design of the members.

The effects of a particular earthquake on a series of structures can be examined using a response spectrum. A response spectrum shows the relative magnitude of the various uniform harmonic waves that combine to give the complex motion of an earthquake record and can be thought of as a plot of velocity, displacement, or acceleration response of a single-degree-of-freedom structure of varying natural frequency and a particular amount of damping to a specific earthquake. It is a function both of the earthquake and the structure. This form of presentation is valuable because most structures can be roughly characterized by a natural frequency and damping. The response spectrum indicates whether the structure is likely to undergo a large response relative to similar structures of other periods and gives an indication of the magnitude of the response for a particular earthquake.

Methods exist whereby the response spectra of potential earthquakes can be predicted from the spectra of recorded earthquakes. Housner produced a set of curves which represents the average

response spectra of several recorded earthquakes for various percentages of critical damping. The curves can be scaled according to the magnitude of the earthquake that is anticipated. Newmark developed a method where spectra are produced for a structure by applying to the ground spectra and multiplication factor which is related to the structural damping. The ground spectra is a curve drawn for convenience to represent the maximum anticipated ground velocity accelerations and displacement; He found that the velocity, which is related to the energy absorbed; the acceleration, which is related to the forces experienced, and the displacement, which is related to the distortion; were critical design parameters in different structural period ranges. The Newmark method produces a design curve that is an envelope of analyzed cases.

The next stage in complexity involves modelling the site to analytically produce a spectrum which typifies the building response. Using an earthquake record that is representative of the motion on bedrock and a model describing the dynamic properties of the soil, the resulting ground surface motions can be mathematically determined and the surface response calculated. If carefully executed, this procedure should yield a response spectrum that is more typical of the local site conditions than the methods previously described.

The final stage in complexity involves linking the structure and soil together through the use of finite elements and modelling the whole system to find the actual response of the structure to a particular earthquake on bedrock. The attempt of this method is to

incorporate the effects of soil structure interaction. This is desirable because the free-field response of soil is not the same as the response of soil which underlies a building. Finite element analysis is also suited to problems where the soil cannot be modelled as semi-infinite horizontal layers. However, this method of analysis is costly, and for general problems may not yield results which are any more reliable than those obtained for the one-dimensional analysis.

A good combination of practicality and accuracy is provided by the dynamic analysis of methods that use the properties of the soil deposits to produce a response spectrum on surface from an assumed earthquake motion at bedrock. Because of their complexity when applied to real problems, these methods generally require the use of a computer. There are two general classes of programs; those which use a lumped mass model and those which provide a solution to the wave equation. The lumped-mass method uses a soil model consisting of discrete masses connected by stiffness elements which characterize the properties of the various soil layers. The wave equation methods are based on the theory of one-dimensional wave propagation in a continuous medium. Both of these classes of analysis are based on the assumption that the earthquake can be respresented by a shear wave propagating vertically through horizontal soil layers. This assumption is more valid for deep than for shallow earthquakes.

Computer programs based on the wave-equation methods use a fourrier transform to develop the fourrier spectrum. Transfer functions which incorporate the dynamic effect of the soil deposit

are developed to produce a fourrier spectrum which describes the ground-surface motion in the frequency domain. Because the fourrrier spectrum contains all the information describing the ground motion, it is possible to produce the predicted ground surface record in the time domain in the form of an acceleration record.

In this study, a wave propagation solution was employed to predict the surface motion characteristics. The SHAKE program developed in Berkley (Schnabel, Lysmer, and Seed, 1972) was used, with a minor modification to allow the use of a greater range of dynamic soil properties. SHAKE uses an iterative visco-elastic method of analysis to solve a non-linear problem. When soil is deformed it follows a hysteritic stress strain path, the shape of which is dependent on the stress strain amplitude, as depicted in fig. 3-1-1. The SHAKE program approximates this behaviour through the use of a secant shear modulus, and a damping ratio. As shown in figure 3-1-2, the shear modulus is defined by a straight line through the end points of the stress loop, and the damping ratio is related to the ratio of the area of the hysteresis loop and the area of a triangular area defined by the shear modulus and the end-point of the loop. The SHAKE program uses this equivalent linear modulus and a viscous damping ratio to determine the strain amplitude which will define a new modulus and damping ratio. The iteration continues until the solution stabilizes. It is assumed that the average strain amplitude is 65% of the peak experienced from the total earthquake amplitude record. The SHAKE program has

the same limitations as other similar dynamic analysis in that it performs a one-dimensional analysis of horizontal semi-infinite beds and uses an approximate mathematical solution.

The input to the SHAKE program consists of a description of the soil profile at the site and an acceleration record to be used as the object motion on bedrock. The soil is described in terms of layers with similar dynamic properties, varying in thickness from less than 2 meters near the surface to up to 50 meters at depth. The dynamic properties are presented in terms of the maximum shear modulus determined at low strain amplitude; attenuation curves describing the reduction in modulus experienced as the strain level increases, and the maximum damping ratio and its variation with strain amplitude.

3-2 Soil Profiles and Dynamic Properties

The dynamic analysis in this study was undertaken in two stages. In the first stage of the analysis, the SHAKE program was used to predict the surface motions of several sites in the Fraser Delta. The 1976 Pender Island earthquake was used as the bedrock input, and the dynamic properties at the sites were calculated from the information gained in the examination of the delta soils. These motions were compared with the actual motions recorded for the 1976 Pender Island earthquake at those sites, to form an estimation of the accuracy of the modelling procedure and input parameters. With this knowledge, the second stage of analysis could be undertaken. This involved subjecting the profile developed in the first stage to data representing earthquakes

of various magnitudes to assess the effect of large motions on the sites.

Because of the necessity of comparison between the predicted and measured earthquake in the first stage, the sites were limited to those where surface records for the 1976 Pender Island earthquake had been obtained. Three sites satisfied this criterion. They consist of one at Roberts Bank, one on Annacis Island and one in the Brighouse area of Richmond, as shown in figure 3-2-1. These sites are widely spaced across the area of the recent delta, and their profiles are representative of the soils found throughout the delta.

The three profiles that were developed and the soil models that were used for the computer analysis are shown in figures 3-2-2, 3-2-3 and 3-2-4. Generally, the nature of the near-surface deposits is well known from drill holes in the vicinity of the site. Below depths of 45 meters to 60 meters, the nature of the deposits. and their properties have been gleaned from a few deep drill holes and a knowledge of the history of the delta formation. The later aids in the extrapolation of known soil characteristics near surface to those at depth. Depths to the top of the till deposits were estimated by projection of the till surface slopes as indicated by drill holes which intercepted the till, and by correlation with a few isolated deep holes. The depth to bedrock was estimated from a few deep drill holes, and vibro-seismic profiles. Figure 1-1-5 shows the large irregularity in the bedrock surface, indicating that the bedrock depths estimated could easily vary by 30 meters from the true depth.

The Brighouse profiles consist of 3.7 meters of clayey silt overlying sand to about 45 meters. Below that is silt grading downwards to clay. Till is estimated to be at 198 meters and bedrock at 305 meters. Because of the sequence of glaciation that effected the present Fraser Delta area, there is a possibility that the till could contain layers of interglacial deposits of sand, clay or silt, though because of their lack of resistance to abrasion and errosion, these deposits may have been completely eliminated.

The Roberts Bank profile consists of 9.1 meters of sandy silt fill and silt overlying sand with some silt layers to about 60 meters. Below this, silt is expected to 107 meters, where till is estimated to occur, again with the possibility of interglacial deposits. Bedrock is estimated to be at 228 meters.

The Annacis Island profile is similar to the Roberts Bank profile. It consists of 6 meters of sandy silt overlying sand to about 37 meters with sandy silt to about 91 meters, where till is estimated to occur, possibly with some interglacial deposits. Bedrock is estimated to be at 220 meters.

The soil model consists of soil layers ranging from a few feet in thickness at the surface, to 30 meters in thickness at depth. This approach is taken since a single value of each dynamic parameter must be selected to be representative of all the soil in each layer. The layers are shown classified by the major soil-type they represent, as this will determine the method used to derive the dynamic properties of the layer.

The dynamic properties of the soils shown in the profile are input in terms of a maximum shear modulus, maximum damping ratio, and reduction curves which show the relationship between these maximum values and the strain level. The dynamic soil characteristics have been determined from relations developed by others using both laboratory and field tests. In the laboratory, the material being tested is well known but it is difficult to apply test conditions that are representative of the situation found in the field, while in field testing the reverse is true. Both laboratory and field tests can be subdivided into two groups; those which attempt to measure the response of the soil system to dynamic excitation, and those which measure the shear wave velocity to the soil, from which the modulus can be calculated. Common laboratory techniques for the measurement of the soil stress strain properties include the resonant column test, ultrasonic pulse tests, shake table tests and cyclic tests. The cyclic tests may be either triaxial, simple shear, or torsional. These cyclic tests can be either stress or strain controlled. Common field tests are seismic refraction survey, cross hole survey, down hole survey, or surface-save techniques. These give the modulus indirectly through measurement of the shear wave velocity. Vibro-seismic methods can also be used, as can the cylindrical insitu test developed by Bratton and Higgins (1978), in which accelerometers on a surface grid measure the response of the soil to an explosion and an iterative procedure is used to determine the soil properties.

Because of the lack of knowledge of the material being tested

in the field, most modulus and damping relations have been developed from laboratory data. It is important, therefore, to establish a correlation between the field and laboratory data, which often differ because of the varying strain levels at which the tests were performed.

The maximum shear modulus has been calculated for the soil layers in the three profiles from several relations and is shown in figures 3-2-5, 3-2-6, and 3-2-7. Hardin and Black (1968) developed the relationship for cohesive and cohesionless soils:

$$G_{max} = \frac{1230(2.973-e)^2}{1+e}(OCR)^k \sigma_o^{\frac{1}{2}} \quad (psi)$$

where the factor K depends on the plasticity index of the soil as follows:

Plasticity Index	K
0	0
20	.18
40	.30
60	.41
80	.48
100 or greater	.50

The above equation relates the maximum shear modulus (G_{max}) to the void ratio (e), the over consolidation ratio (OCR), a factor related to the plasticity index (K) and the mean normal effective stress (σ_o). Seed and Idriss (1970) developed separate relations for sand and for clay. For sand they use the relationship:

$$G_{max} = 1000\ (K_2)_{max}\ (\sigma_o)^{\frac{1}{2}} \quad (psf)$$

Here σ_o is the mean normal effective stress and $(K_2)_{max}$ is a factor which depends upon the relative density of the sand. For clay soils the following relationship was developed:

$$G_{Max} = Su\ (K) \quad (psf)$$

Here, Su is the undrained strength, and K is a constant which ranges from 1100 to 4000 with an average of 2200. Ohsaki and Iwasaki (1973) bypass the steps required to ascertain the relative density by using the folowing formulation:

$$G_{Max} = 1200\ (N)^{.8} \quad (t/m^2)$$

They relate the maximum shear modulus directly to the standard penetration test blow count (N), Murphy et al (1978) have developed a graphical relationship for the glacial till used in their study which relates the maximum shear modulus to the mean consolidation stress and maximum past pressure.

The maximum shear modulae of the various layers in the profiles were calculated from these equations using the soil data presented in Chapter 2. The plasticity index was read directly from the plots shown in Chapter 2, as was the undrained shear strength, though the lack of information at depth made it impossible to obtain a measure of the $\frac{c}{p}$ ratio accurately enough to extrapolate the silt data. The blow count data was taken directly from the curves of blow count for 0.15 to 0.45 meter penetration for the site area in question, as shown in Chapter 2. The relative density values were computed from the blow count curves using the Schultze and Menzenback relationship. The void ratios were computed from the water content of the clays and silts, and the relative densities of

the sands. The void ratio data was extrapolated to depth by assuming that the change in void ratio was due only to consolidation of the material under the weight of the overburden, an assumption that was supported by the data collected in Chapter 2. This allowed the void ratio to be computed using the coefficient of consolidation. In cases where the soil had been over consolidated by glaciation, the rebound of the soil was considered. The mean principle effective stress was computed from the void ratio, specific gravity and using an assumed value of the coefficient of lateral pressure which varied from 0.6 for the soft clays to 0.4 for the tills. The overconsolidation ratio was determined at the surface from the plots of undrained shear strength versus depth, and the $\frac{c}{p}$ ratio. At depth the overconsolidation ratio was determined from a knowledge of the glacial history. The engineering properties of the tills were taken from the values presented by Klohn (1965), Radhakrishna and Klym (1974), Clarke (1966) and Murphy et al (1978). The properties of the rocks are based on average values for the rock type anticipated, as presented by Clark (1966).

The values of maximum shear modulus computed using these methods are shown for the three soil profiles in figures 3-2-5, 3-2-6, and 3-2-7. It can be seen that despite the change in soil type between layers, the modulus predicted by each method increases smoothly with depth, there being no major discontinuities, except where the till and rock layers are encountered. In figure 3-2-7, for the Brighouse profile the range of the maximum shear modulus was shown. This range was based on the maximum range anticipated in

those parameters which are used to calculate the modulus. The range, though large is still smaller than the range between the modulus values determined by different methods, which suggests that efforts should be made to make a choice between the analysis methods used rather than concentrating on the possible errors in the data. The plots show that the Ohsaki and Iwasaki method generally predicted the highest modulus, and the Hardin and Black method the lowest, with the Seed and Idriss method lying in between. This is in keeping with the findings of Anderson et al (1978), who compared these methods with values measured in the field. They found that the Hardin and Black method underestimated the field value by a factor of 1.8, that the Seed and Idriss method underestimated the field value by 1.6 and the Ohsaki and Iwasaki method overestimated the field value by a factor of 1.4. The trends seen in the profiles calculated for the Fraser Delta sites are similar to those found by Anderson et al, but the magnitude of the variation is not as great.

In the till layer, the use of the relationship formulated by Murphy et al gave values of shear modulus increasing with depth. For the Brighouse profile, values of shear modulus were also calculated using the Harden and Black formulation for till, and for layers of clay and sand interbedded between till layers. The modulus predicted for the interglacial clay and till was about 80% of that predicted for till by Murphy's method. The modulus of the inter-glacial sand was less than 50% of the value for till predicted by Murphy's method, because of the lack of any cohesion or over-consolidation effect.

For the computer analysis, the Harden and Black mean curves were used in the sediments above the till because they gave values of the modulus in all soil layers. The data available was not sufficient to permit accurate use of the Seed and Idriss formula in deep silt layers. The Ohsaki and Iwasaki method could not be used in silt because it was not designed for that, and could not be used in clay because of lack of data. The modulus predicted by Murphy et al was used in till layers.

The maximum damping ratio is an important input parameter for the dynamic analysis. Seed and Idriss (1970) show plots of damping ratio versus strain for sands and clays from a large number of tests by various researchers. They show the maximum damping ratio in sands to be from 21% to 28%, and that of clay from 26% to 32%. Hardin and Drnevich (1972) developed relationships from experiments on various soil types. They found that for saturated sands:

$$D_{Max} = 28 - 1.5 \ (\log n)$$

For saturated silts:

$$D_{Max} = 26 - 4\sigma_o'^{\frac{1}{2}} + .7f^{\frac{1}{2}} - 1.5 \ (\log n)$$

and for clays:

$$D_{Max} = 31 - (3 + .03f)\sigma_o'^{\frac{1}{2}} + 1.5f^{\frac{1}{2}} - 1.5 \ (\log n)$$

Here σ_o' is the mean effective principal stress in kg/cc, f is the frequency in cycles/second and n is the number of cycles.

A variation within a reasonable range of n and f does not have a large effect on values of maximum damping ratio. These two parameters form part of the equation because the laboratory

samples which were tested to form the relationship were subject to cycles of complete stress reversal at a certain frequency. The stress-strain characteristics could be determined for any particular cycle. For this computer analysis, values for n and f must be selected which are representative of the irregular motion of the significant part of the earthquake. Seed,Idriss and Kiefer (1969) present a relationship which correlates the earthquake magnitude with the distance from the source of energy release and the predominant period. For the nearby earthquakes analyzed in this study a frequency of 3.3 cycles per second was chosen using their relationship. The true value will vary with the earthquake used for the object motion and the soil layer considered. Methods have been developed (Seed, Idriss,Makdisi and Banerjee (1975) whereby an irregular stress-strain history can be represented by a uniform stress series, however because the input to the computer program consists of the average damping over several soil layers experiencing a range of of earthquake motions, this analysis would not be of benefit, so a mean value of 15 was selected.

The maximum damping ratios computed using these relationships are shown for the three profiles in figures 3-2-8, 3-2-9, and 3-2-10. The damping ratio for the till soils was taken from the average of those presented by Murphy et al. Insufficient data was available to attempt to characterize a change in damping ratio with depth in the till. The damping ratio anticipated in layers of sand, clay and silt which might be present as interglacial deposits

between till layers is shown in the Brighouse profile. The interglacial sand and clay would have higher damping ratios than the till, while the interglacial silt would have lower damping. The damping characteristics of the rock were obtained from average values presented by Schnabel, Lysmer and Seed (1972).

Both the shear modulus and damping ratio vary with the strain amplitude. Seed and Idriss (1970) present damping reduction curves for clay and sand, however, they indicate only a range of values with an average for each soil type. Hardin and Drnevich (1972) present a method of calculating the relationship between the maximum shear modulus, and the shear modulus at any given strain level. It has the following formulation:

$$\frac{G}{G_{Max}} = \frac{1}{1 + \gamma_h} \qquad \text{where} \qquad \gamma_h = \frac{\gamma}{\gamma_r} \, 1 + a \exp \frac{(-\gamma b)}{\gamma_r}$$

Here:

γ = strain level

G =the shear modulus at strain level

G_{Max} =the maximum shear modulus

a =a cycle factor which depends on the soil type

b =a soil coefficient

γ_r =the reference strain

The reference strain can be thought of the strain that the soil would experience if it had a constant shear modulus of G_{Max} and was strained to failure. It can be computed from G_{Max} and a Mohr plot of the soil stress state.

The modulus reduction curves were computed by this method for the sands, silts, clays and the till layers in the profiles. The reduction curves for all the silt and clay layers were virtually identical, as were all the curves of the sand layers and of the till layers. The mean of each curve set is plotted in figure 3-2-11 along with the relation for rock obtained from Schnabel et al (1972) and another curve for till from Murphy et al (1978). This additional till curve was obtained by replotting the laboratory data developed by Murphy et al without arbitrarily forcing the curve to go through an end-point that was determined by geophysical methods. This additional curve predicted a greater reduction in modulus at a particular strain level than did the Hardin and Drnevich curves.

Hardin and Drnevich also proposed the following relationship describing the dependence of the damping ratio on the strain level:

$$\frac{D}{D_{Max}} = 1 - \frac{G}{G_{Max}}$$

Here D is the damping ratio at strain level γ, and D_{Max} is the maximum damping ratio. This relation, applied to the curves in figure 3-2-11 yields the relationship for sands, clays and silts and till shown in figure 3-2-12. The damping reduction curve for rock was obtained from Schnabel et al (1972).

For the computer analysis the Hardin and Drnevich damping reduction curves were used for the sands, silts, clays and tills, and the Schnabel et al curves were used for rock. The Seed and

Idriss reduction curves for soil were too general and the Murphy et al curve did not follow the pattern set by the Hardin and Drnevich curves. Anderson (1976) found that the Hardin and Drnevich curves were more representative of sample behaviour than the Seed and Idriss curves. Arango et al (1978) present data which also indicates that the Hardin and Drnevich equations are superior to those of Seed and Idriss.

3-3 Pender Island Earthquake Correlation

Ground surface acceleration records were obtained for the 1976 Pender Island earthquake, from the Pacific Geoscience Centre in Victoria. The object was to compare the surface motions recorded at the three sites at which profiles had been developed, with the surface records obtained by dynamic analysis, using the SHAKE program and the motions recorded on rock for the same earthquake at the Lake Cowichan Satellite Station as the base input motion. The soil properties developed in Section 3-2 were used in the analysis. Variations were made in these properties and profiles to determine the extent to which inaccurate data would effect the analysis results.

The question as to whether scaling of the input earthquake motion (Lake Cowichan record) would be necessary was examined. This scaling could be necessary because of a difference in the distance from the earthquake source to the Lake Cowichan site and the Fraser Delta sites, or a difference in the rock type through which the seismic waves passed. Scaling could also be necessary because the motions recorded at the

surface rock outcrop would be different than those experienced by a buried rock surface, even if both sites were close together. In examining these problems it was necessary to keep in mind the accuracy of our knowledge of the dynamic soil properties at the sites and the potential magnitude of errors that could be induced by an invalid assumption regarding the scaling required.

The epicentral distance of the Lake Cowichan site is 54km, while the epicentre distance of the Fraser Delta sites ranges from 37 km to 52km. Figures presented by Schnabel and Seed (1972) give a relationship between the maximum acceleration, the magnitude of the earthquake, and the distance from the source of energy release. This relationship compares well with other similar relationships, as shown by Trifunac and Brady (1975), who found that for distances greater than 30km the acceleration amplitude varied inversely with the square of the distance to the source. For a small earthquake, such as the Pender Island earthquake with a magnitude in the order of 5 to 5.5, these relationships show that the difference in maximum accelerations for these sites would be small. The earthquake was not scaled on the basis of distance from the source since other factors which could not be accounted for, such as bedrock topography, would have a greater effect on the maximum accelerations.

The bedrock underlying the three Fraser Delta sites consists of relatively low shear wave velocity sandstone, conglomerate, and shale, overlying higher velocity granitic rocks. Since the low velocity rocks are present in thicker

strata at the Fraser Delta sites than at the Lake Cowichan site, it is possible that seismic waves travelling to the delta sites would experience more damping than those travelling to the Lake Cowichan site. Because of the difficulty in assessing the magnitude of these effects no attempt was made to compensate for them by scaling. This effect may compensate to some degree for the difference from the epicentre to the Lake Cowichan and Fraser Delta sites.

The theory of shear wave propagation in a one-dimensional system is described by Schnabel, Lysmer, and Seed (1972). They point out that the horizontal displacements at any layer in the system are caused by two components of the shear wave. One component is due to the incident wave travelling upwards towards the surface and the other is caused by the reflected wave travelling back into the earth. At the free surface, the magnitude of the incident and reflected waves are the same. It is reasonable to assume that the incident waves at the rock outcrop will be of the same amplitude as the incident waves at a nearby buried rock layer, since the incident waves are not effected by the overlying soils. However, while the reflected wave at the rock outcrop is equal to the incident wave, the relected wave amplitude at the buried rock surface will be less than the incident wave amplitude because of the damping qualities of the overlying soil layers. From this it can be seen that the amplitude of the buried base rock motion will be between 50% and 100% of the amplitude of the rock outcrop motion. It would be 50% if the wave propagating up from the buried rock surface and reflected back had been

completely absorbed before it reached the rock surface again. It would be 100% if the wave had not changed in character on its return to the buried rock layer. The actual ratio of amplitudes would depend on the damping in the deposit, the impedence ratio between the deposit and the rock, and the frequency distribution of the wave energy in the rock relative to the resonant frequency of the deposit (Schnabel, Lysmer, Seed, 1972). This means that the difference in the response spectra for a profile which had been computed using the true motion on the buried rock layer and the response spectra for the same profile which had been computed using a nearby measured rock outcrop motion would be greatest at the periods where the largest amplification had taken place between the rock motion and the surface motion.

Lysmer, Seed, and Schnabel (1971) performed a series of analyses on profiles consisting of up to 90 meters of sand and clay over rock, and found that the maximum acceleration in the buried rock layers was between 85% and 92% of the maximum acceleration on nearby rock outcrops, for rock having a shear wave velocity of 1800 m/s, and between 80% and 85% of the maximum acceleration for rocks having a shear wave velocity of 1200 m/s. The three sites in the Fraser Delta were analyzed using a base rock modulus of 16,000 MPa, which corresponds to a shear wave velocity of less than 2400 m/s. Lysmer et al (1971) also found that the response spectra for the surface motions were essentially the same in shape whether computed using the rock outcrop motion or the actual motion on

the buried rock as the object motion.

Because there was little difference in the response spectra, and the difference in the rock outcrop motion and buried motion was dependant on the properties of the overlying soil and not easily scaled, it was decided to perform the analysis using the unscaled records obtained from the Lake Cowichan site rock outcrop, which we are assuming would have similar motion to a rock outcrop in the Fraser Delta, if such an outcrop existed. The results of the analysis could be examined in the light of the known effects that this variation from reality would produce.

Comparison of the computed motions and recorded motions for the three sites was made using acceleration response spectra. This was done because the ground surface accelerations are related to the maximum forces experienced by structures at the site, and because the spectra presents the acceleration that would be experienced by structures of varying fundamental periods. The acceleration response spectra were produced for single degree of freedom structures having 5% of critical damping. This corresponds to the amount of damping that would be present in most buildings when the structure had reached yield, where most of the energy of the earthquake would be absorbed. Response spectra were produced for the layers that marked the division between soils of different types to permit an assessment of the relative effects of each soil type on the ground motion. The response spectrum that was used for comparison with the actual recorded surface spectrum was one which was computed at a 1.5

meter depth below the soil surface. This was done to try to account for the fact that the accelerographs were on rigid concrete floor slabs in buildings, which added a normal load. In the case of the Brighouse recording, the accelerograph was in a basement.

3-4 Seismicity and the Design Earthquake

The Fraser River Delta lies in one of the most seismically active zones in Canada. A network of accelerographs has been set up by the Earth Physics Branch of the Department of Energy, Mines and Resources, to monitor earthquake activity in this area. Through information obtained from these recorders and from others in the United States, an understanding of the magnitude and frequency of the earthquakes in this area, and the causitive mechanism as related to plate tectonics, has emerged.

The records magnify the ground motions to give plots of the earthquake motions in three coordinate directions. By examining the phases of the records produced by the arrival of body and surface waves, it is possible to estimate the distance and asimuth to the epicentre and the depth to the focus. All accelerograph records that show the particular event can be used to locate the epicentre. Inaccuracies in the location can result from inaccurate acceleration records, or a poor knowledge of the time at each of the recording stations. The velocity characteristics of the earth's crust must also be modelled, so the solution cannot be expected to be exact.

The accuracy of location will vary with the size of the earthquake and the location of the recording stations, so that

both scattering and systematic errors are introduced. Earthquakes of small magnitude, or those at a large distance from recording centres may not be detected. A relatively unbiased map of epicentres can be produced by eliminating the low magnitude earthquakes, which are detected only in areas where there are nearby seismographs. Bias due to the locations of the recording stations is a particular problem with historically old earthquakes, which may have occurred at a time when there were very few recording stations. They would be detected only if they were large and near an inhabited area and could not be so accurately located. Figure 3-4-1 from Milne et al (1978) shows distribution of earthquakes greater than magnitude 2 in the Puget Sound -Strait of Georgia area. The earthquakes which are of a magnitude which is subject to regional bias because of the distribution of accelerographs are marked with an"X", while others are graded by magnitude.

On a regional scale, the boundaries between the major lithosperic plates (Figure 3-4-2) correspond to areas of high seismic activity. Milne et al (1978) have described this relationship. The Queen Charlotte-Fairweather fault, the northern equivalent of the San Andreas fault, marks a division between the Pacific and America plates. These plates have a relative motion of about 5 cm/year. South of 51 degrees latitude, the ridge fracture zone between the Juan de Fuca and Explorer plates marks the area of interaction between these two small plates and the Pacific plate. In the continental area the Explorer and Juan de Fuca plates are subducting under

the America plate at a rate of 2½ cm/year. Mile et al (1978) found that the seismic records indicate that the interaction between the two oceanic plates and the America plate is in the form of a strike slip fault rather than the thrust fault normally expected in areas of subduction. This is due to the oblique convergence of the plates. Rogers and Hasegawa (1978) point out that the majority of larger earthquakes in this continental region occur at depth, within the continental crust. The tectonic forces causing these earthquakes probably result from the motion of the upper plates in the subduction zone.

An assessment of the maximum probable earthquake motion to occur in the Fraser Delta can be made on the basis of several criteria, which must consider both the magnitude of the earthquake, and its horizontal distance and depth from the site, since the earthquake characteristics change as the waves propogate through the lithosphere. These criteria are the strain release versus time relations, magnitude versus time relations and the anticipated mechanism.

Strain release is a measure of the total energy released by an earthquake, and is related to its magnitude. By plotting strain release against time and assuming a constant rate of potential strain accumulation, estimates can be made of the maximum expected earthquake on a particular fault system. In figure 3-4-3 Milne et al (1978) show the possibility of a significant earthquake, greater than magnitude 7, in the Georgia Strait- Puget Sound area.

Various methods of examination of accelerograph records are used to determine the magnitude of an earthquake. These

methods may give results which vary by one unit. It is possible to find empirical relationships between earthquake magnitude and return period for a particular area. These relationships are difficult to determine accurately because of the bias in magnitude estimates. At low magnitudes, events may go undetected, and at high magnitudes events may be quite rare. Milne et al (1978) have analyzed the data for the Georgia Strait - Puget Sound area and have formed a relationship which can be represented as shown in figure 3-4-4. This relation predicts that a one-hundred-year earthquake in the Fraser Delta area would have a magnitude of about 7.4

The maximum magnitude of an event is limited by the mechanism and by the extent of the faulting. Milne et al (1978) estimate that the maximum magnitude earthquake in the Puget Sound - Georgia Strait area would be greater than 8 for thrust faulting, which is the most common fault type found in subduction zones. However, the earthquakes in this area appear to exhibit strike slip or normal faulting mechanisms so the maximum magnitude is likely to be less than 8.

The distance from the Fraser Delta sites to the source of energy release is an important factor in assessing the earthquake motion since it effects the predominant period and the accelerations experienced. Large magnitude events, due to the tectonic forces developed in the subduction process, are likely to occur at depths of up to 60km within the continental lithosphere (personal communication G. Rogers). These events would probably not cause surface rupture, so they would not necessarily be

associated with the presence of surface faults. Such earthquakes could reasonably be expected to have a source of energy release 20 or 30km within the earth's crust.

An earthquake with a hypocentre closer to the earth surface has a greater likelihood of being related to an existing fault with surface expression. Rogers and Hasegawa (1978) point out that the magnitude 7.2 British Columbia Earthquake of 1946 may have resulted from rupture along the projection of an existing fault. Some geological interpretations have inferred that there is a fault existing in the Strait of Georgia. Muller (1977) shows this interpretation, while others, (Jackson and Seraphin (1976)), do not indicate the presence of a fault. The existance or otherwise of a fault in the Strait of Georgia, where surface rock exposures cannot be mapped, is difficult to verify and would be open to the interpretation of individual geologists, based on an understanding of the regional geology and seismic patterns. Because the presence of a fault is not generally accepted, the assumption is made in this study that if such a fault exists in the Strait of Georgia, and if it could undergo movements due to an earthquake, that the source of energy released would be no closer to the Fraser Delta sites than the 20 or 30km expected from the deep earthquake.

For the purposes of this work earthquakes of several magnitudes were studied. On the basis of the information just outlined, an earthquake of magnitude 7.4 at a distance of 30km was selected as the maximum probably earthquake. In order to assess the effect of earthquake intensity on the soils, earthquake

of magnitude 8.0, possible if there was faulting in a thrust mechanism, and of magnitude 6.5 were also selected for analysis.

Several design earthquakes were used in an attempt to observe the effects of earthquakes in general, since it is unlikely that the actual earthquake occurring at the site would resemble completely any particular design earthquake. Ideally, the design earthquakes should have the same characteristics as the potential earthquake. They should be caused by the same mechanism, have the same magnitude, and have the same distance to the hypocentre through similar geologic formations. Because of the form of the analysis used, the input must be an earthquake recorded on rock. The Western Washington earthquake of 1949 and the Puget Sound Earthquake would be the ideal design earthquakes if recordings had been obtained on rock, since they satisfy the above criteria. It would be possible to perform an analysis similar to that now being undertaken, to obtain a base rock motion at the recording sites of these two earthquakes using the surface record, if the soils deposits at the site were well known. This was not done because the data were not readily available and such an analysis would introduce additional errors into the Fraser Delta analysis.

Recordings made on rock outcrops of earthquakes of similar magnitude and distance from source to site were used in the computer analysis. This eliminated the need to scale the period, which as can be seen from Figure 3-4-5 is not a well defined or accurate procedure. The earthquakes chosen were the N21E component of the magnitude 7.6 Kern County earthquake of 1952

as recorded 56km from the source at Taft, the S69E component of magnitude 6.6 San Fernando earthquake as recorded 26km from the source at Lake Hughes Station #4, and the N21E component of the magnitude 6.6 San Fernando earthquake as recorded 21km from the source at Lake Hughes station #12. The Kern County earthquake is of a larger magnitude but with a source at greater distance than the principle design earthquake for the Fraser Delta sites, while the two San Fernando earthquakes are of a smaller magnitude but a shorter distance. Figure 3-4-5 shows that it is likely that all three recordings would have a predominant period similar to the anticipated earthquake. The San Fernando earthquake exhibits predominately lateral slip motion, which is the type of motion most likely to occur in the Fraser Delta area.

The analysis used in the SHAKE program is based on the assumption that the earthquake record input as the excitation motion repeats itself to produce a continuous record. The records used in the analysis were the first 16 seconds of recorded motions of the selected earthquakes. This time-period contains the major part of the strong motions.

The three design earthquakes were scaled according to the relation developed by Schnabel and Seed (1972) and reproduced in figure 3-4-6. This relationship was developed from earthquakes which occurred in California, but Nuttli (1973) stated that"there is no evidence for a marked contrast in attenuation properties of the earth as observed in California and in Western North America". At a distance of 30km from the source of energy release this relation gives the maximum acceleration due to magnitude

8.0, 7.4, and 6.5 earthquakes as 0.33g, 0.25g, and 0.16g respectively. The earthquake recordings were not scaled in any other way, to facilitate comparison of the results on the basis of only one changing parameter.

CHAPTER 4

RESULTS

4-1 Pender Island Earthquake Correlation

The results of the dynamic analysis using the profiles developed in Section 3 and the Lake Cowichan earthquake as object motion, are presented in the form of acceleration response spectra. They are compared to the spectra of the actual surface motion as recorded at the three sites. The degree of correspondence between the recorded and computed curves is examined and the significance of the curve shape as a function of varying soil properties is investigated.

The acceleration response spectra for a single-degree-of freedom structure with 5% of critical damping produced when the Lake Cowichan record of the Pender Island Earthquake was used as the object motion on the profiles developed in Section 3, are shown with the spectre of the actual surface record for the same earthquake in figure 4-4-1, 4-1-2 and 4-4-3. The spectra of the ground motions recorded on two mutually perpendicular component axes are shown for both the recorded and the computed motions. It will be noticed that the abscissa axis has been plotted using a variable scale, to show the important detail at low periods while allowing a full range of periods to be presented. The curves were not smoothed to develop a single curve to represent the characteristics of each of the recorded and computed motions. This was done to show the variability between the spectra of two components of the same earthquake, and because producing a smooth curve from such a data base

could be misleading.

Figure 4-1-1, shows the spectra of the recorded and computed motions at the Annacis Island site. The two curve sets compare very favorably. There is a major peak in the spectra at a period of 0.25 seconds to a magnitude of about 0.14g and a minor peak at a period of 0.8 seconds to magnitude of 0.08g. The spectra of the computed motion shows a peak in the high period range, where none was observed in the spectra of the recorded motion. This is probably the result of the mechanics of the analysis and will be discussed later.

The spectra developed from the computed and recorded motions at the Brighouse site are shown in figure 4-1-2. A major peak to an acceleration of 0.11g is present at a period of 0.2 seconds. The curves are similar in shape, though the spectra developed from the computed motions do exhibit minor peaks in the high period range, which are not obvious in the spectra of the recorded motions.

The spectra developed for the Roberts Bank motion are shown in figure 4-1-2. The general shape of the computed and recorded spectra is the same. The major excitation is at a period of 0.2 seconds with smaller peaks in the period range of 0.5 seconds to 0.8 seconds, but the magnitude of the accelerations shown in the spectra of the computed motions is larger. As at the other two sites, the spectra developed from the computed motions are less smooth than those developed from the recorded motions and show larger peaks in the high period range.

Generally, the spectra of the recorded and computed motions compared well. The major peaks occurred at the same periods and with the exception of the Roberts Bank site, showed the same acceleration. The chief difference between the spectra was that those developed from the computed motion were less smooth and show small acceleration peaks at high periods where they were less evident in the spectra developed from the recorded motions.

The better agreement between spectra at the Brighouse and Annacis Island sites than at the Roberts Bank site suggests that the method of analysis used is appropriate but the parameters used at Roberts Bank were less representative of the actual situation than those used at the other sites. It is unlikely that the dynamic soil profile developed was less accurate at the Roberts Bank site because reasonable soil data was available in that area. A more probable explanation is that the object motion used for the analysis at the Roberts Bank site was not as representative of the true object motion as it was at the other two sites. This could be due to the effect of buried bedrock topography on the earthquake waves. It may also be due to the positions of the site relative to the earthquake source and the underlying geology. The object motion used was the surface bedrock motion recorded at Lake Cowichan. Seismic waves travelling from the source at Pender Island to Lake Cowichan would travel primarily through igneous and metamorphic rock which have a high shear wave velocity. To the east of Pender Island the surface rocks are sedementary, with lower shear wave velocity and higher damping than the granitic rocks. Because the Roberts Bank site is closer to the epicentre than the Annacis Island

site, which has a similar soil profile, seismic waves reaching the Roberts Bank site may have travelled more through the low shear wave velocity upper layer sedementary rocks, and may therefore have been more subject to damping than those waves reaching the Annacis Island site. This could account for the recorded motion being less severe than the computed motion at the Roberts Bank site.

The analysis involves the division of the soil profile into discreet layers which can be represented by specific soil properties. The number of layers that may be used is limited by the cost of additional computing time. Obviously such a model using layers of soil with discreet divisions where dynamic properties change is not completely accurate. Each of these small sublayers used in the analysis will have a predominant period which can be estimated in the elastic range by the equation:

$$T_n = \frac{4H}{V_s\ (2n-1)} \qquad \text{eq'n 4-1-1}$$

Here T_n is the natural period, H is the layer thickness, V_s is the shear wave velocity of that material, and n is the mode. The result of this is that every sublayer will be excited at slightly different periods of motion. Although these excitations will be modified by the effects of the other surrounding layers, the response spectrum will mirror these small excitations as small perturbations. The spectra of the actual recorded motions are smooth because the properties of any soil type will change gradually with depth, so the spectra will not be influenced by the resonance of artificial layers.

Where major layers of soil with greatly different dynamic properties exist in the same profile, major peaks in the response spectra can be observed. Each peak reflects the characteristics of a particular soil group. These acceleration peaks are at periods which correspond roughly to the natural period range calculated for the major soil group using equation 4-1-1, since at the low level of excitation of the Pender Island earthquake, the soils are near their elastic response range. Changing the properties of a particular soil group (Rock, till, or soft sediment) will have a primary effect on the peak in the response spectra caused by the resonance of that particular soil group and secondary effect on the general shape of the spectra. The interaction of the various soil groups in the development of the earthquake motions from that causing the excitation at the base of a soil deposit to the resulting surface motion can be seen in figure 4-1-4. This figure shows plots of the response spectra of the motion at various levels in the soil deposit for the Annacis Island profile, with the Pender Island earthquake recorded at Lake Cowichan as object motion. The object motion is shown to have a predominant period of 0.2 seconds with very little excitation at high periods. The motion at the top of the till layer shows one peak in acceleration at the same period as seen in the object motion. It also shows another at a period of 0.85 seconds which is close to the natural period of 0.7 seconds calculated for the till layers using equation 4-1-1. The response spectrum of the surface motion shows these two peaks in approximately the same position, along with a new area of increased excitation at larger periods

caused by the soft sediments overlying the glacial till.

The characteristics of any response spectrum will be modified slightly by minor changes in the dynamic properties of any soil layer and by changes in the configuration of the soil profile. In any real situation, it is not possible to select particular values for the dynamic properties of the soil with complete confidence, nor is it always possible to have complete confidence in the thickness of the various soil layers which make up the profile. Field investigation and laboratory analysis yield a range of values that may represent the field situation.

For the three sites examined, changing the input parameters within their probable range did not greatly effect the general shape of the response spectra. The peaks in acceleration occurred at the same periods, but the magnitude of the peak could change by up to 50%.

The most important parameter in determing the shape of the response spectra is the depth to bedrock, followed by the thickness of the overlying till layer. This is what one would expect since the shear modulus and damping differ by orders of magnitude between the rock, glacial till and soft sediments. By comparison, the difference in dynamic properties between sand, silt, and clay, and the range in properties likely for any given layer are small.

Because of the interaction between layers in the profile, seen mathematically as an interrelationship between the strain dependant damping ratio and shear modulus, it is not possible to make meaningful comment on the specific effects of changes in

the parameters. In general, however, changing the damping and modulus strain relationships for soil layers had, as one would expect, a primary effect in the period range of the spectra where those layers produced excitation and a lesser effect at other periods. Increasing the modulus to stiffen a particular layer produced larger accelerations at given periods, as would reducing the damping of the layer.

4-2 Analysis Using the Design Earthquake

The close correlation between the response spectra of the observed motion caused by the Pender Island Earthquake, and the response spectra of the computed motion using the Lake Cowichan record as object motion at the Brighouse and Annacis Island sites confirms the suitability of the soil profiles and the analysis method. Using the same soil profiles, and the object motions for larger earthquakes as described in section 3-4, the same dynamic analysis was performed. The surface response at each of the two sites was computed using the SHAKE program with each of the three chosen object motions scaled to give three different accelerations at bedrock. This produced nine response spectra at each site. These response spectra were compared with each other and with general relationships developed by others, to determine the significance of the results to this area.

The response spectra of the three design earthquakes used as the object motions, scaled to 0.25g maximum acceleration, are shown in figure 4-2-1. Figure 4-2-2 shows the response

spectra developed from the three sets of surface motion at the Annacis Island site, that were computed from these three input earthquakes scaled to a maximum acceleration of 0.16g. These three curves exhibit the same general characteristics, with a peak in the surface acceleration for periods of about one second. The response spectra developed from surface motions due to an object motion scaled to 0.25g and 0.33g are shown in figures 4-2-3 and 4-2-4 respectively. The same series of curves for the Brighouse site are presented in figures 4-2-5, 4-2-6, 4-2-7. The spectra produced at a given site using the three different object motions, scaled to the same value of maximum acceleration, are similar in form and in magnitude in every case.

For ease in comparison, the three response spectra curves shown on each of the aforementioned figures have been fitted with a smooth curve so that the spectra developed at three different acceleration levels may be summarized for each site on one page. The response spectra of the surface motion caused by a base layer excitation by earthquakes of three different magnitudes are shown for the Brighouse site in figure 4-2-8, and for the Annacis Island site in figure 4-2-9. The most striking characteristic of these curves is that changing the maximum acceleration on bedrock by over 100% produces very little difference in the spectra of the surface motions. For these three relatively large magnitude earthquakes, increasing the acceleration of the object motion results in a very small increase in the acceleration at the ground surface. When considering

the potential damage to buildings it is important to remember that the accelerations experienced are only one of the factors involved. The duration of these strong accelerations is also important, since the capacity of a structure to absorb the energy of the earthquake is finite. Larger magnitude earthquakes would be of longer duration. The predominant period of the surface motion, as shown by the peak in the surface acceleration response spectra, is also important because buildings which have a predominant period similar to that of the earthquake will experience much larger accelerations than those which do not. The period of peak acceleration for the three design earthquakes has changed dramatically from the predominant periods for the rock motion and the low magnitude Pender Island earthquake surface motion. However, differences in the predominant period of the surface acceleration caused by a single object motion scaled to the three different large accelerations cannot be significantly observed with the database used.

The till layers have a shear modulus which is substantially greater than that of the overlying soft sediments, but is still significantly less than that of the underlying bedrock. If an analysis which applied an object motion to the glacial till surface would yield similar results to an analysis which applied the same motion to the bedrock surface, modelling the site for dynamic analysis would be simplified, because data on till properties and the depth to bedrock would not be required. Figure 4-2-10 and 4-2-11 show the response spectra for the three design earthquakes scaled to .25g and applied as object motions

to the top of the till layer at the Brighouse and Annacis Island sites. Comparison with figures 4-2-6 and 4-2-3, which show the spectra for the same analysis performed with the object motion applied to bedrock, demonstrates that the thick till layer has a significant effect on the shape of the spectra and the magnitude of the acceleration. If the results of an analysis are to be meaningful, the object motion must be applied to the surface of the bedrock and the dynamic effects of the till accounted for in the analysis.

When comparing the spectra for the two sites it can be seen that at the Annacis Island site both the maximum surface acceleration and the acceleration peak on the spectra are larger than at the Brighouse site. This may be because the Annacis Island profile has less thickness of soft sediments above the bedrock, so the damping is less. The period at which the peak acceleration occurs is larger for the Annacis Island site than for the Brighouse site. In terms of physical results, this means that for the design earthquakes used, structures with periods of about 0.8 seconds would be most susceptible to large motions and the resulting damage at the Brighouse site, and structures with periods of about 1.0 seconds would be most susceptible at the Annacis Island site. Generally, ground accelerations and the acceleration of buildings, as represented by the response spectra, at the Brighouse site were less than the accelerations at the Annacis Island site.

Comparison of the spectra developed from the object motion and those developed from the computed surface motions shows the

shift in predominant period of the motion from about 0.25 seconds for the earthquakes recorded on rock and used as object motion, to 0.8 seconds or 1.0 seconds for the earthquake motions computed at the surface of the deep soil deposits. This general observation of an increase in the predominant period of the earthquake motion recorded at the surface of deep soil deposits over that recorded on rock is in accordance with the trends observed by others, (Seed, Ugas, Lysmer 1976). Figure 4-2-12 is a plot of the mean response spectra of the object motions scaled to 0.25g, with a plot of the resulting surface motions at the Annacis Island site. The relationship between the curves is typical of what was found at both sites using the three large magnitude earthquakes. These reponse spectra can be thought of as plots of the acceleration that a single degree of freedom structure with 5% of critical damping would experience, as its period was changed. Figure 4-2-12 shows that the relation between the peak in acceleration and the building period is more important than the ground acceleration in determining the behaviour of the structure during an earthquake.

Using the approximation that the period of a structure is equal to 0.1 times the number of stories, the Figure 4-2-12 shows that a building of 2 or 3 stories with a predominant period of about 0.25 sec. would experience very large accelerations if built on bedrock, while an identical building in the Fraser Delta would experience much smaller accelerations. A 10 storey building, with a period in the order of 1.0 sec. would

experience greater accelerations in the delta area than it would if constructed on bedrock. These observations apply for the large magnitude earthquakes analyzed. The analysis of the Pender Island Earthquake indicated that the maximum building acceleration due to smaller magnitude earthquakes occurred at small periods whether the structure was on rock or a deep soil deposit.

The relation between the maximum acceleration recorded on rock and the maximum acceleration recorded at the ground surface, is shown in figure 4-2-13. The data developed in this analysis are shown with the average curves produced from recorded data by Seed, Murarka, Lysmer and Idriss (1976). The general shape of the curve developed from the data produced in this study is similar to the curve for other deep soil deposits developed by Seed et al (1976). Low magnitude earthquakes produce larger accelerations on the surface of deep soil deposits than they do on rock, while larger magnitude earthquakes produce smaller accelerations on the surface of deep soil deposits than they do on rock. Low magnitude earthquakes excite the soil deposits and cause them to strain only slightly so the soils remain close to their elastic stress strain range, and damping is small even though the soil is being displaced by the earthquake. Large magnitude earthquakes cause larger movement of the soil particles, which strain greatly and follow their hysteritic stress strain path to produce large amounts of damping, which reduce the acceleration of the soil.

The correlation between the data developed in this analysis and the average curve shown in figure 4-2-13 is good. The curve shape is similar, though the curve developed for the Fraser Delta soil deposits predicts smaller surface accelerations for the same rock acceleration than do the average curves of Seed et al (1976). The data from this analysis should not be expected to fall close to the Seed et al (1976) curve because their curve shows the average results from many different sites, none of which will be identical to the sites analyzed in this study. The curve developed from the data in this study indicates that as the magnitude of the earthquake increases, the surface acceleration of a deep soil deposit becomes an increasingly smaller percentage of the rock acceleration. This is in keeping with the findings of Trifunic and Brady (1975), who noted that the maximum accelerations were reached by earthquakes of magnitude 6.5 to 7.0, which for the area and configuration that we are dealing with, corresponds to a maximum acceleration of about 0.2g. Larger magnitude earthquakes do not produce a noticeable increase in maximum acceleration, though the duration will be larger. The curves from Seed et al (1976) exhibit this trend, but not as markedly as the curve for the data developed in this study. This may be in part because the Seed et al curves have been extrapolated beyond the 0.3g acceleration.

The specific results of this analysis can be compared with the recommendations of the National Building Code. The National Building Code recommends that design in the Fraser Delta area

incorporate the effects of acceleration due to an earthquake of 0.08g on firm ground and 0.12g on soft sediments. The results of this work are somewhat different. Based on the study of the seismicity of this area, a design earthquake of magnitude 7.4 is expected, which could result in an acceleration of 0.25g on rock. The dynamic analysis has predicted that the maximum acceleration on the surface of the deep soil deposits due to such an earthquake would be in the order of 0.16g. The maximum accelerations predicted by this analysis are more severe than those predicted by the National Building Code, though Byrne (1977) has pointed out that the ductility of most buildings is such that if designed according to the National Building Code criteria, they could actually resist greater accelerations than the code would predict. Design should also incorporate the effects of the shift of predominant period of the earthquake that is observed where large magnitude earthquakes occur in areas of deep soil deposits. The shift in predominant period results in buildings on deep soil deposits experiencing greatly different accelerations from buildings on bedrock, quite apart from what the ground accelerations might be.

CHAPTER 5

COMMENT ON THE LIQUEFACTION POTENTIAL OF THE FRASER DELTA

A detailed description of the mechanics of liquefaction and a study of the factors involved and their relation to the sites being investigated is beyond the scope of this work. Empirical methods of estimating liquefaction potential have been developed through field investigation of many sites. These methods were applied to the Fraser Delta sites using the soils data presented in Chapter 2 to provide a simple measure of the liquefaction potential at these sites. Refinements on the results presented here could be made using the more complicated analytical procedures that are in existence.

Areas of saturated soil subjected to cyclic shear stresses such as those caused by an earthquake, may experience increased pore pressures. If these pore pressures increase until they are equal to the overburden pressure, the effective stress in the soil will become zero. Soil in this state is said to have liquefied, since it cannot resist shear stresses and its behavior resembles that of a dense fluid.

A liquefied soil can pose a threat to man in several ways. Liquefied soil cannot resist shear stresses, so horizontal forces applied to the soil cannot be resisted, and large deflections result. The other major problem is that liquefied soil behaves like a fluid, so structures in or on the soil will change elevation until their buoyant force is equal to the weight of the displaced fluid. Buildings could sink into the soil and

buried structures such as storage tanks or sewers could rise to the surface.

The factors influencing the earthquake induced liquefaction potential of a site are related both to the characteristics of the soil and the characteristics of the earthquake motion. These factors have been investigated in the laboratory under well known conditions, and in the field where generally the liquefaction potential has been correlated to Standard Penetration Test data. The data developed from the laboratory analysis is extensive enough that the process of liquefaction can be modelled analytically (Finn, Byrne and Martin 1976). However, there may be difficulty in applying the results of these analyses to field situations because the correlation between the laboratory and field soil properties must be done using Standard Penetration Test results if it is to be done on a wide basis using existing data. The problems involved in obtaining a representative correlation between the results of the Standard Penetration test and other soil properties have been outlined in Chapter 2.

The field data was developed using the Standard Penetration Test values directly, so the problem of choosing a suitable correlation is eliminated. However, the results of these empirical relations are not specific since the soil properties have been considered through a single parameter only. These empirical relations do provide a simple method of estimating the liquefaction potential of a site.

Oshaki (1970) proposed the criteria that if the blow count at some depth from the standard penetration tests is

equal to two times the depth in meters, liquefaction will not occur. Kishida (1969) proposed a relationship also based on the blow count of the Standard Penetration Test. These two methods consider the properties of the soil but not the properties of the earthquake. Christian and Swiger (1975) attempt to consider the effects of the earthquake by relating the stress ratio to the relative density determined from the Gibbs and Holtz criteria at field sites. For a particular site, this relation can be expressed as a relationship between the blow count and depth as shown in appendix 3. Seed, Murarki, Lysmer, and Idriss (1976) have developed a method which relates the stress ratio to a normalized blow count. This can also be expressed as a relation between blow count and depth, as shown in appendix 3.

These four relations which separate soils that have been known to liquefy from those that have not, are shown in figure 5-1 for a magnitude 7.4 earthquake at 30 km. These relations define a band of blow count values where liquefaction may occur. The Seed et al relationship, which is more finely developed than the others, occupies a mean position within the group of curves. Curves obtained using the Seed et al relationship with the three design earthquakes under consideration in this study are shown in figure 5-2 . The accelerations used in the analysis are 0.1g for the magnitude 6.5 earthquake, 0.16g as an upper limit for the magnitude 7.4 earthquake, and 0.18g for earthquakes of magnitude greater than 8, as shown in Figure 4-2-13. These curves are shown superimposed on the curves

presenting the relations between blow count and depth for various areas in the Fraser Delta. An examination of this figure indicates that when sand soils exist above the 6 meter depth, liquefaction is likely to occur in most areas of the delta when subjected to a magnitude 7.9 earthquake at 30km, while below the 6 meter depth, most sand areas are unlikely to liquefy when subjected to the same earthquake. Under the influence of a larger earthquake, of magnitude greater than 8, liquefaction is likely at depths less than 9 meters, while for a magnitude 6.5 earthquake, liquefaction is unlikely at any depth. Examination of these figures also reveals that there are profiles that do not conform to this generalization, and more importantly that the application of different criteria give different results for the same site.

These empirical methods give a general idea of the liquefaction potention of the Fraser Delta. For more specific results at a particular site, more rigorous analysis is needed. To make this analysis useful, close correlation is needed between field and laboratory conditions.

CHAPTER 6

CONCLUSIONS AND SUGGESTIONS FOR FUTURE RESEARCH

6-1 Conclusions

1) The correlation developed between the blow count recorded 0 to 12 inches penetration and that recorded for 6 to 18 inches penetration in the Standard Penetration Test gives meaningful results, and allows data recorded in both manners to be used together.

2) The relationship between relative density and the blow count of the Standard Penetration Test developed by Schultze and Menzenbach best typifies the behavior of the sands found in the Fraser Delta.

3) The correlation between the friction angle of sands and the blow count of the Standard Penetration Test developed by de Mello gives reasonable results in the Fraser Delta soils.

4) The dynamic analysis used in the SHAKE computer program gives effective representation of the surface motions resulting from an object motion acting at the base of a soil profile, the dynamic properties of which have been determined from more readily available soil information.

5) In the dynamic analysis, the most critical parameters of the soil profile are the depth to bedrock and the thickness of the glacial till existing above the bedrock. The difference in dynamic properties between clay, silt and sand layers is not as significant.

6) A suitable design earthquake for dynamic analysis in the Fraser Delta is one of magnitude of 7.4 at a distance of 30km, which produces a bedrock acceleration of about 0.25g. However, the possibility of larger earthquakes of magnitude greater than 8 should not be ruled out.

7) Use of the dynamic analysis with design earthquakes of magnitudes 6.5, 7.4 and 8.0 at two sites in the delta yielded surface motions with a predominant period of 0.8 to 1.0 seconds, and a maximum ground acceleration of about 0.16g. For the large magnitude earthquakes used, an increase in the magnitude of the object motion did not greatly affect the predominant period or the maximum acceleration at the ground surface. The maximum ground acceleration at these magnitudes was much less than the bedrock acceleration. The predominant period of the surface motion under the large magnitude earthquakes had increased greatly from the predominant period of both the bedrock motion under large magnitude earthquakes, and the surface motion under small magnitude earthquakes.

8) The dynamic effects of the till layer are important and must be modelled with the other soil layers.

9) The liquefaction potential estimated from empiracal relationships suggests that for an earthquake of magnitude 7.4 liquefaction is likely in the upper 6 meters of sand sediments, but less likely below the 6 meter depth. Under a severe earthquake of magnitude greater than 8, liquefaction is unlikely to occur in sands below the 9 meter depth.

6-2 Suggestions for Further Research

1) For laboratory data to be applied to field situations a reliable method is needed to determine the field relative density. Research which develops accurate field technique for determining the relative density and relating it to the Standard Penetration Tests would be valuable.

2) The liquefaction potential of the Fraser Delta could be investigated using rigorous analytical methods as well as the empirical methods used in this study.

3) The Fraser Delta contains a large proportion of silt soils. Because of the problems involved in sampling and testing these soils where permeability is in a mid range between that of clay and sand, little field or laboratory investigation of dynamic properties has been done. An investigation into the dynamic properties of silt, and a method of defining its properties by simple field tests would be valuable.

4) The Western Washington Earthquake of 1949 and the Puget Sound Earthquake of 1965 are large-magnitude earthquakes which would probably resemble the type of earthquakes that would effect the Fraser Delta area. An analysis similar to the one performed in this study could be undertaken to produce the bedrock motion of these earthquakes from the motion recorded at ground surface. These bedrock motions could then be used as the object motions for analysis in the Fraser Delta area.

Suggestions for Further Research cont'd

5) The analysis performed in this study has ignored the effects that a building would have on the underlying soils. To get a better idea of the effect of the earthquake on a structure, soil structure interaction should be considered.

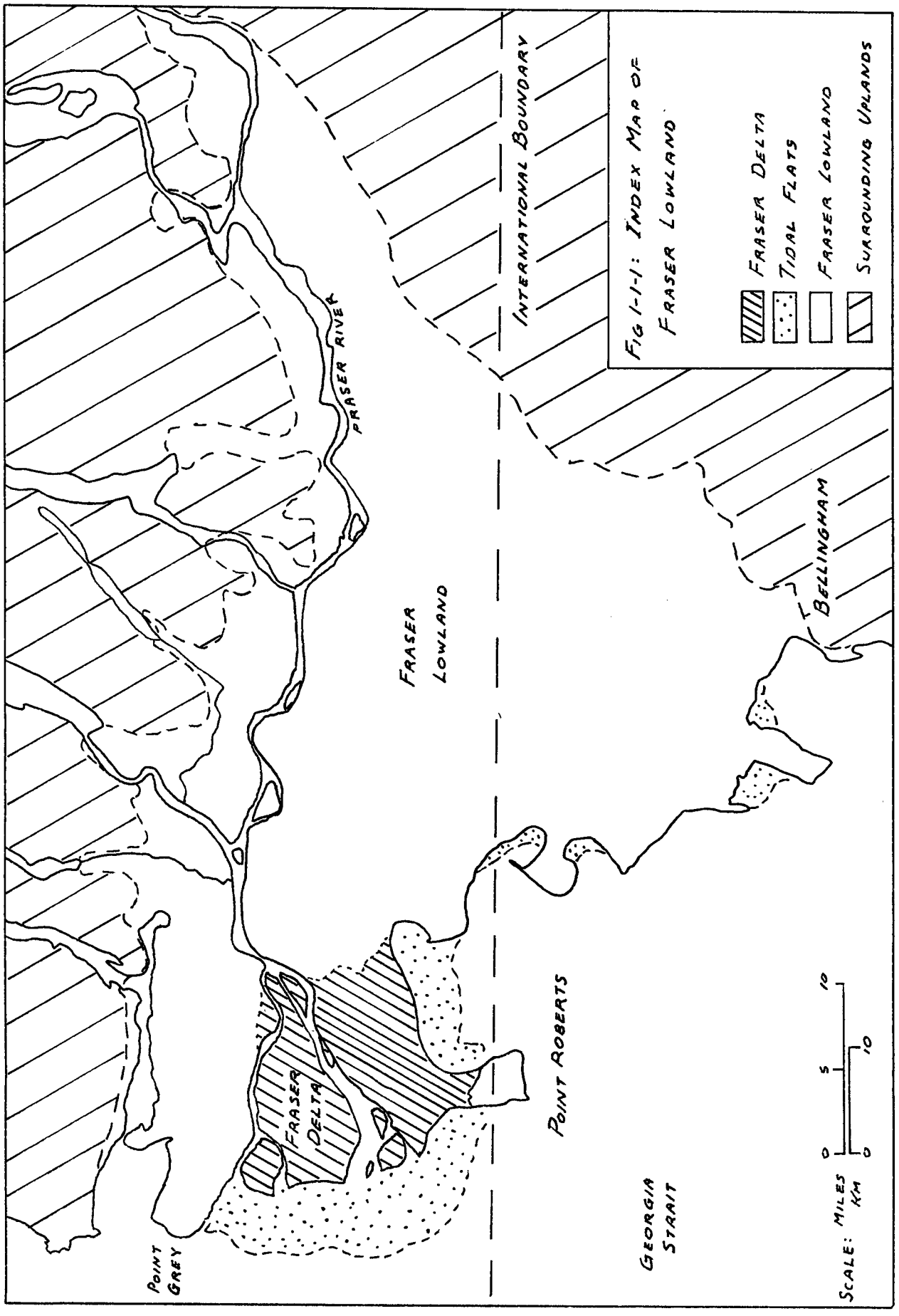
FIG 1-1-1: INDEX MAP OF FRASER LOWLAND
FRASER DELTA
TIDAL FLATS
FRASER LOWLAND
SURROUNDING UPLANDS
INTERNATIONAL BOUNDARY
FRASER RIVER
FRASER LOWLAND
BELLINGHAM
POINT ROBERTS
GEORGIA STRAIT
POINT GREY
FRASER DELTA
SCALE: MILES KM
0 5 10
0 10

FIG. 1-1-2 : PHYSIOGRAPHIC REGIONS

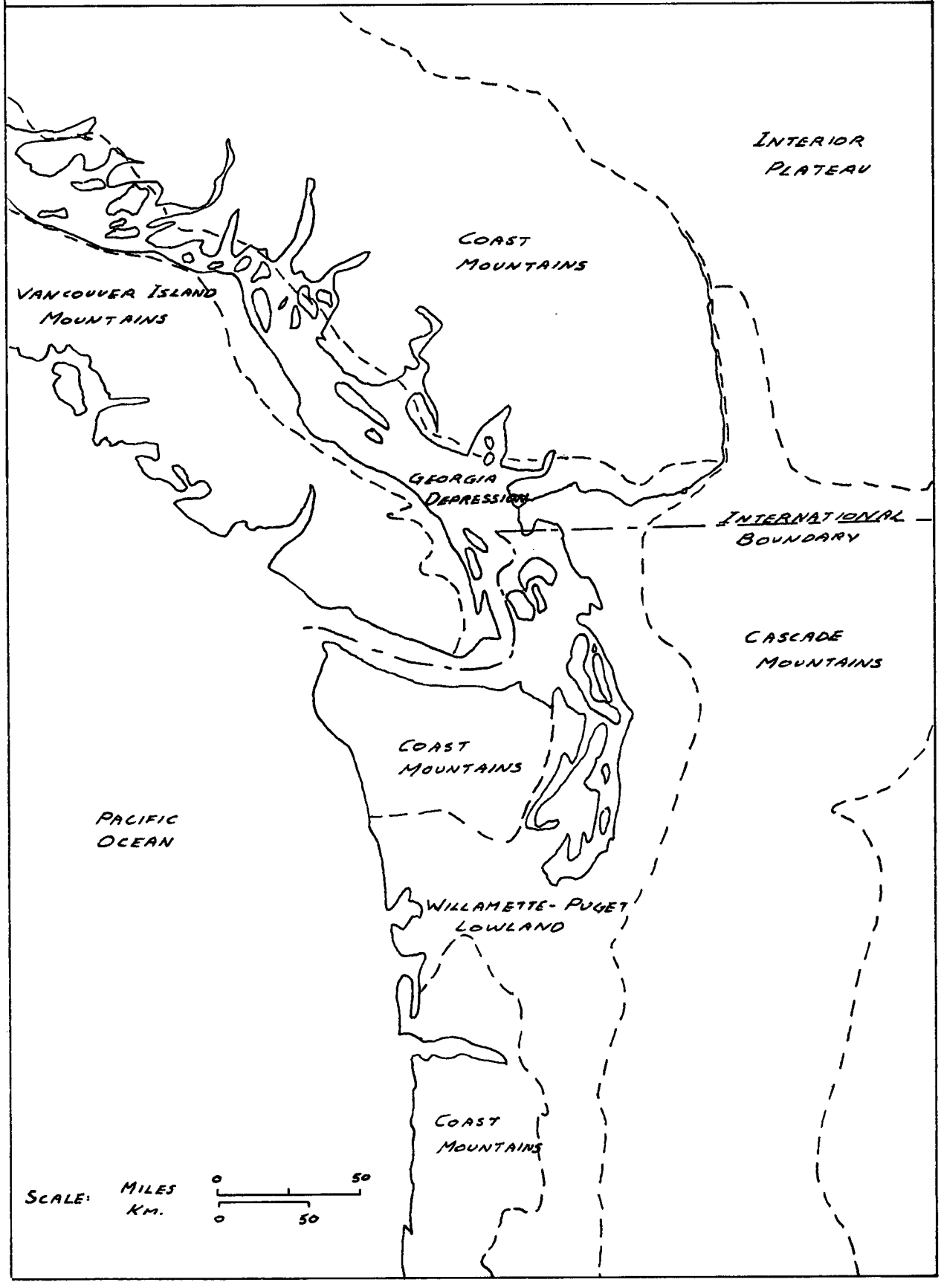

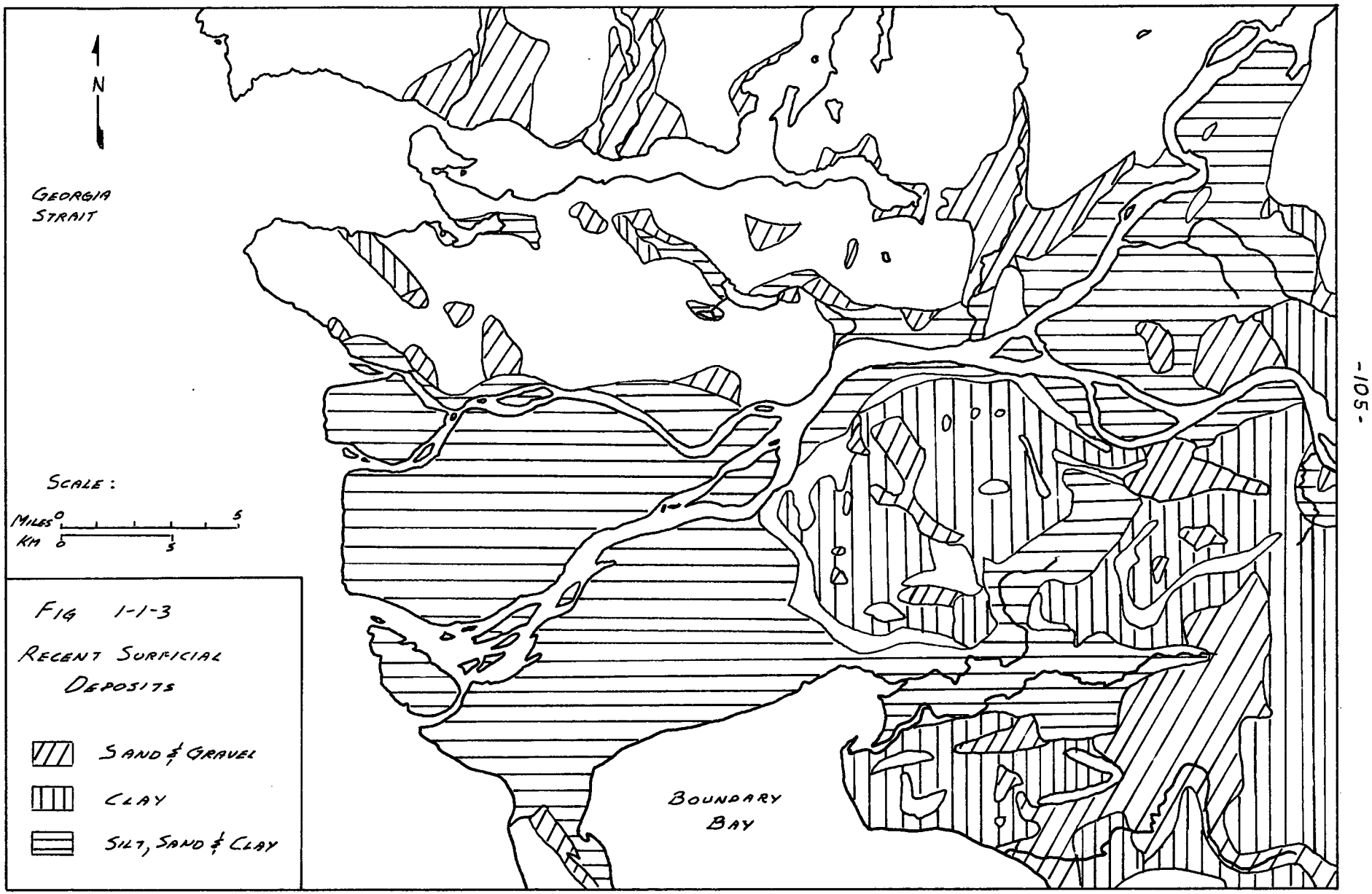
N
GEORGIA STRAIT
SCALE :
MILES 0 5
KM 0 5
FIG 1-1-3
RECENT SURFICIAL DEPOSITS
SAND & GRAVEL
CLAY
SILT, SAND & CLAY
BOUNDARY BAY

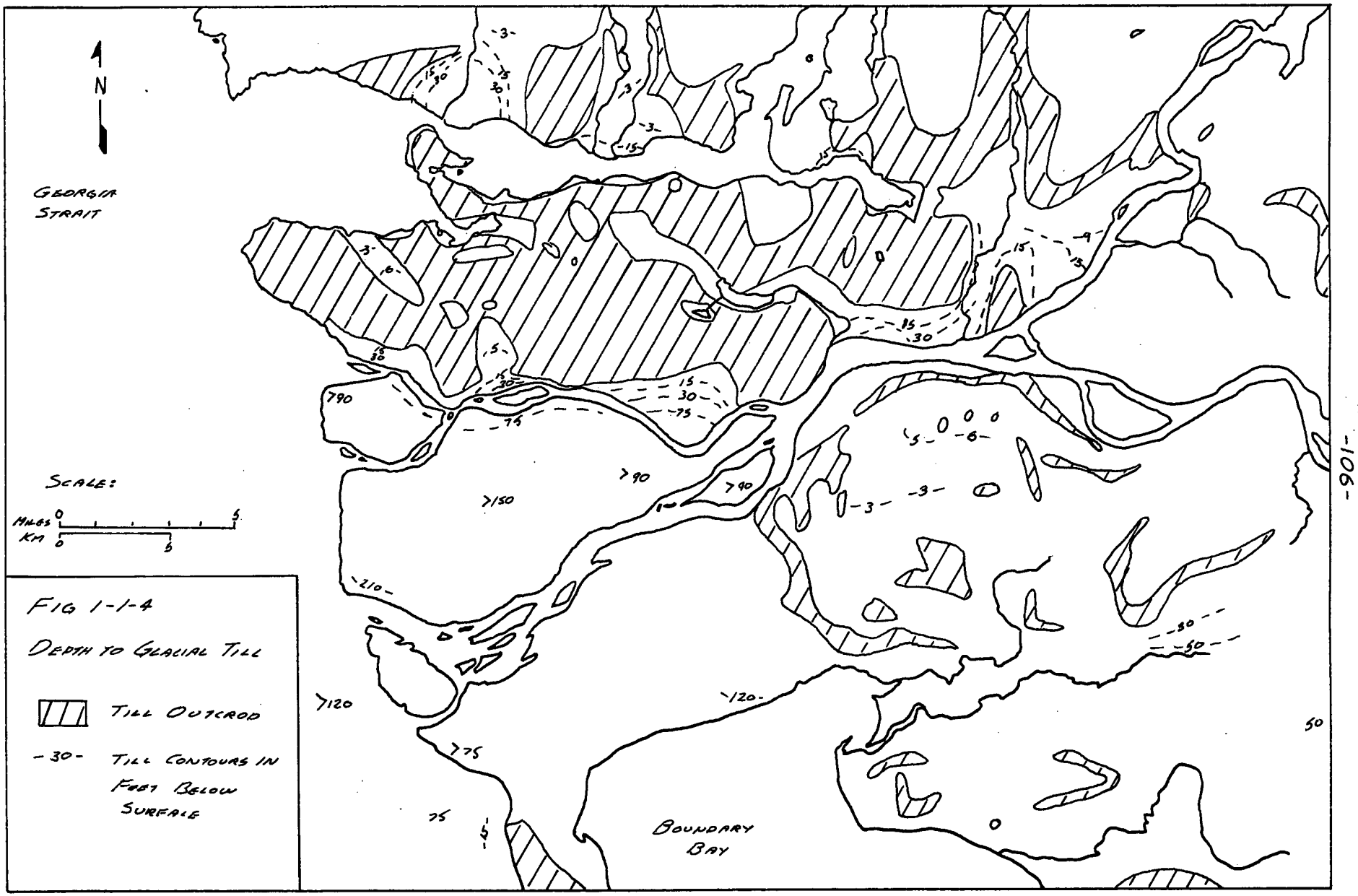
N
GEORGIA STRAIT
SCALE:
MILES 0 5
KM 0 5
FIG 1-1-4
DEPTH TO GLACIAL TILL
TILL OUTCROP
-30- TILL CONTOURS IN FEET BELOW SURFACE
BOUNDARY BAY
>150
>90
>120
>75
-210-
-120-
790
50

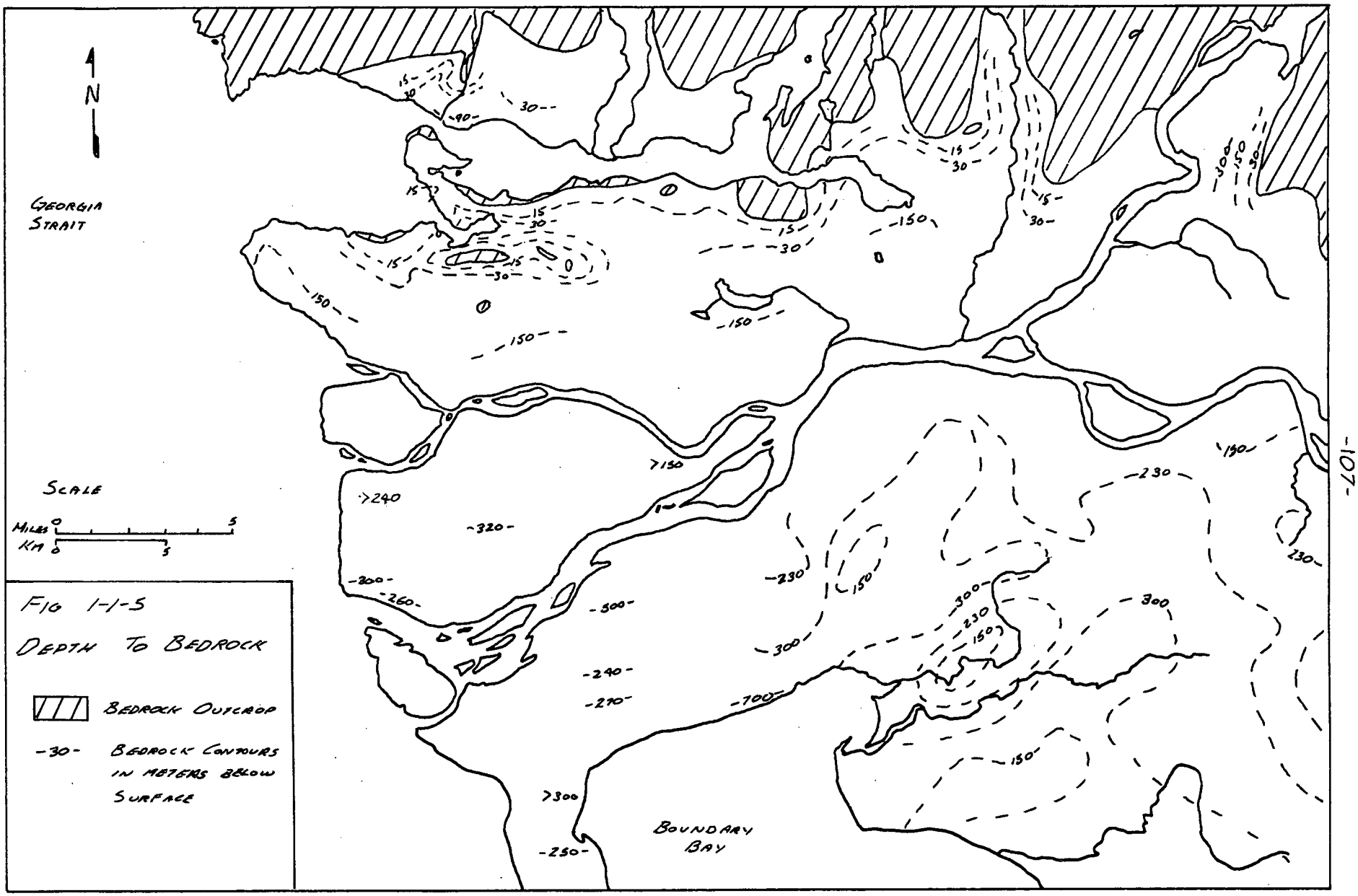
N
GEORGIA STRAIT
SCALE
MILES 0 5
KM 0 5
FIG 1-1-5
DEPTH TO BEDROCK
BEDROCK OUTCROP
-30- BEDROCK CONTOURS IN METERS BELOW SURFACE
BOUNDARY BAY
15
30
90
150
240
320
200
260
500
240
270
700
300
250
230

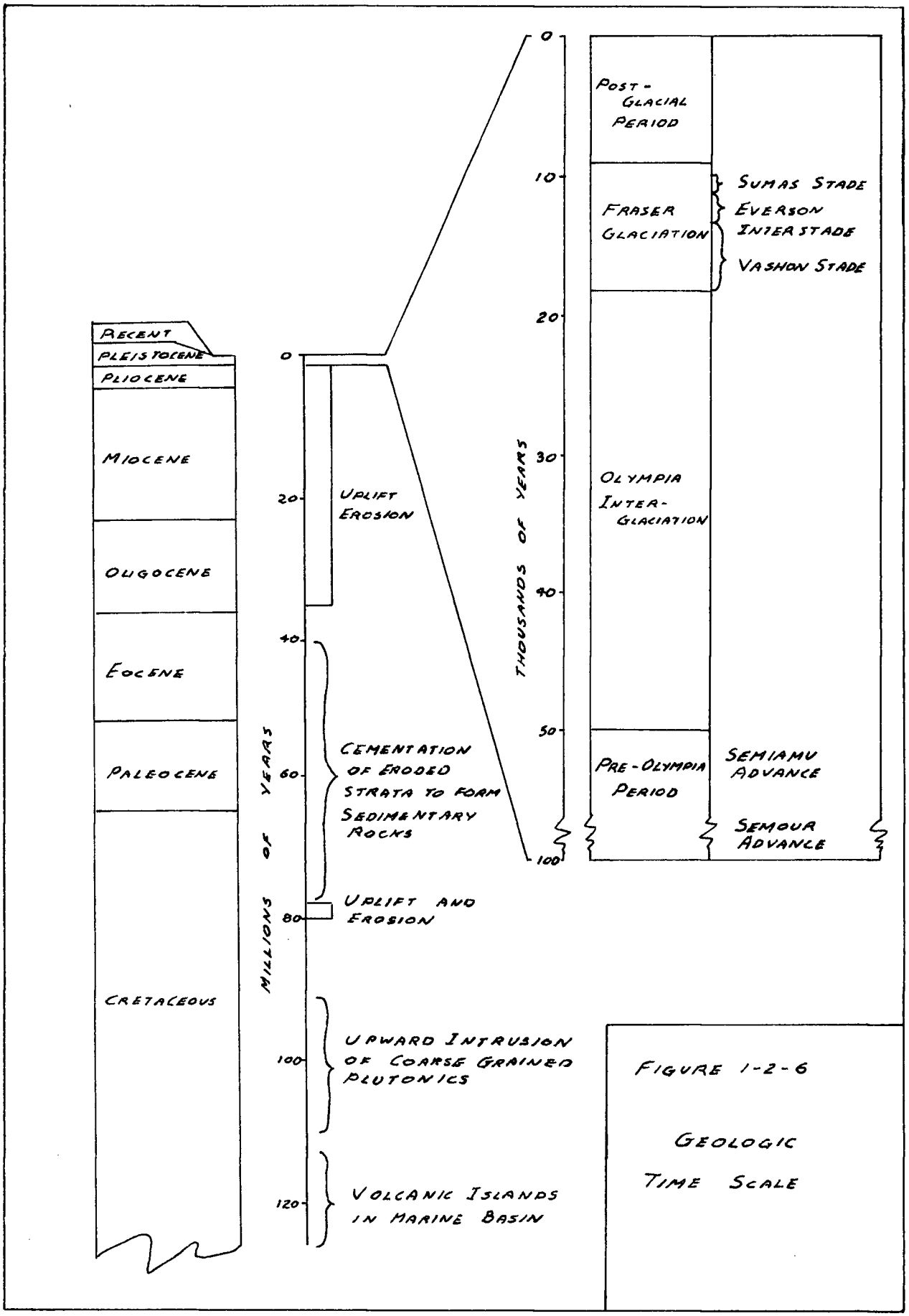

FIGURE 1-2-6

GEOLOGIC TIME SCALE

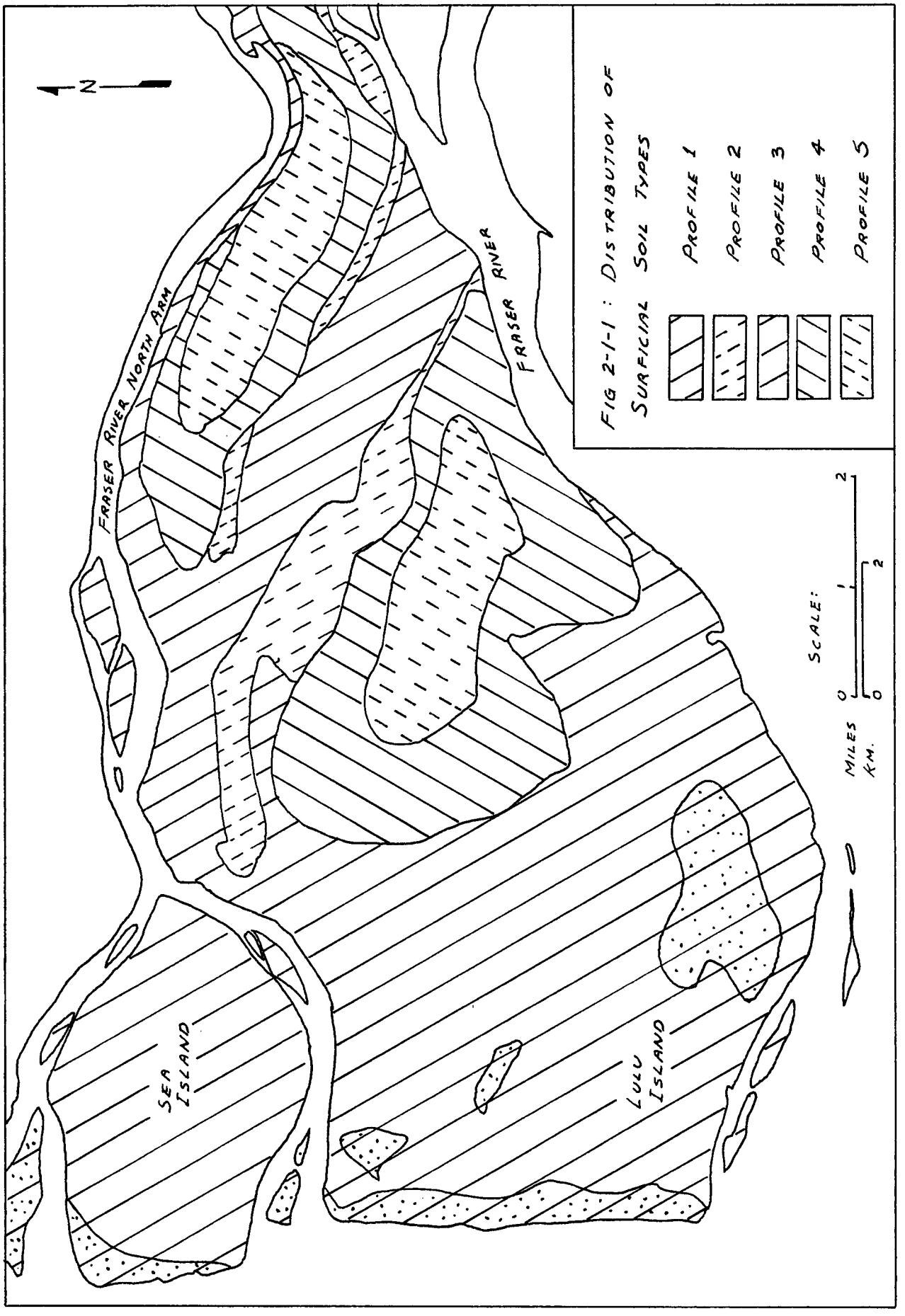
N
FRASER RIVER NORTH ARM
FRASER RIVER
SEA ISLAND
LULU ISLAND
FIG 2-1-1 : DISTRIBUTION OF SURFICIAL SOIL TYPES
PROFILE 1
PROFILE 2
PROFILE 3
PROFILE 4
PROFILE 5
SCALE:
0 1 2
0 1 2
MILES
KM.

FIG. 2-1-2 : SURFICIAL SOIL PROFILES

PROFILE 1

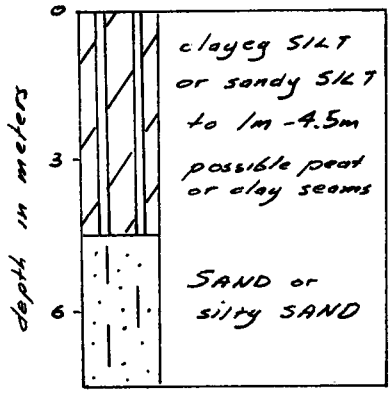

PROFILE 2

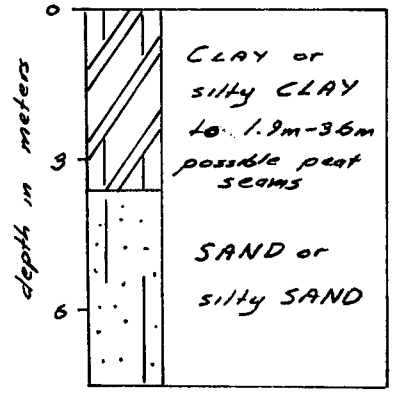

PROFILE 3

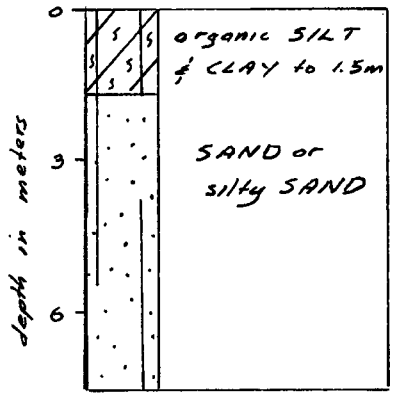

PROFILE 4

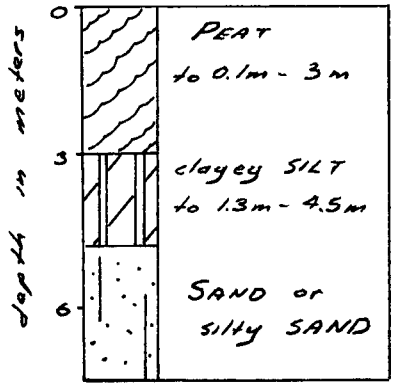

PROFILE 5

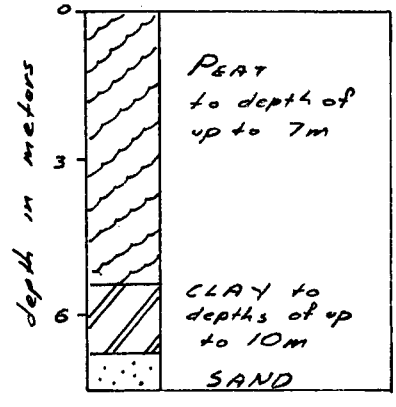

FIG 2-4-1 CLAY: WATER CONTENT VS DEPTH

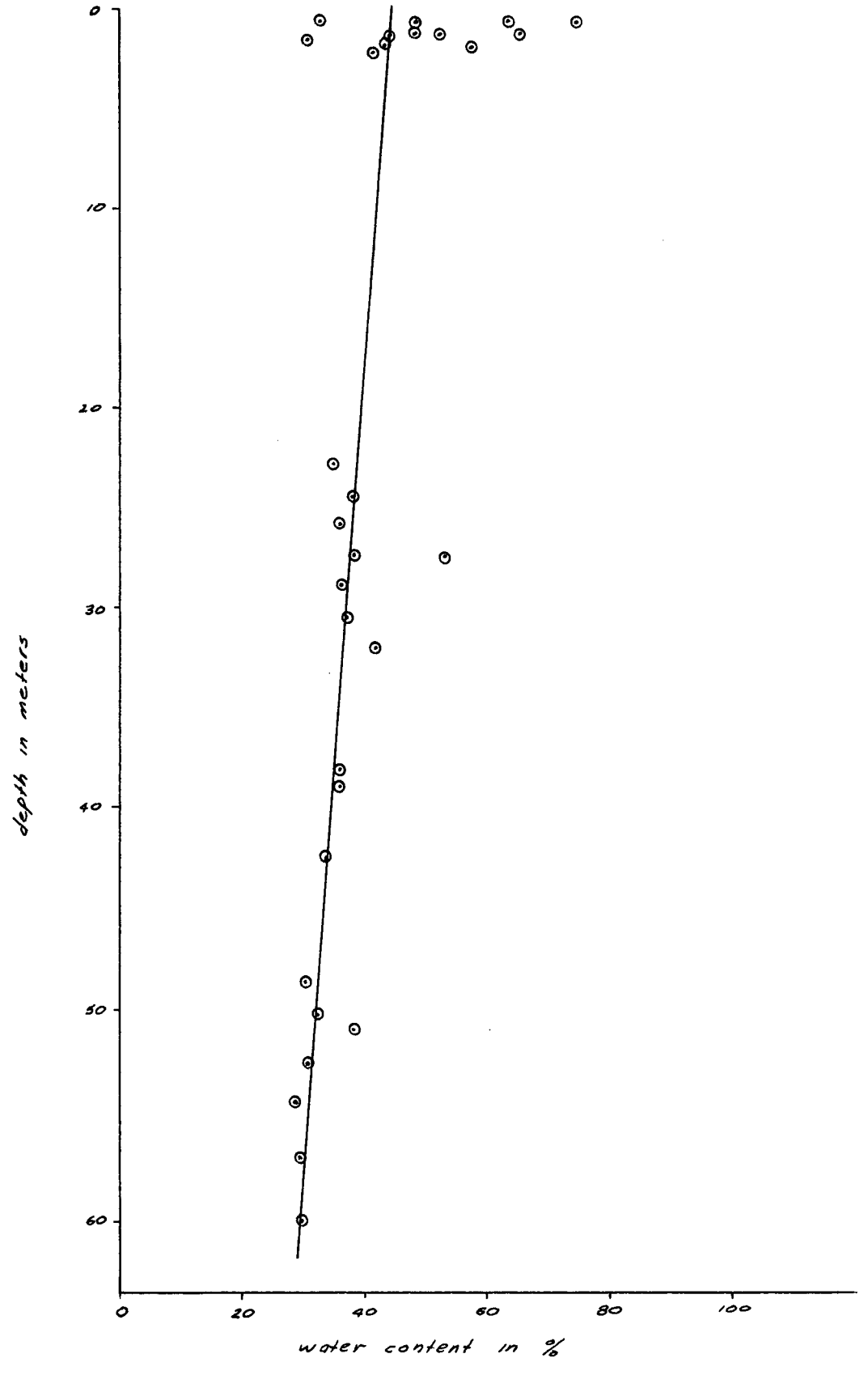

FIG 2-4-2 SILT: WATER CONTENT VS DEPTH

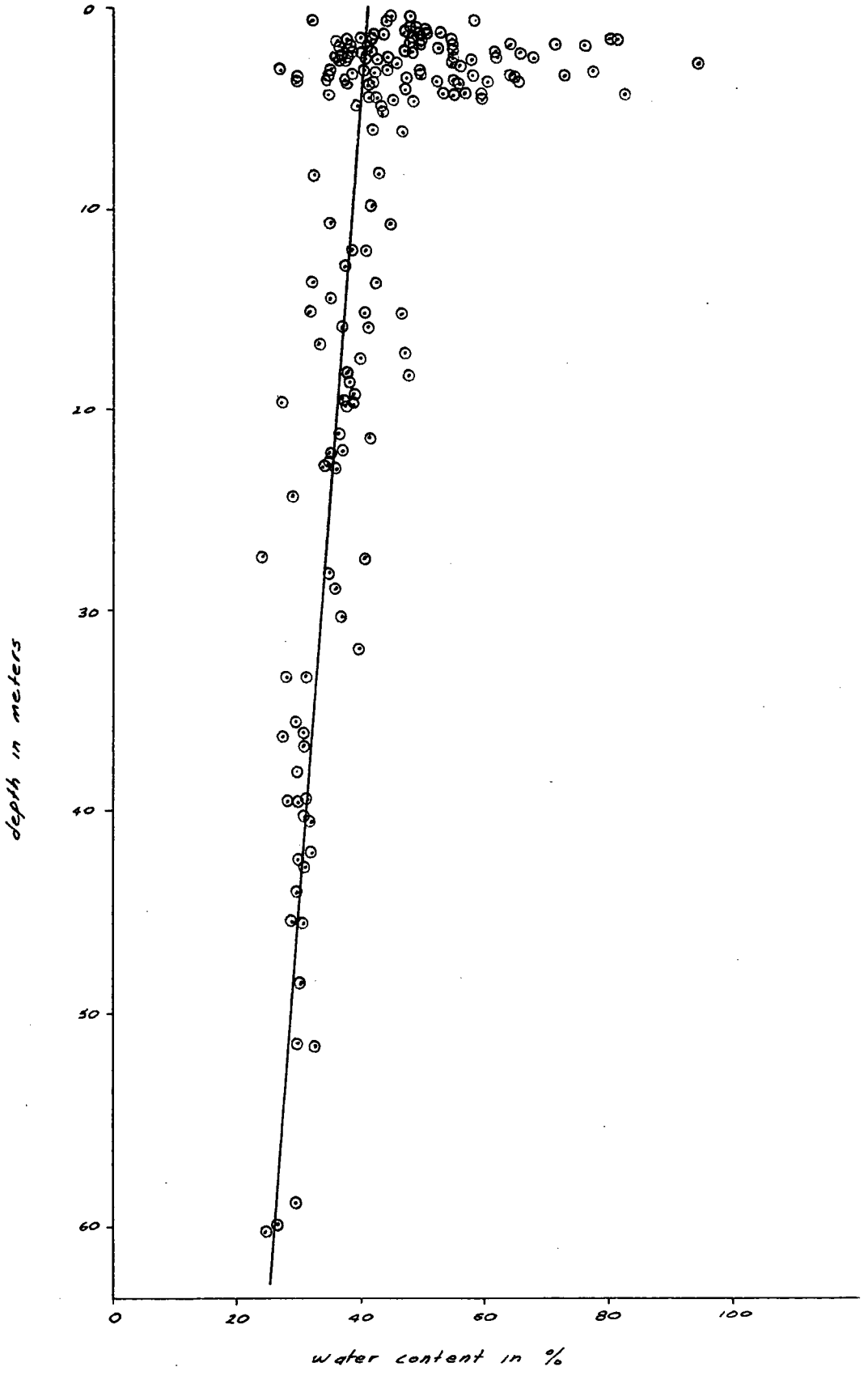

FIG 2-4-3 PEAT: MOISTURE CONTENT VS DEPTH

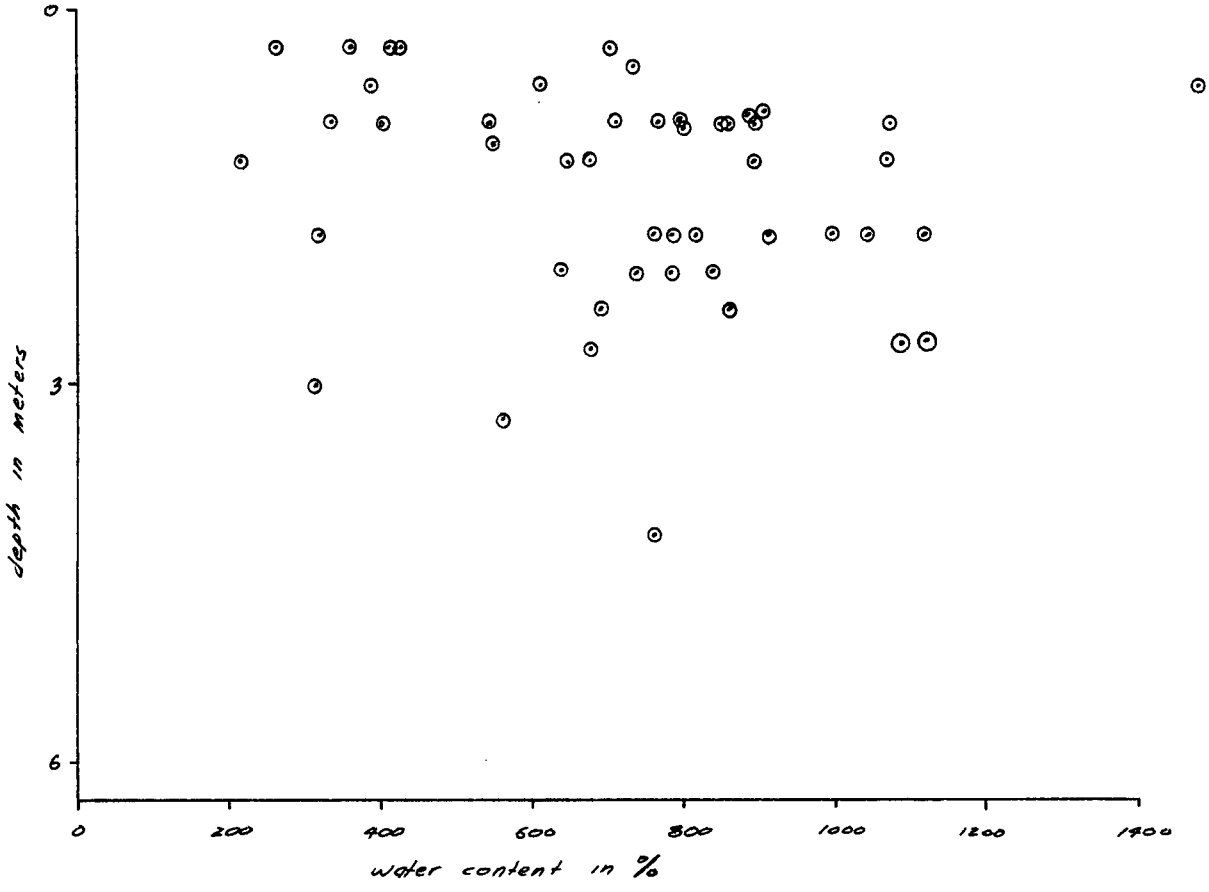

FIG 2-5-1 CLAY: LIQUID LIMIT AND PLASTIC LIMIT VS. DEPTH

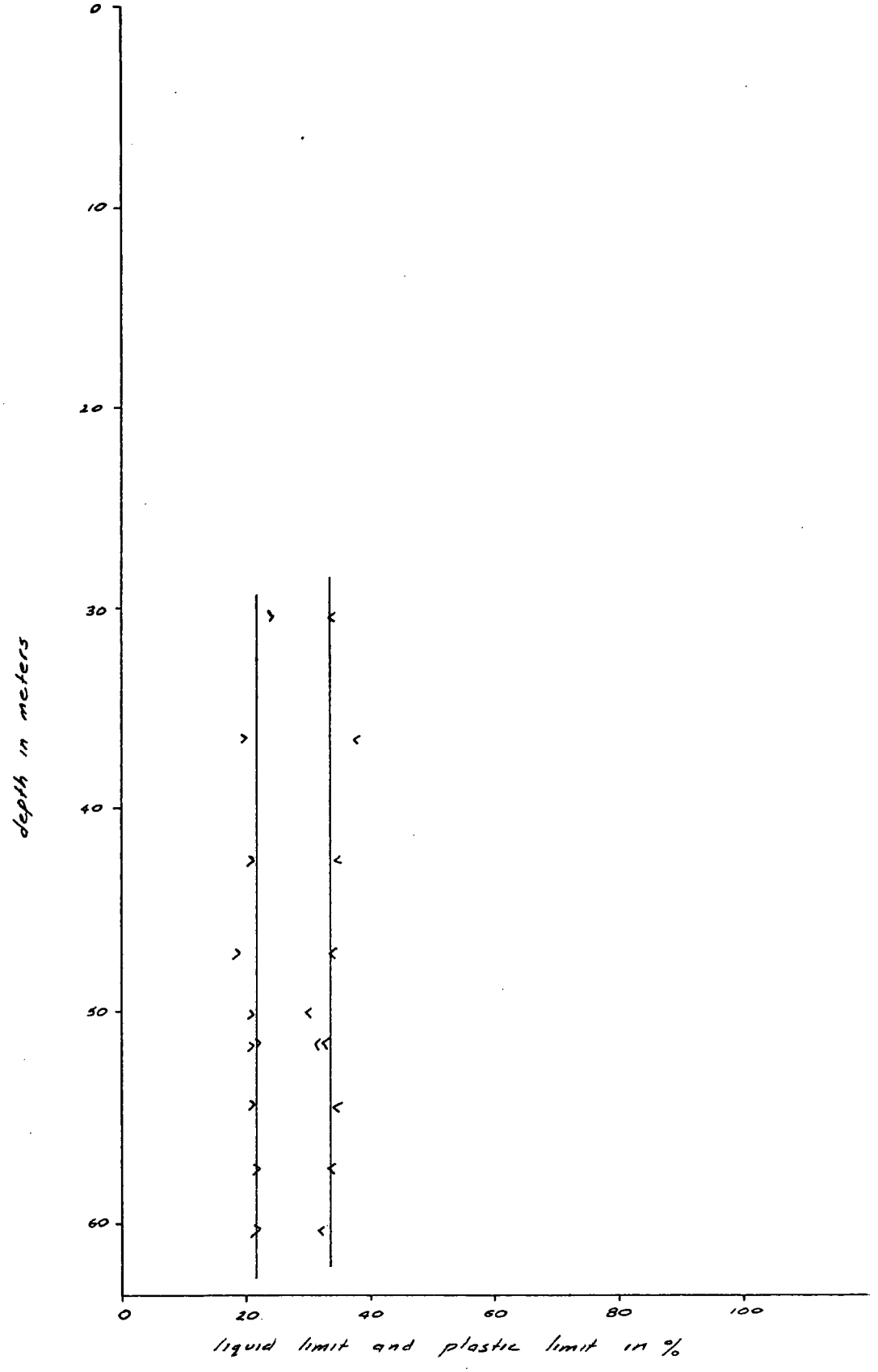

FIG 2-5-2 SILT: LIQUID LIMIT AND PLASTIC LIMIT VS. DEPTH

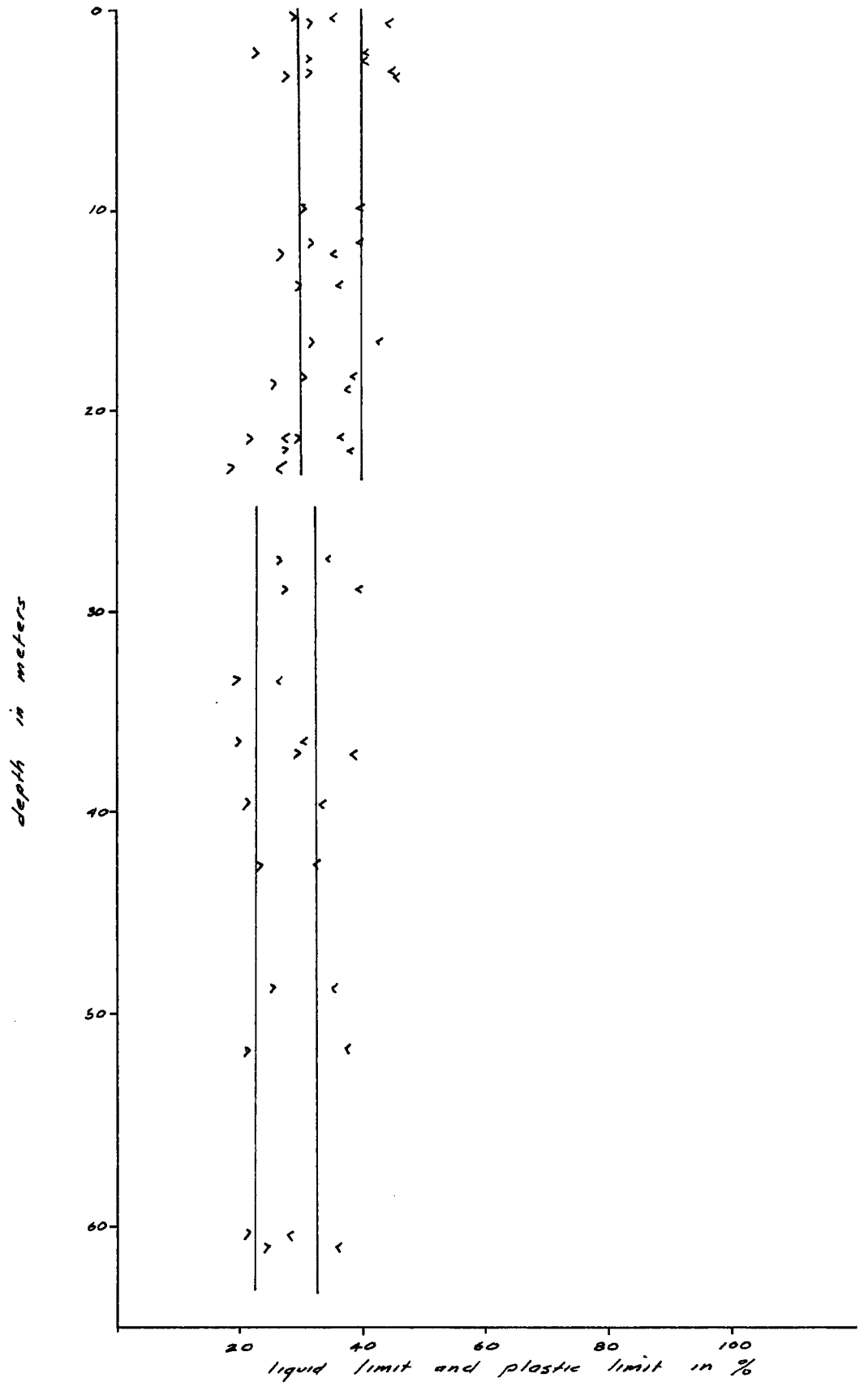

FIG 2-5-3 SILT: PLASTICITY INDEX VS. DEPTH

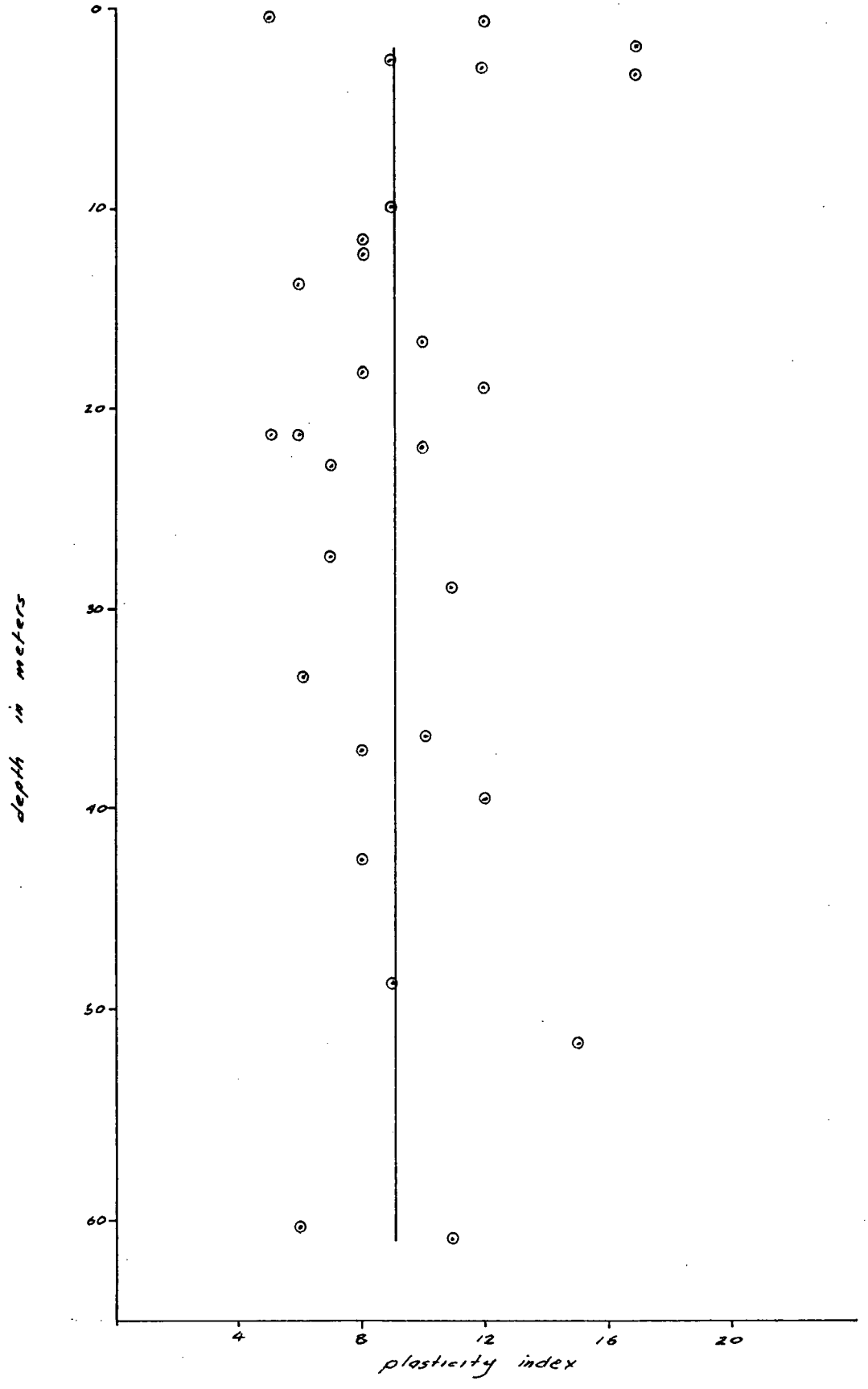

FIG 2-5-4 CLAY: PLASTICITY INDEX VS. DEPTH

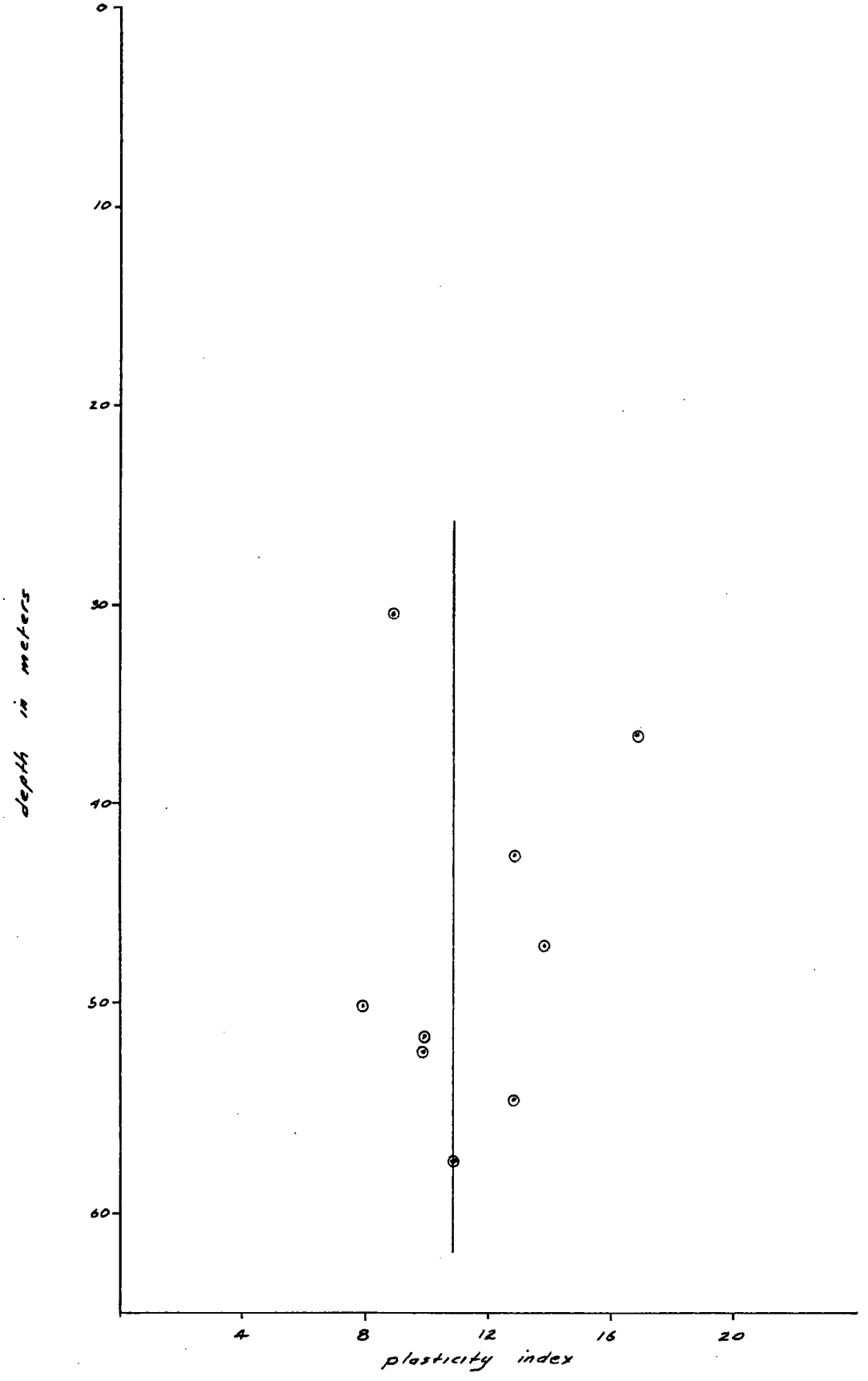

FIG 2-5-5 PLASTICITY CHART

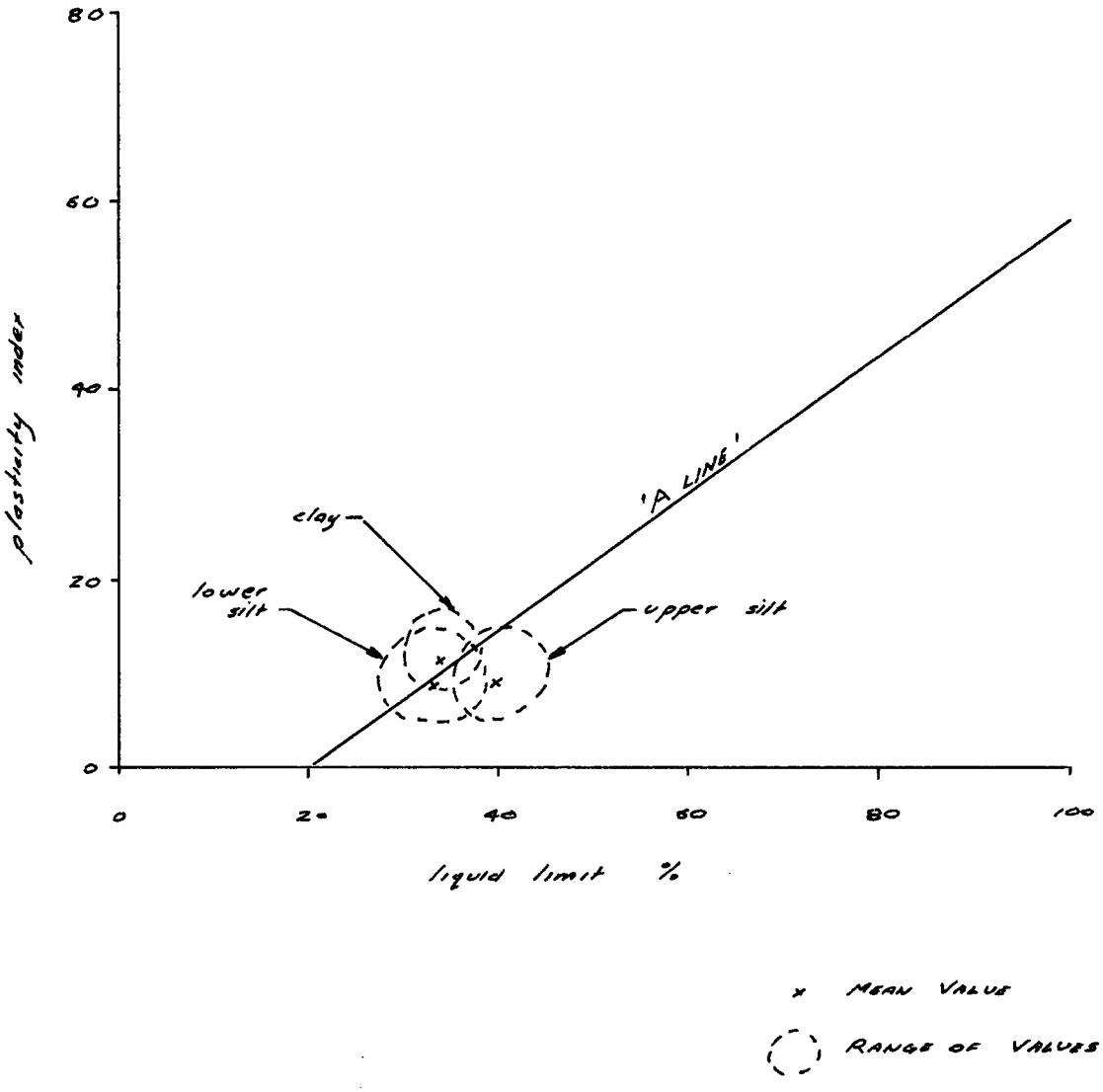

FIG 2-6-1 SILT: COMPRESSION INDEX VS. DEPTH

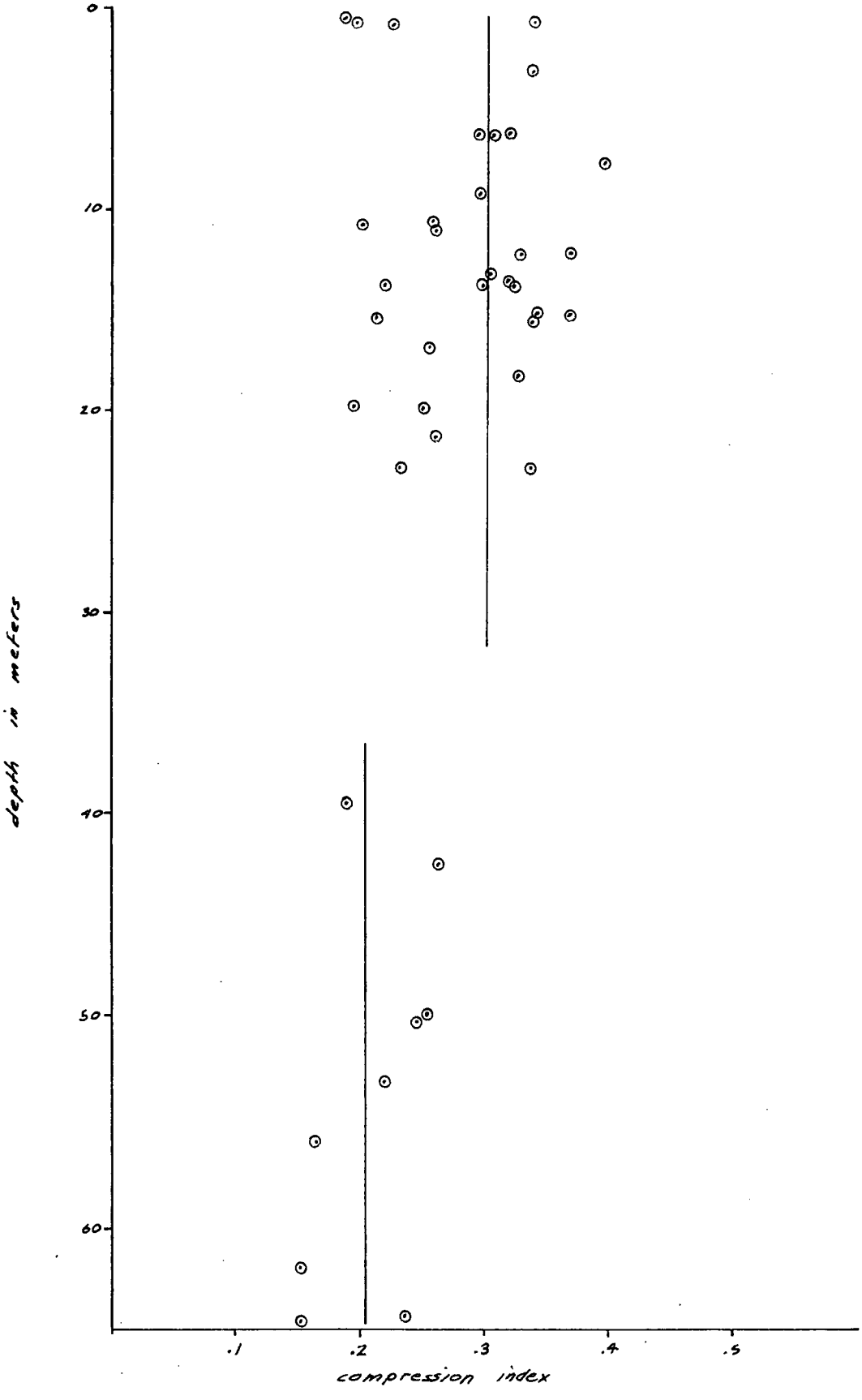

FIG 2-6-2 CLAY: COMPRESSION INDEX VS. DEPTH

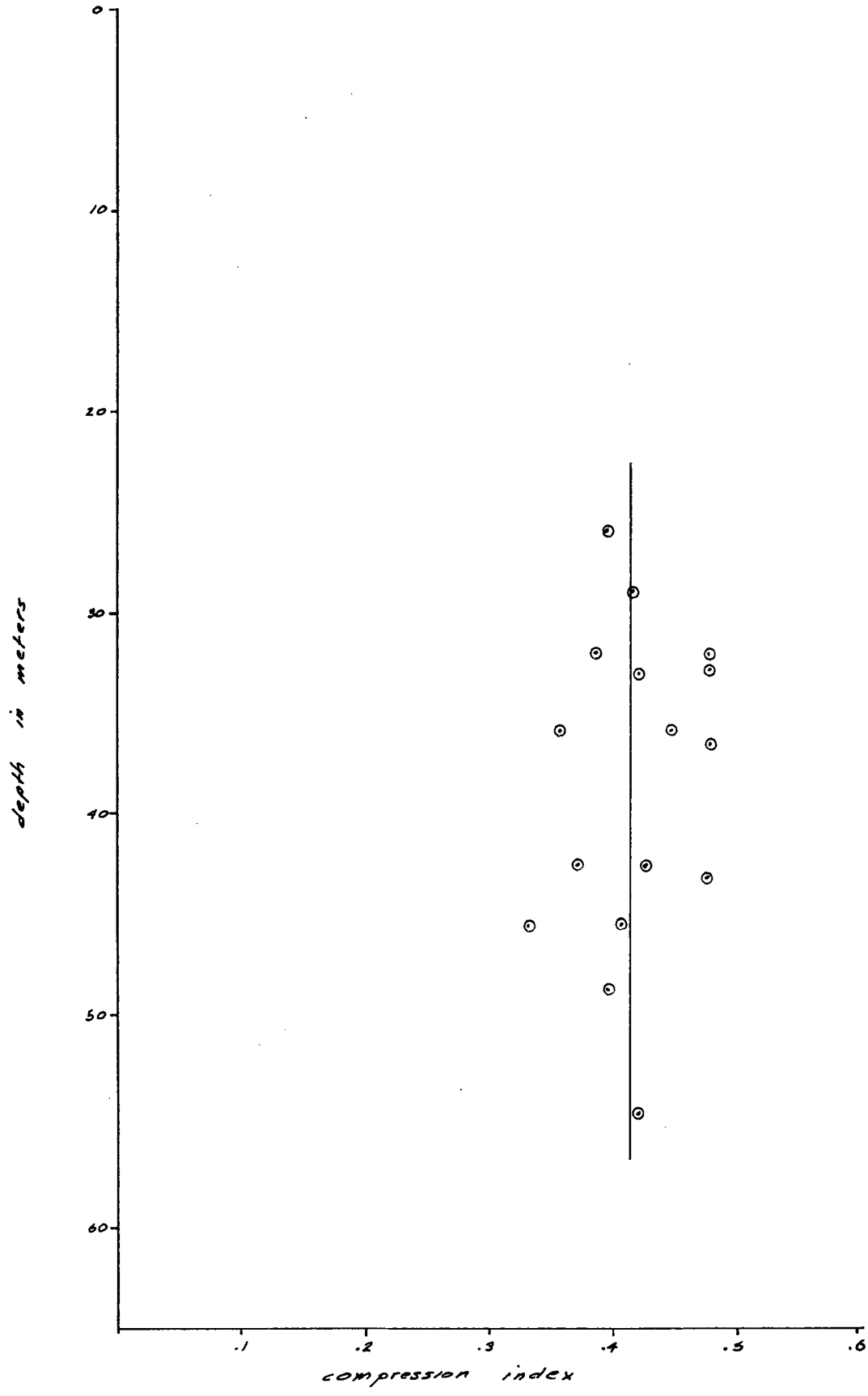

FIG 2-7-1 CLAY: UNDRAINED SHEAR STRENGTH VS DEPTH

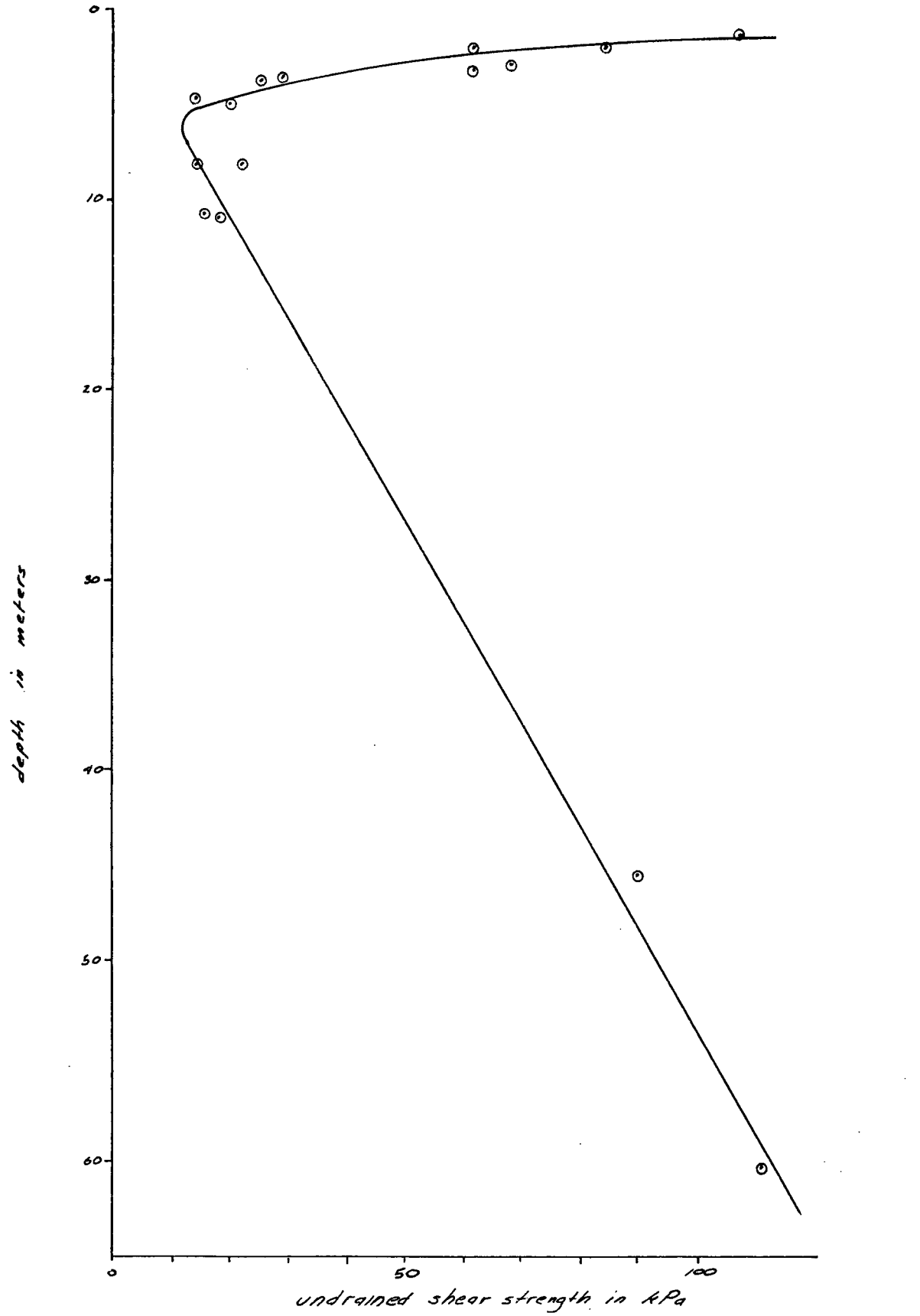

FIG 2-7-2 SILT : UNDRAINED SHEAR STRENGTH VS. DEPTH

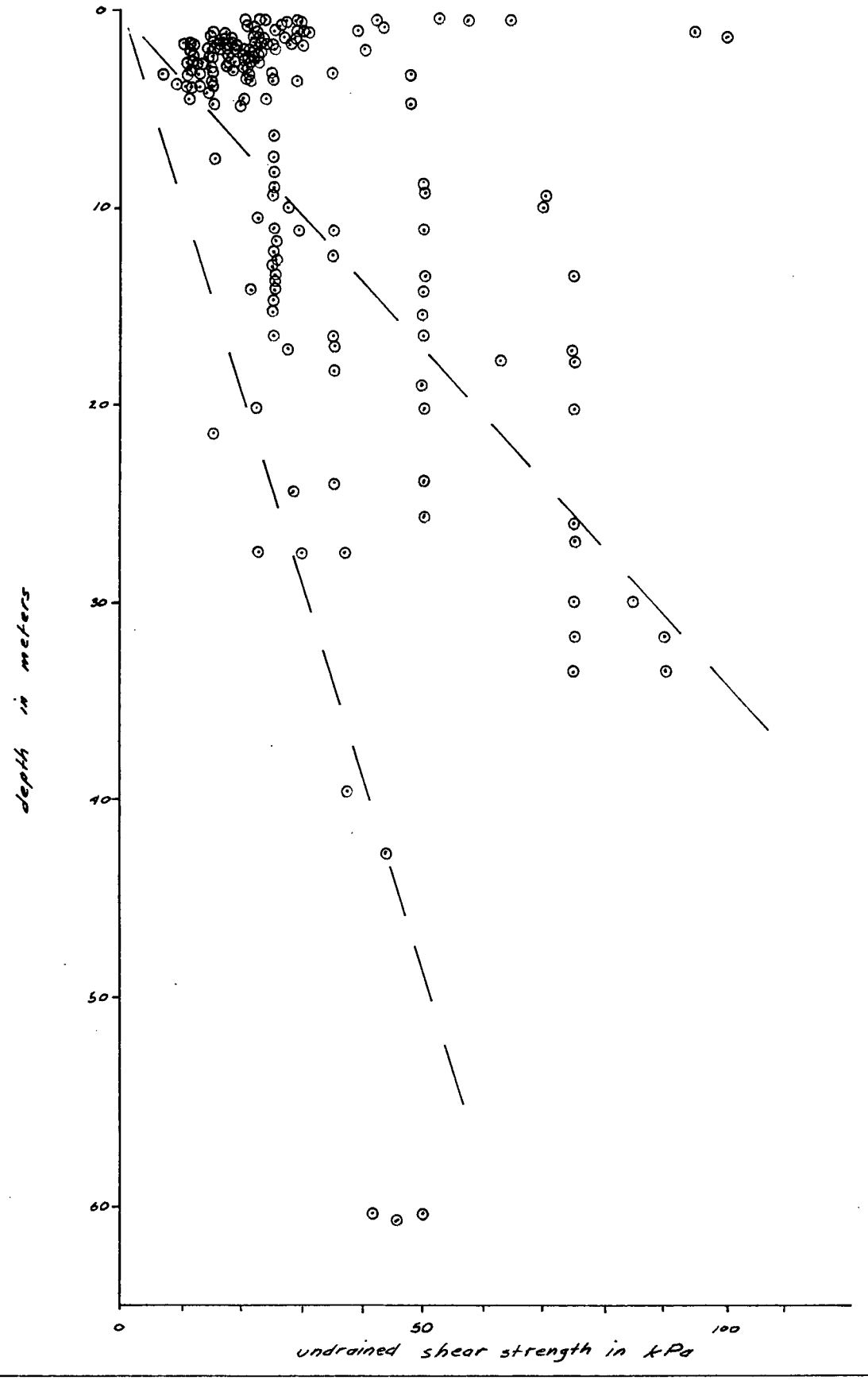

FIG 2-8-1 SAND : DRY DENSITY vs DEPTH

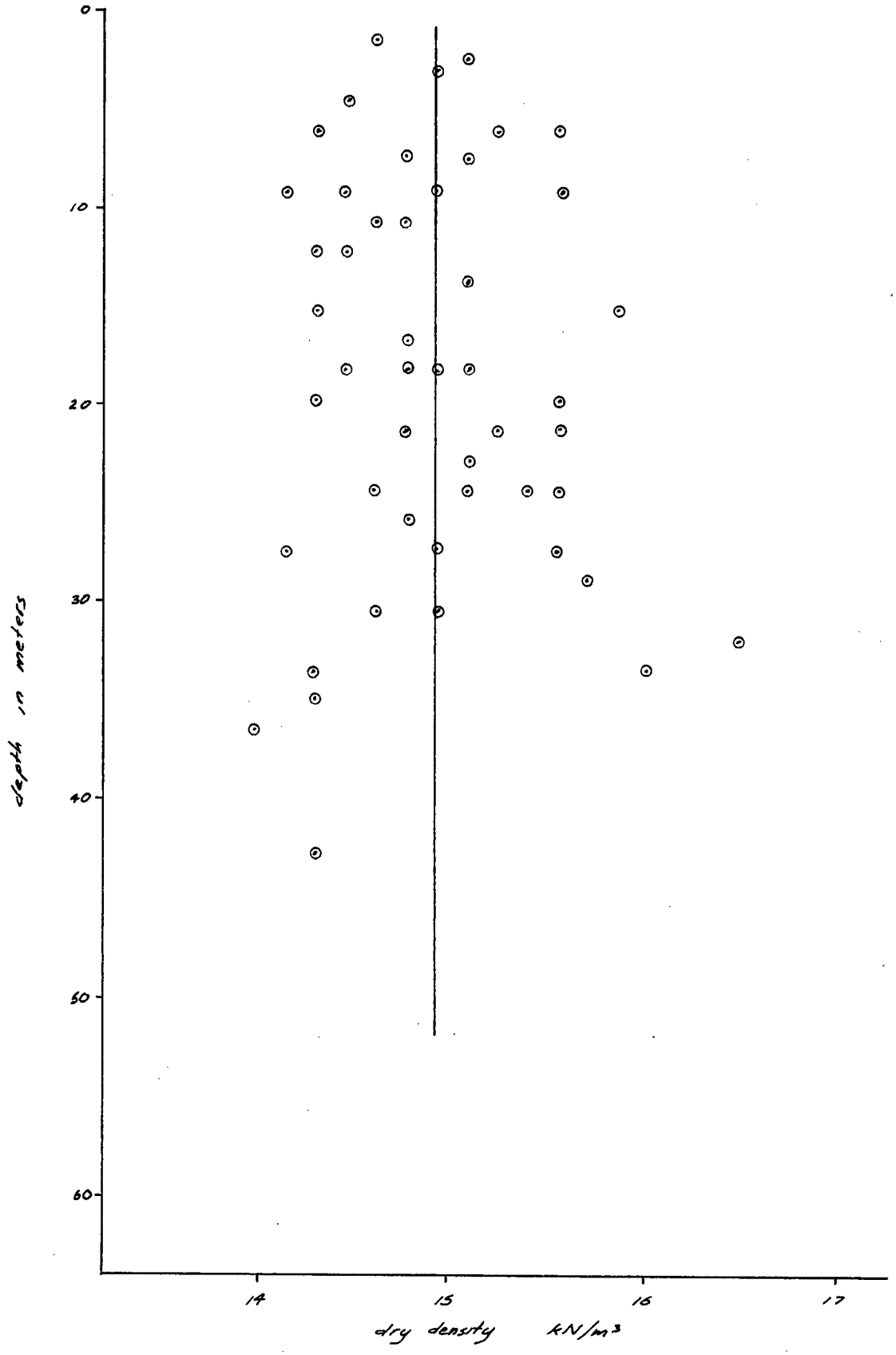

FIG 2-9-1 BLOW COUNT vs. DEPTH IN SAND (TYPICAL)

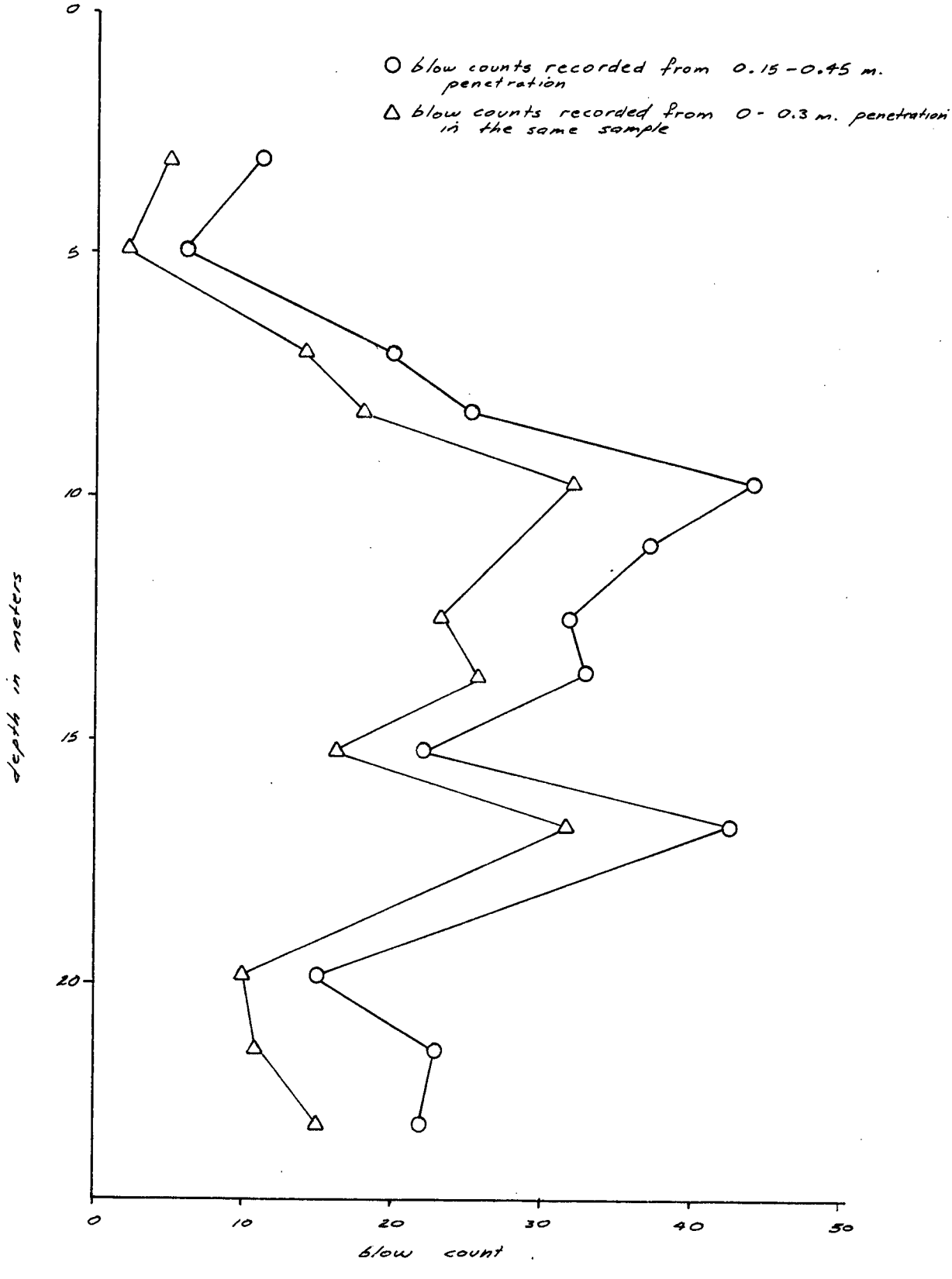

FIG 2-9-2: COEFFICIENT OF RELATIVE CURVE SMOOTHNESS VS DEPTH FOR S.P.T. IN SAND: COMPARISON BETWEEN BLOWS COUNTED FROM 0-0.3m AND FROM 0.15-0.45m. ON EACH SAMPLE, DATA FROM 3 SITES.

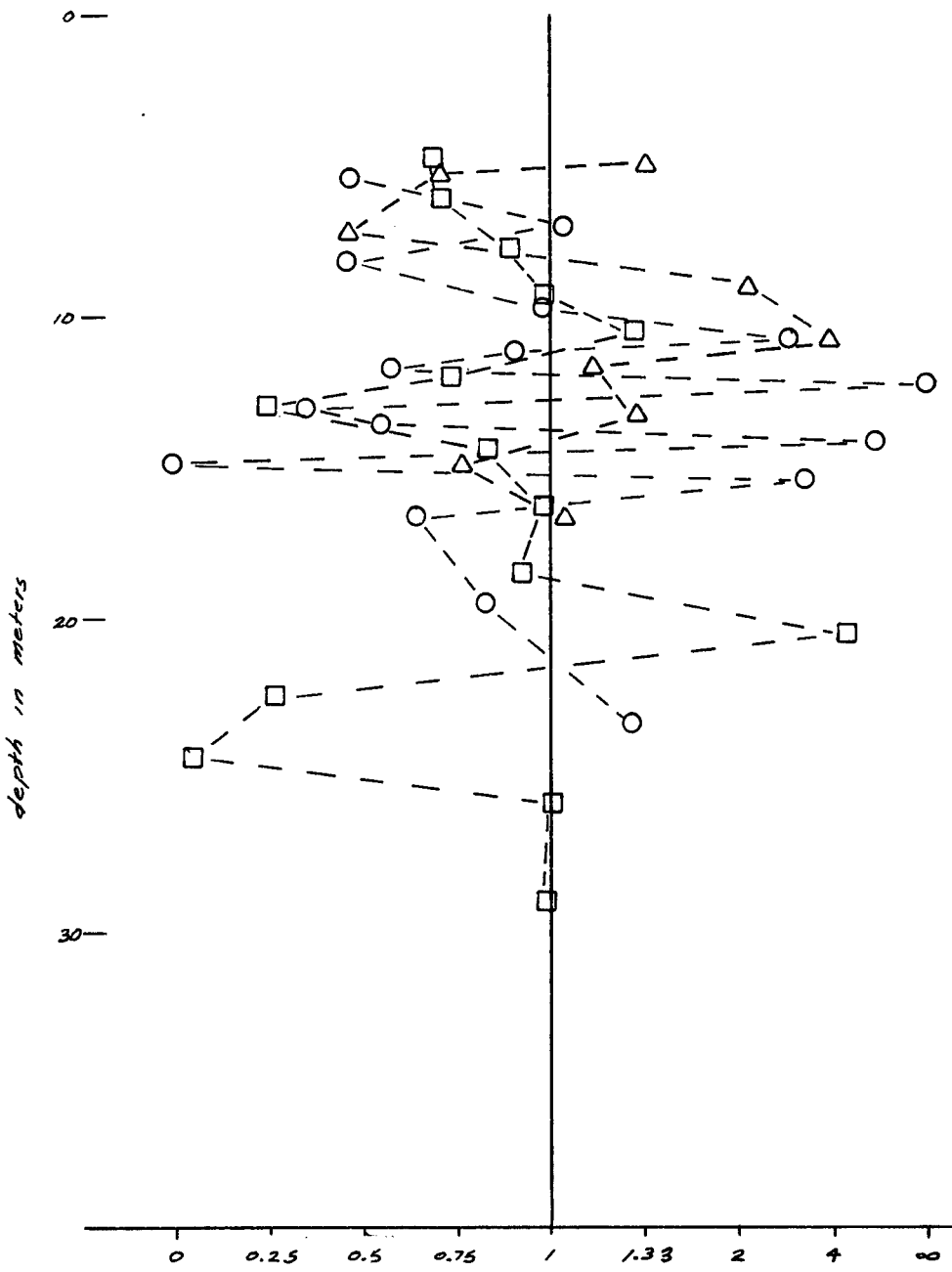

$$\text{coefficient of relative curve smoothness} = \left[\frac{\left(\frac{\Delta N}{N_{avg}}\right)_{0.15-0.45}}{\left(\frac{\Delta N}{N_{avg}}\right)_{0-0.3}} \right] \text{ for each 2 consecutive values of } N$$

FIG 2-9-3 COEFFICIENT OF RELATIVE CURVE SMOOTHNESS VS DEPTH FOR S.P.T. IN SAND : COMPARISON BETWEEN BLOWS COUNTED FROM 0-0.3m. AND FROM 0.3-0.6m. ON EACH SAMPLE, DATA FROM 3 SITES.

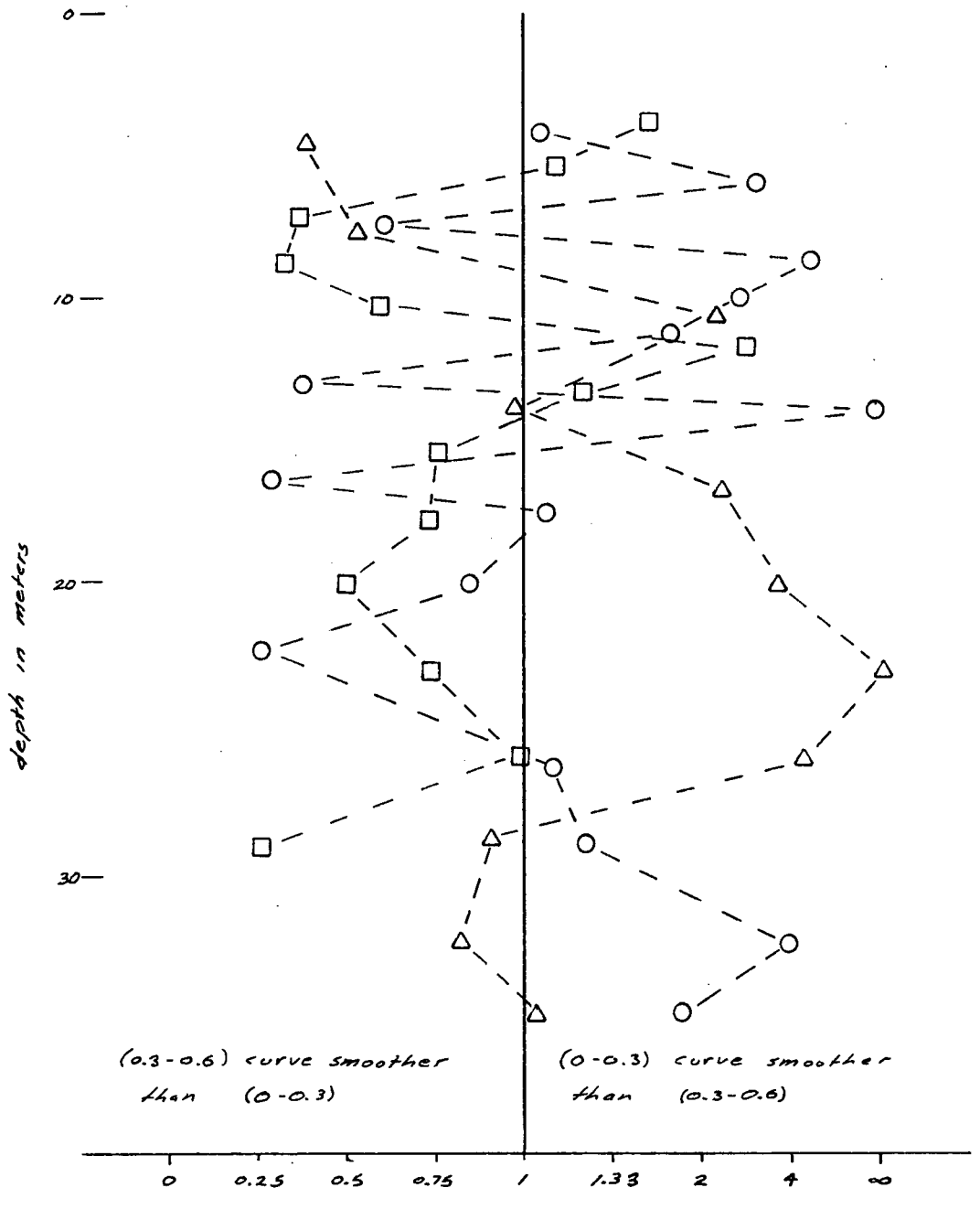

$$\text{coefficient of relative curve smoothness} = \left[\frac{\left(\frac{\Delta N}{N_{avg}}\right)_{0.3-0.6}}{\left(\frac{\Delta N}{N_{avg}}\right)_{0-0.3}} \right] \text{ for each 2 consecutive values of } N$$

FIG 2-9-4 COMPARISON OF S.P.T. BLOW COUNTS RECORDED IN FIRST 0.3m. WITH THOSE RECORDED FROM 0.15m - 0.45m ON SAME SAMPLE OF SAND, DATA FROM 3 SITES

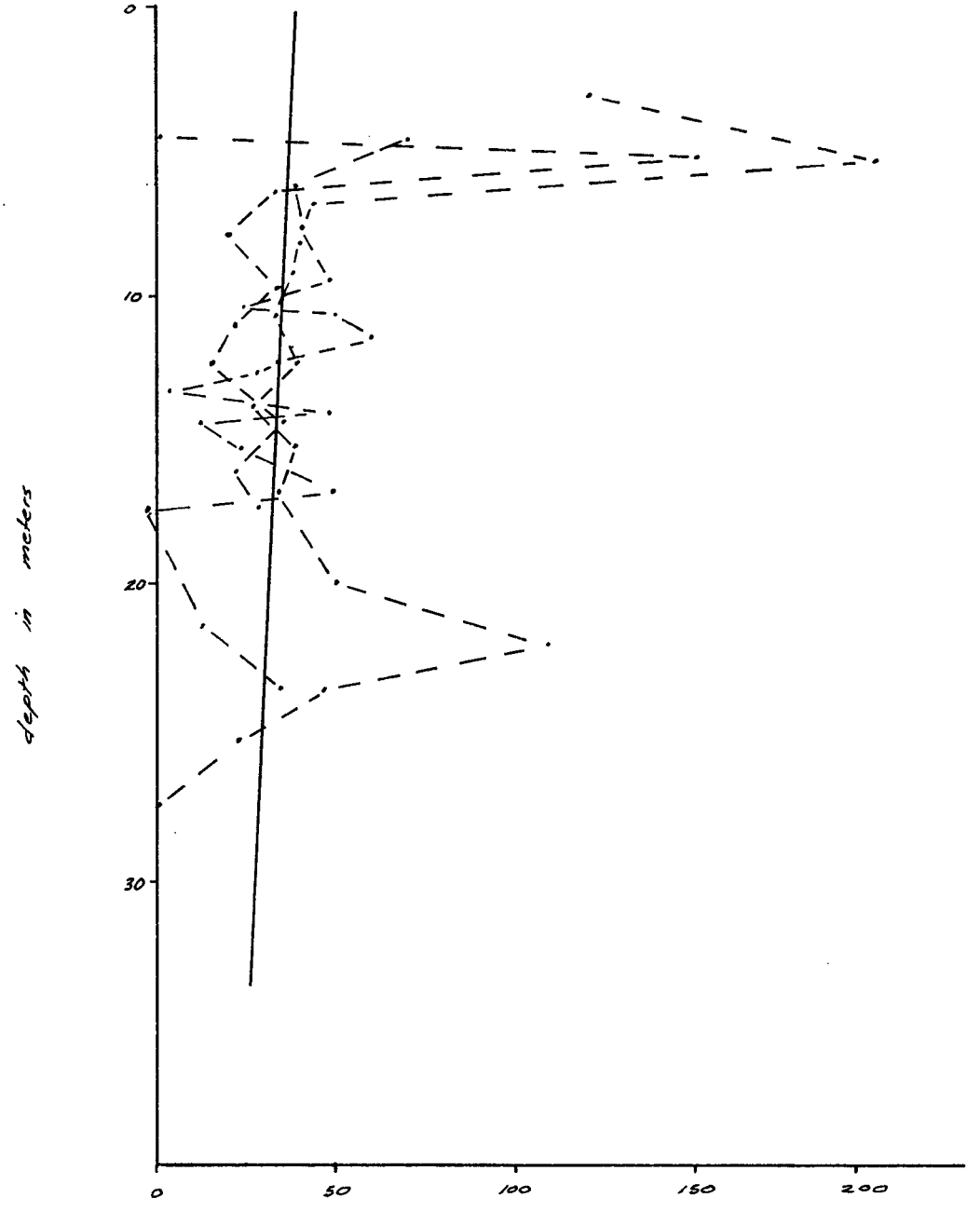

$$\% \text{ difference} = \frac{N_{(0.15-0.45)} - N_{(0-0.3)}}{N_{(0-0.3)}} \times 100$$

FIG 2-9-5 COMPARISON OF S.P.T. BLOW COUNTS RECORDED IN FIRST 0.3 m. WITH THOSE RECORDED FROM 0.3 - 0.6 m. ON THE SAME SAMPLE OF SAND, DATA FROM 3 SITES

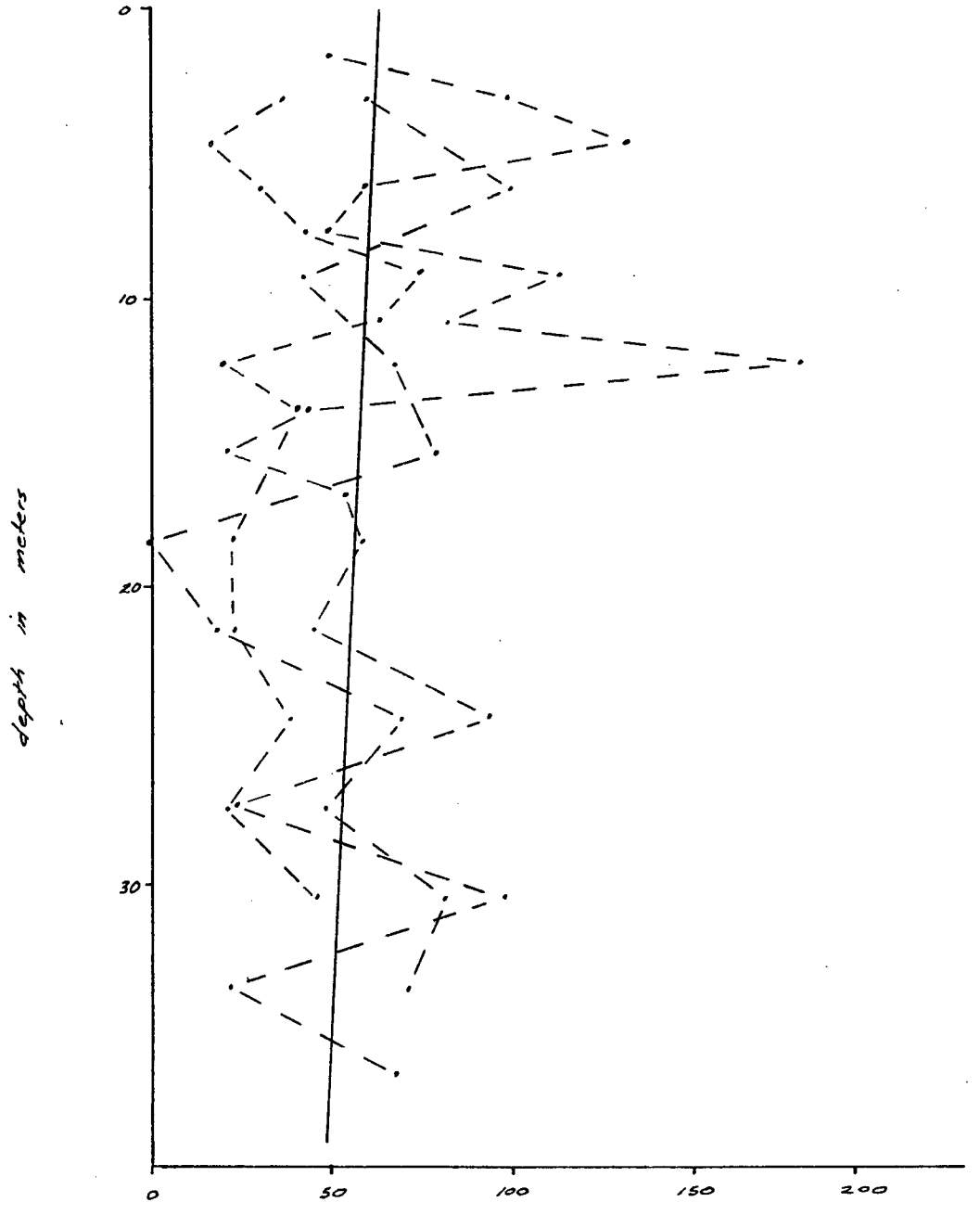

$$\% \text{ difference} = \frac{N_{(0.3-0.6)} - N_{(0-0.3)}}{N_{(0-0.3)}} \times 100$$

FIG 2-9-6 COMPARISON OF S.P.T. BLOW COUNTS RECORDED IN FIRST 0.3 m. WITH THOSE RECORDED AT OTHER POSITIONS ON THE SAME SAMPLE OF SAND.

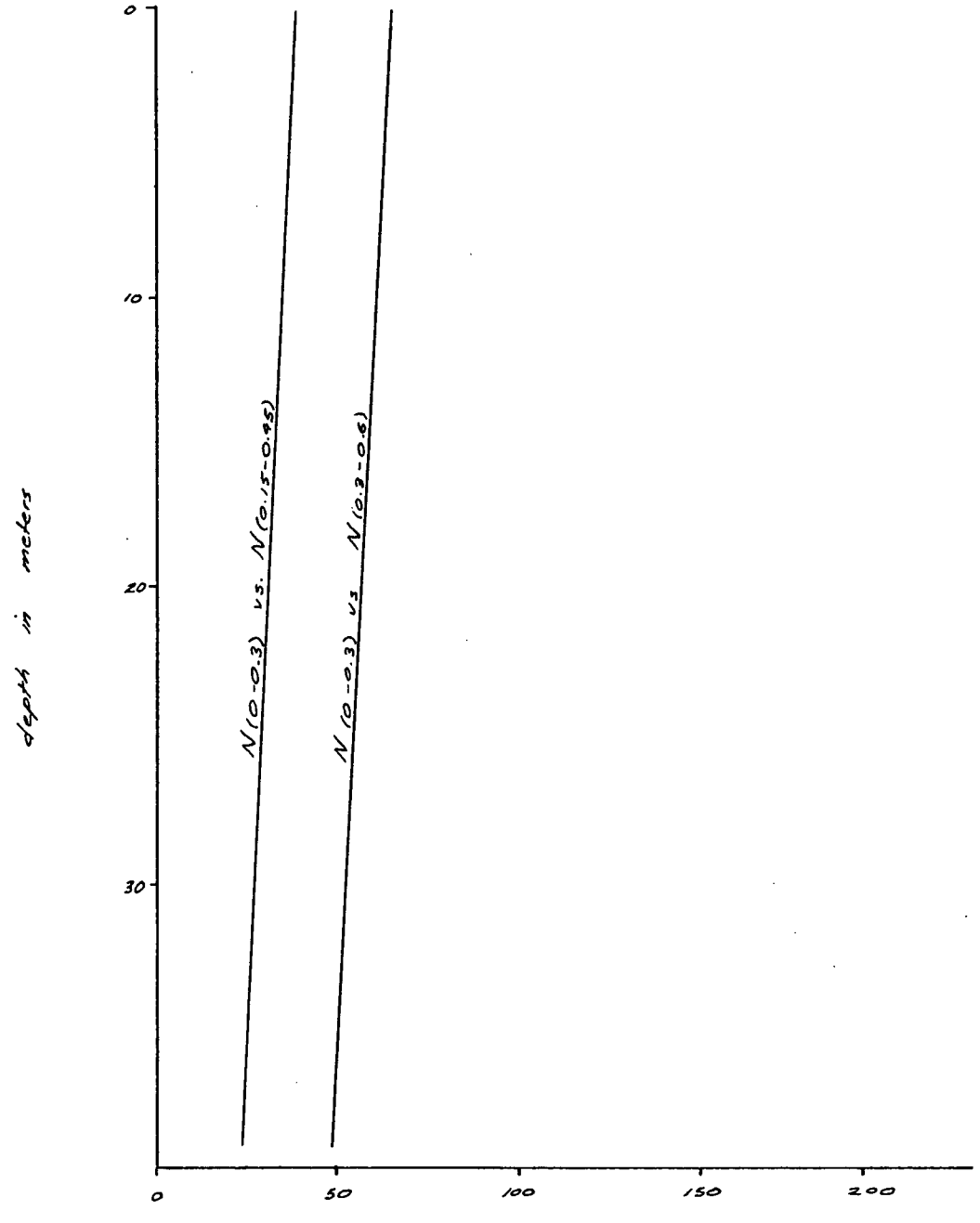

$$\% \text{ difference} = \frac{N_{(other)} - N_{(0-0.3)}}{N_{(0-0.3)}} \times 100$$

FIG 2-9-7 COMPARISON SITE: BLOW COUNT VS. DEPTH IN SAND, BLOW COUNTS RECORDED FOR PENETRATION FROM 0 - 0.3 m.

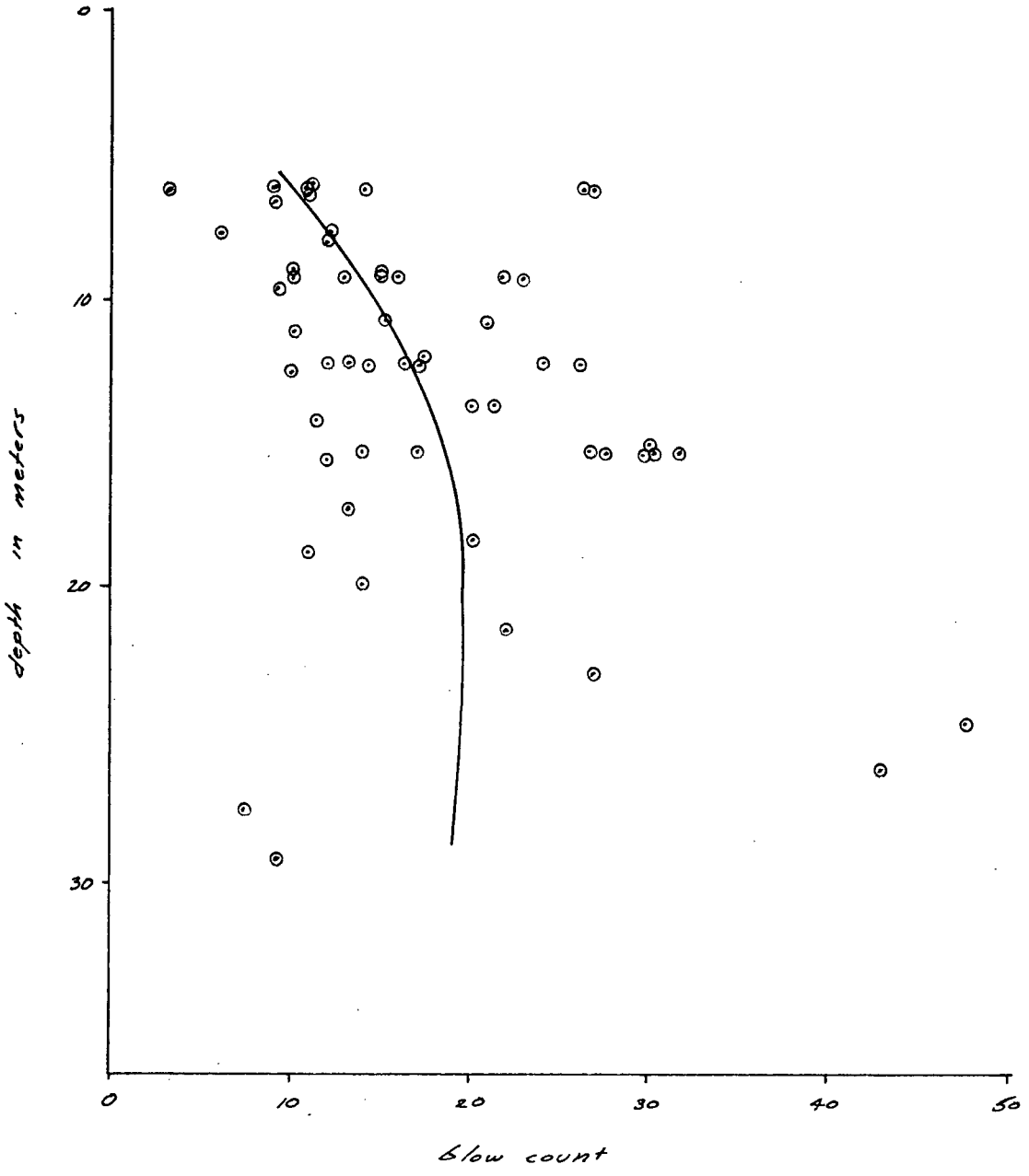

FIG 2-9-8 COMPARISON SITE: BLOW COUNT VS. DEPTH IN SAND, BLOW COUNTS RECORDED FOR PENETRATION FROM 0.15 - 0.45 m.

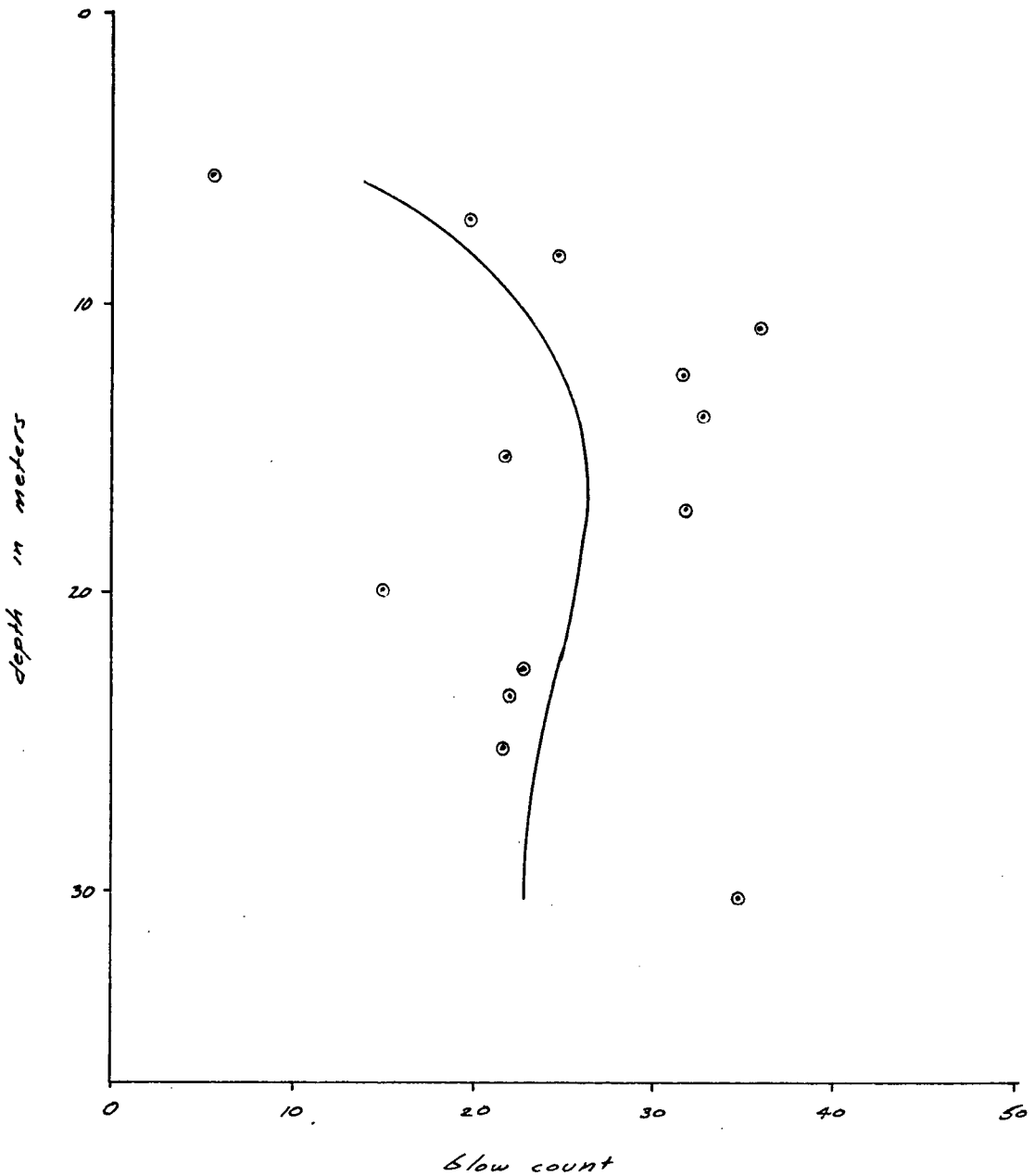

FIG 2-9-9 COMPARISON SITE: BLOW COUNT VS. DEPTH IN SAND

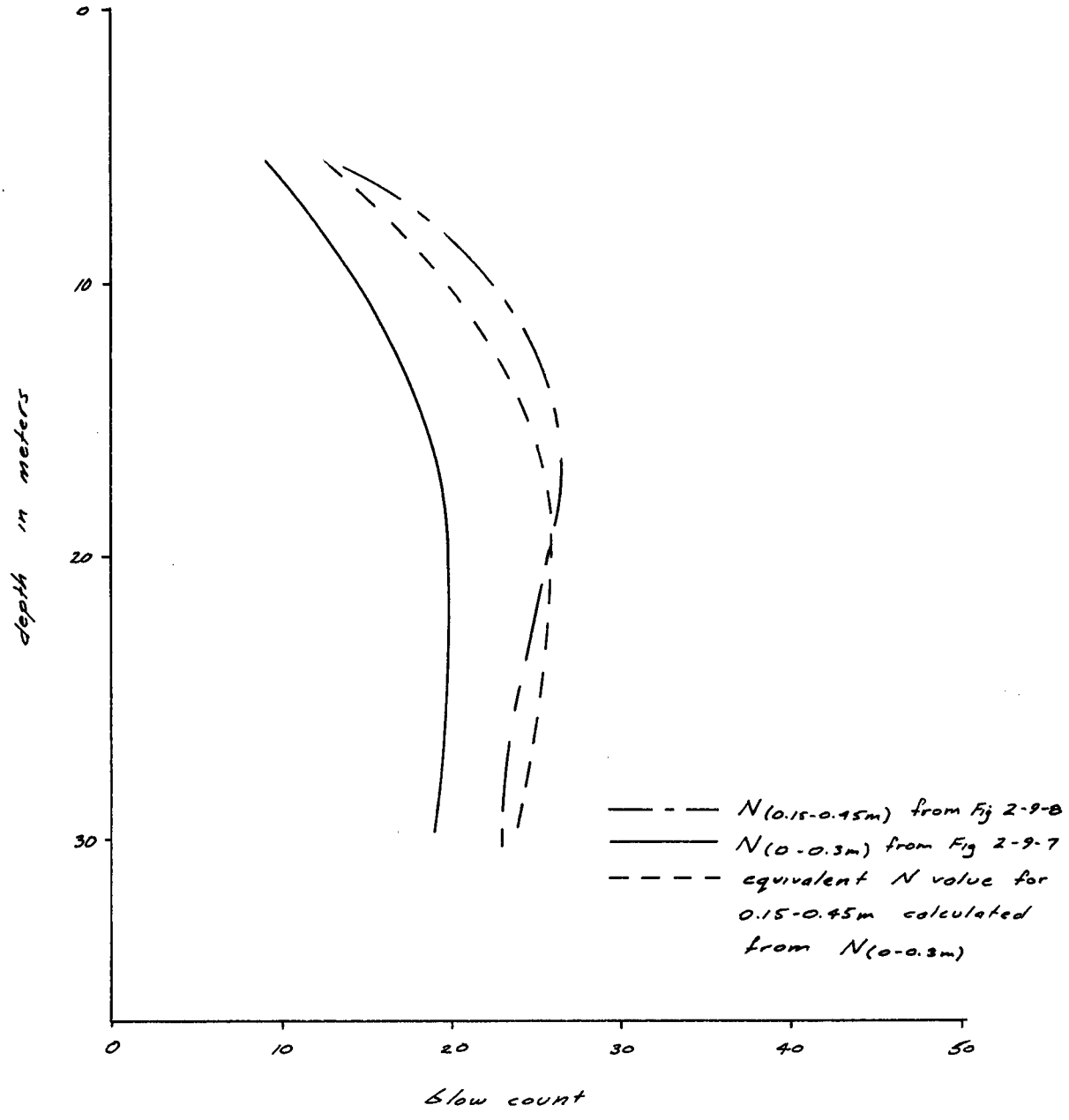

FIG 2-9-10 : ROBERTS BANK, BLOW COUNT VS DEPTH IN SAND

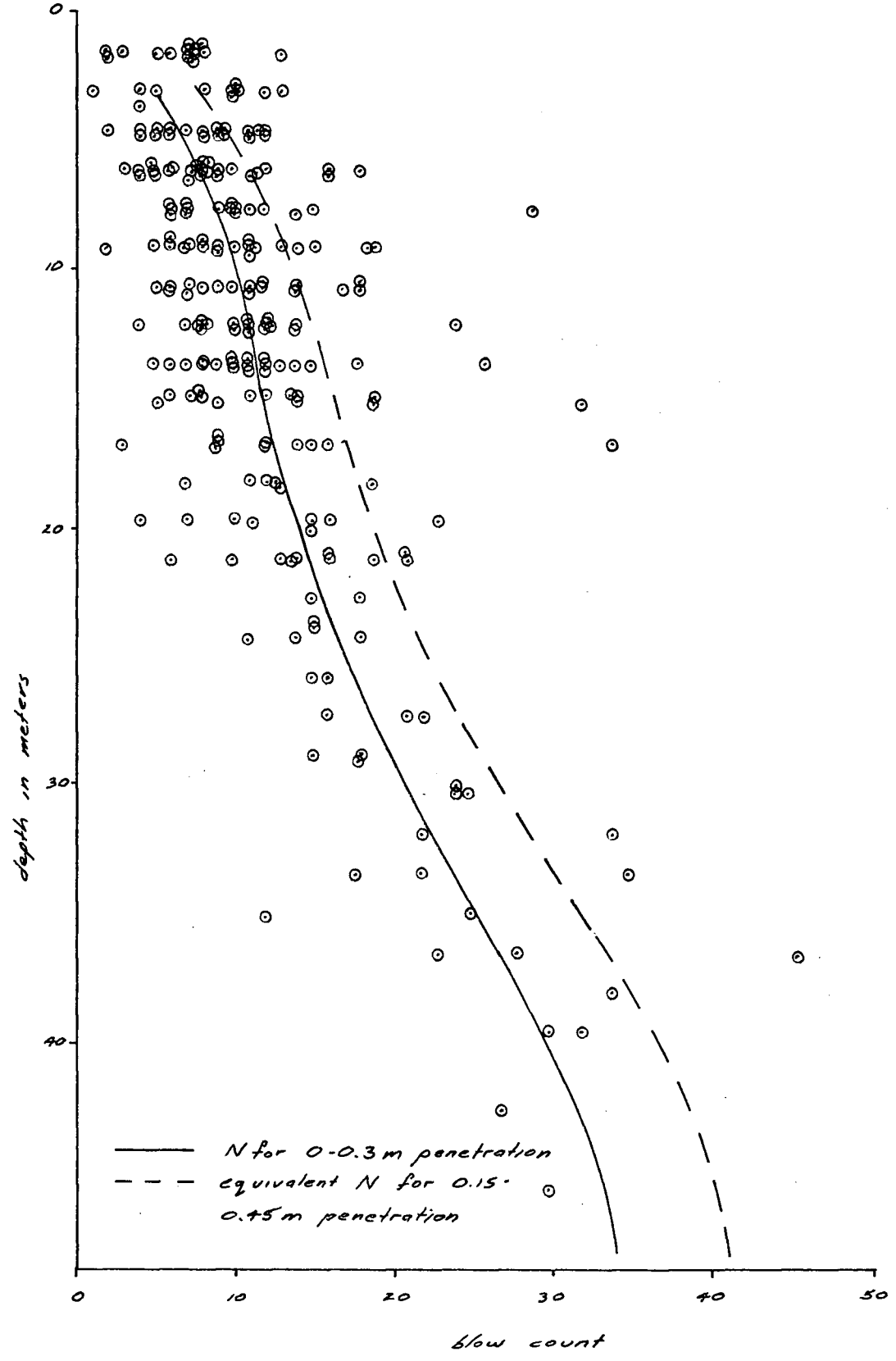

FIG 2-9-11 STURGEON BANK, BLOW COUNT VS. DEPTH IN SAND

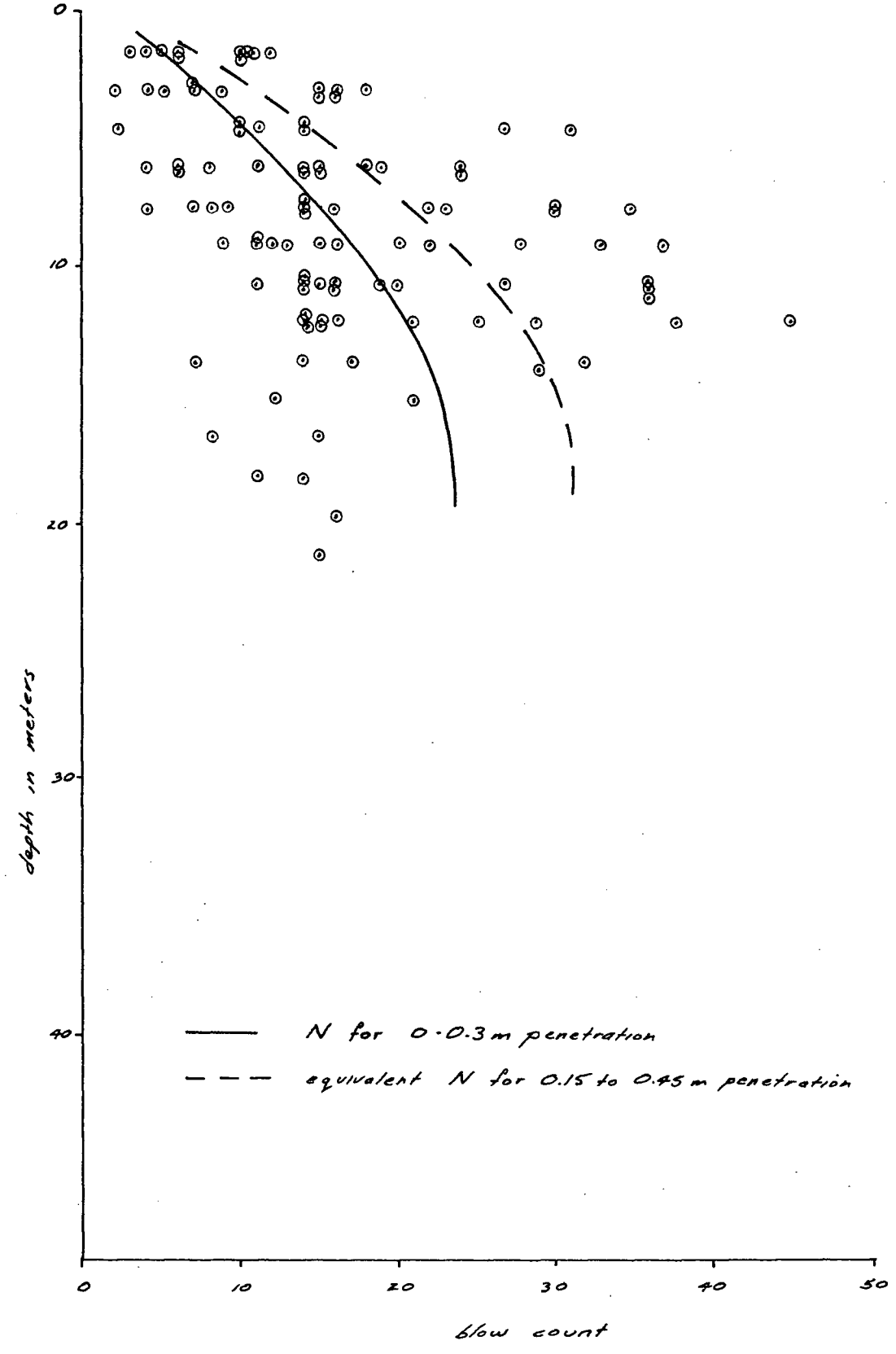

FIG 2-9-12 : TILBURY ISLAND, BLOW COUNT VS. DEPTH IN SAND

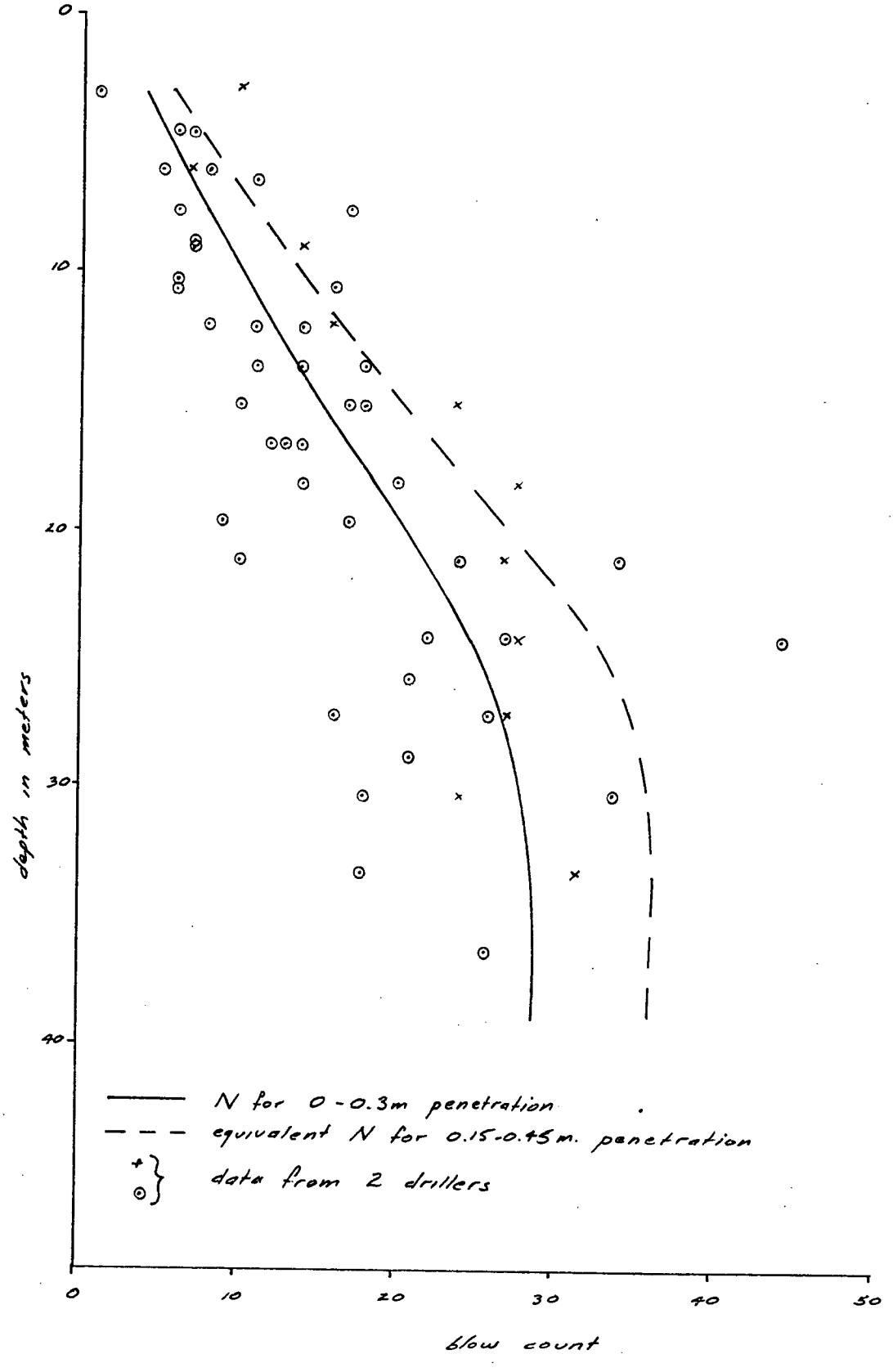

FIG 2-9-13 : SEA ISLAND, BLOW COUNT VS DEPTH IN SAND

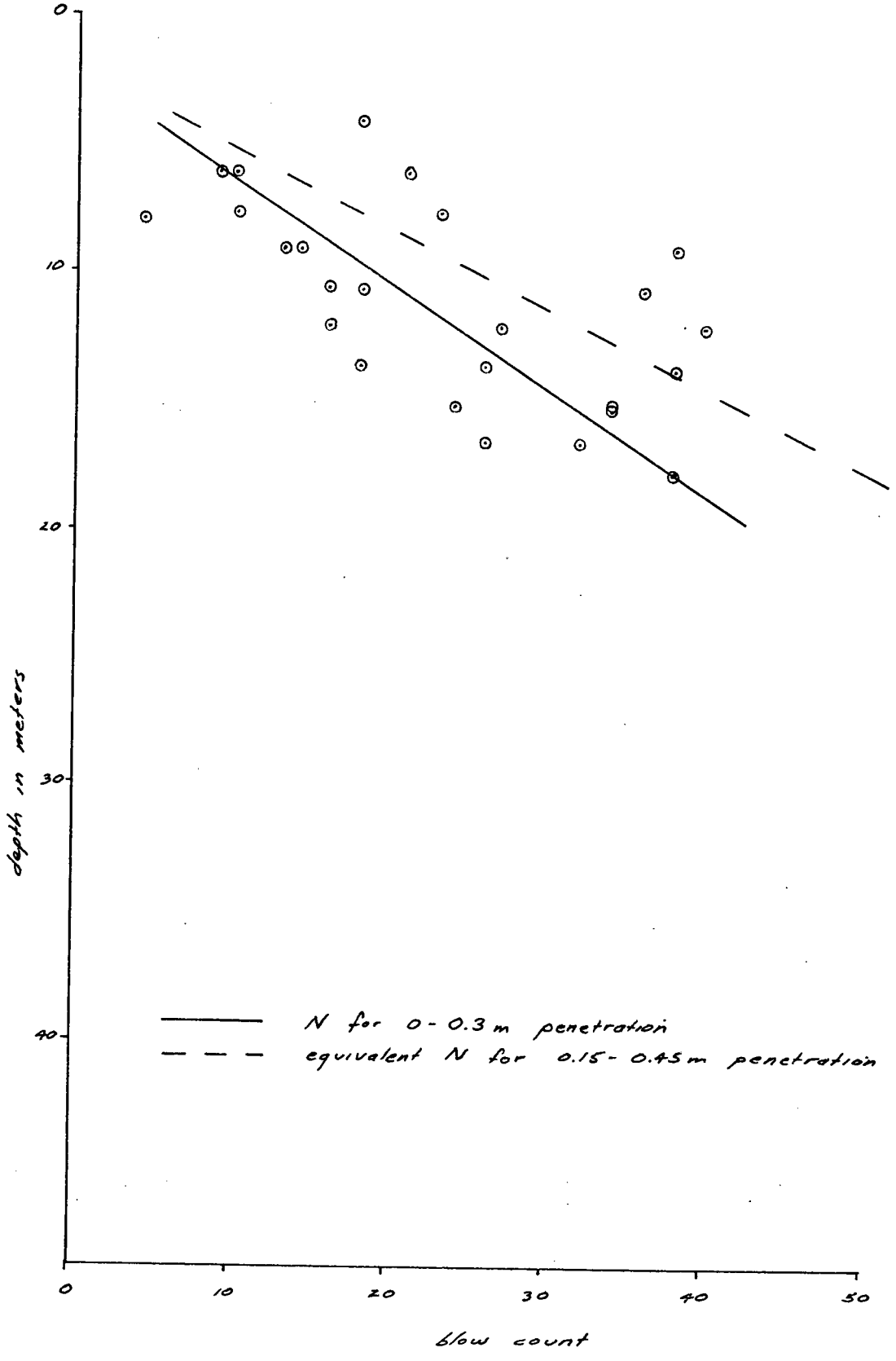

FIG 2-9-14: LADNER, BLOW COUNT VS DEPTH IN SAND

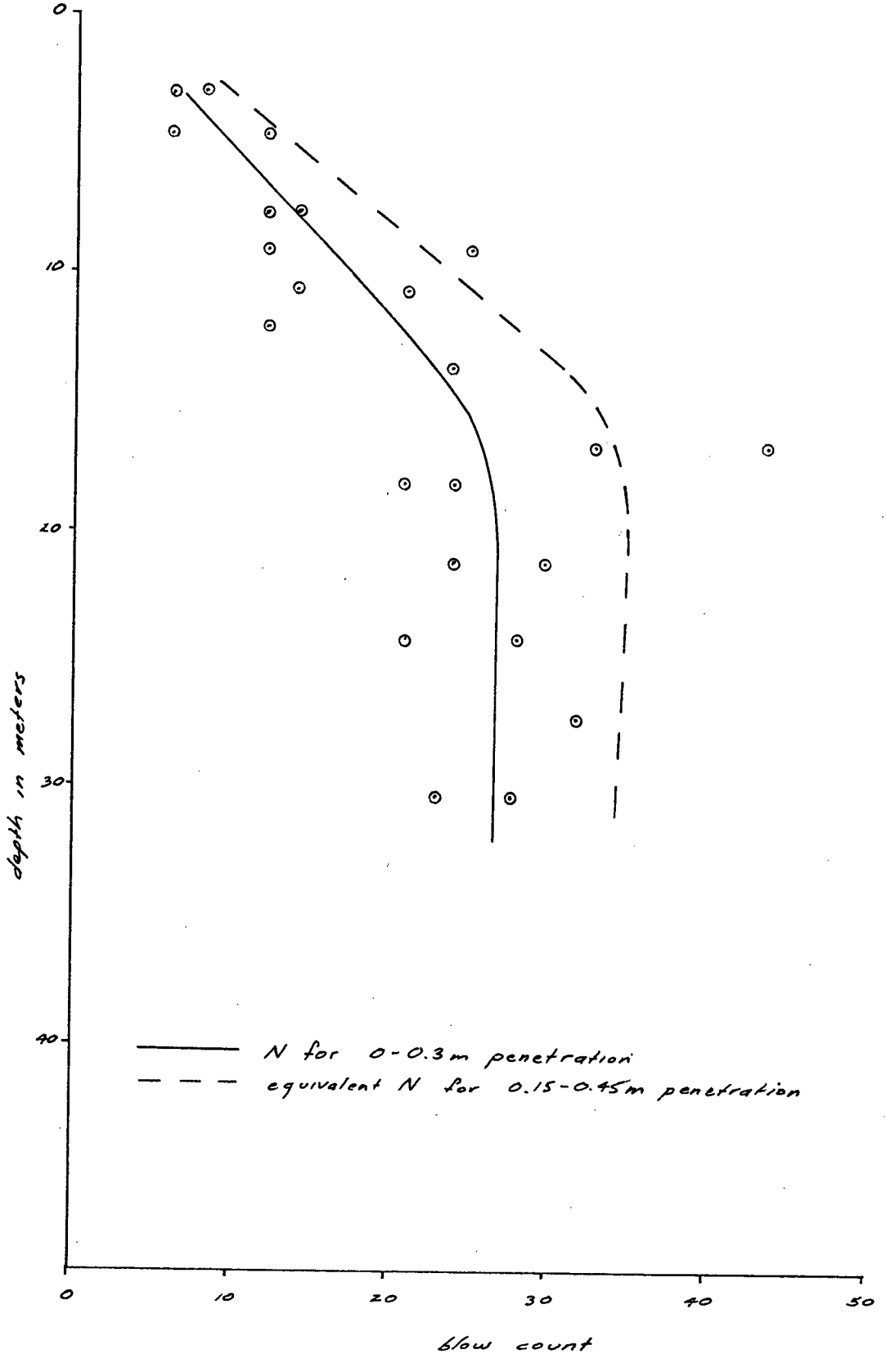

FIG 2-9-15 : ANNACIS ISLAND, BLOW COUNT VS DEPTH IN SAND

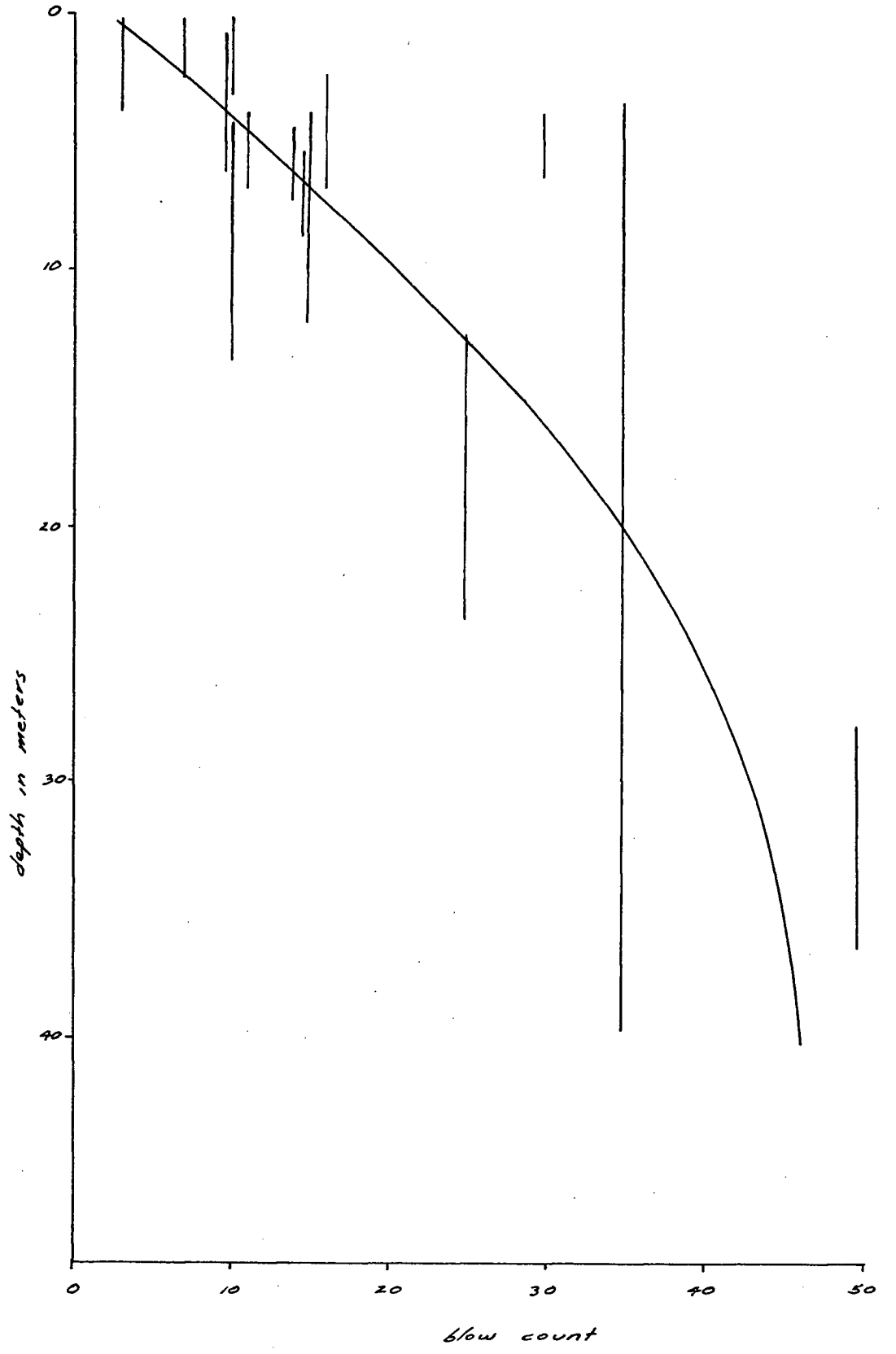

FIG 2-9-16: ANNACIS ISLAND, BLOW COUNT VS. DEPTH IN SAND

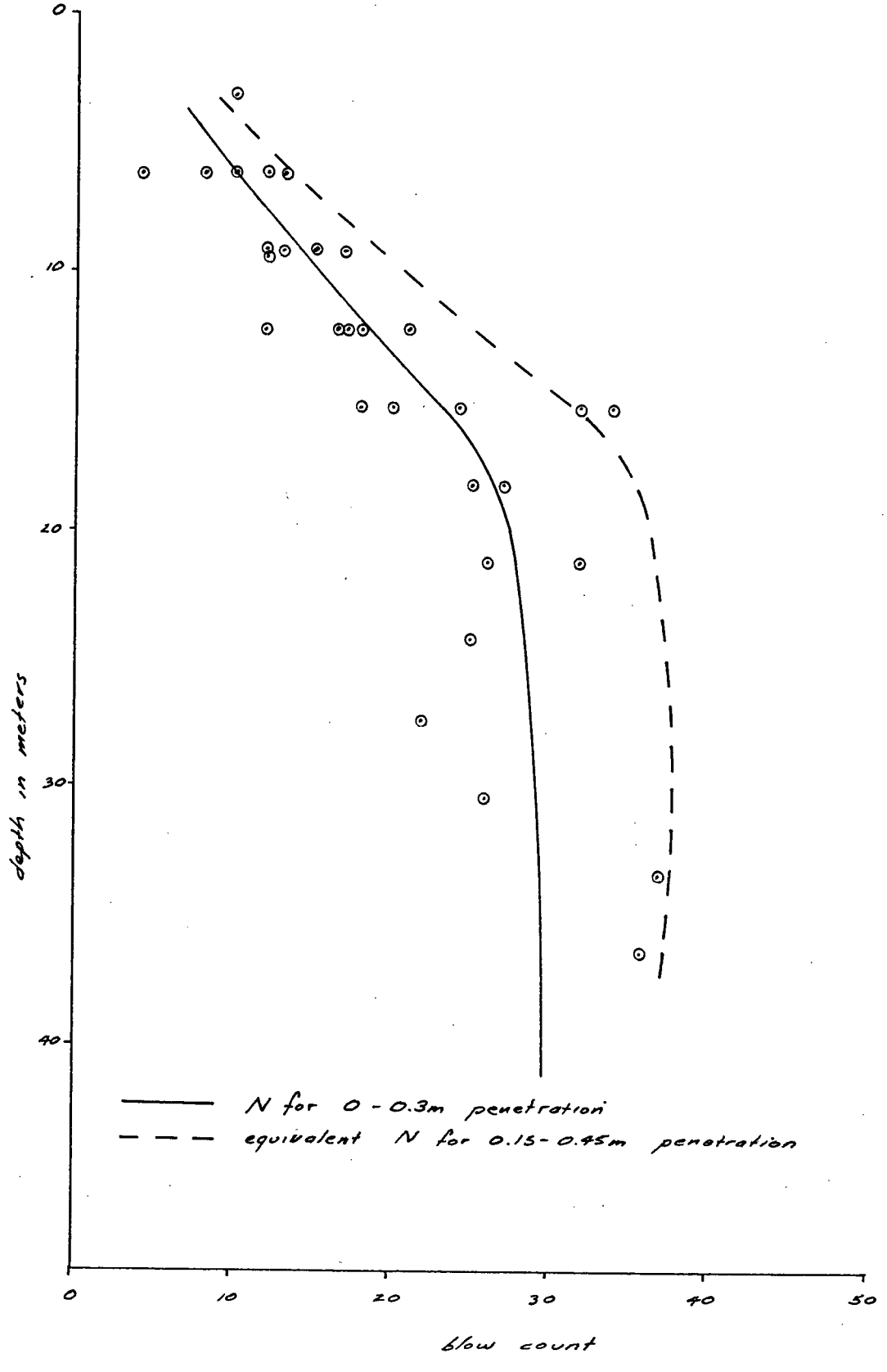

FIG 2-9-17: RICHMOND, BLOW COUNT vs. DEPTH IN SAND

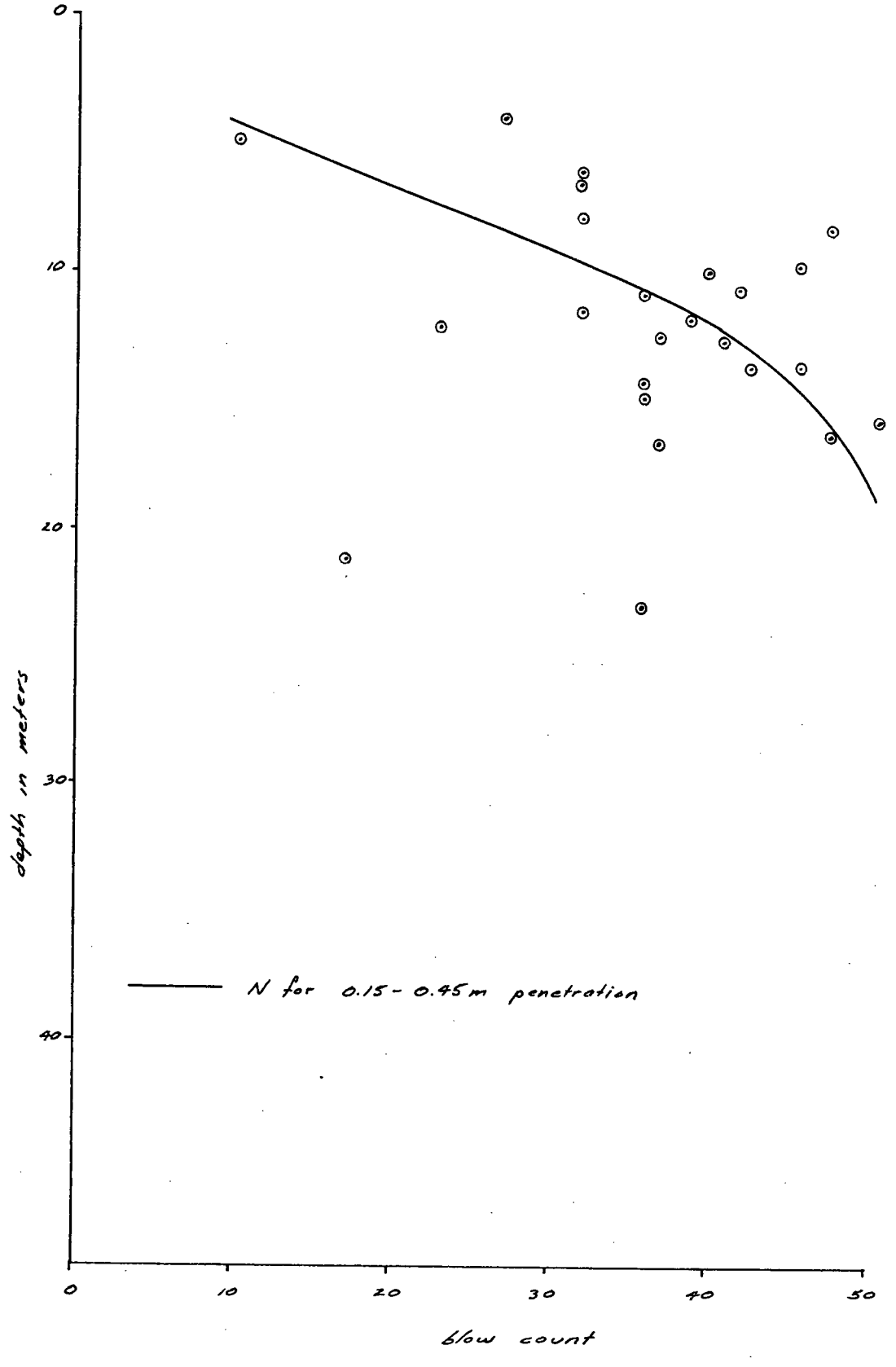

FIG 2-9-18 : HEAD OF DELTA, BLOW COUNT VS DEPTH IN SAND

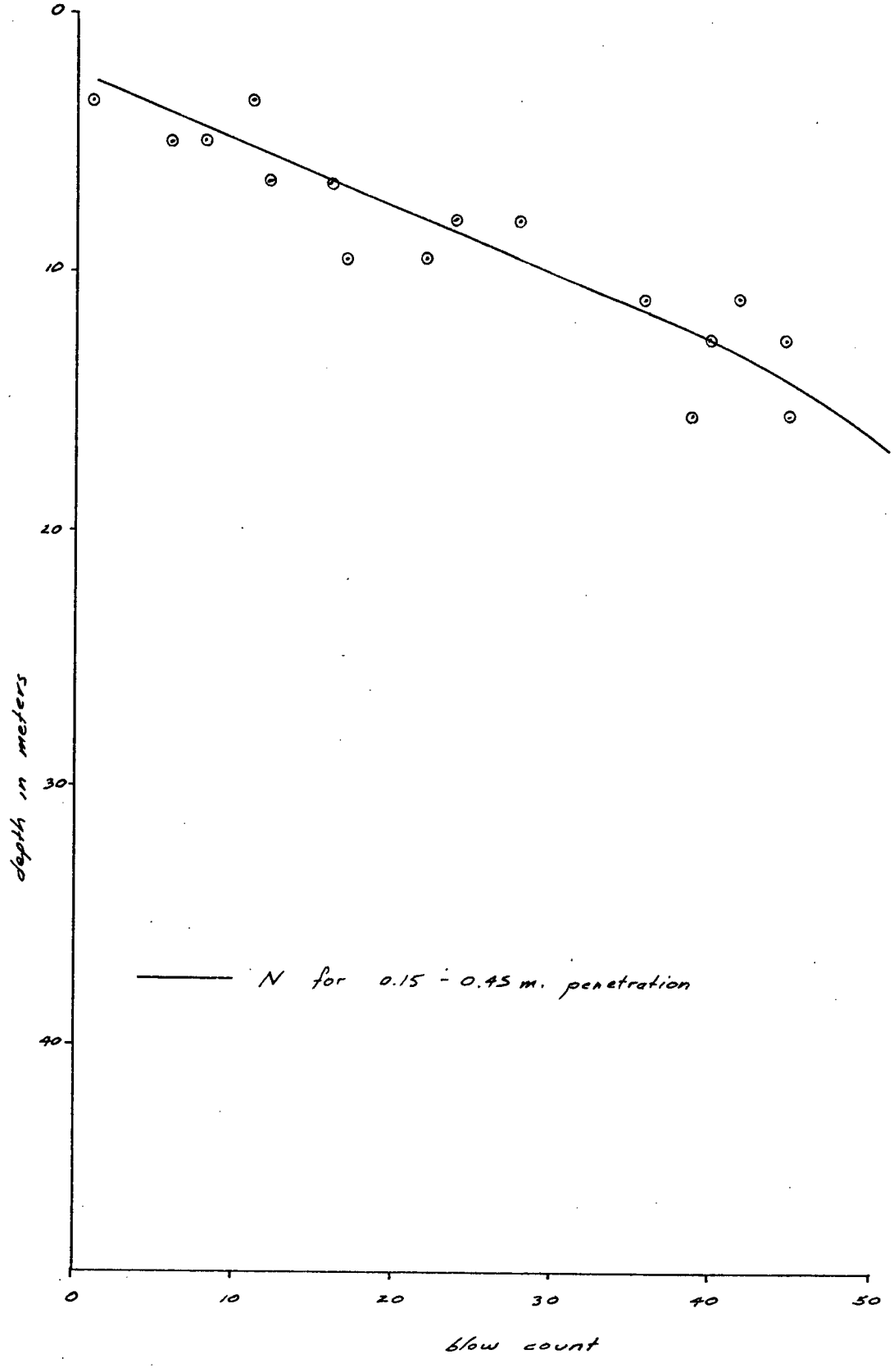

FIG 2-9-19: BYRNE RD., BLOW COUNT VS. DEPTH IN SAND

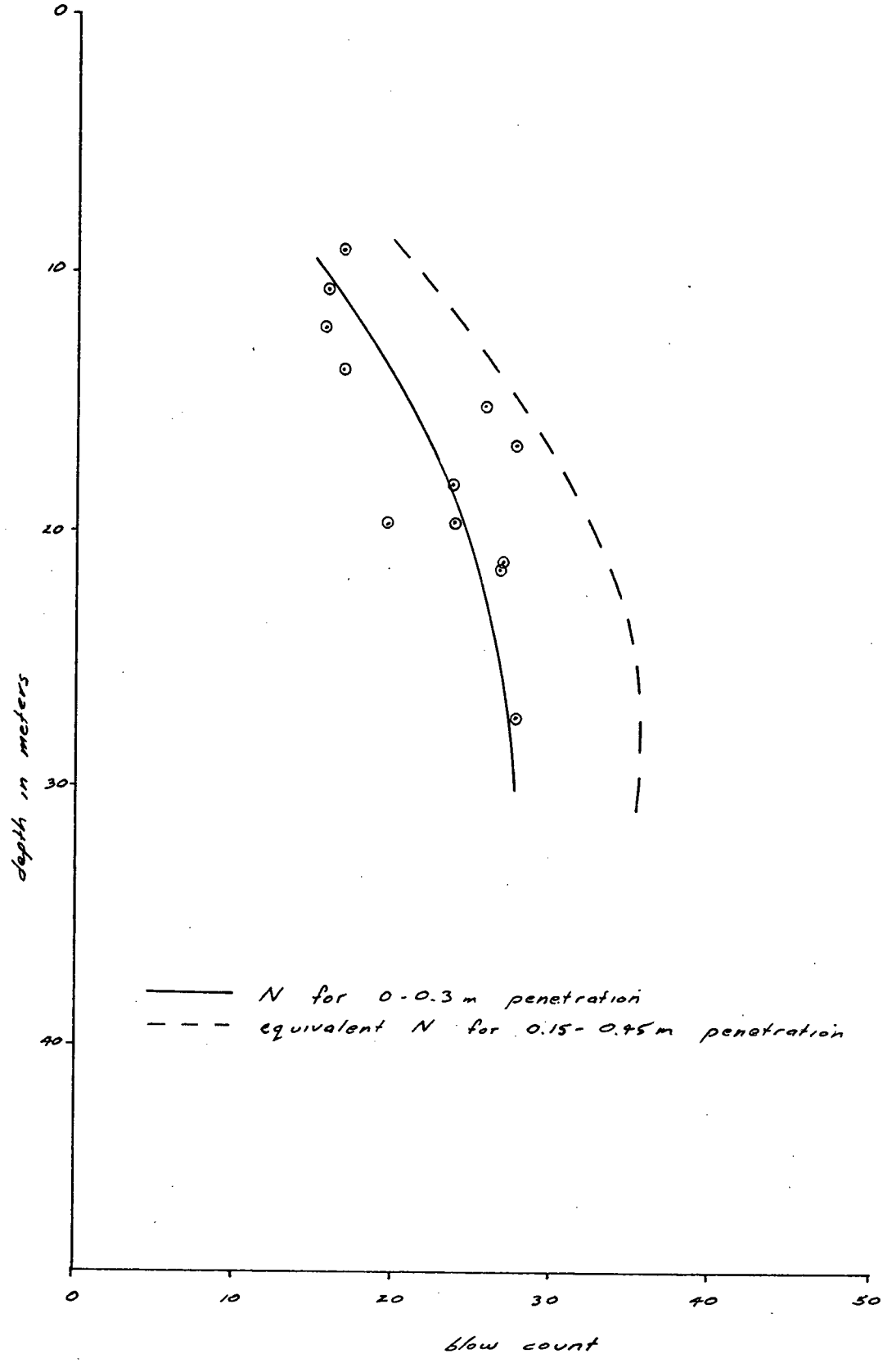

FIG 2-9-20: LULU ISLAND, BLOW COUNT VS. DEPTH IN SAND

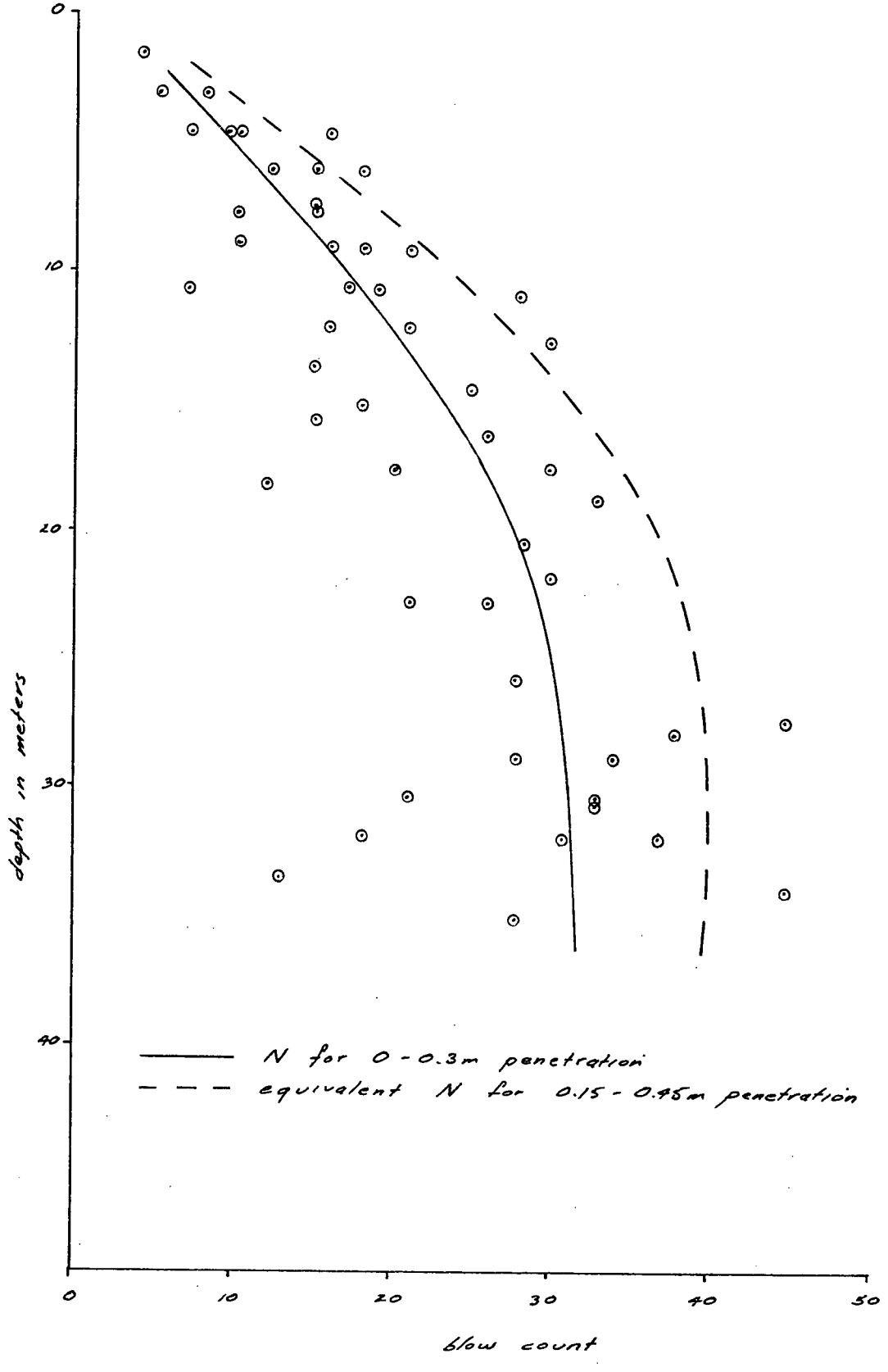

FIG 2-9-21: NORTH RICHMOND, BLOW COUNT VS DEPTH IN SAND

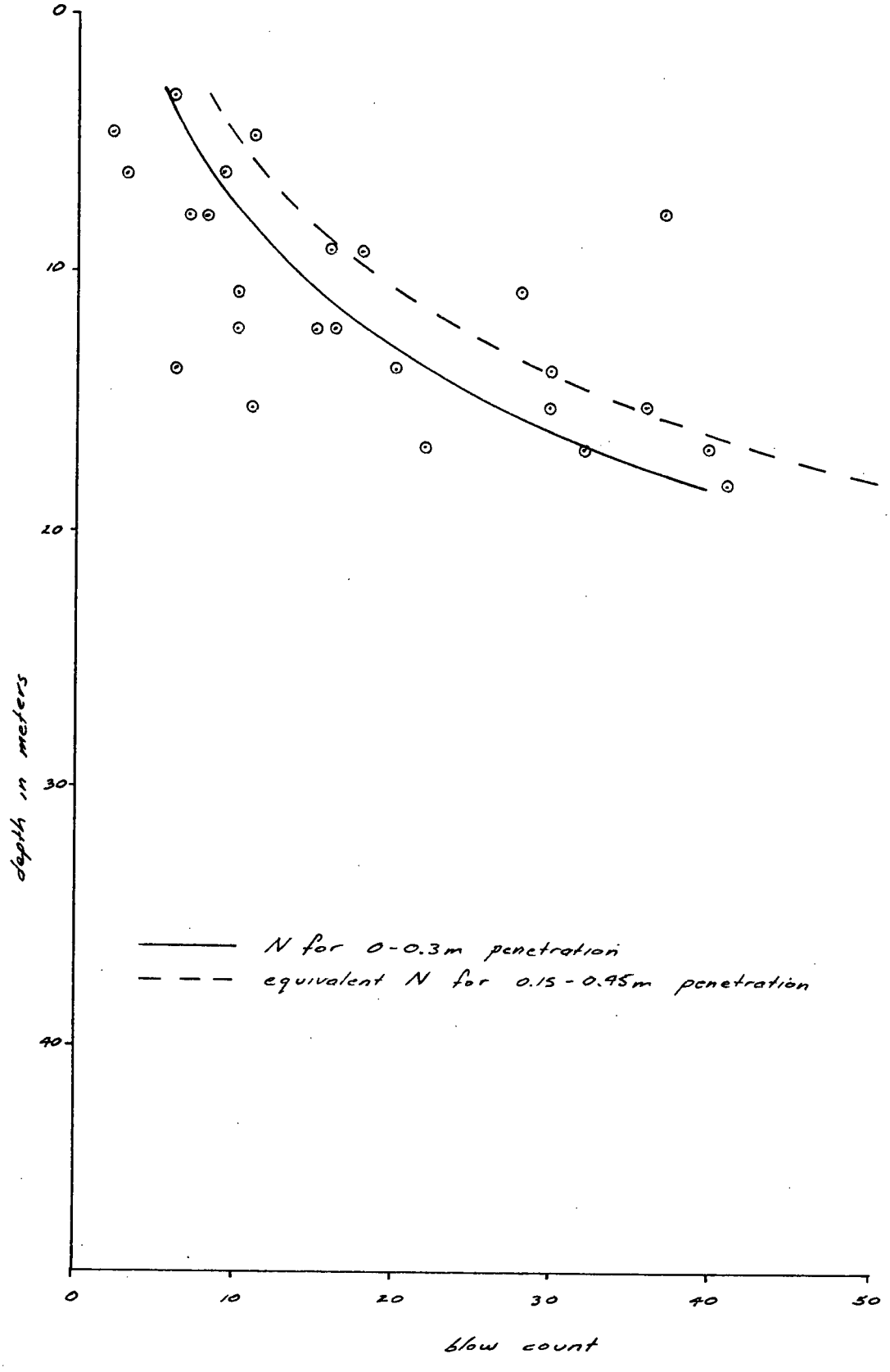

FIG 2-9-22 : SUMMARY, BLOW COUNT vs DEPTH IN SAND

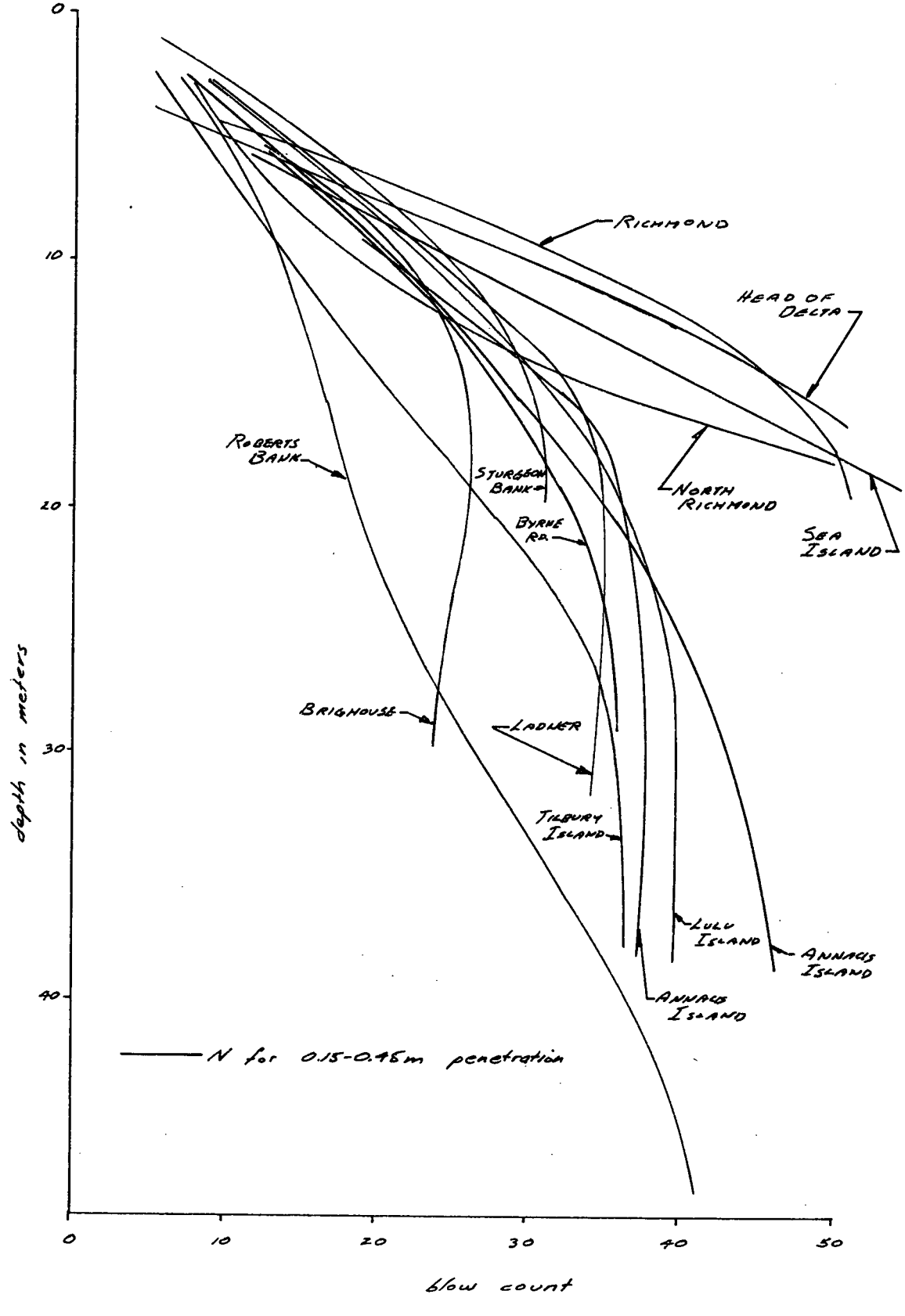

TABLE 2-10-1

RELATIVE DENSITY DATA

DEPTH meters	DRY DENSITY kN/m³	RELATIVE DENSITY %	BLOW COUNT 0-0.3m PENETRATION	EQUIVALENT BLOW COUNT 0.15-0.75m PENETRATION
1.5	14.6	45	8 9	11.2
6	15.5	74	13 22	17.9
10.6	14.6	62	16 26	21.7
20	15.1	29	22 40	30
29	16.0	76	29 41	37.1

FIG 2-10-1 : BLOW COUNT - RELATIVE DENSITY RELATIONSHIPS

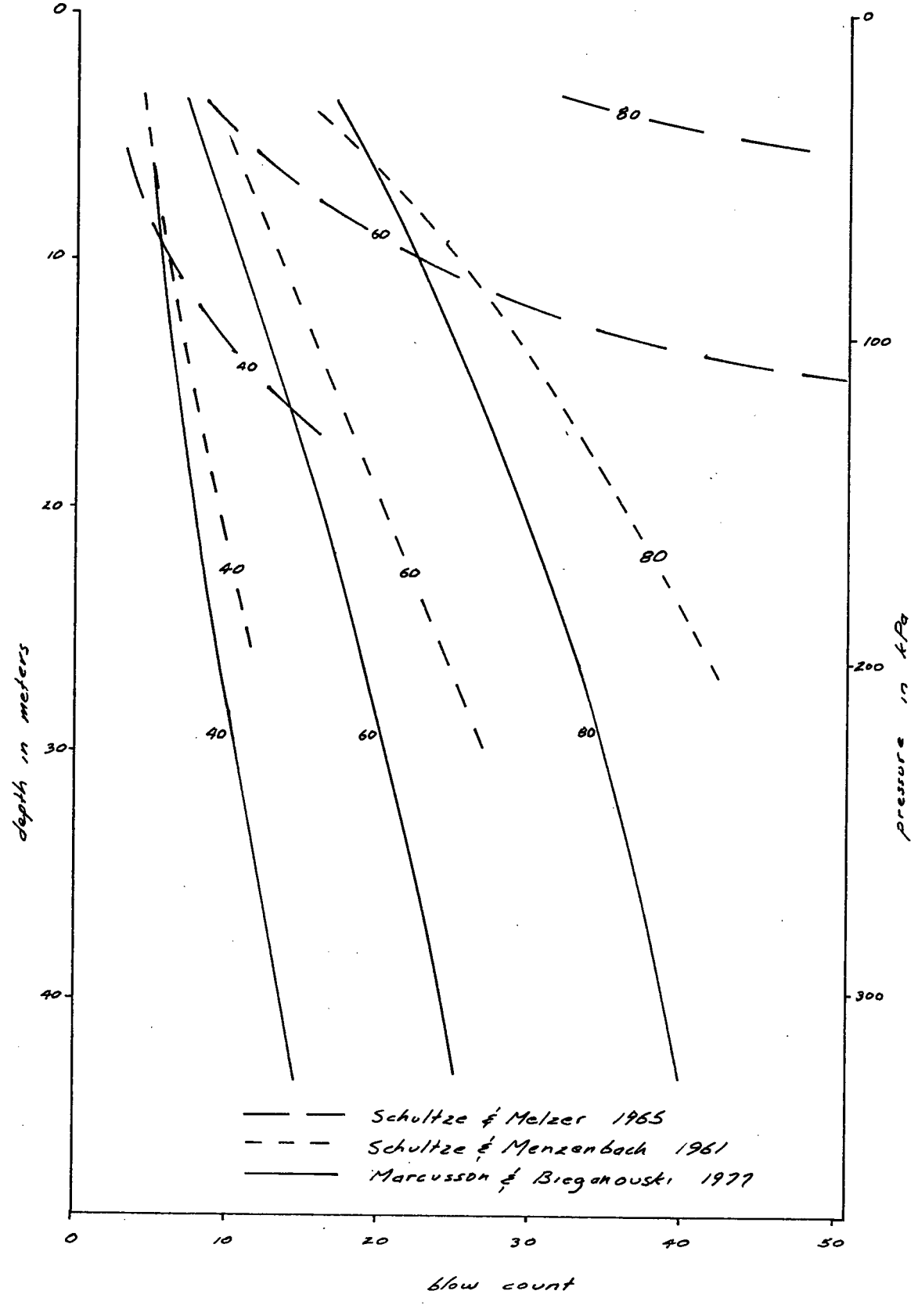

FIG 2-10-2 : BLOW COUNT - RELATIVE DENSITY RELATIONSHIPS

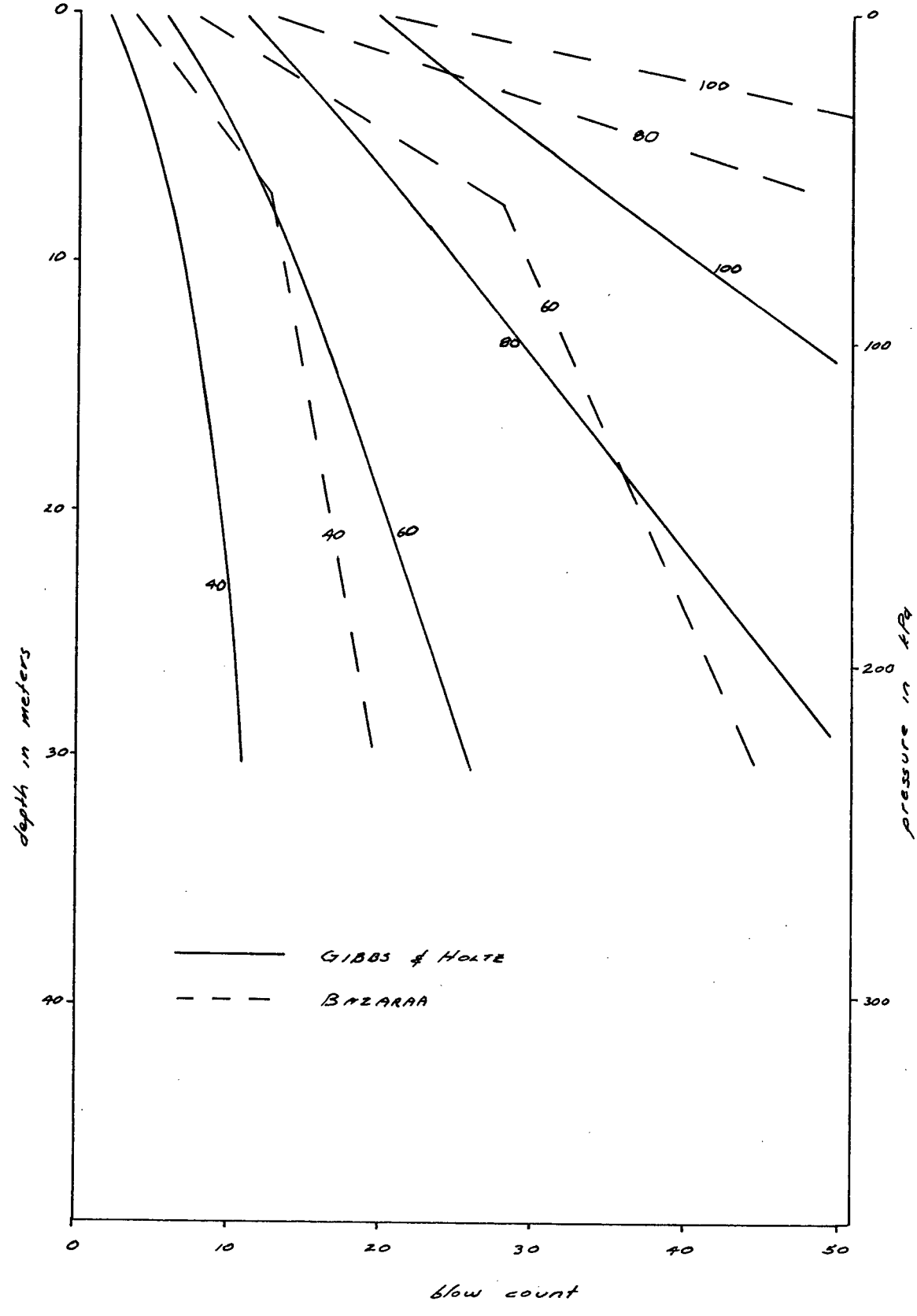

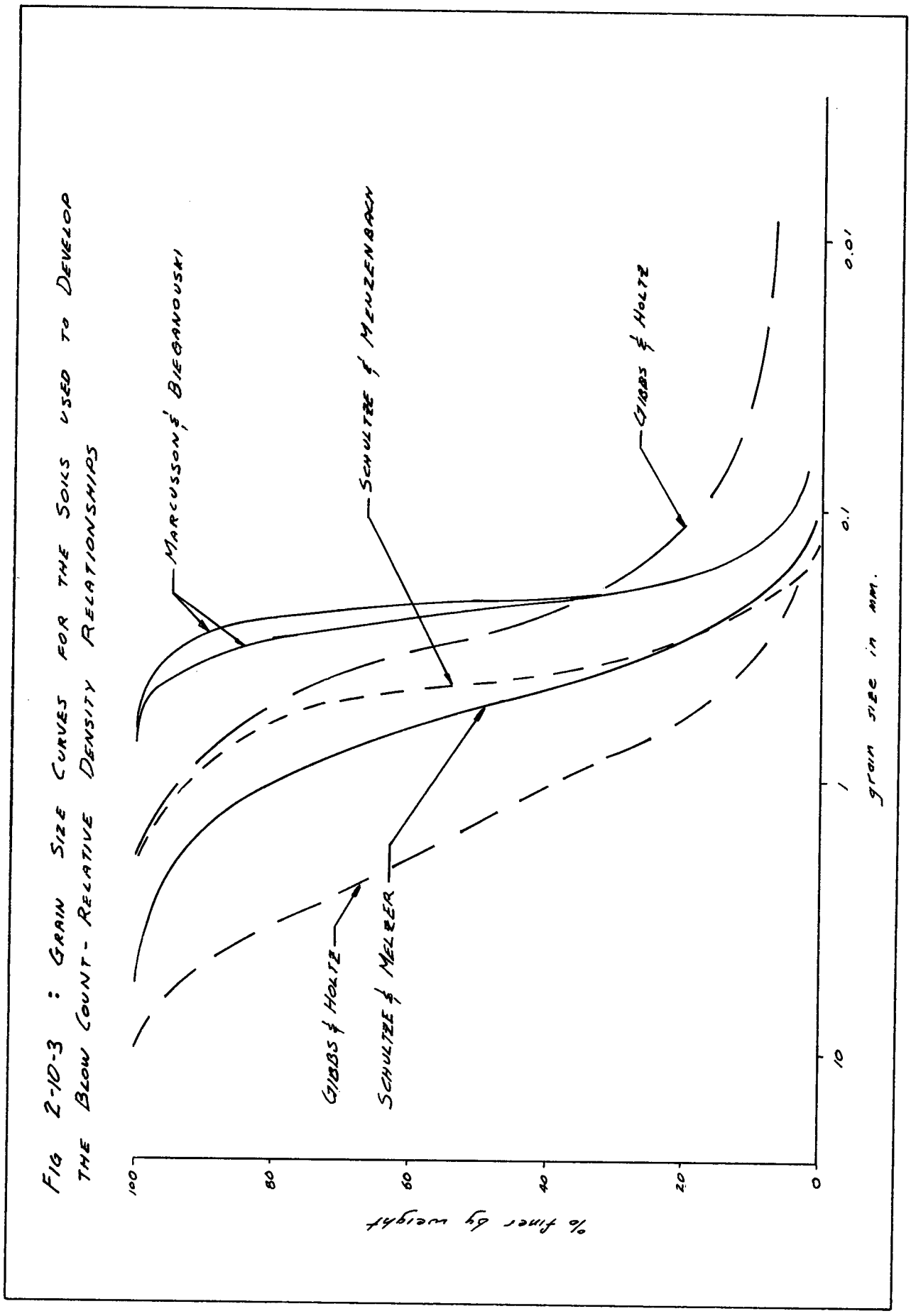

FIG 2-10-3 : GRAIN SIZE CURVES FOR THE SOILS USED TO DEVELOP THE BLOW COUNT - RELATIVE DENSITY RELATIONSHIPS

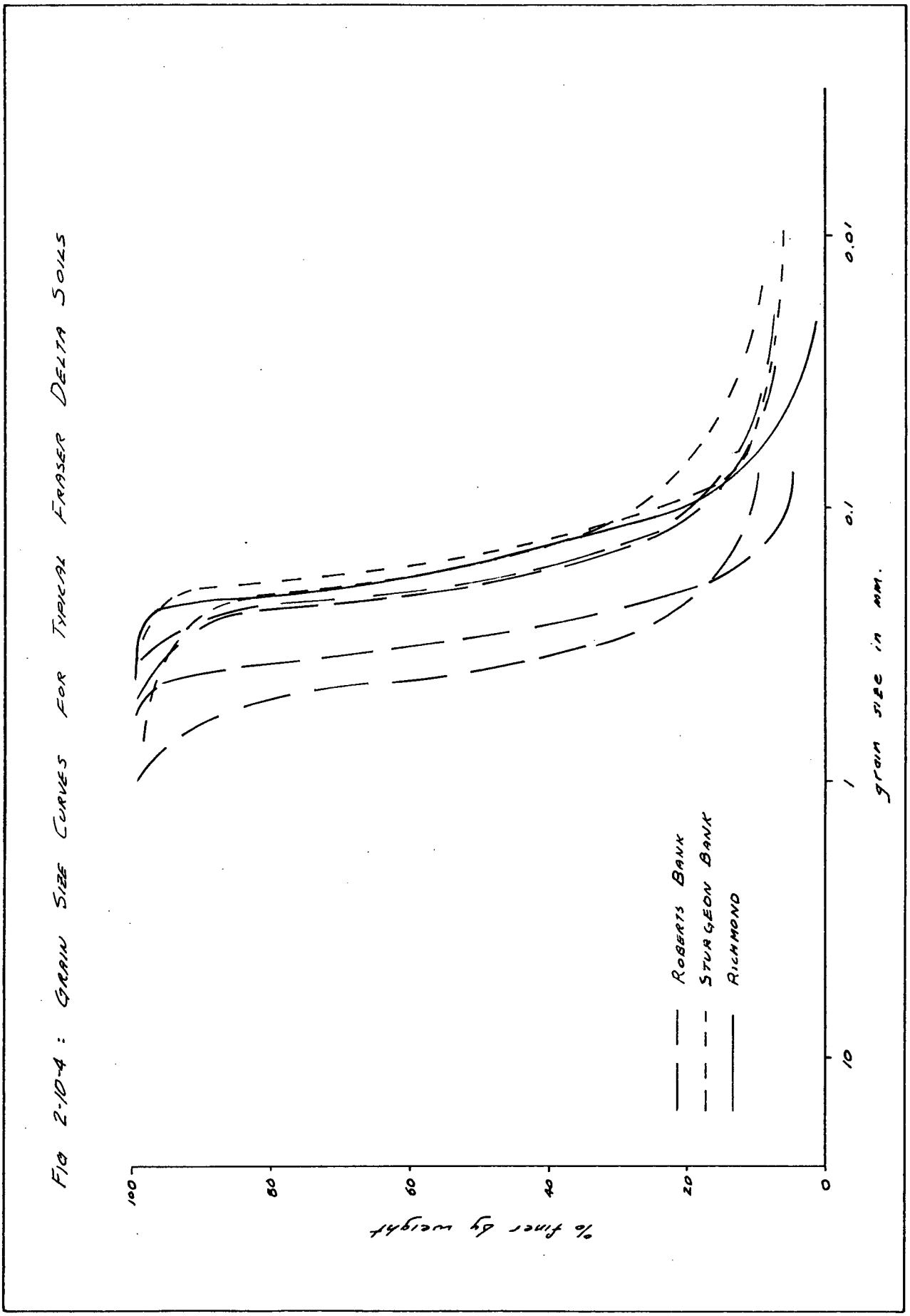

FIG 2-10-4 : GRAIN SIZE CURVES FOR TYPICAL FRASER DELTA SOILS

FIG 2-10-5: RELATION BETWEEN RELATIVE DENSITY AND BLOW COUNT WITH DEPTH AT A PARTICULAR SITE

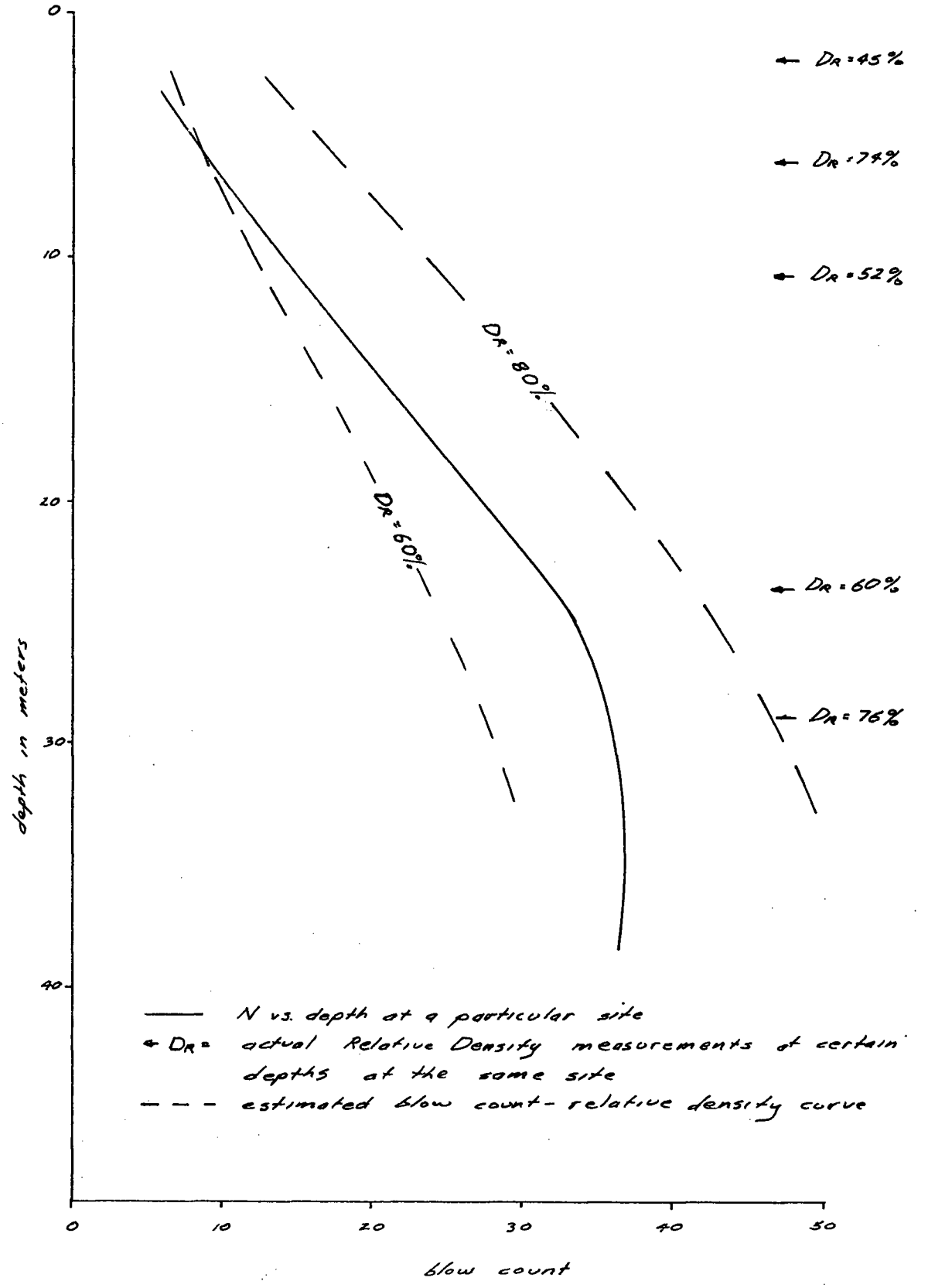

FIG 2-11-1 : SAND, FRICTION ANGLE vs DRY DENSITY

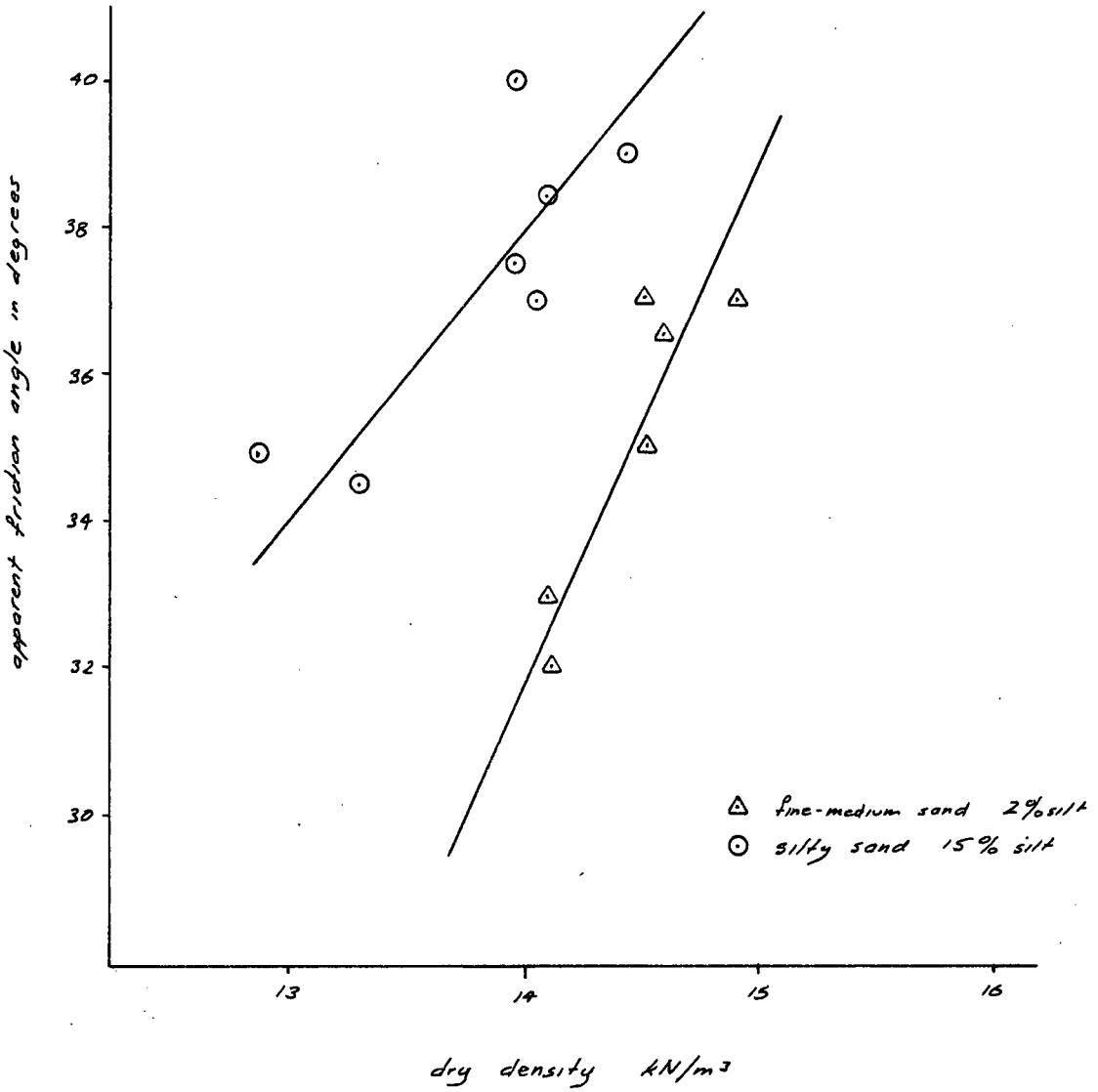

FIG 2-11-2: VARIATION OF BLOW COUNT WITH DEPTH & FRICTION ANGLE

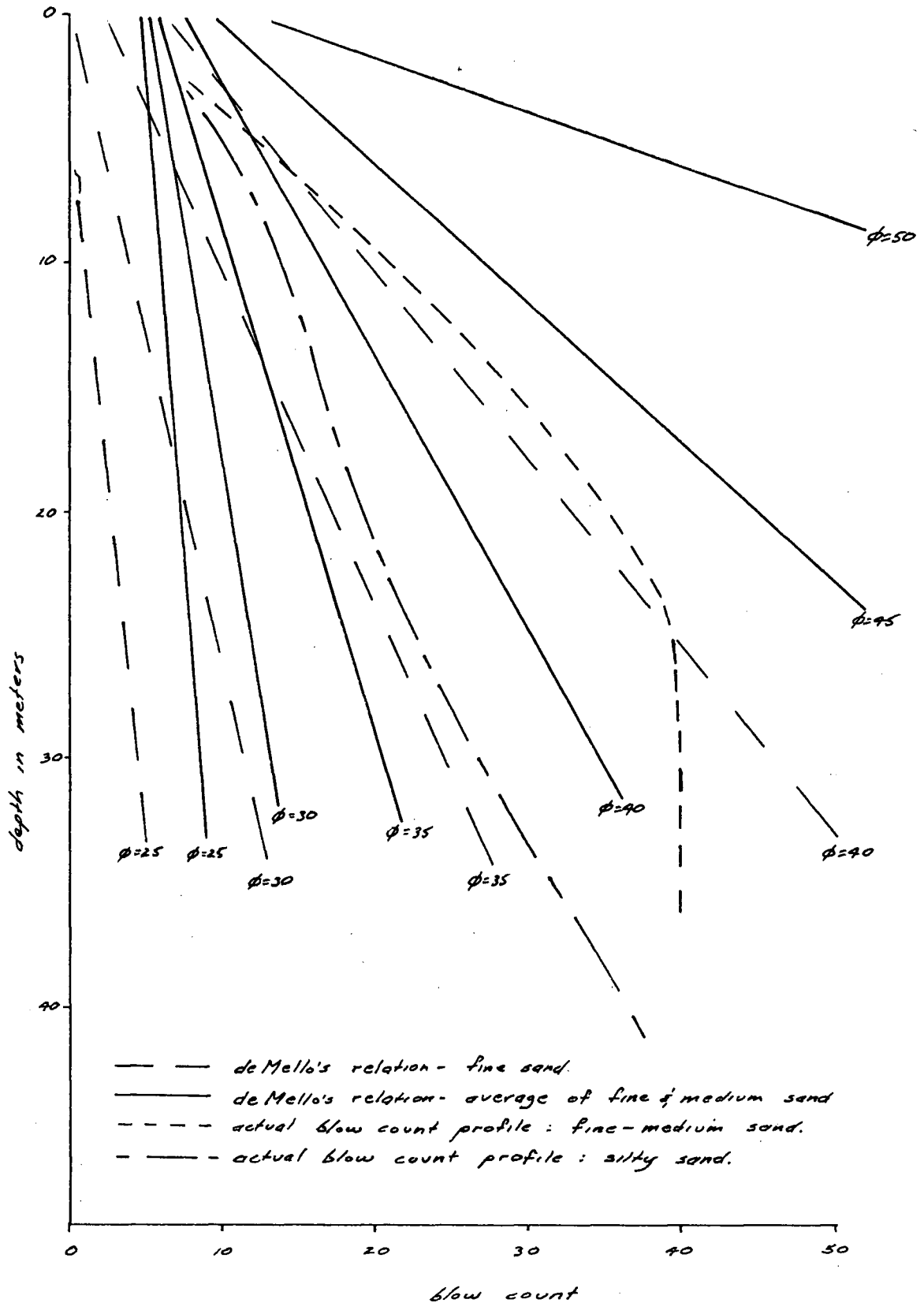

FIG 3-1-1 : HYSTERETIC STRESS-STRAIN PATH

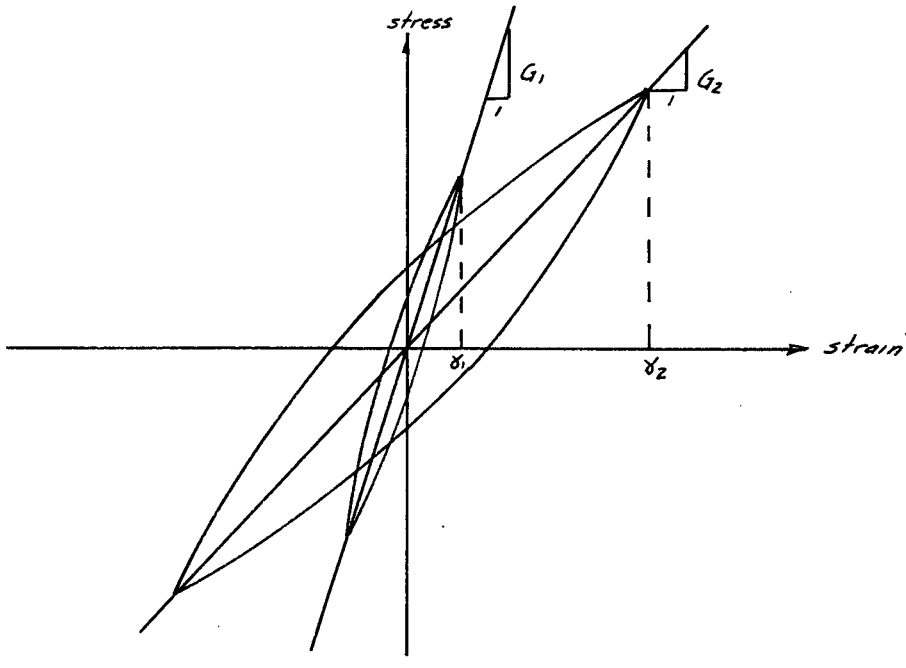

FIG 3-1-2 : DEFINITION OF SHEAR MODULUS AND DAMPING

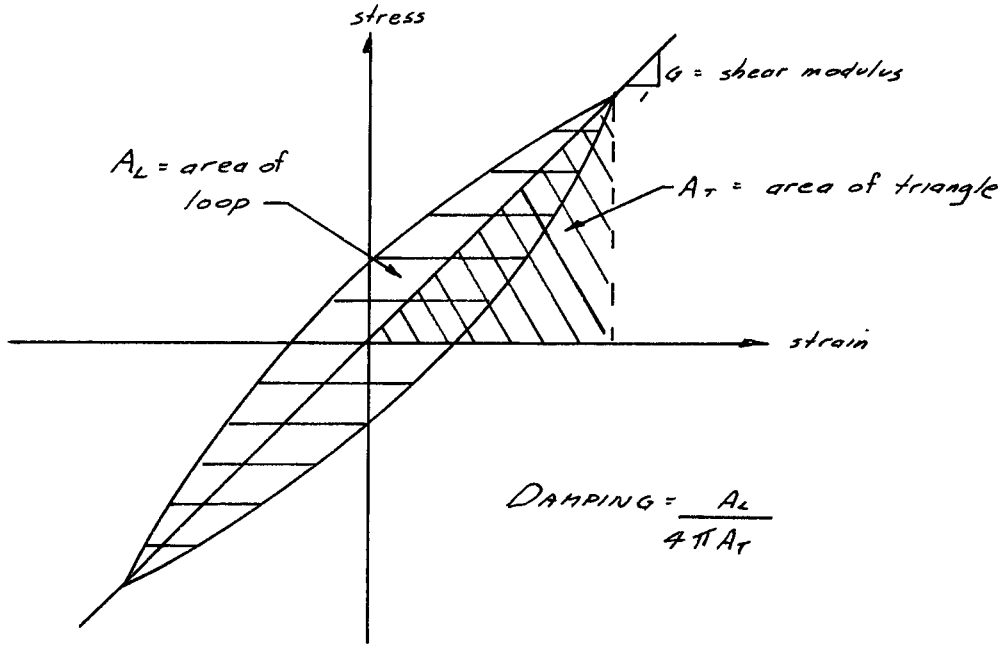

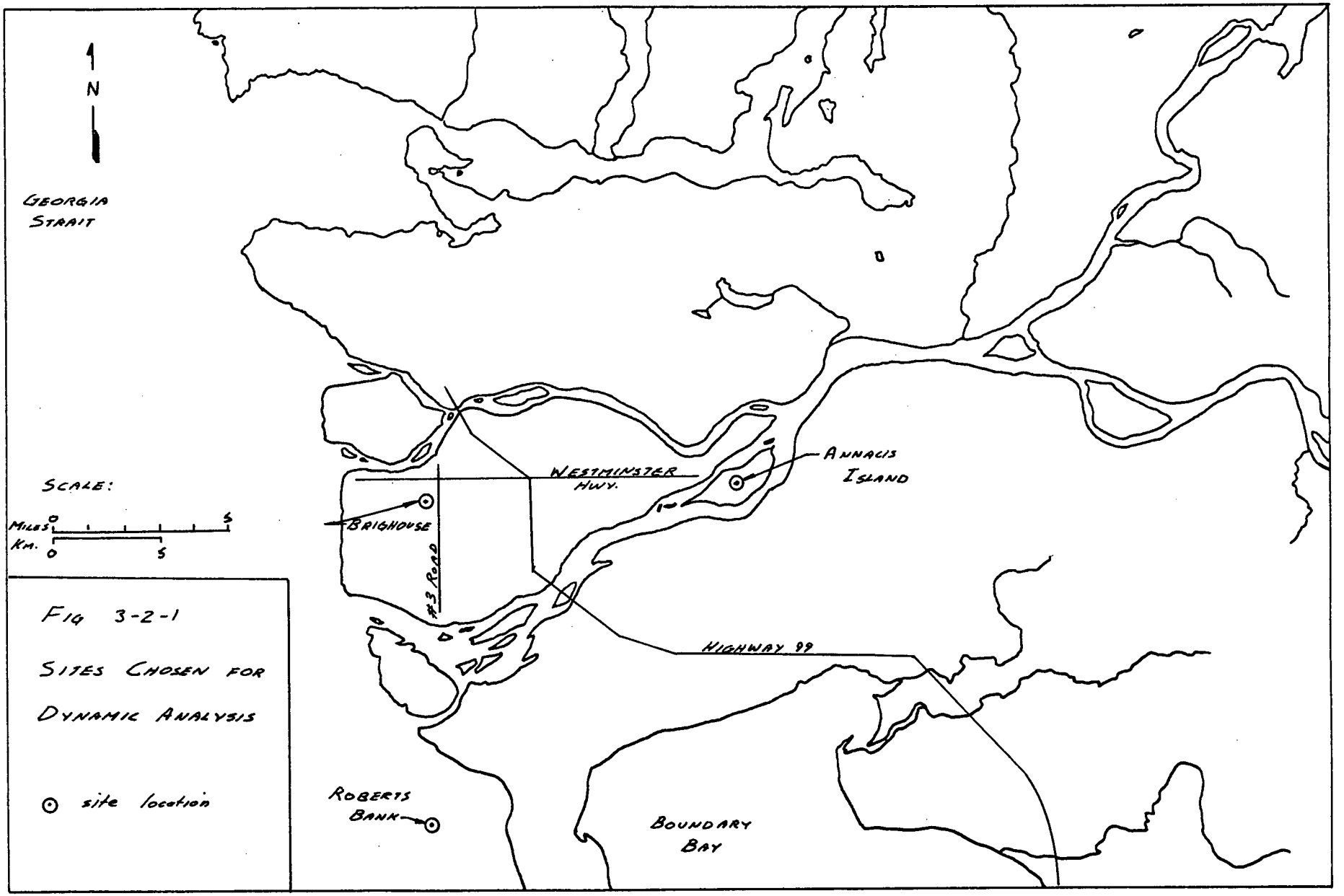

FIG 3-2-1

SITES CHOSEN FOR DYNAMIC ANALYSIS

⊙ site location

FIG 3-2-2 ROBERTS BANK : SOIL PROFILE & SOIL MODEL

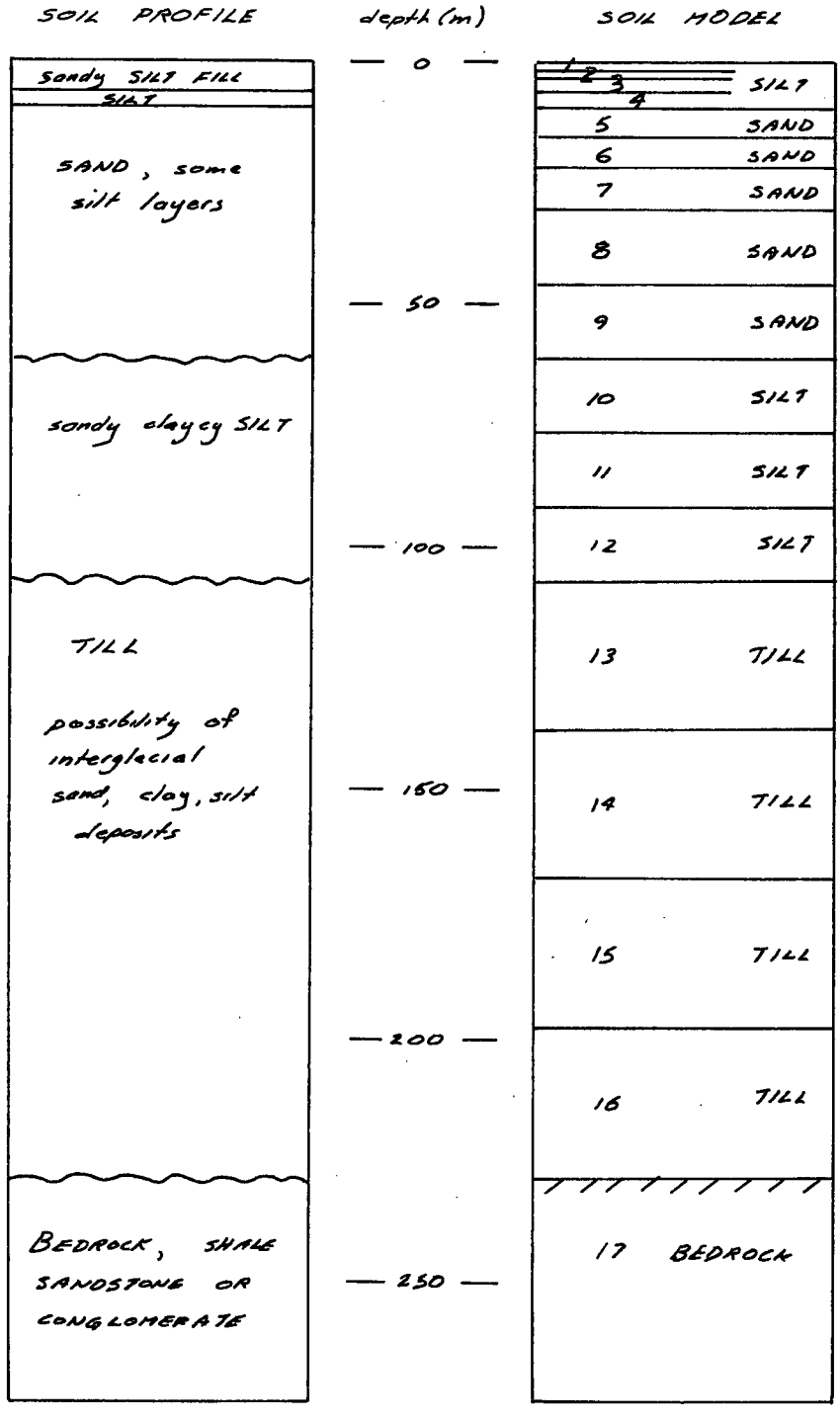

FIG 3-2-3 ANNACIS ISLAND : SOIL PROFILE & SOIL MODEL

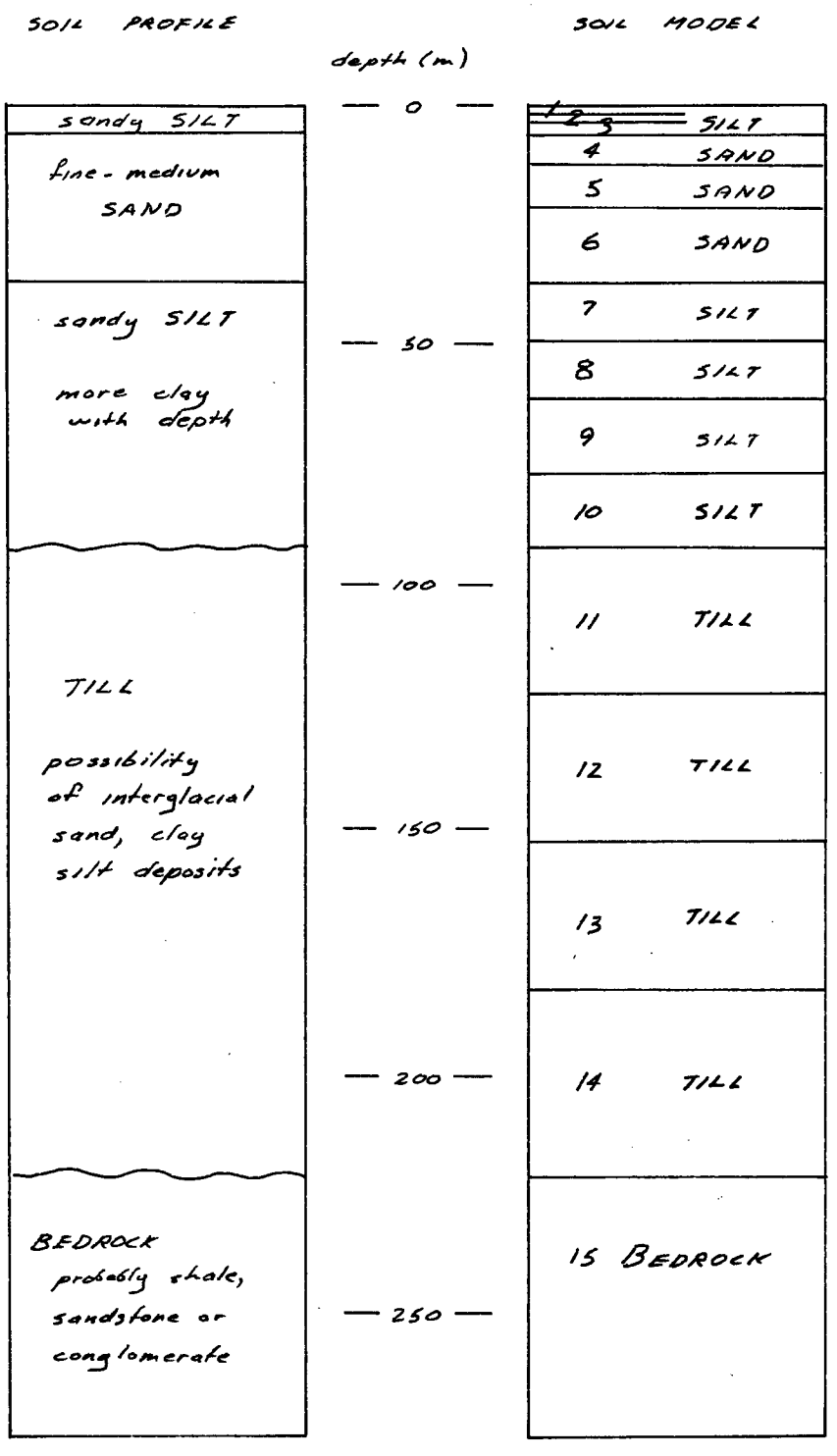

FIG 3-2-4 BRIGHOUSE: SOIL PROFILE & SOIL MODEL

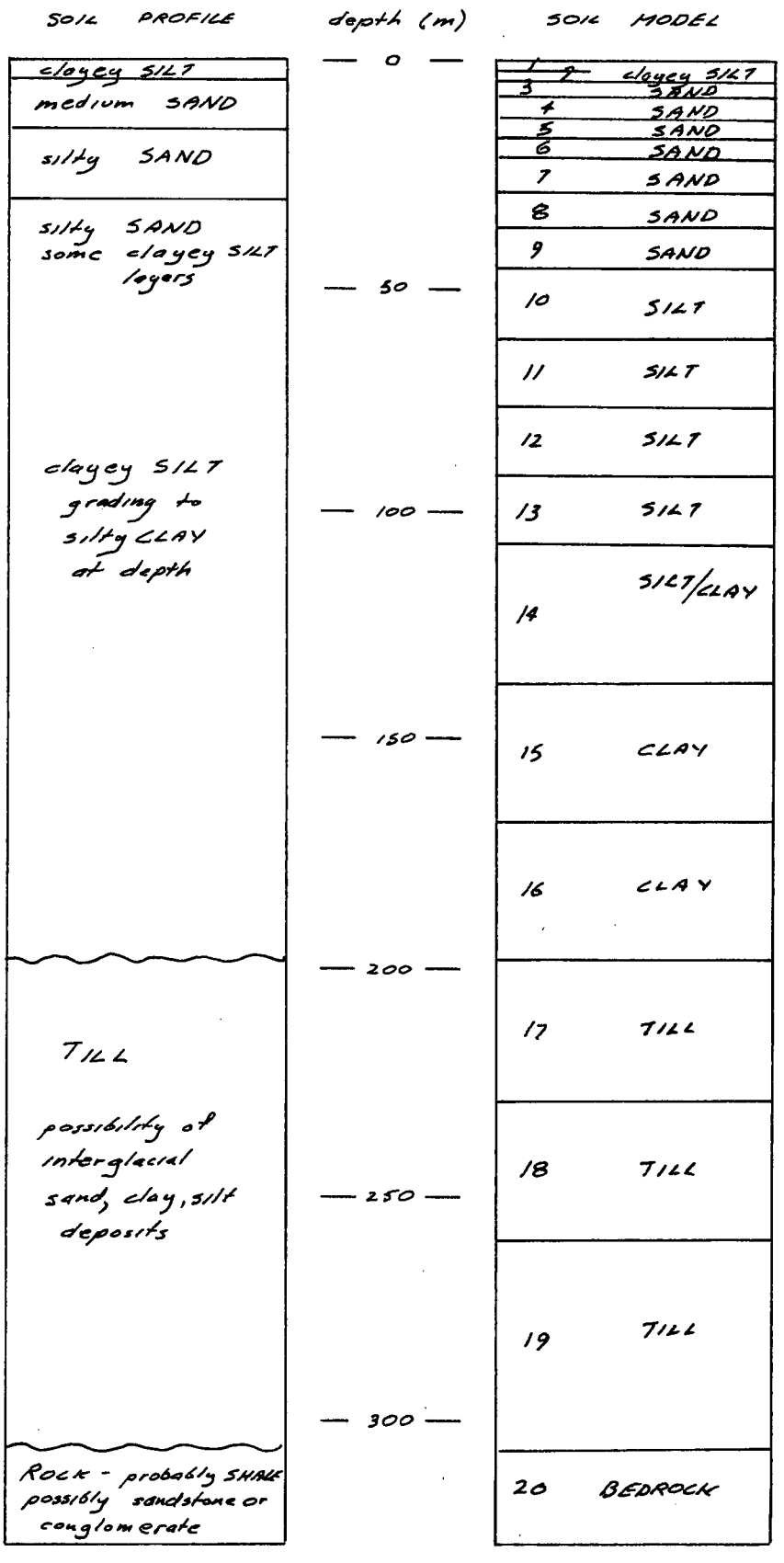

FIG 3-2-5 ROBERTS BANK : MAXIMUM SHEAR MODULUS

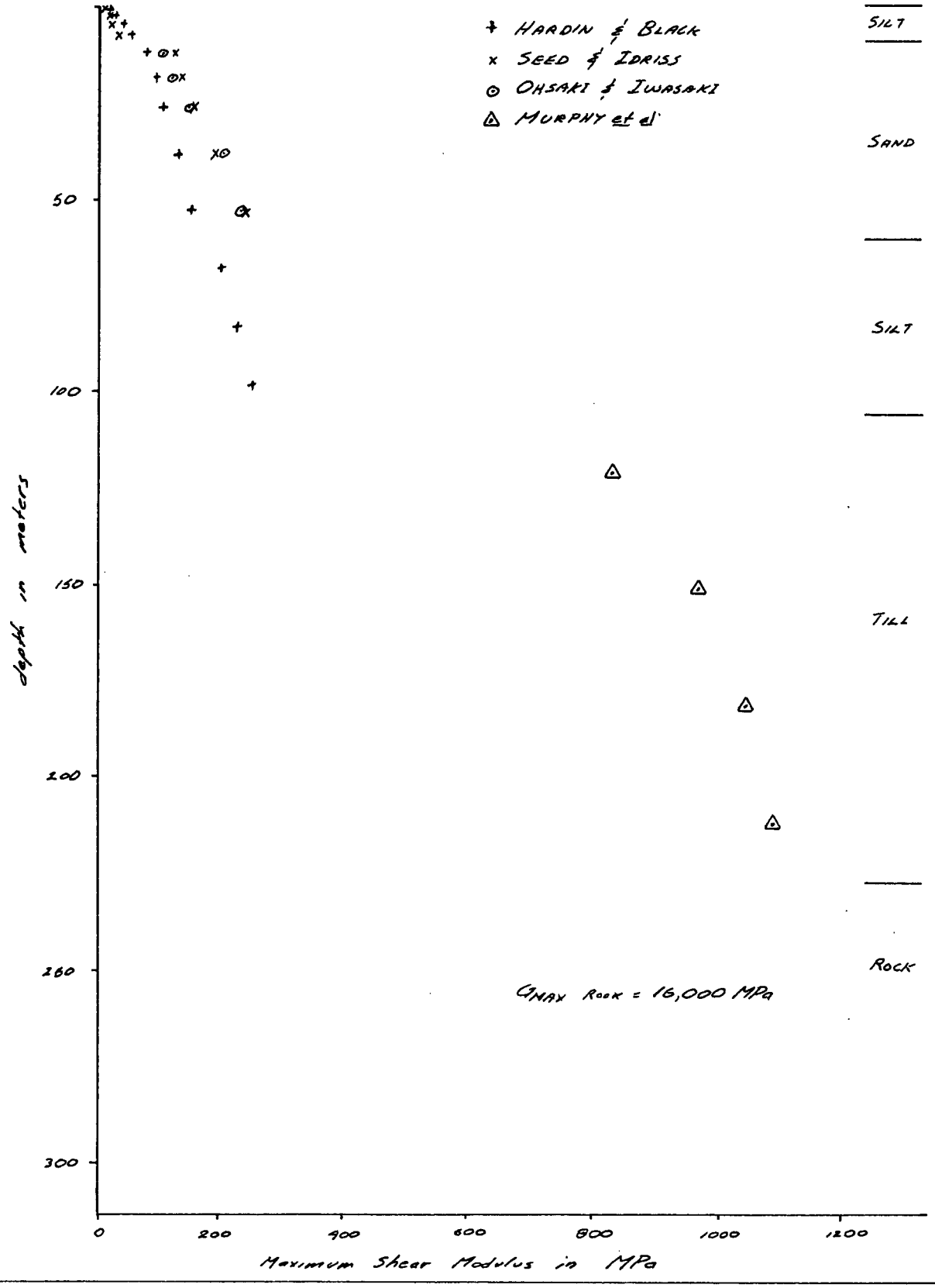

FIG 3-2-6: ANNACIS ISLAND: MAXIMUM SHEAR MODULUS

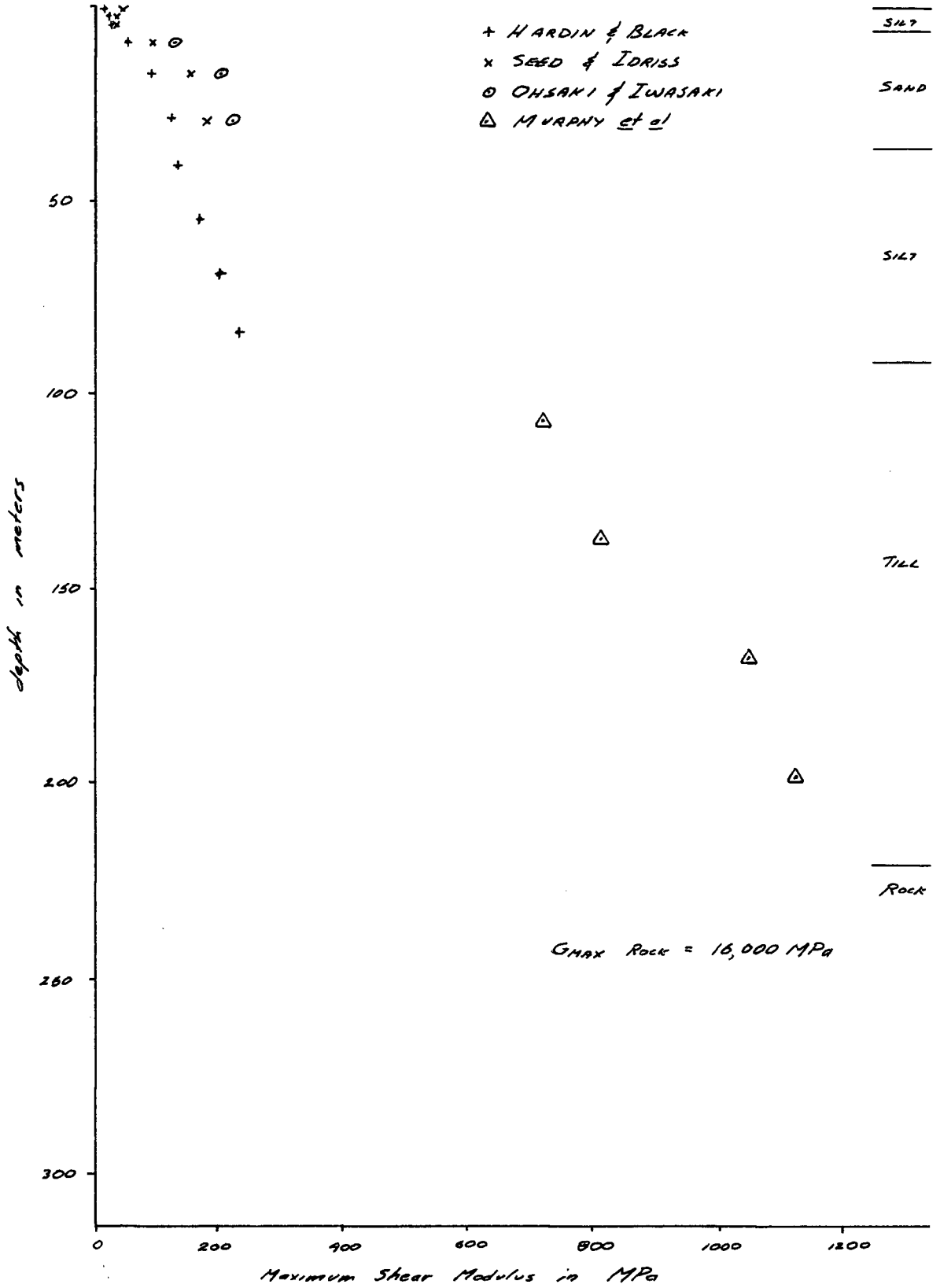

FIG 3-2-7 BRIGHOUSE : MAXIMUM SHEAR MODULUS

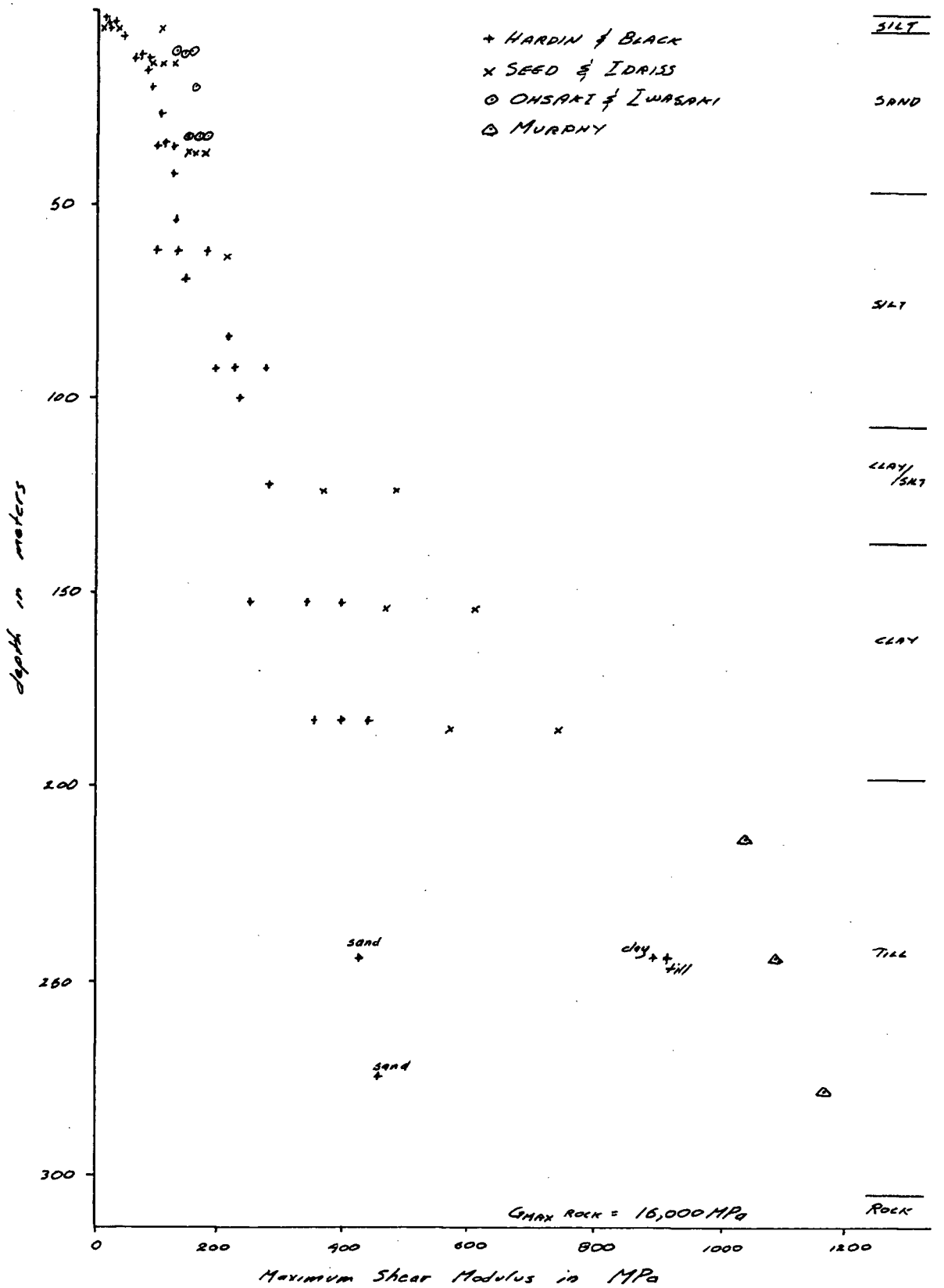

FIG 3-2-B ROBERTS BANK : MAXIMUM DAMPING RATIO

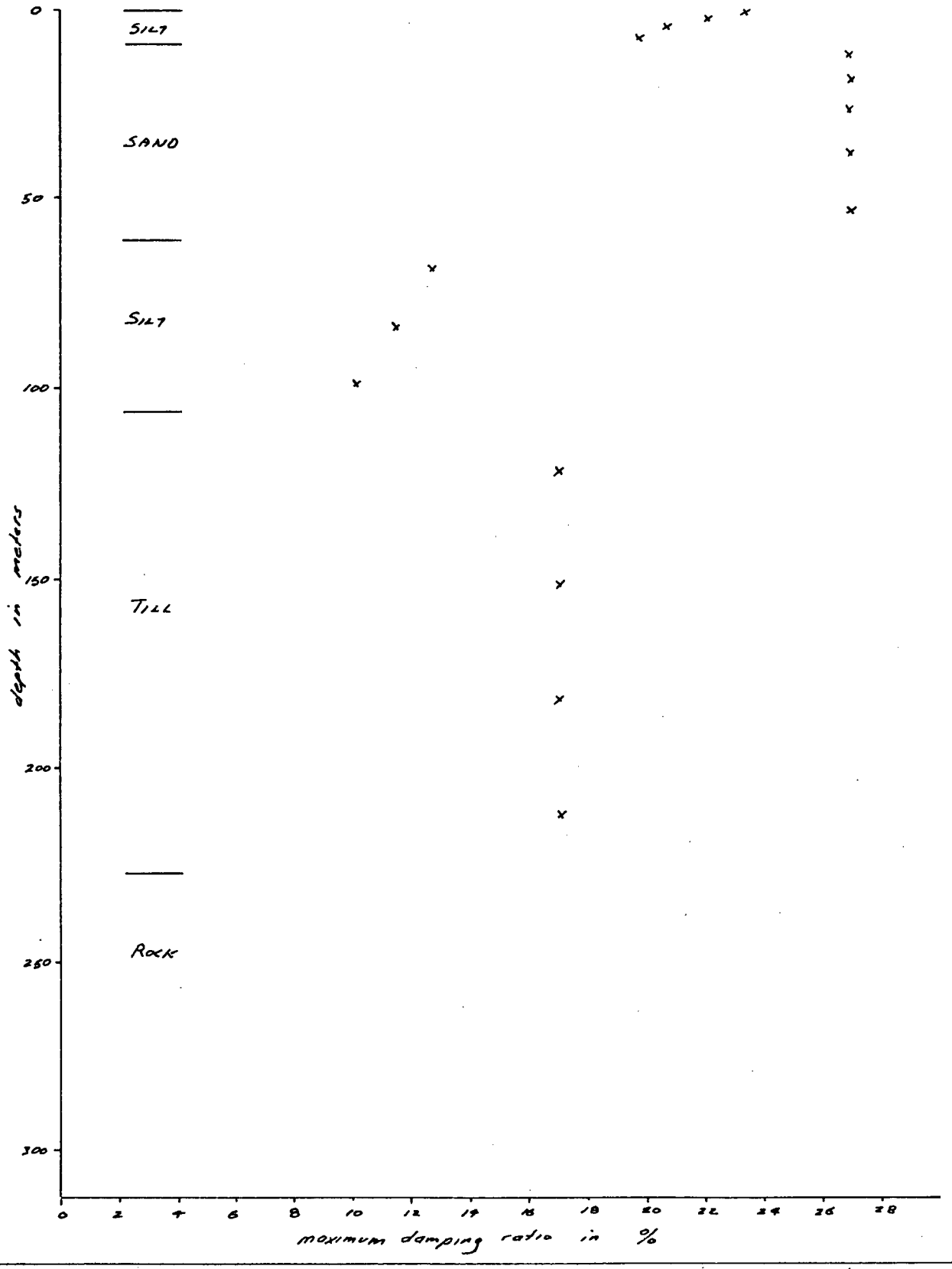

FIG 3-2-9 ANNACIS ISLAND : MAXIMUM DAMPING RATIO

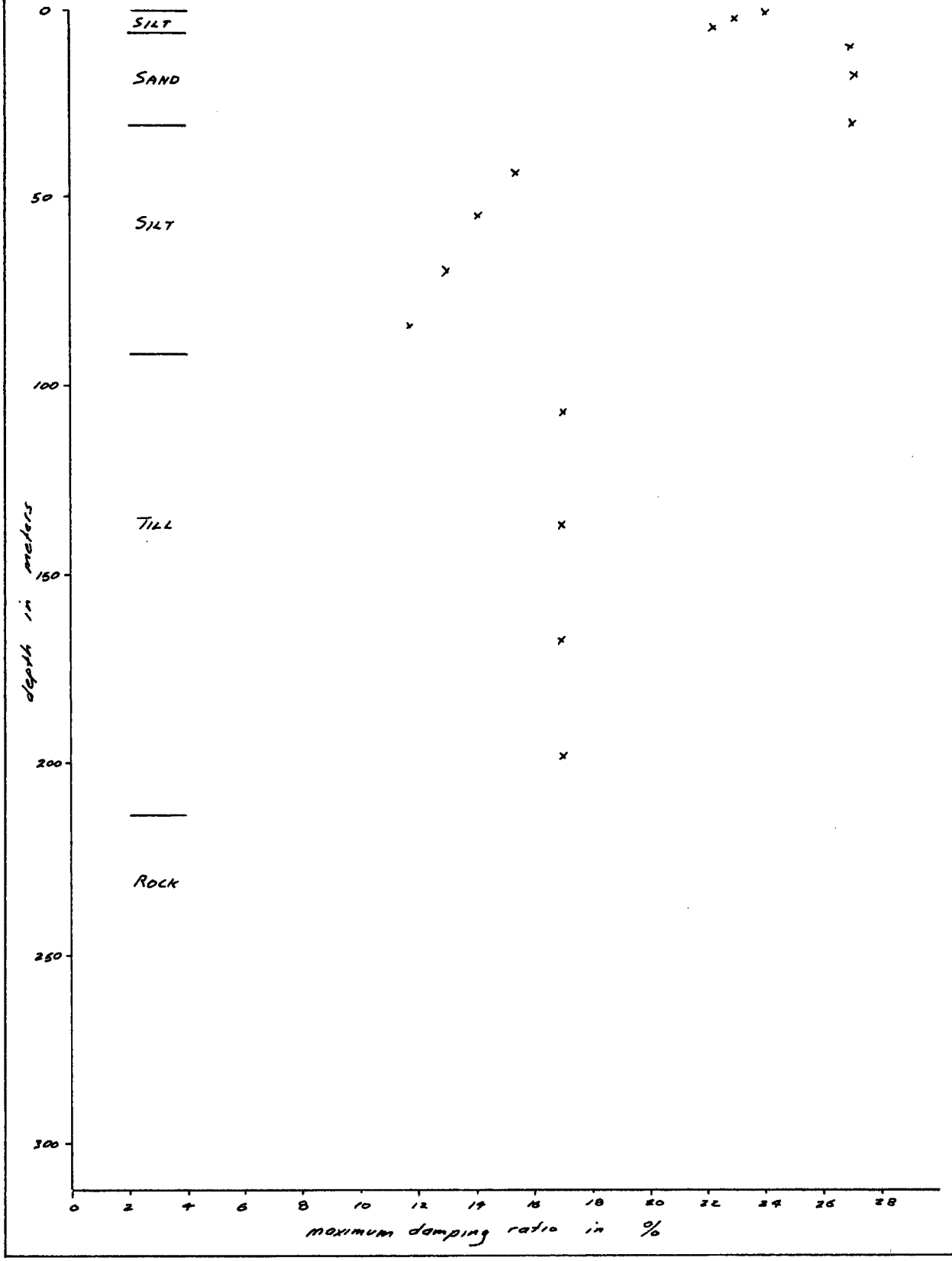

FIG 3-2-10 BRIGHOUSE : MAXIMUM DAMPING RATIO

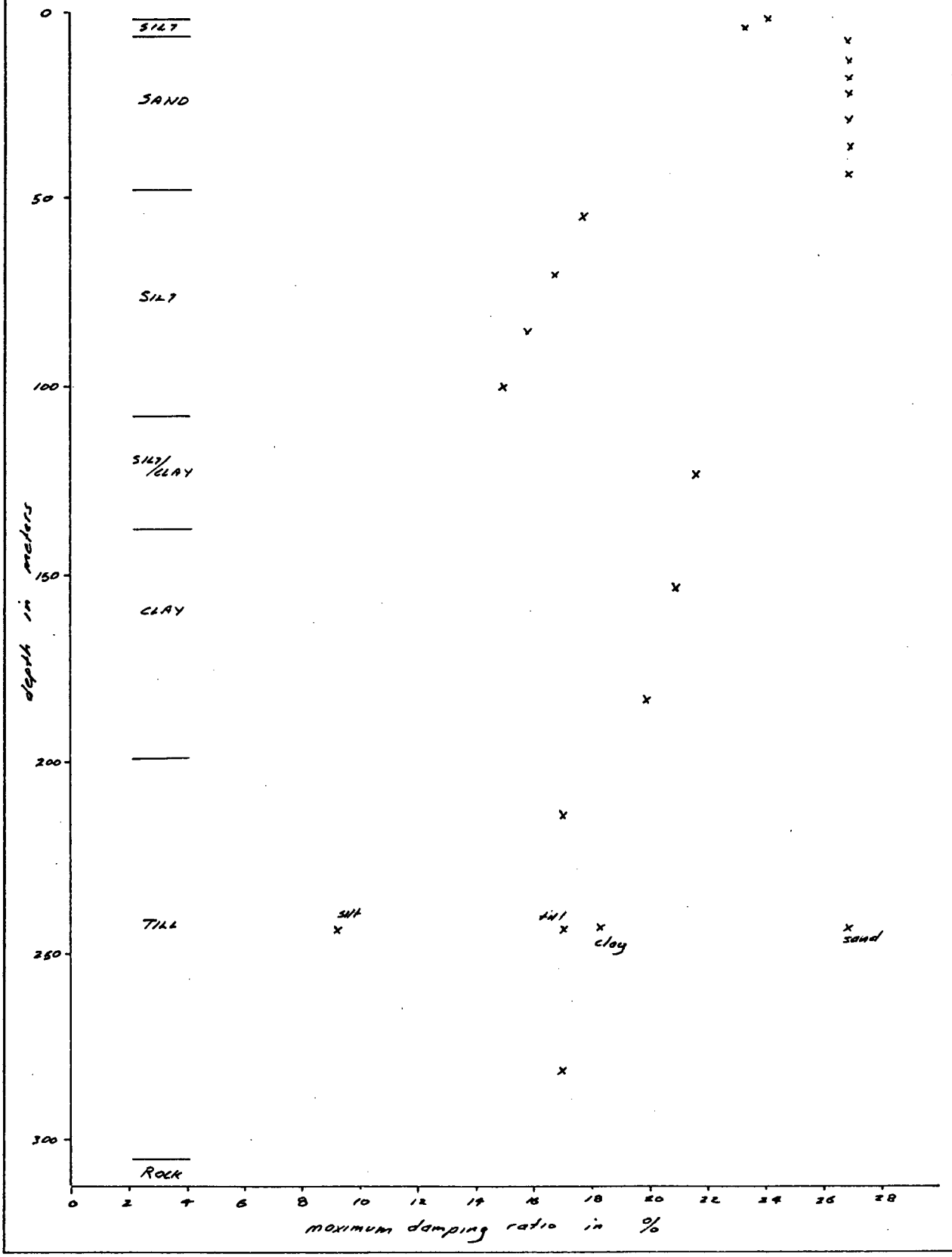

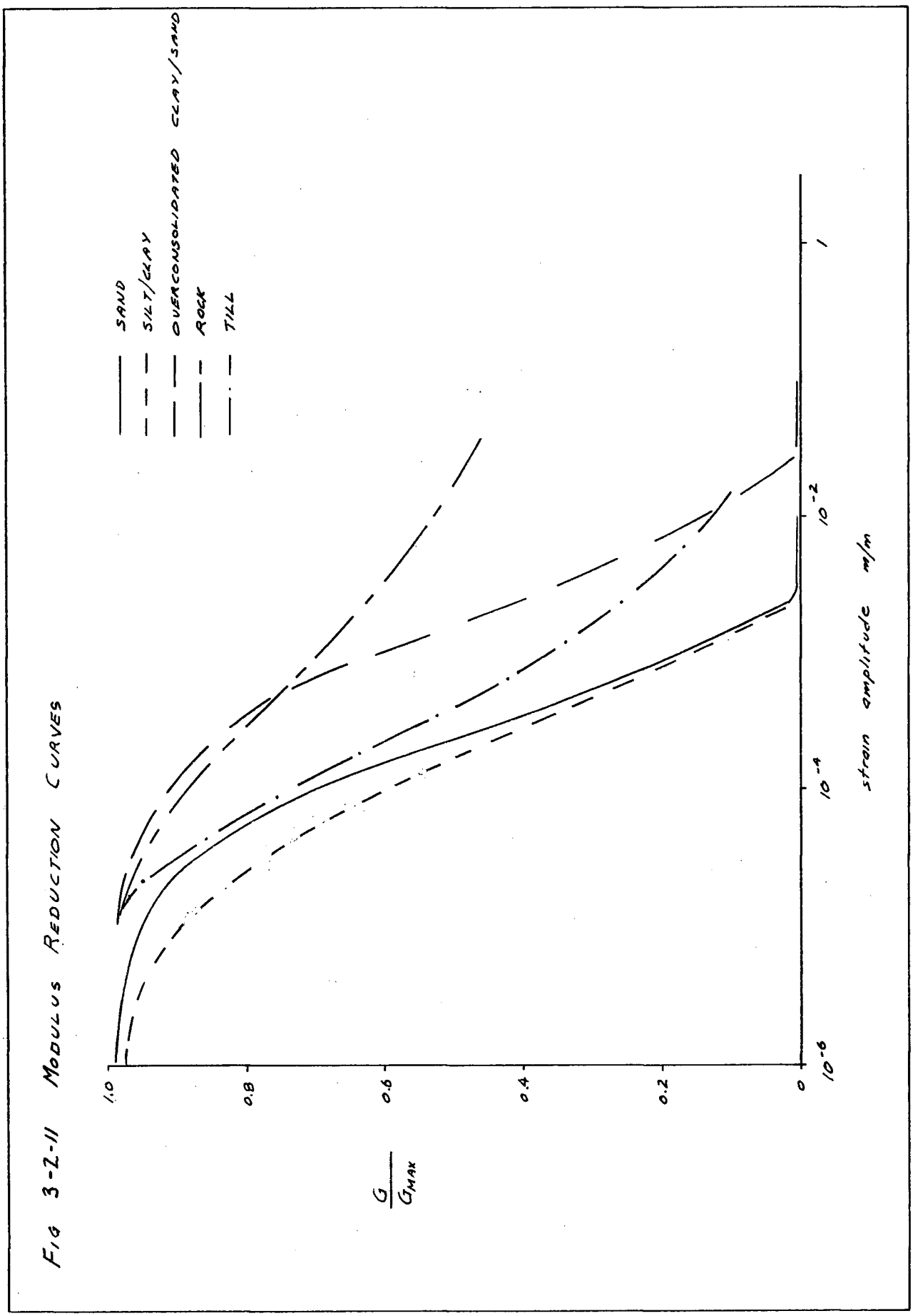

FIG 3-2-11 MODULUS REDUCTION CURVES

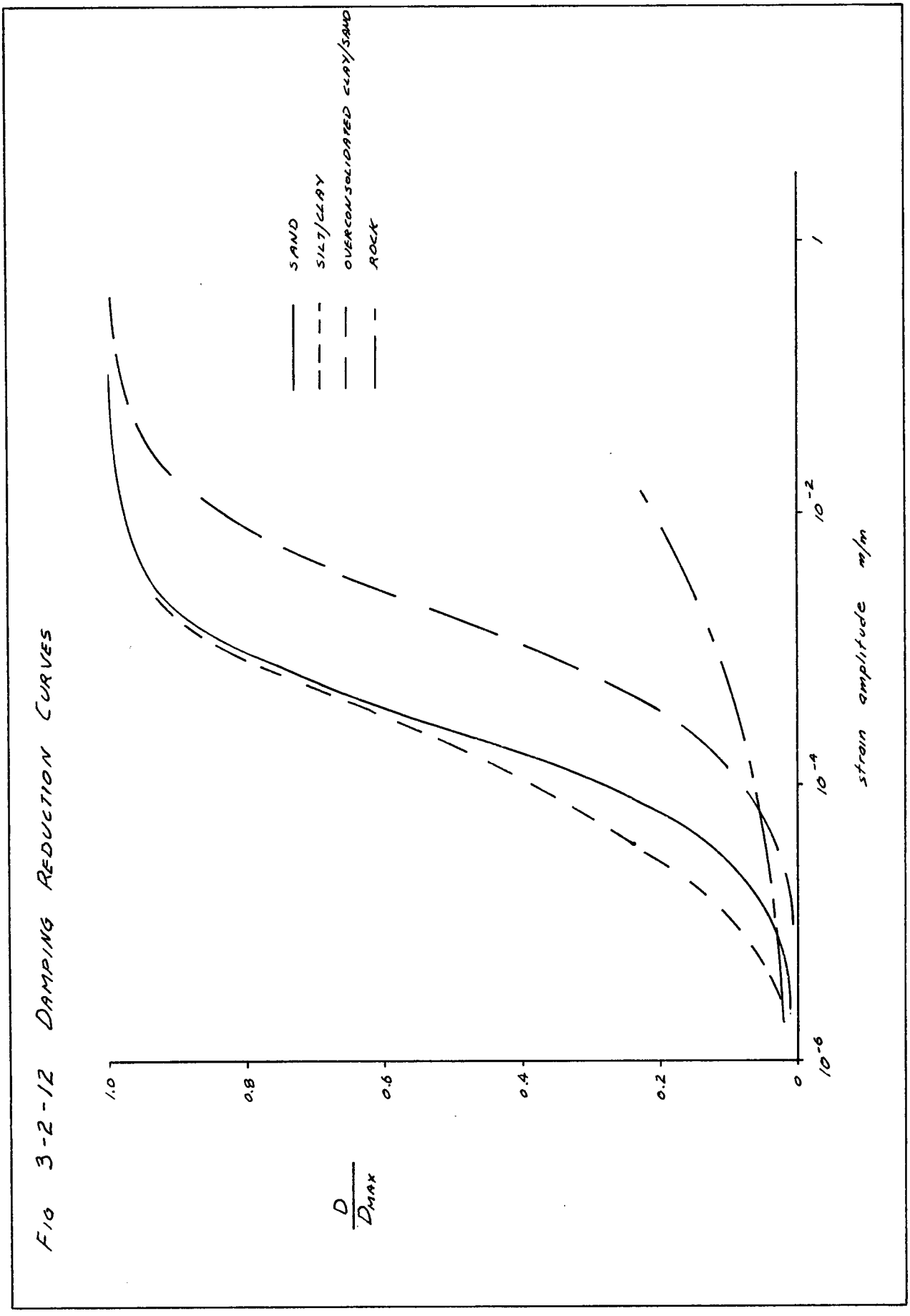

Fig 3-2-12 Damping Reduction Curves

FIG 3-4-1: DISTRIBUTION OF EARTHQUAKES IN STRAIT OF GEORGIA-PUGET SOUND AREA FROM MILNE et al 1978

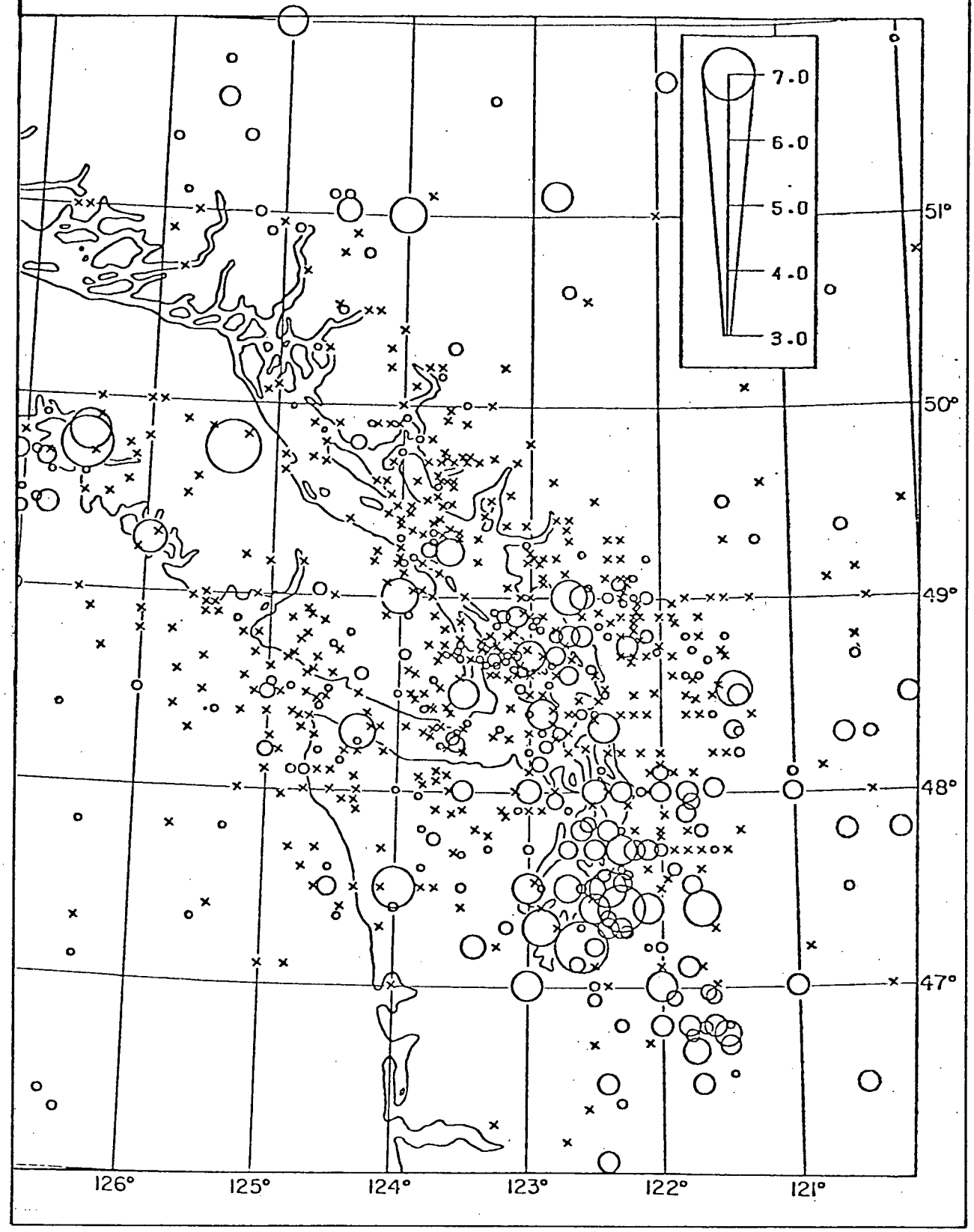

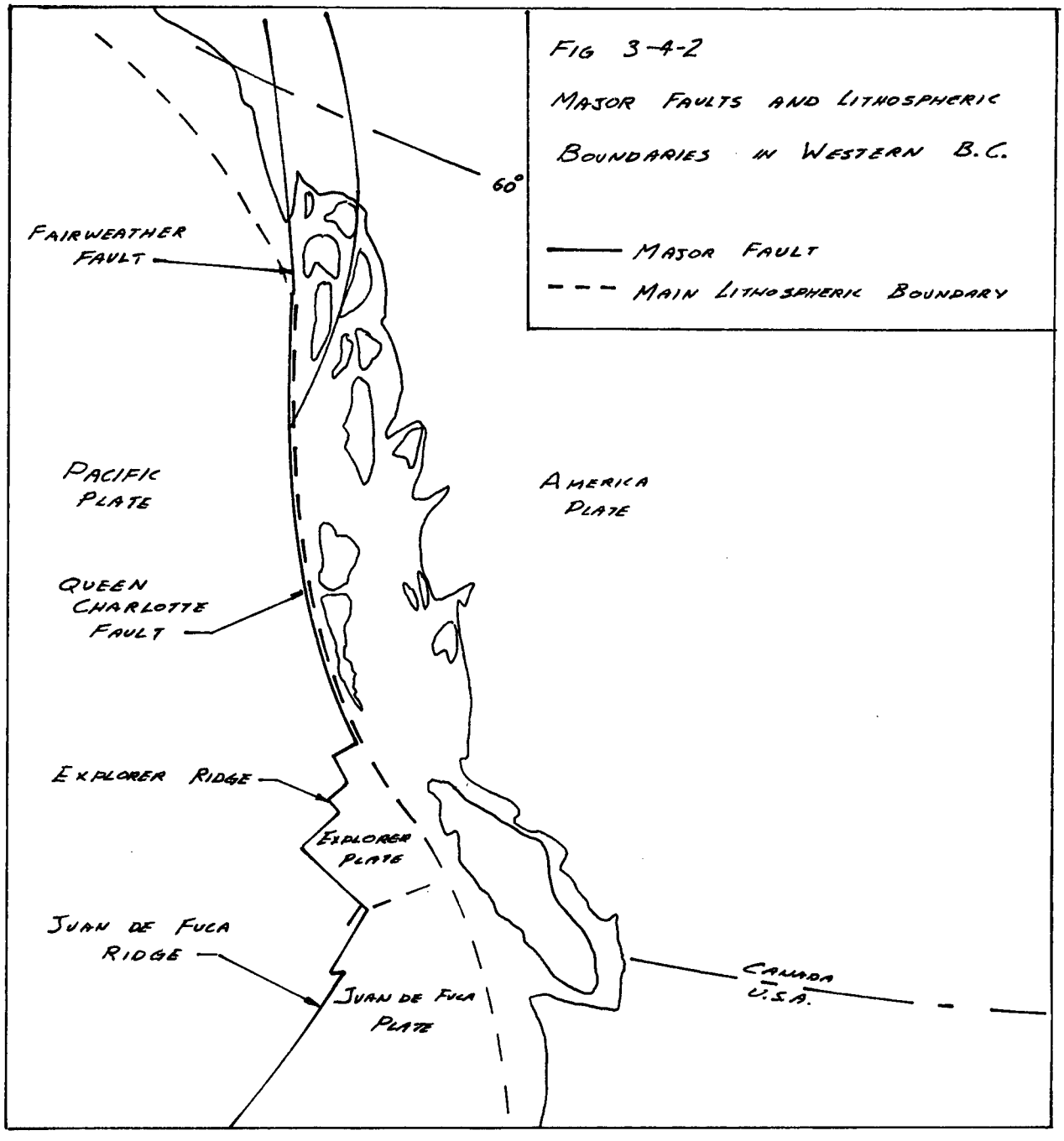

FIG 3-4-2

MAJOR FAULTS AND LITHOSPHERIC BOUNDARIES IN WESTERN B.C.

——— MAJOR FAULT

- - - MAIN LITHOSPHERIC BOUNDARY

FIG 3-4-3: STRAIN RELEASE VS TIME IN CONTINENTAL AREA

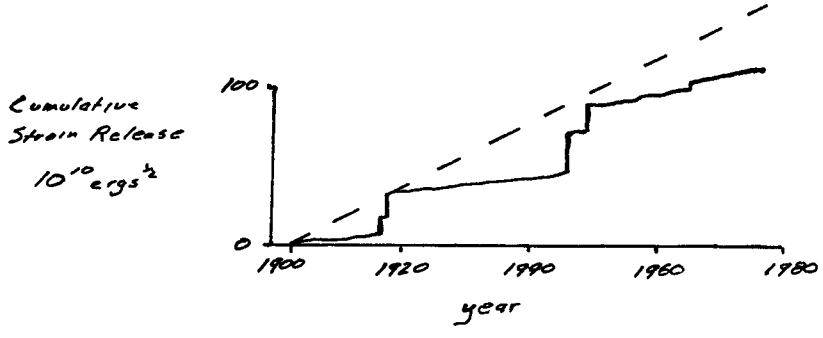

from Milne et al. (1978)

FIG 3-4-4: MAGNITUDE vs TIME RELATION FOR GEORGIA STRAIT - PUGET SOUND AREA, (From MILNE ET AL 1978)

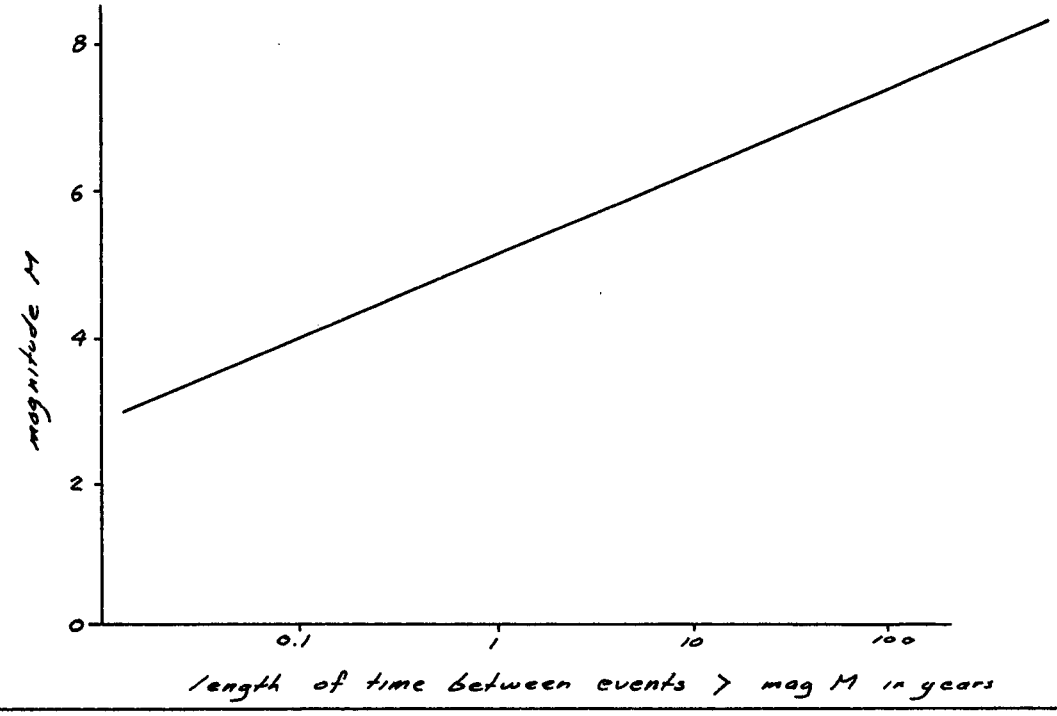

FIG 3-4-5: PREDOMINANT PERIODS FOR ACCELERATION IN ROCK (FROM SEED IDRISS & KIEFER 1969)

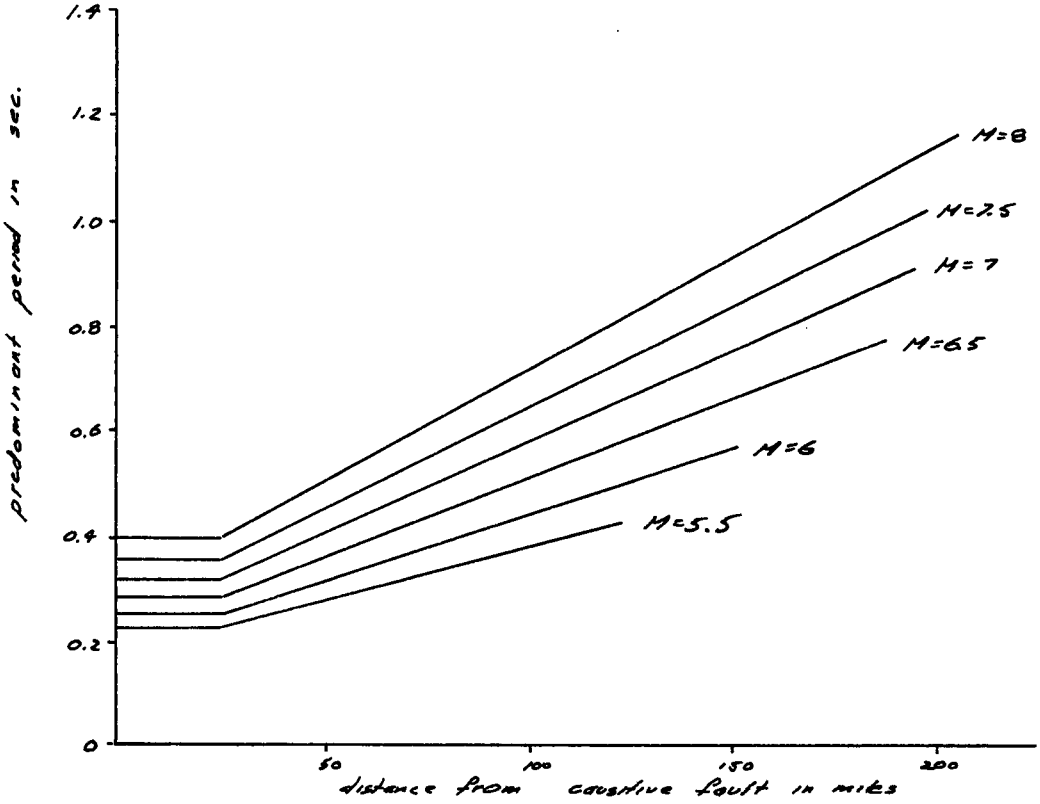

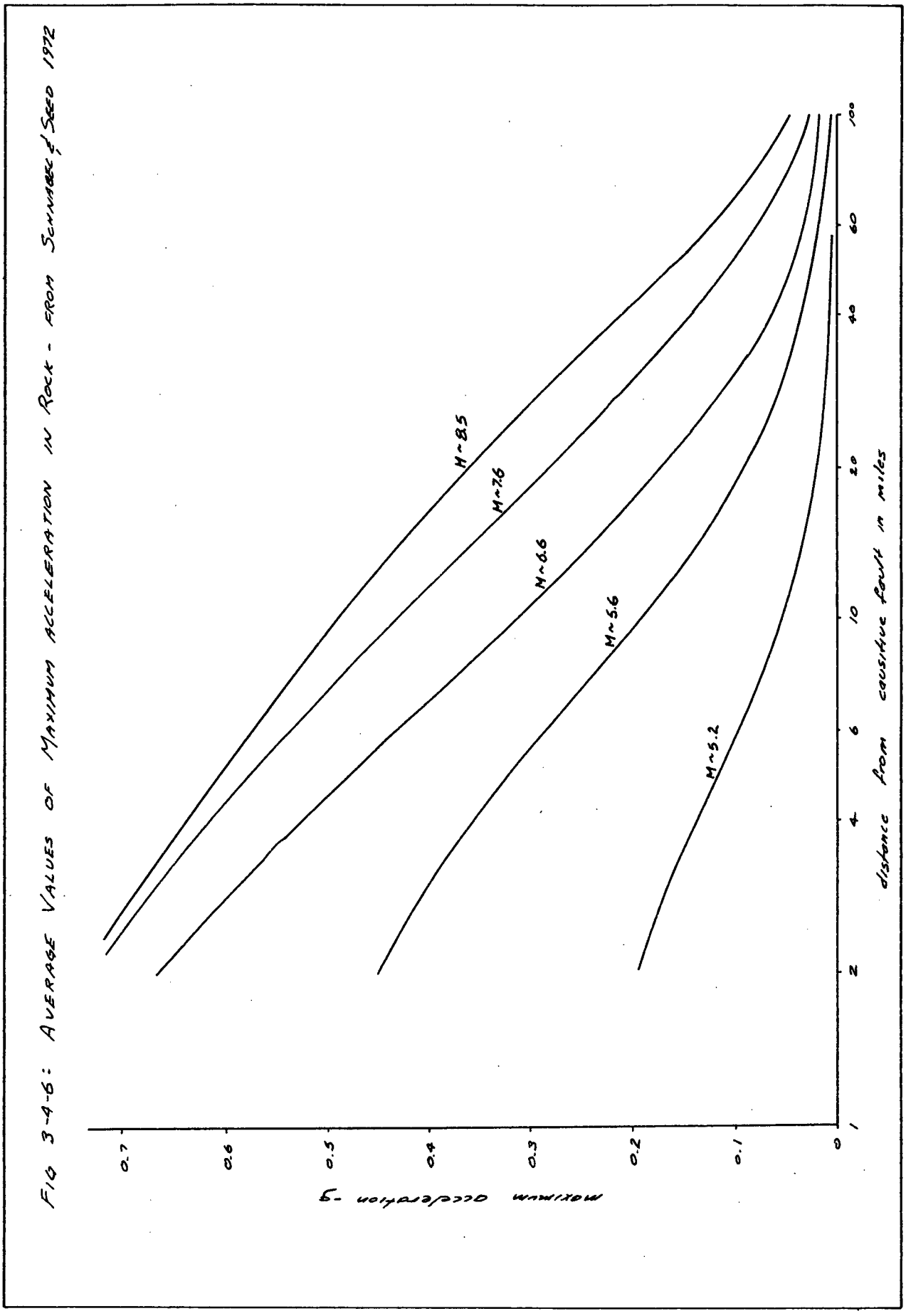

FIG 3-4-6: AVERAGE VALUES OF MAXIMUM ACCELERATION IN ROCK - FROM SCHNABEL & SEED 1972

FIG 4-1-1 ANNACIS ISLAND : RESPONSE SPECTRA OF COMPUTED AND RECORDED SURFACE MOTIONS DUE TO PENDER ISLAND EARTHQUAKE

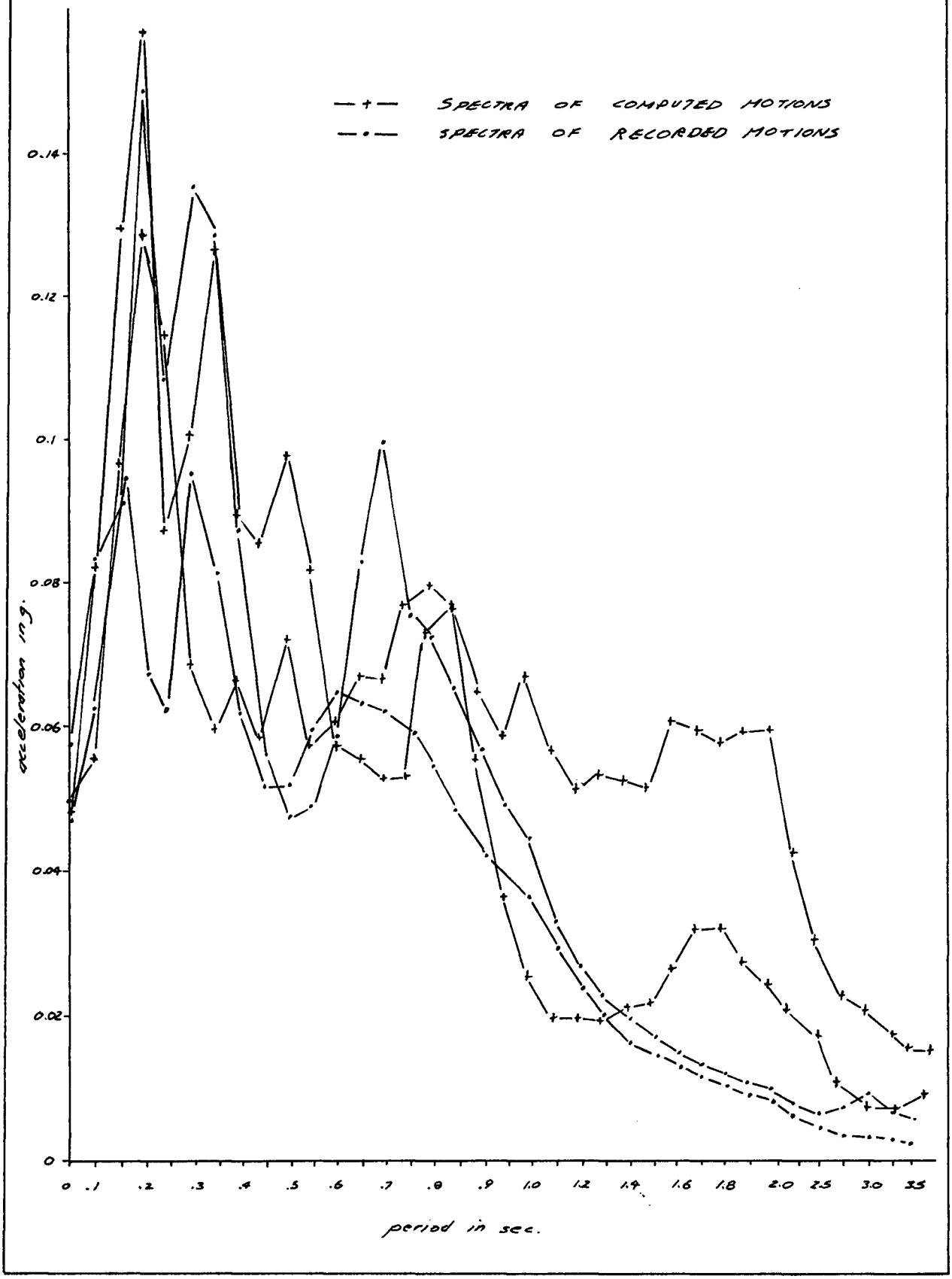

FIG 4-1-2 BRIGHOUSE: RESPONSE SPECTRA OF COMPUTED AND RECORDED SURFACE MOTIONS DUE TO PENDER ISLAND EARTHQUAKE

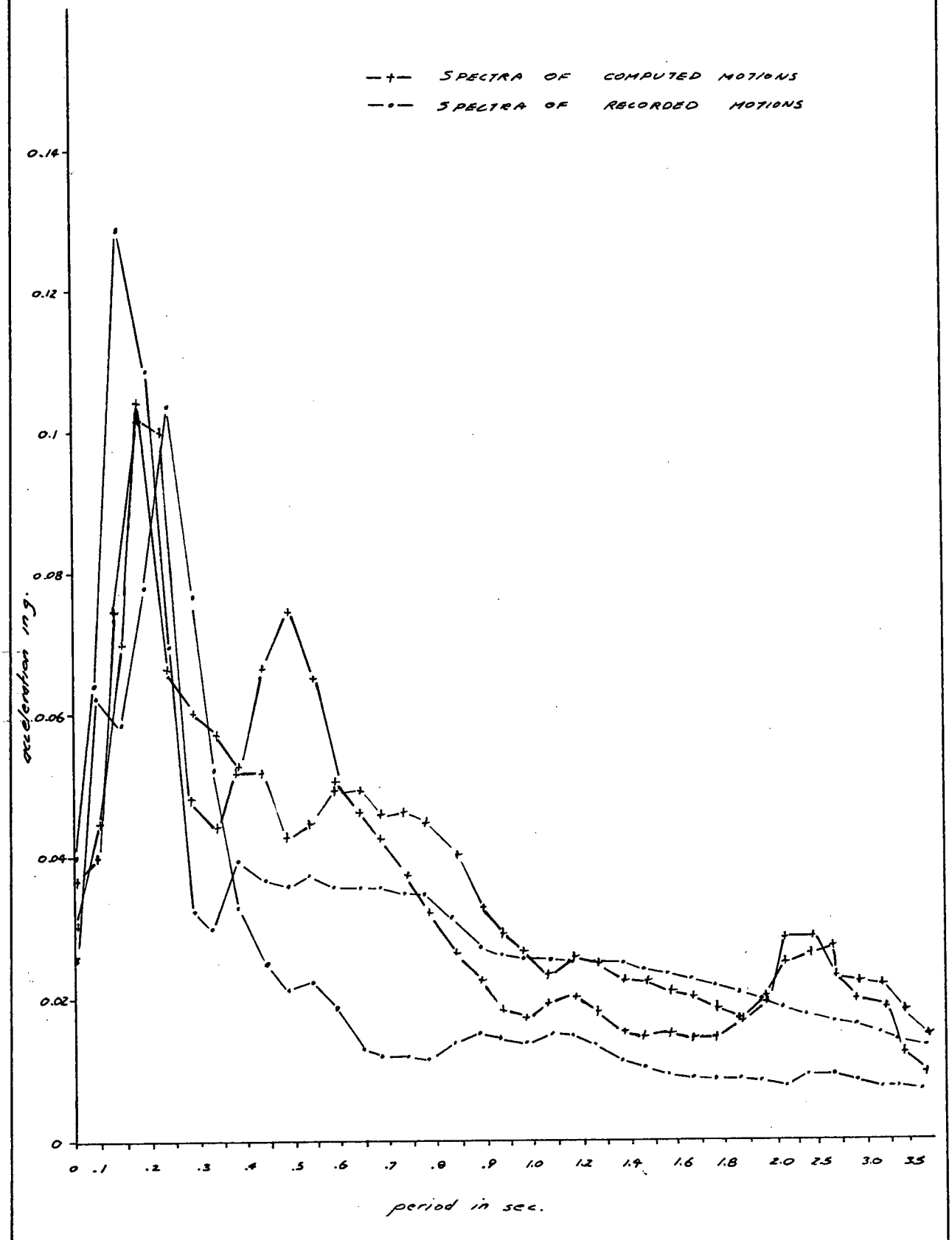

FIG 4-1-3 ROBERTS BANK: RESPONSE SPECTRA OF COMPUTED AND RECORDED SURFACE MOTIONS DUE TO PENDER ISLAND EARTHQUAKE

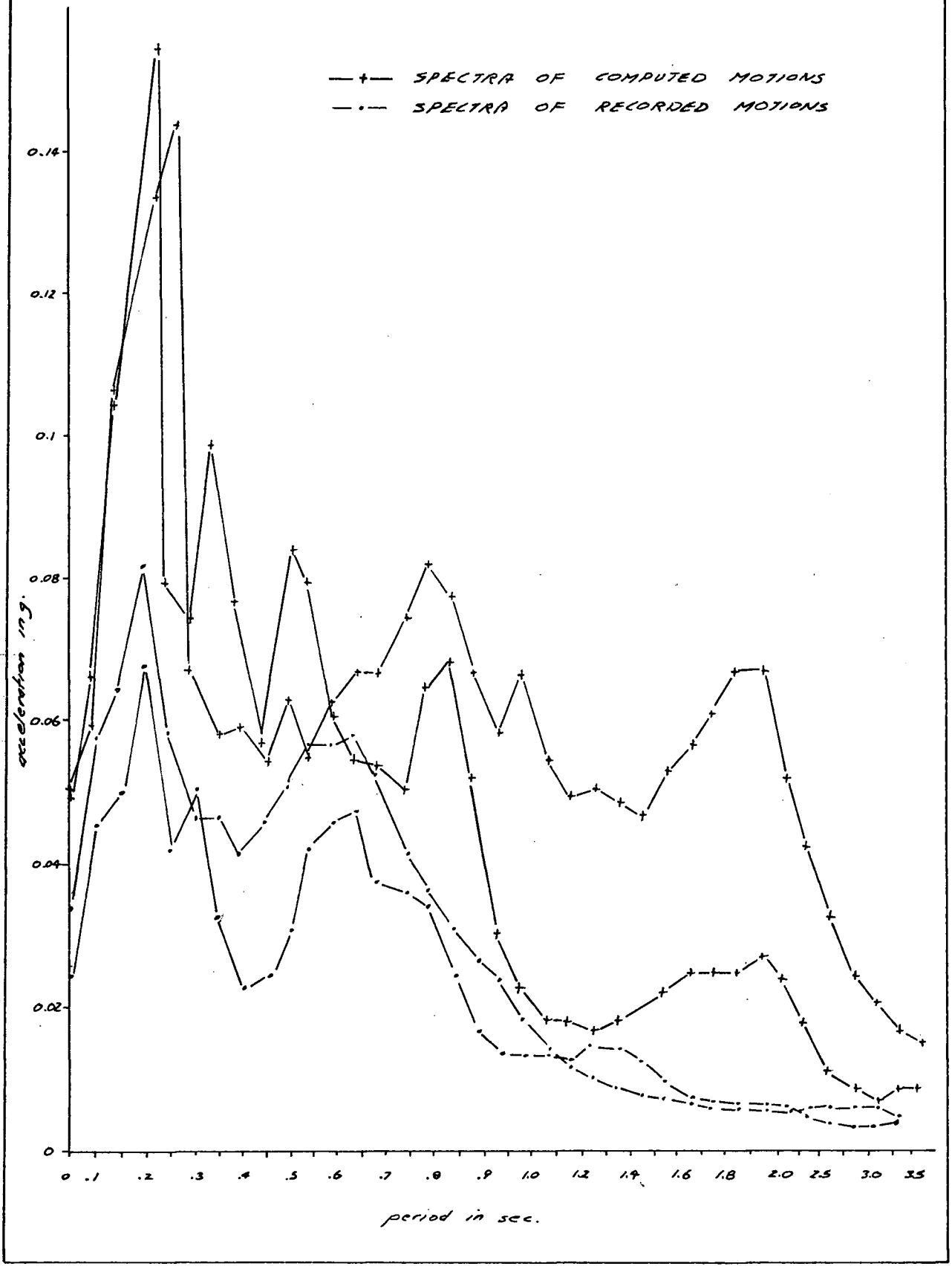

FIG 4-1-4 : ANNACIS ISLAND: RESPONSE SPECTRA OF MOTIONS COMPUTED WITHIN THE SOIL PROFILE, DUE TO PENDER ISLAND EARTHQUAKE

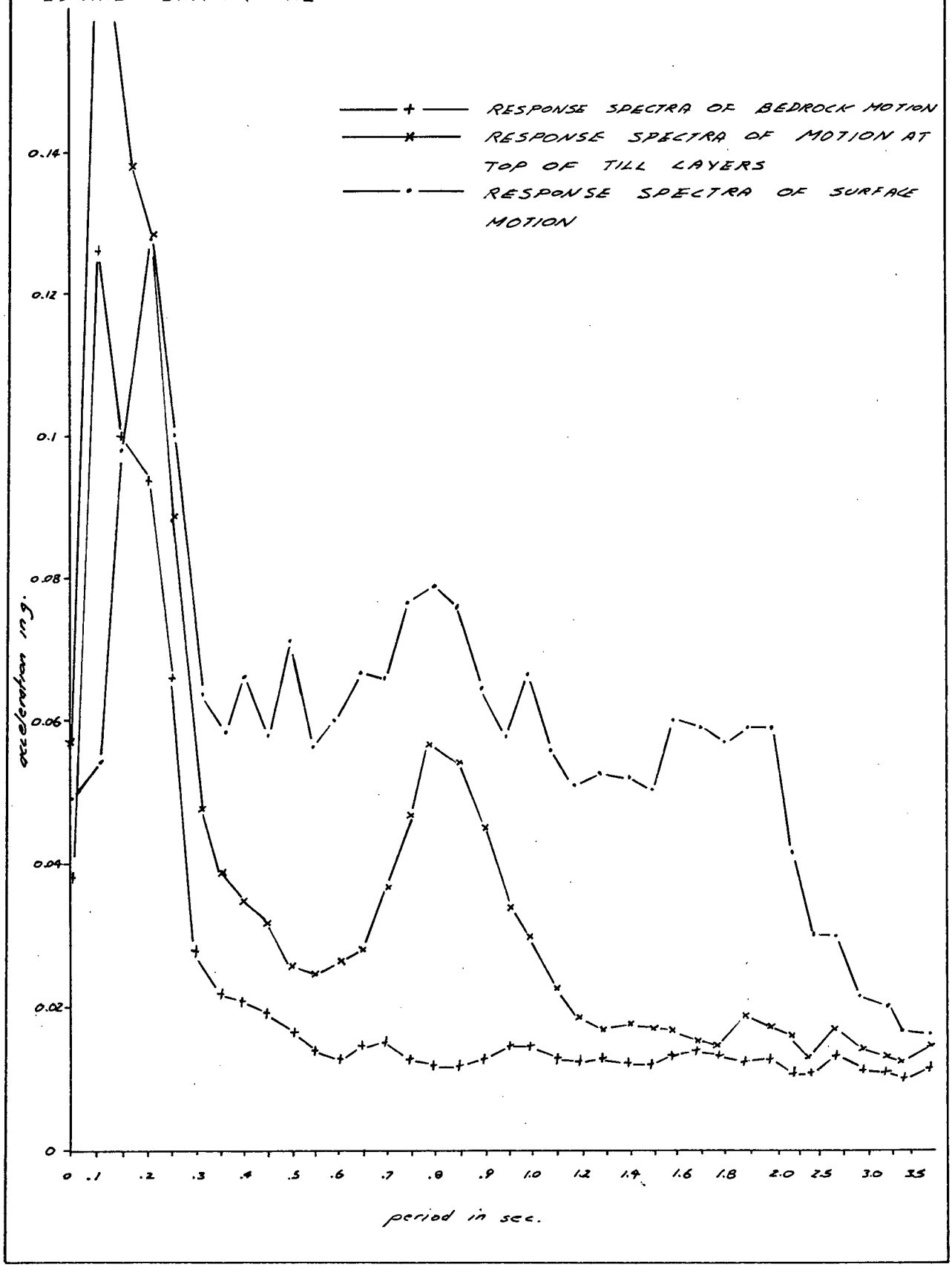

FIG 4-2-1 RESPONSE SPECTRA OF DESIGN EARTHQUAKES SCALED TO MAXIMUM ACCELERATION OF 0.25g

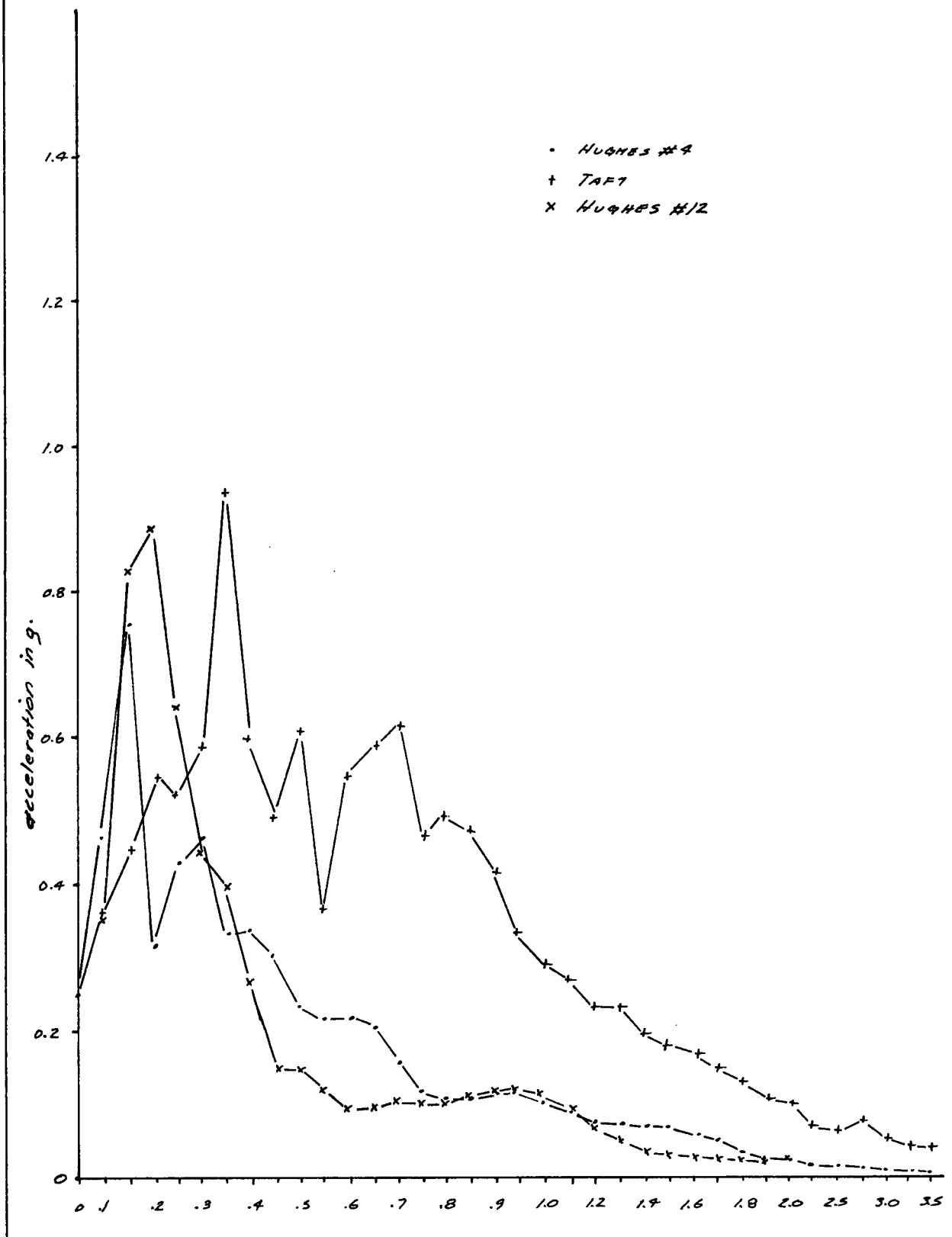

FIG 4-2-2: ANNACIS ISLAND, RESPONSE SPECTRA OF SURFACE MOTION FOR DESIGN EARTHQUAKES SCALED TO $A_{MAX} = 0.16g$

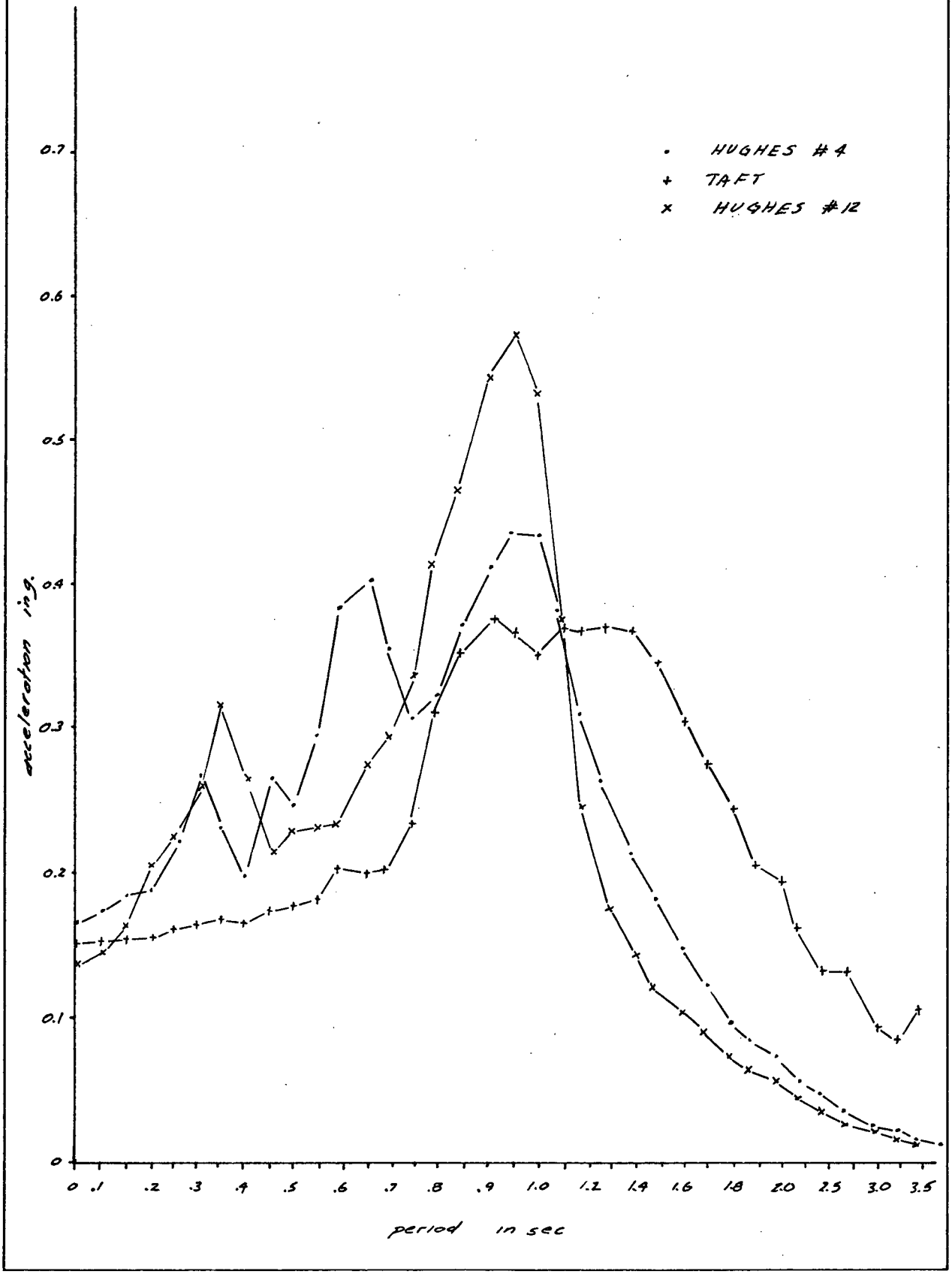

FIG 4-2-3 : ANNACIS ISLAND, RESPONSE SPECTRA FOR SURFACE MOTION, FOR DESIGN EARTHQUAKES SCALED TO A_{MAX} = 0.25g

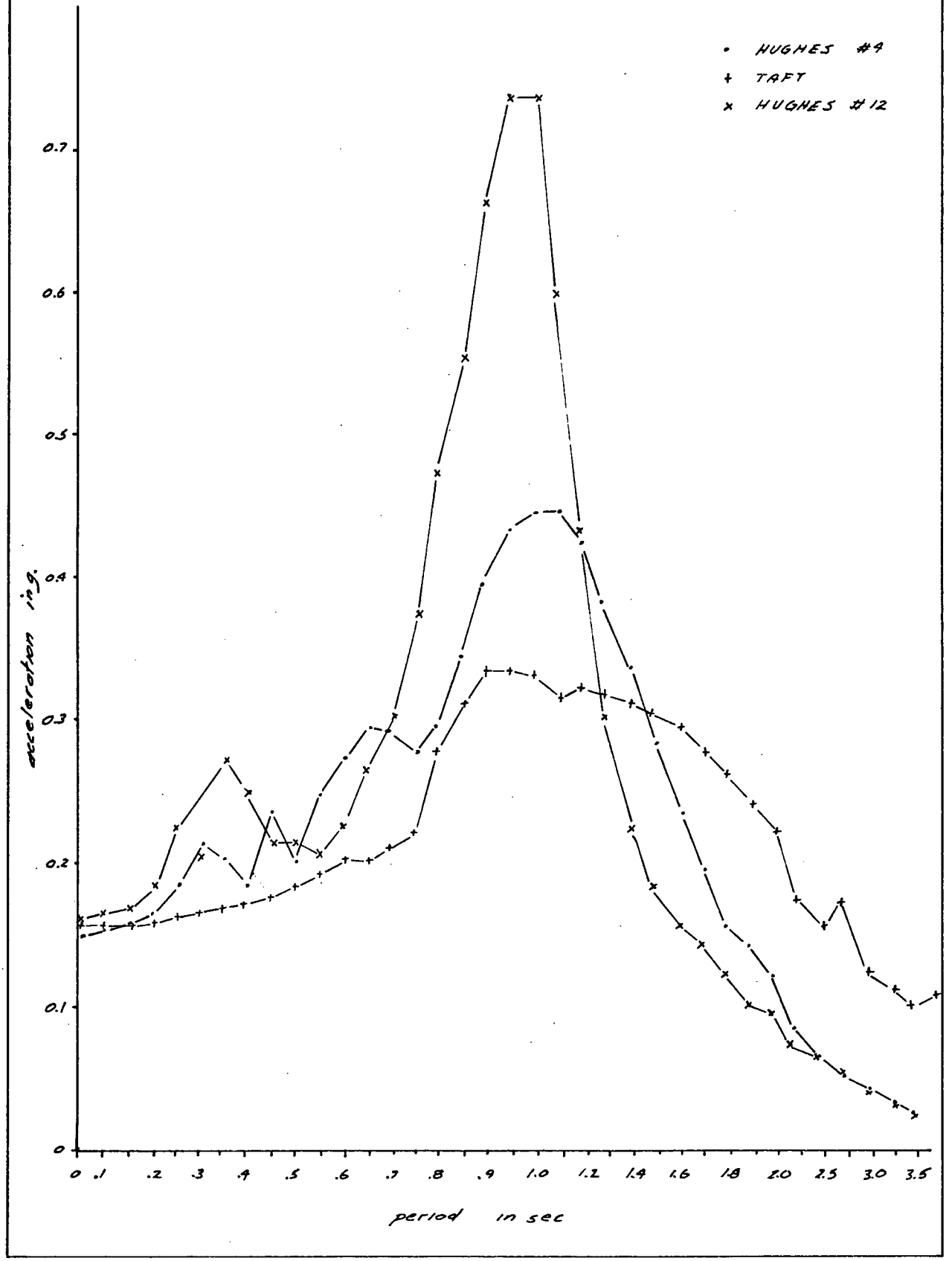

FIG 4-2-4: ANNACIS ISLAND, RESPONSE SPECTRA OF SURFACE MOTIONS FOR DESIGN EARTHQUAKE SCALED TO $A_{MAX} = 0.33g$

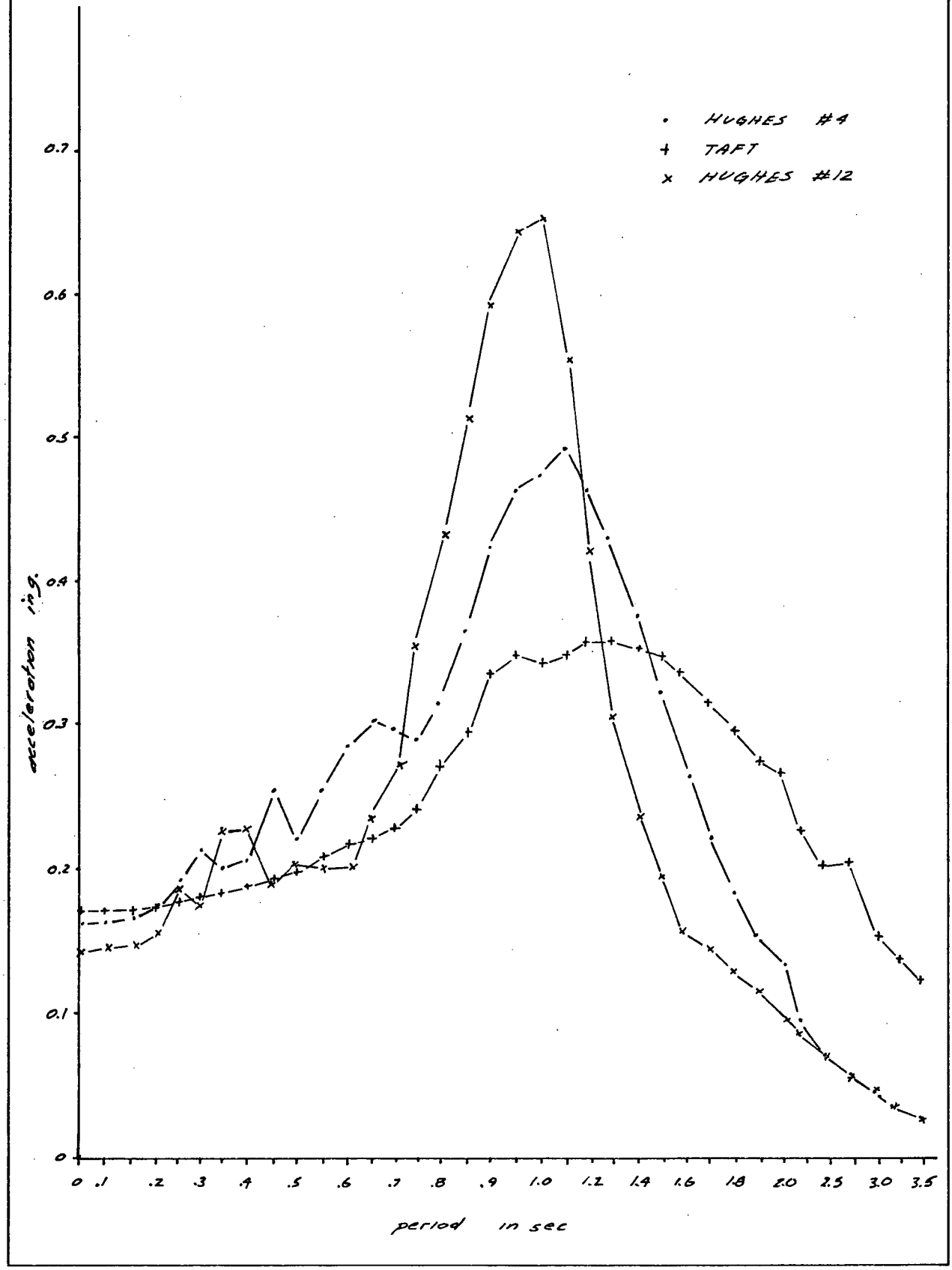

FIG 4-2-5 : BRIGHOUSE, RESPONSE SPECTRA OF SURFACE MOTIONS FOR DESIGN EARTHQUAKES SCALED TO $A_{MAX} = 0.16g$

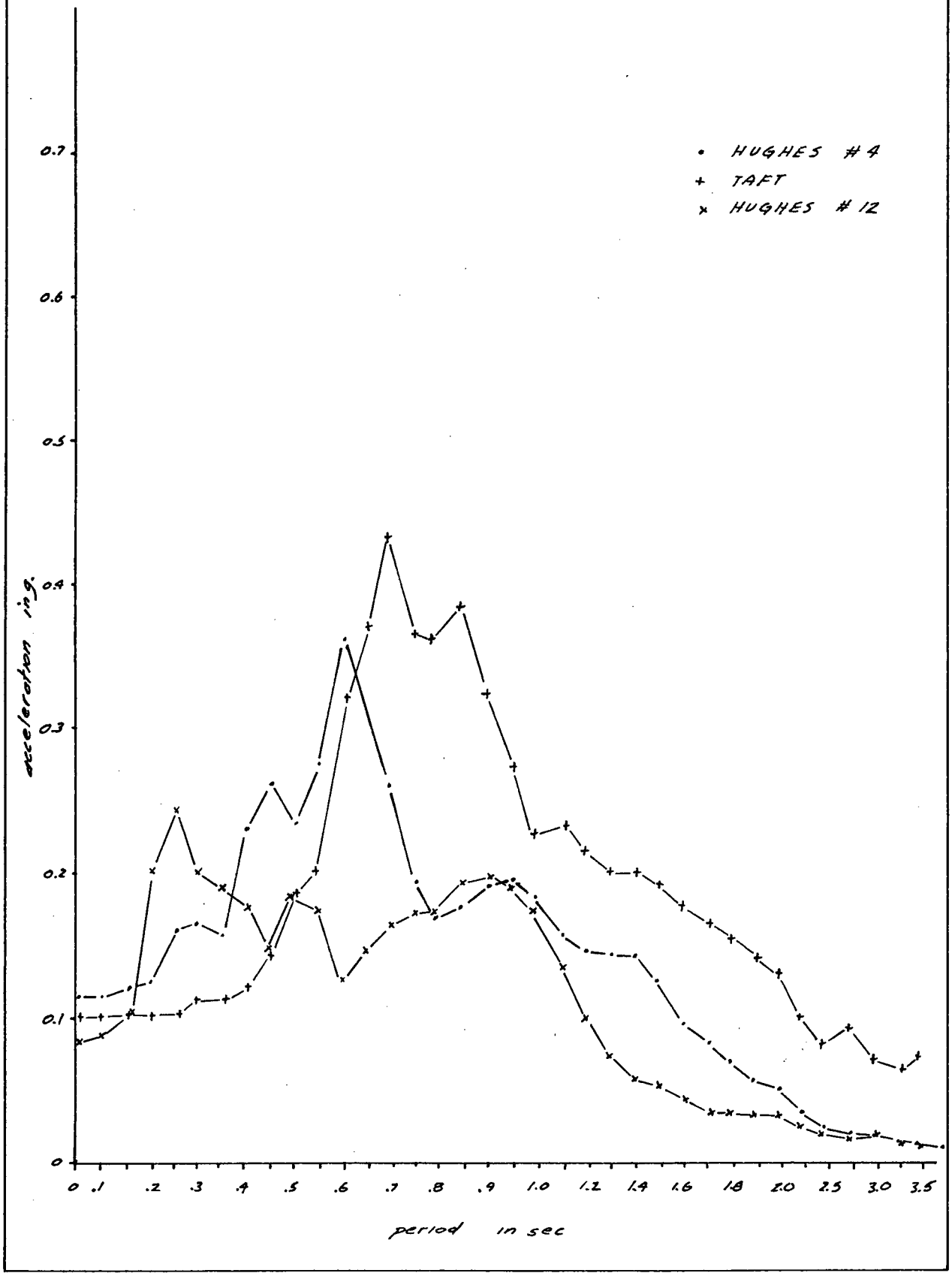

FIG 4-2-6 : BRIGHOUSE, RESPONSE SPECTRA OF SURFACE MOTION, FOR DESIGN EARTHQUAKES SCALED TO A_{MAX} = 0.25g

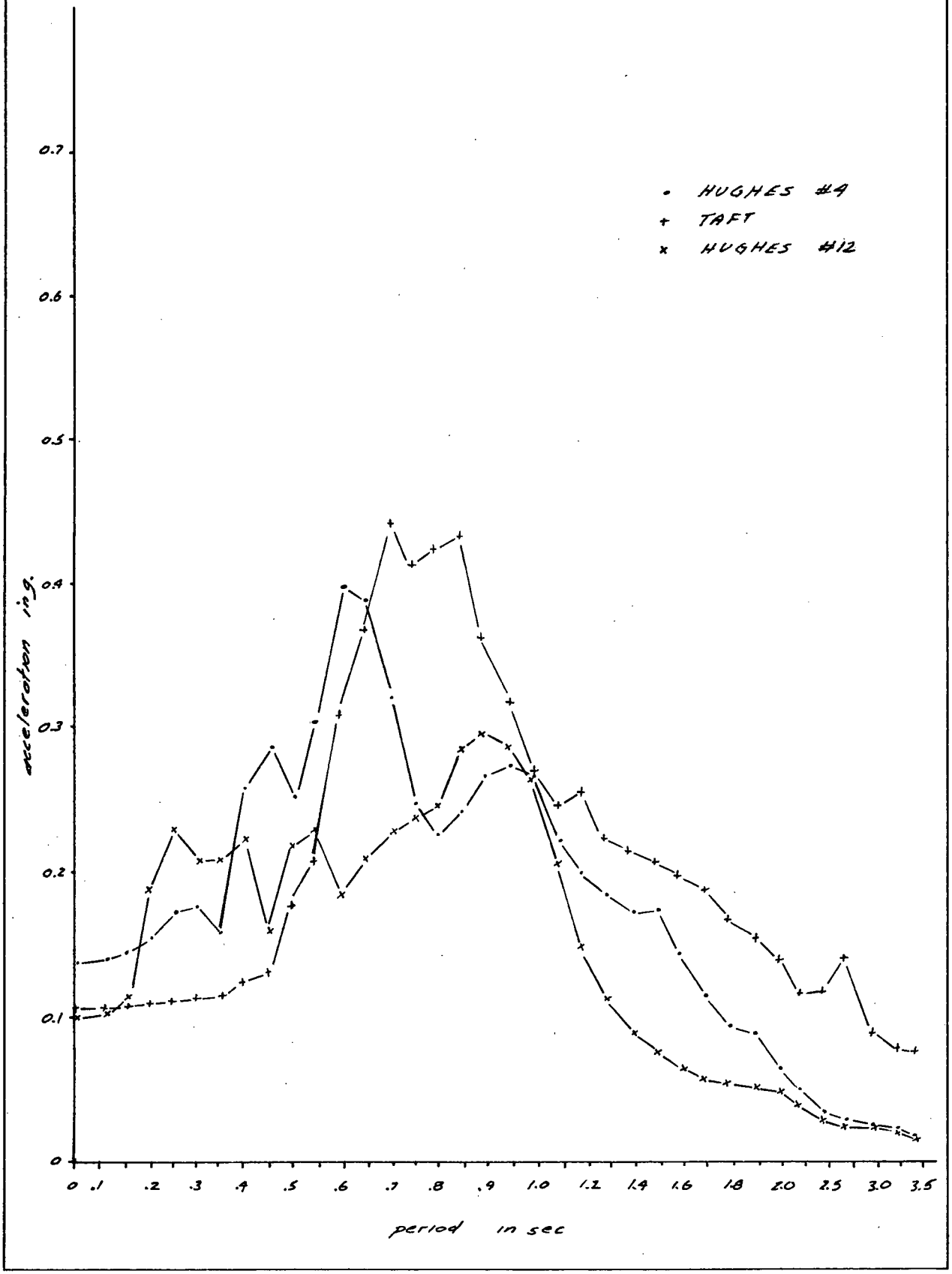

FIG 4-2-7 : BRIGHOUSE, RESPONSE SPECTRA OF SURFACE MOTIONS FOR DESIGN EARTHQUAKES SCALED TO $A_{MAX} = 0.33g$

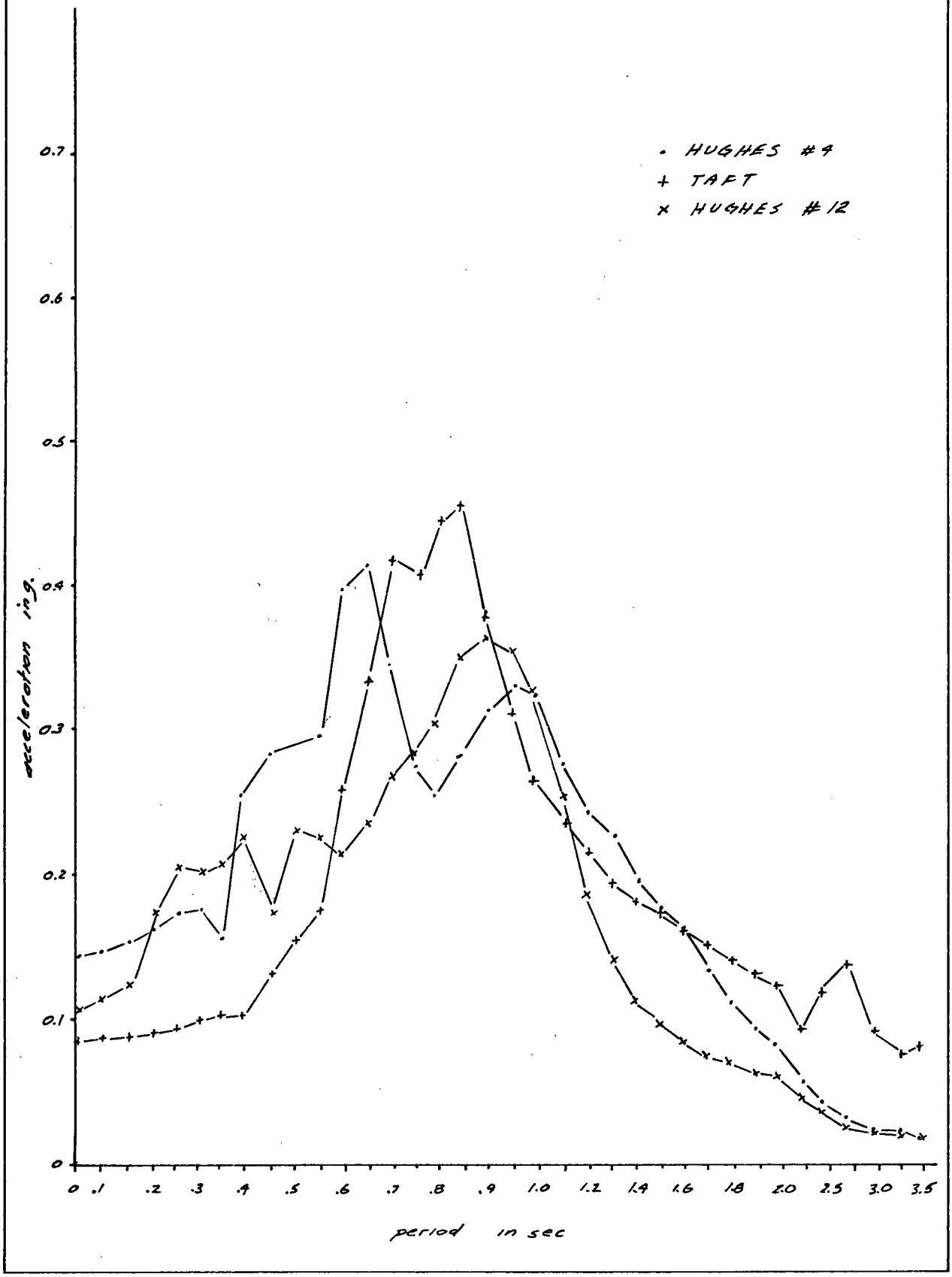

FIG 4-2-8 : BRIGHOUSE, MEAN OF THE RESPONSE SPECTRA FOR THREE DESIGN EARTHQUAKES OF A PARTICULAR A_{MAX}

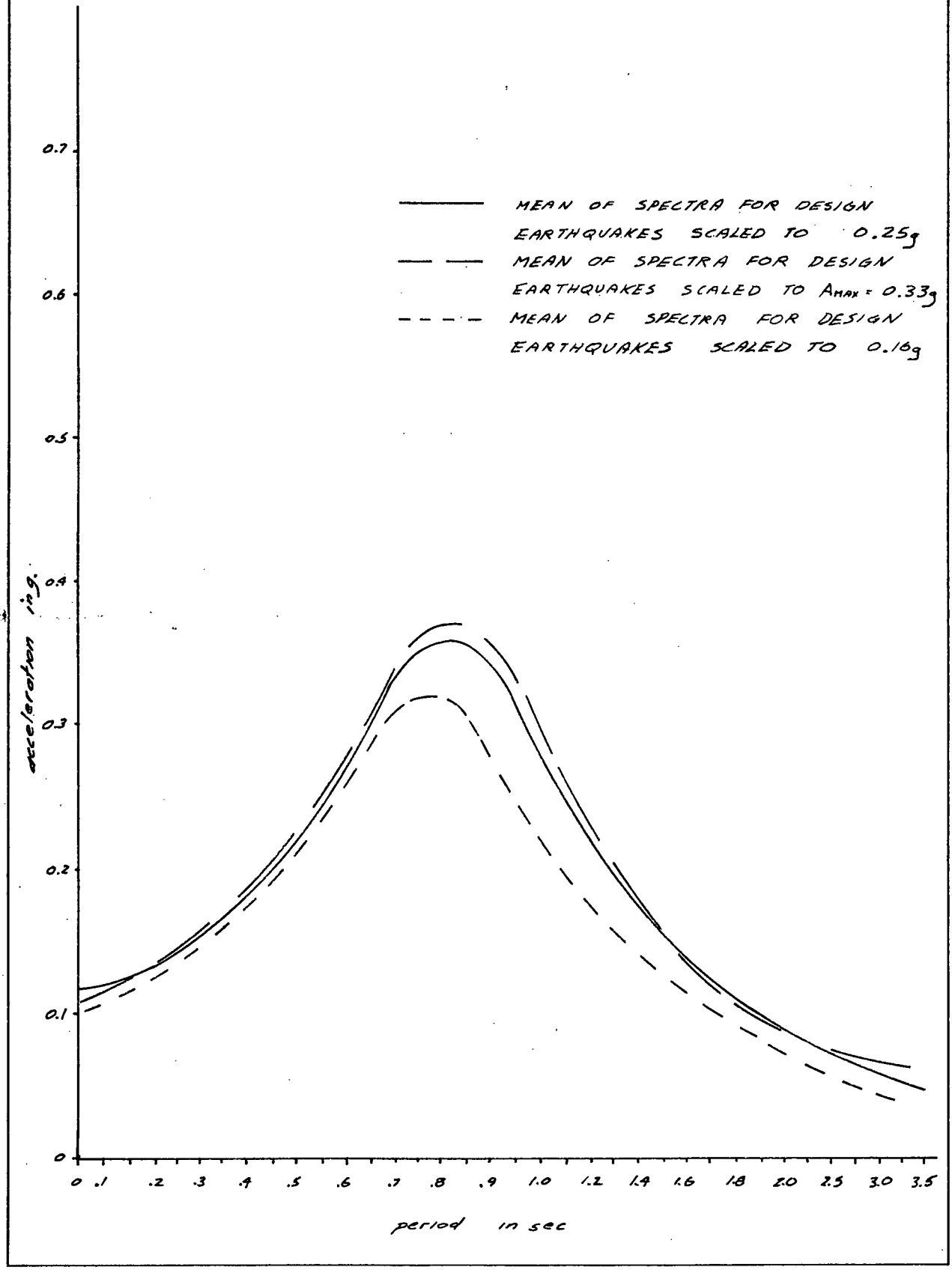

FIG 4-2-9 : ANNACIS ISLAND, MEAN OF THE RESPONSE SPECTRA FOR THREE DESIGN EARTHQUAKES OF A PARTICULAR A_{MAX}

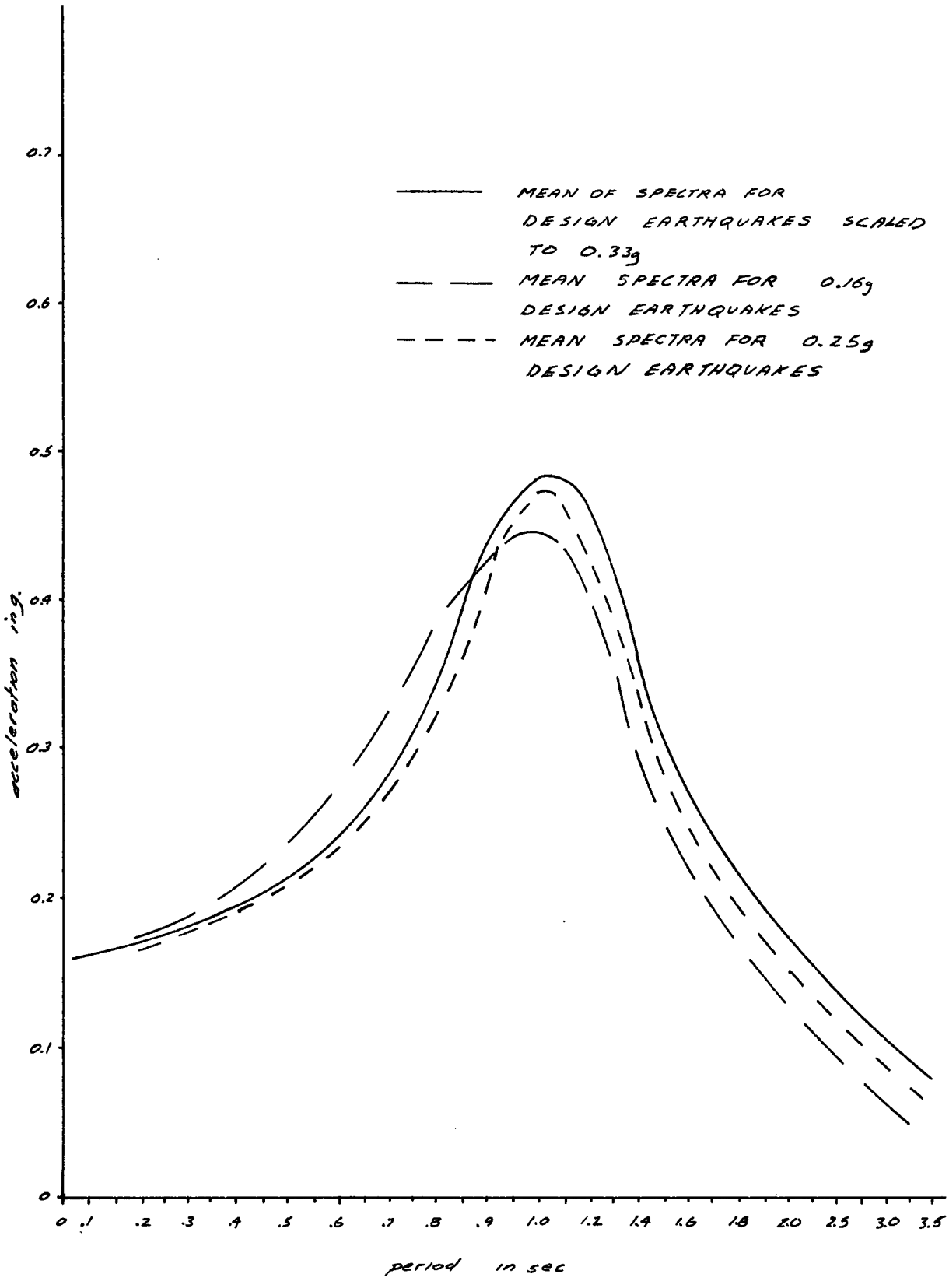

FIG 4-2-10: BRIGHOUSE, RESPONSE SPECTRA OF SURFACE MOTIONS FOR DESIGN EARTHQUAKES SCALED TO A_{MAX} = 0.25g AND OBJECT MOTION APPLIED TO TOP OF GLACIAL TILL

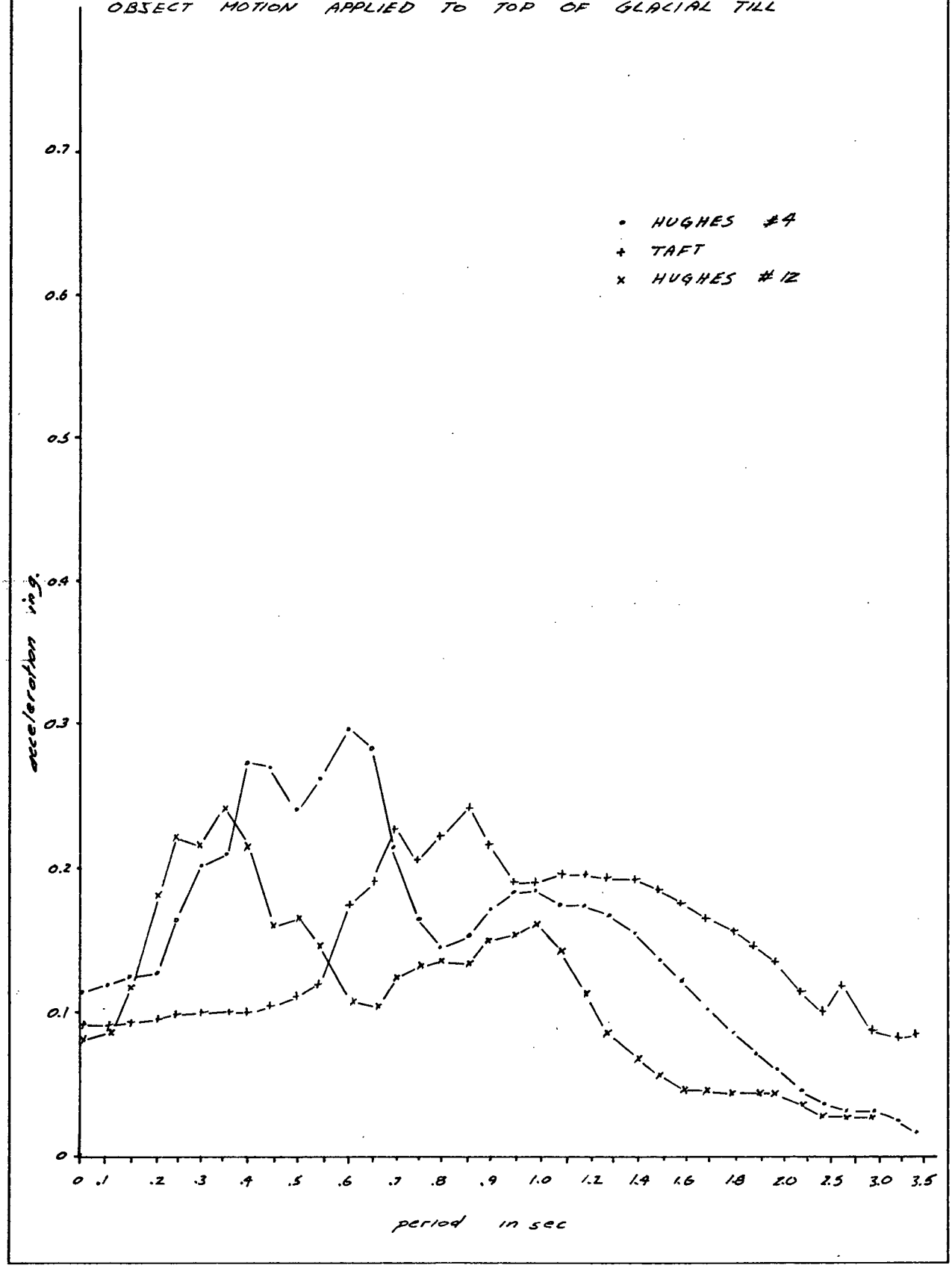

FIG 4-Z-11 : ANNACIS ISLAND, RESPONSE SPECTRA OF SURFACE MOTIONS FOR DESIGN EARTHQUAKE SCALED TO A_{MAX} = 0.25g AND OBJECT MOTION APPLIED TO TOP OF GLACIAL TILL

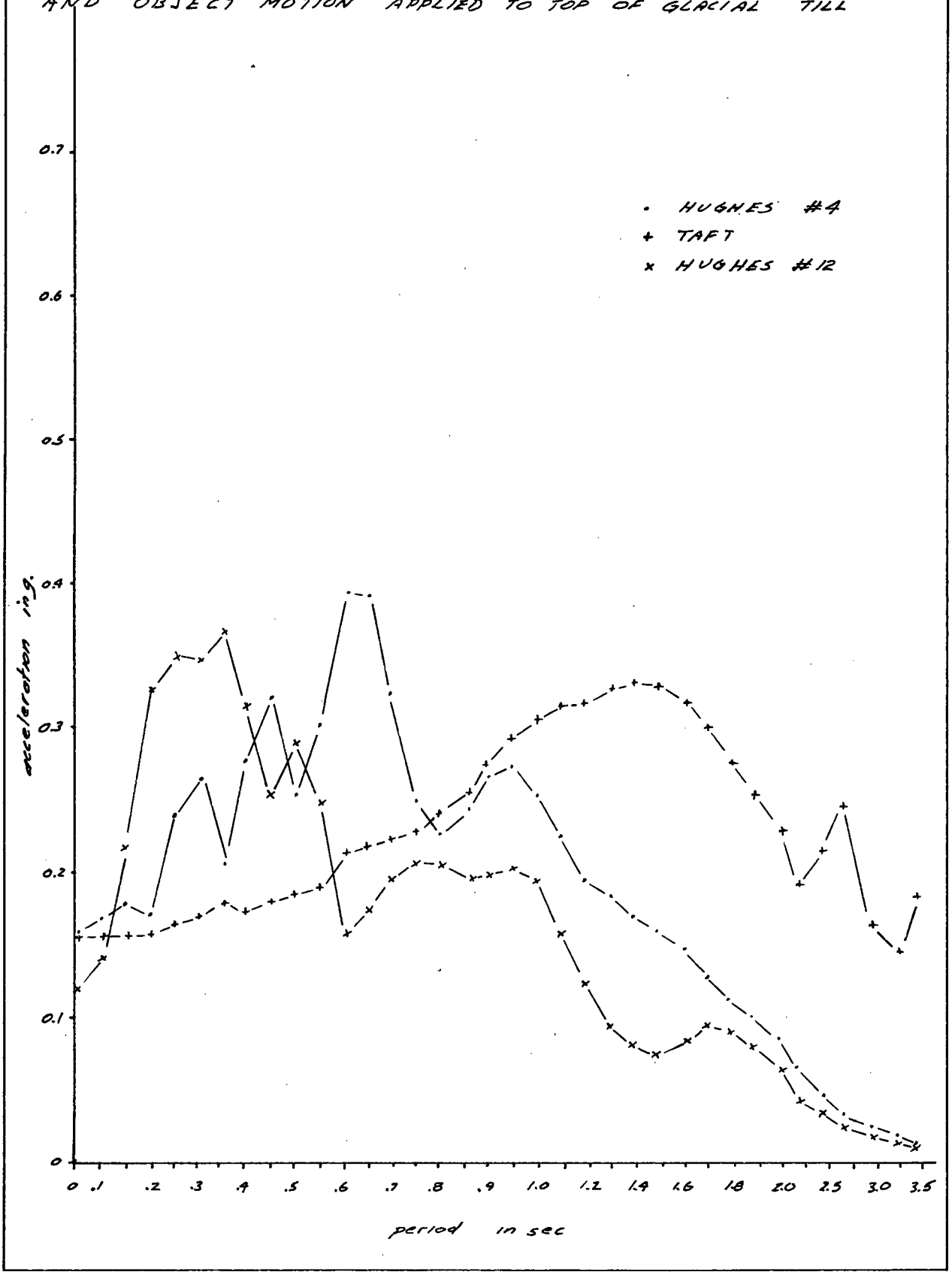

FIG 4-2-12: ANNACIS ISLAND: MEAN RESPONSE SPECTRA OF ROCK MOTION AND OF SURFACE MOTION FOR $A_{MAX\ ROCK} = 0.25g$

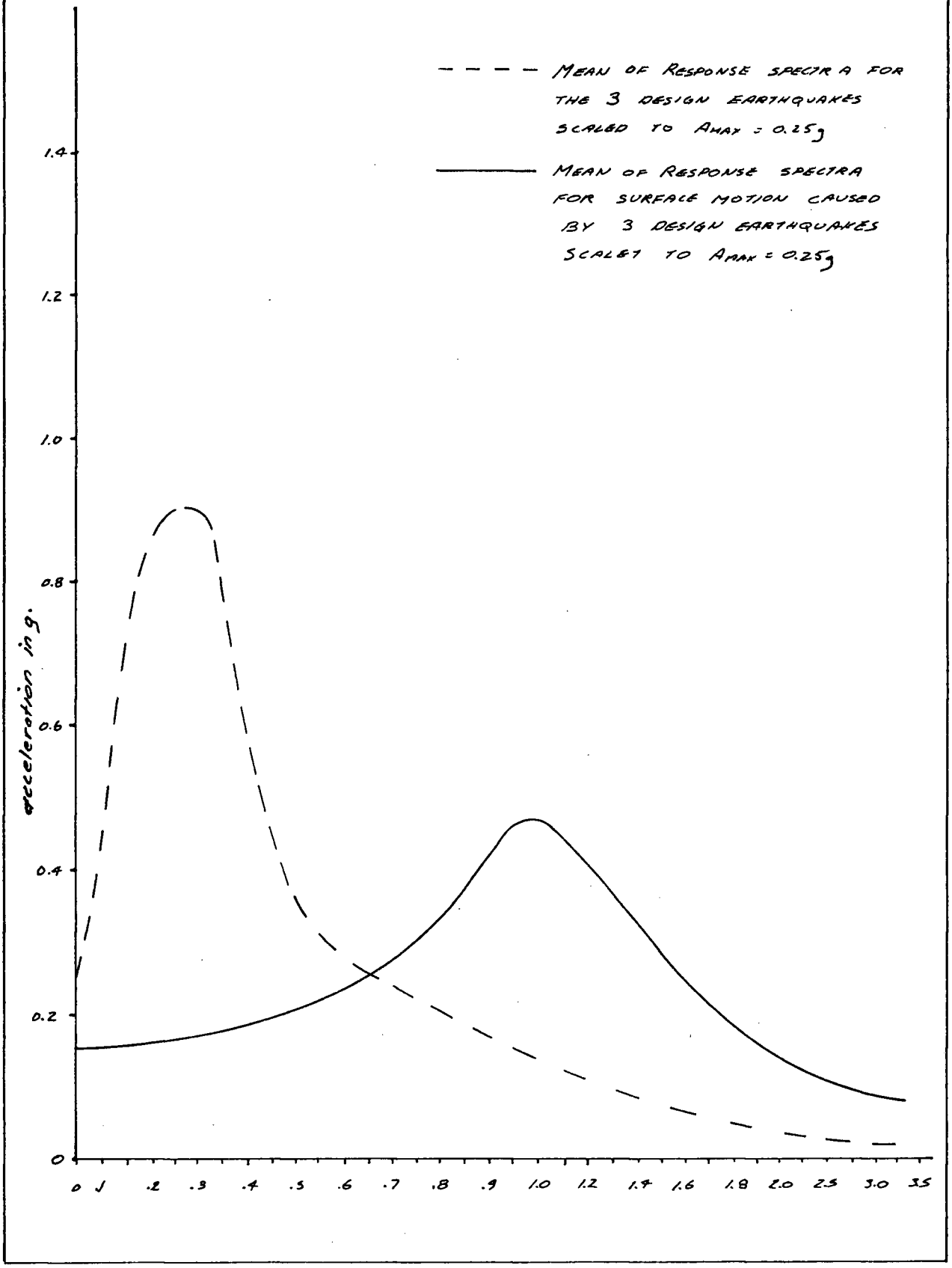

FIG 4-2-13: MAXIMUM ACCELERATION ON ROCK VS. MAXIMUM ACCELERATION AT GROUND SURFACE

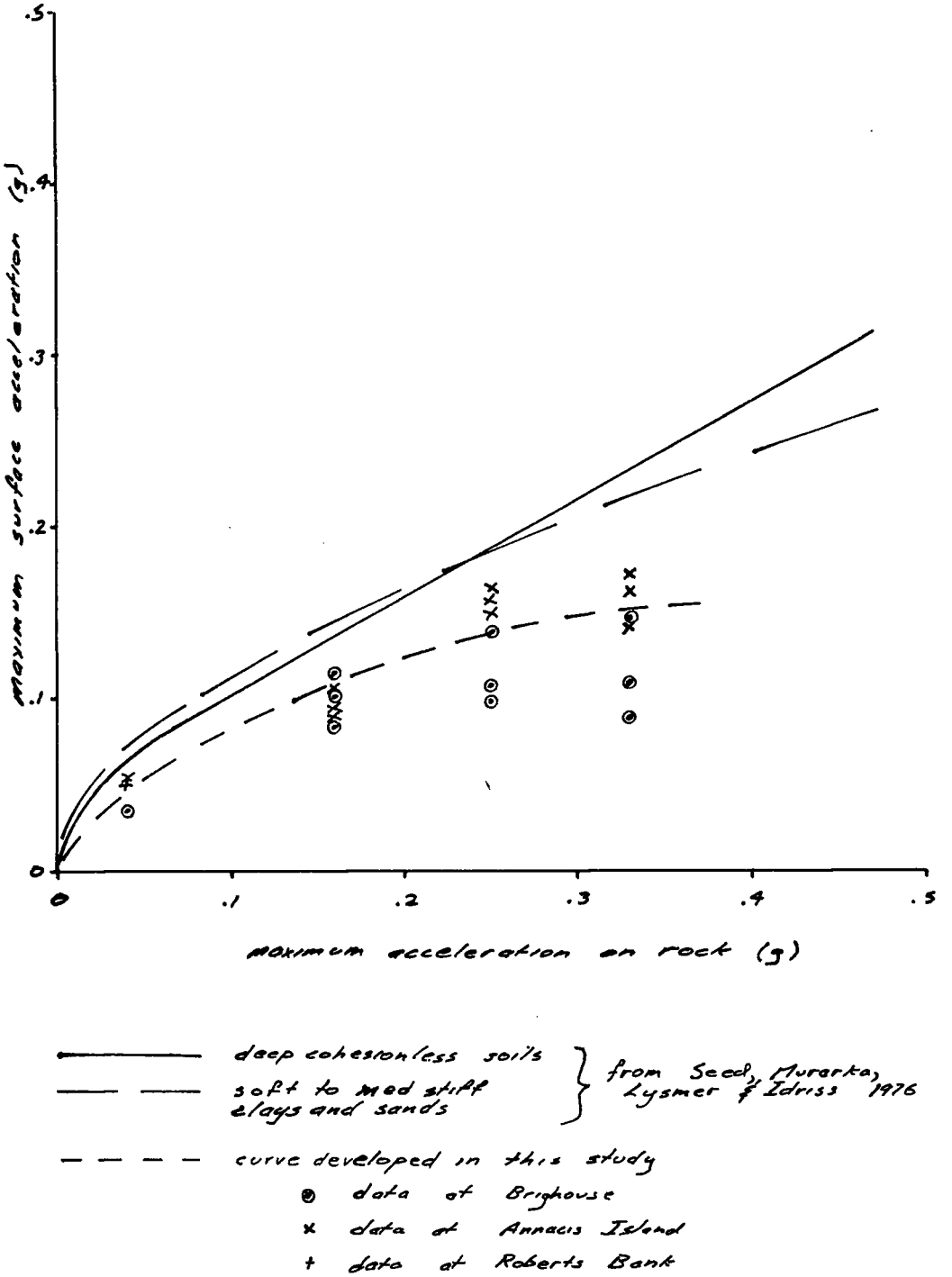

FIG 5-1: BLOW COUNT - LIQUIFACTION POTENTIAL RELATIONS

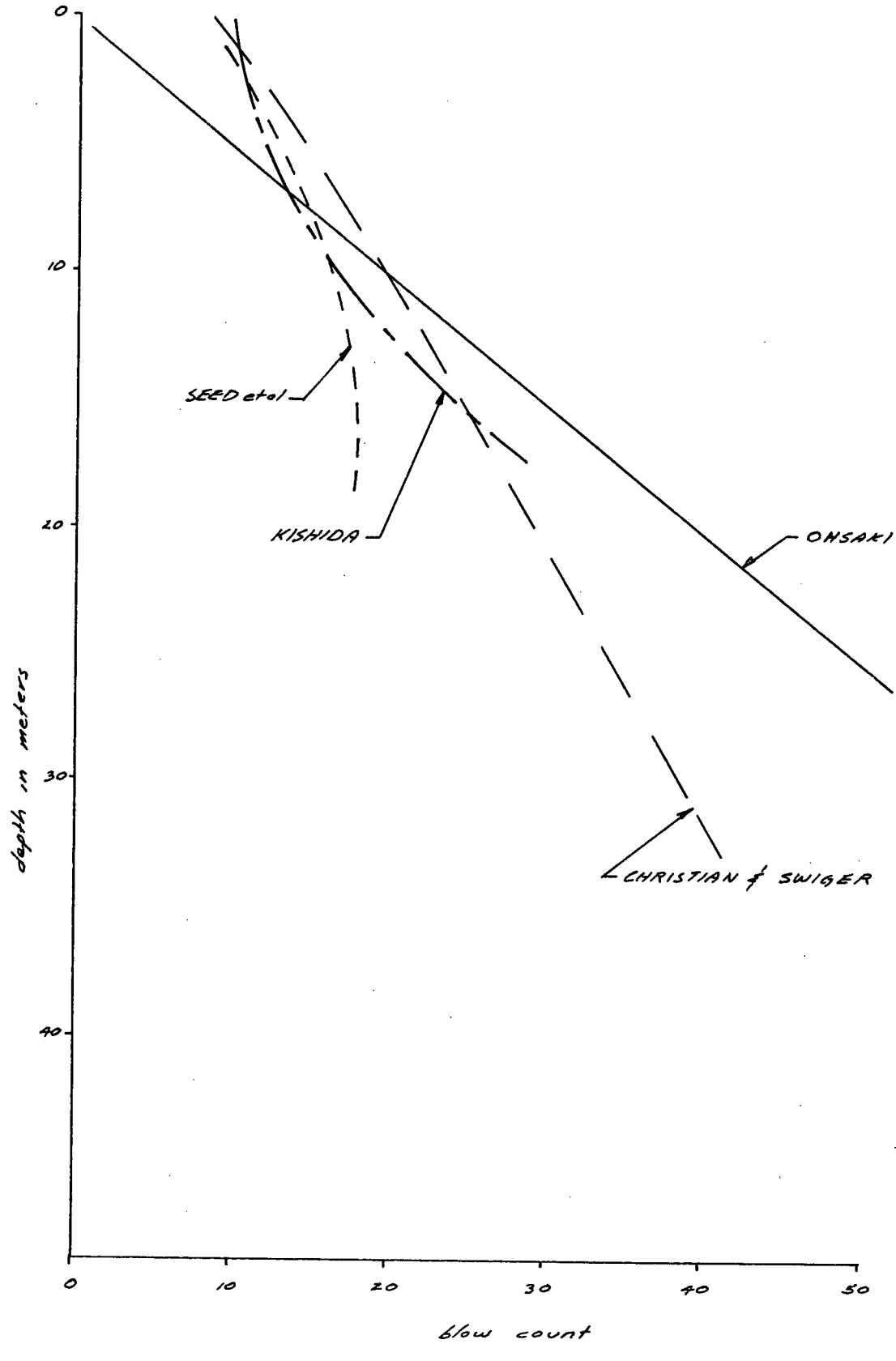

FIG 5-2 : LIQUIFACTION POTENTIAL OF THE FRASER DELTA

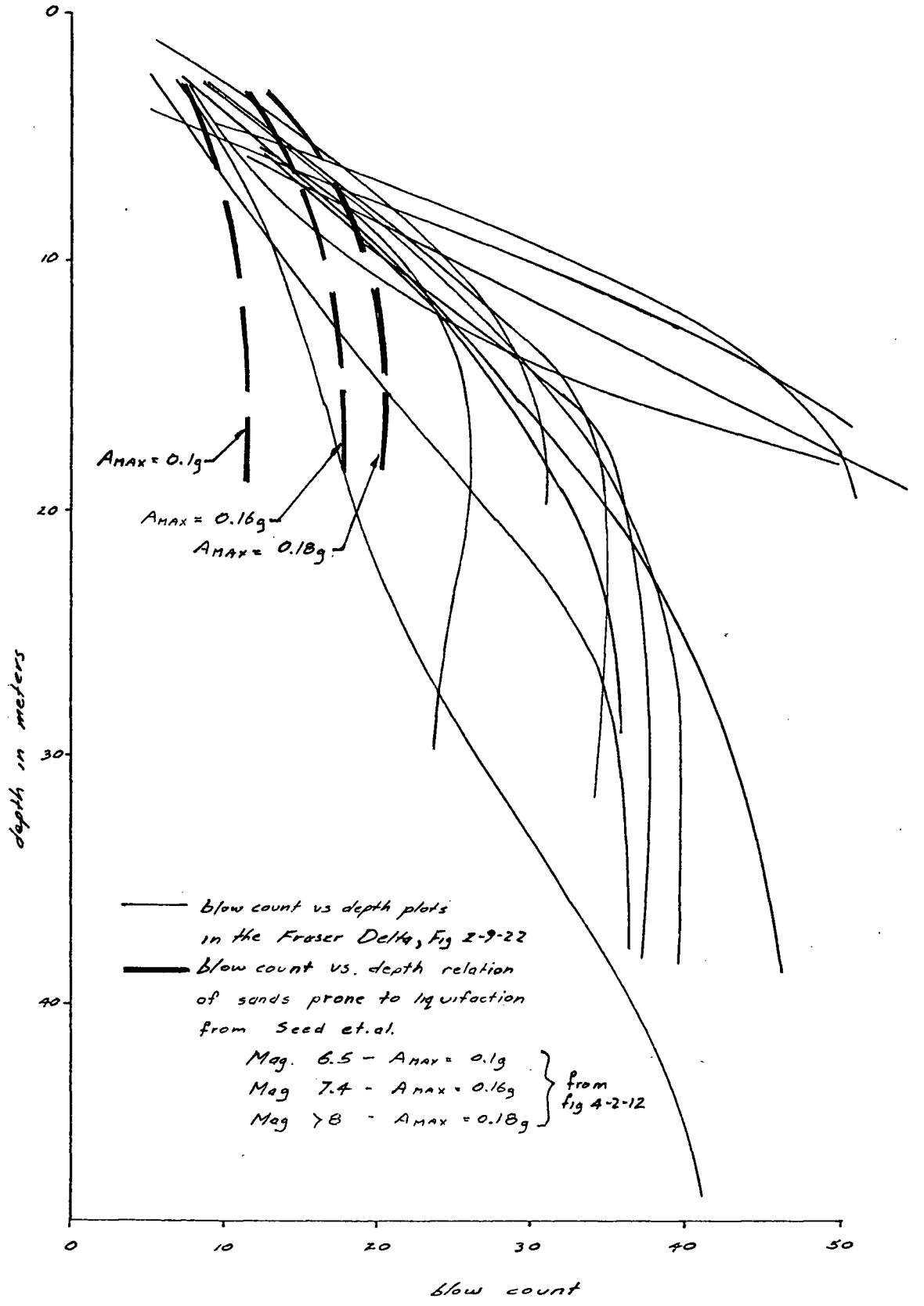

REFERENCES

Anderson, A.M., Espana, C., McLamore, V.R., 1978, Estimating In-Situ Shear Moduli at Competent Sites", Earthquake Engineering and Soil Dynamics Specialty Conference, Pasadena, 181-197.

Arango, I., Moriwaki, Y., Brown, F., 1978, "In Situ and Laboratory Shear Velocity and Modulus." Earthquake Engineering and Soil Dynamics Specialty Conference, Pasadena, pp. 198-212.

Armstrong, J.E., 1956, "Surficial Geology of Vancouver Area, B.C." G.S.C. Paper 55-40.

Armstrong, J.E., 1957, "Surficial Geology of New Westminster Map Area, B.C." G.S.C. Paper 57-5.

Armstrong, J.E., 1960, "Surficial Geology of Sumas, New Westminster, B.C." G.S.C. Map 44-1959.

A.S.T.M. 1969, "Standard Method for Relative Density in Cohesionless Soils". ASTM Designation D2049-69.

Bazaraa, A., 1967, "Use of the Standard Penetration Test for Estimating Settlements of Shallow Foundations on Sand." Ph.D. Dissertation, University of Illinois, Urbana, Illinois.

Blunden, R.H., 1973, "Urban Geology of Richmond, B.C." University of British Columbia, Department of Geology Report No. 15.

Bratton, J.L., Higgins, C.J., 1978, "Measuring Dynamic In Situ Geotechnical Properties." Earthquake Engineering and Soil Mechanics Specialty Conference, Pasadena. pp. 273-289.

Byrne, P.M. 1977, "An Evaluation of the Liquefaction Potential of the Fraser Delta." University of British Columbia, Department of Soil Engineering, Soil Mechanics Series No. 30.

Christian, J.T., Swiger, W.F., 1975, "Statistics of Liquefaction and SPT results." ASCE Jour. of Geotechnical Eng. Div. Vol. 101-pp. 1135-1150.

Clarke, S.P., 1966, "Handbook of Physical Constants." G.S.A. Memoir 97.

Danner, W.R. 1968, "An Introduction to the Stratigraphy of South-Western B.C. and Northwestern Washington." Guide Book for Geological Field Trips in Southwestern B.C., University of British Columbia, Department of Geology, Report No. 6.

deMello, V., 1971, "The Standard Penetration Test." 4th Pan American Conference on Soil Mechanics and Foundation Engineering, pp. 1-86.

Finn, W.D.L., Byrne, P.M., Martin, G.R., 1976, "Seismic Reponse and Liquefaction of Sands." ASCE Jour. Geotechnical Engineering Division, Vol. 102, pp. 841-856.

Gibbs, H.J., Holtz, W.G., 1957, "Research on Determining the Density of Sands by Spoon Penetration Testing." Proceeding, 4th Int. Conf. Soil Mechanics and Foundation Engineering, London, Vol. 1, pp.35-39.

Hardin, B.O., Black, W.L., 1968, "Vibration Modulus of Normally Consolidated Clay." ASCE Jour. of Soil Mechanics and Foundations Division, Vol. 94, pp. 453-464.

Hardin, B.O., Drnevich, V.P., 1972, "Shear Modulus and Damping in Soils: Measurement and Parameter Effects." ASCE Jour. Soil Mechanics and Foundations Division, Vol. 98, pp. 603-624.

Holland, S.S., 1976, "Landforms of British Columbia: A Physiographic Outline." B.C. Dept. Mines and Petroleum Resources, Bulletin 4B.

Hoos, L.M., Packman, G.A., 1974, "The Fraser River Estuary, Status of Environmental Knowledge to 1974." Report of the Estuary Working Group, Department of Environment, Regional Board, Pacific Region.

Hopkins, W.S., 1966, "Palyntology of Tertiary Rocks of Whatcom Basin, Southwestern B.C. and Northern Washington" Ph.D. Dissertation, University of British Columbia.

Jackson, E.V., Seraphin, R.H., 1976, Map: "Faults, Porphyry Deposits and Showings and Tectonic Belts of the Canadian Cordillera." C.I.M.M. Special Volume 15.

Johnston, W.A., 1923, "Geology of the Fraser River Delta Map Area." G.S.C. Memoir 135.

Kishida, H. 1969, "Characteristics of Liquefied Sands During Mino-Owari, Tohnankai, and Fukui Earthquakes." Soils and Foundations, Vol. 9, pp. 75-92.

Klohn, E.J., 1965, "The Elastic Properties of a Dense Glacial Till Deposit." Cdn. Geotechnical Journal, Vol. 11, pp. 116-140.

Kovacs, W.D., Evans, J.C., Griffith, A.M., 1977, "Towards a more Standardized Standard Penetration Test." Proceedings of the 9th International Conference on Soil Mechanics and Foundation Engineering Vol. II.

Luternauer, J., Murray, J., 1973, Sedimentation on the Western Delta Front of the Fraser River, B.C." Cdn. Jour. of Earth Sciences Vol. 10 #11, pp.1642-1663.

Lysmer, J., Seed, H.B., Schnabel, P.B., 1971, "The Influence of Base Rock Characteristics on Ground Response".

Marcusson, W.F., Bieganousky, W.A., 1977, "Laboratory Standard Penetration Tests on Fine Sand" Jour. of Soil Mechanics and Foundation Div. A.S.C.E. Vol. 103 pp. 565-588.

Mathews, W.H., Fyles, J.G., Nasmith, H.W., 1970, "Postglacial Crustal Movements in Southwestern B.C. and Adjacent Washington State." Cdn. Jour. Earth Sciences Vol. 7, pp. 690-702.

Mathews, W.H., Shepard, F.P., 1962, "Sedimentation of the Fraser Delta, B.C." Bul. of the Am. Assoc. of Petroleum Geologists, Vol. 46, pp. 1416-1438.

McTaggart, K.C., Dolmage, V., 1977 "Vancouver Geology-Field Excursion #11 Guide Book." G.S.C.

Milne, W.G., Rogers, G.C., Riddihou, R.P., McMechan, G.A., Hyndman, P.D., 1978, "Seismicity of Western Canada." Cdn. Jour. of Earth Sciences Vol. 15, pp. 1170-1193.

Muller, J.E., 1977, "Evolution of the Pacific Margin, Vancouver Island and Adjacent Regions." Cdn. Jour. Earth Sciences, Vol. 14, pp. 2062-2085.

Murphy, D.J., Koutsoftas, D., Covey, J.N., Fischer, J.A., 1978, "Dynamic Properties of Hard Glacial Till." Earthquake Engineering and Soil Dynamics Specialty Conference, Pasadena.

Nuttli, O.W., 1973, "Seismic Wave Attenuations and Magnitude Relations for Eastern North America." S.Geophys. Res. Vol. 78, pp. 876-885.

Ohsaki, Y., 1970, "Effects of Sand Compaction on Liquefaction during the Tokachiaki Earthquake." Soils and Foundations, Vol. 10, No. 2

Ohsaki, Y., Iwasaki, R., 1973, "On Dynamic Shear Moduli and Poissons Ratio of Soil Deposits." Soil Mechanics and Foundations, Vol. 13, No. 4, pp. 61-73.

Radhakrishna, H.S., Klym, T.W., 1974, "Geotechnical Properties of Dense Glacial Till". Cdn. Geotechnical Jour. Vol. 11, pp. 396-408.

Roddick, J.A., 1965, "Vancouver North, Coquitlam, and Pitt Lake Map Areas, B.C.." G.S.C. memoir 335.

Rogers, G.C., Hasegawa, 1978, "A Second Look at the B.C. Earthquake of 23 June, 19 46." Bulletin of Seimological Society of America, Vol. 68, pp. 653-675.

Saito, A., 1977, "Characteristics of Penetration Resistance of a Reclaimed Sandy Deposit and their Change through Vibratory Compaction." Soils and Foundations Vol. 17 #4, pp. 31-43.

Schmertman, J.H., 1971, Discussion on Paper by V. deMello, 4th Pan American Conference on Soil Mechanics and Foundation Engineering, pp. 91-98.

Schnabel, J., 1971, Discussion on Paper by V. de Mello, 4th Pan American Conference on Soil Mechanics and Foundation Engineering. pp. 89-98.

Schnabel, P.B., Lysmer, J., Seed, H.B., 1972, "SHAKE-A Computer Program for Earthquake Response Analysis of Horizontally Layered Sites." EERC 72-12 Earthquake Engineering Research Centre, University of California, Berkeley.

Schnabel, P.B., Seed, H.B., 1972, "Accelerations in Rock for Earthquakes in the Western United States." Report No. EERC 72-2, Earthquake Engineering Research Centre, University of California, Berkeley.

Schultze, E., Melzer, K.J., 1965, "The Determination of the Density and Modulus of Compressibility of Non-Cohesive Soils by Soundings." Proceedings 6th Int. Conf. Soil Mechanics and Foundation Engineering, Montreal, Vol. 1 pp. 517-521.

Schultze, E., Menzenbach, E., 1961, "Standard Penetration Test and Compressibility of Soil." 5th Int. Conf. Soil Mechanics and Foundation Engineering, Vol. 1, pp.527-531.

Scotton, 1977, "The Outer Banks of the Fraser River Delta, Engineering Properties and Stability Considerations." M.A.Sc. thesis, U.B.C.

Seed. H.B., Idriss, I.M., 1970, "Soil Moduli and Damping Factors for Dynamic Response Analysis." EERC Report No. 70-10, Earthquake Engineering Research Centre, University of California, Berkeley.

Seed, H.B., Idriss, I.M, 1971, "Simplified procedure for Evaluating Soil Liquefaction Potential." Journal of Soil Mechanics and Foundation Division, ASCE, Vol. 97, No. 5 pp. 1249-1273.

Seed, H.B., Idriss, I.M.,Keifer, F.W., 1969, "Characteristics of Rock Motions During Earthquakes." Jour. Soil Mechanics and Foundations Div. ASCE, Vol. 95, No. 5, pp.1199-1218.

Seed, H.B., Idriss, I.M. Makdise, F., Banerjee, N., 1975, "Representation of Irregular Stress Time Histories by Equivalent Uniform Stress Series in Liquefaction Analyses." EERC 75-29, Earthquake Engineering Research Centre, University of California, Berkeley.

Seed, H.B., Mori, K., Chan, C.K., 1977, "Influence of Seismic History on the Liquefaction of Sands." Jour. of Geotechnical Engineering Division, ASCE, Vol. 103, No. G74, pp. 257-270.

Seed, H.B., Murarka, R., Lysmer, J., Idriss, I.M., 1976, "Relationships of Maximum Acceleration, Maximum Velocity, Distance from Source, and Local Site Conditions for Moderately Strong Earthquakes." Bulletin of Seismological Society of America, Vol. 66 No. 4, pp. 1323-1342.

Seed, H.B., Vgas, C., Lysmer, J., 1976, "Site Dependent Spectra for Earthquake Resistant Design." Bulletin of Seismological Society of America, Vol. 66 No. 4, pp. 221-243.

Tavenas, F.A.,Ladd, R.S., La Rochelle, P., 1972, "The Accuracy of Relative Density Measurements: Results of a Comparative Test Program." Department de Genie Civil, Universite Laval.

Trifunac, M.D., Brady, A.G., 1975, "Correlations of Peak Acceleration Velocity and Displacement with Earthquake Magnitude Distance, and Site Conditions.

APPENDIX 1

GEOLOGIC TIME SCALE

ERA	PERIOD	APPROXIMATE NUMBER OF YEARS AGO*
	Quaternary	Last 10,000
	Recent	10,000 to 1,000,000
	Pleistocene (Ice Age)	
Cenozoic	Tertiary	(Millions)
	Pliocene	1 to 13
	Miocene	13 to 25
	Oligocene	25 to 36
	Eocene	36 to 58
	Paleocene	58 to 63
Mesozoic	Cretaceous	63 to 135
	Jurassic	135 to 181
	Triassic	181 to 230
Palaeozoic	Permian	230 to 280
	Pennsylvanian and Mississippian	280 to 345
	Devonian	345 to 405
	Silurian	405 to 425
	Ordovician	425 to 500
	Cambrian	500 to 600
Proterozoic	Keweenawan	600 to 2,000
	Huronian	
Archaean	Temiskaming	2,000 to 4,800
	Keewatin	

*Science, April 14, 1961, p.1111

APPENDIX 2

USE OF FRICTION CONE S.P.T. FORMULA TO SEPARATE PENETRATION RESISTANCE DUE TO END BEARING AND FRICTION

From Schmertmann (1971) we have

$$F = Fe + Fs$$

$$Fe = Ae \cdot qc$$

$$Fs = \pi (Di + Do)\, L fs$$

$$FR = fs/qc$$

where F = to sampler resistance to advance
Fe = end bearing component of resistance
Fs = frictional component of resistance
Ae = horizontally projected end area of SPT sampler
qc = end bearing resistance, at same depth from static cone test
Di = inside diameter of sampler
Do = outside diameter of sampler
L = length of sampler imbedded in soil
fs = local friction from static cone penetration test
FR = Friction ratio, a function of soil type

Take the ratio of end bearing and frictional components:

$$\frac{Fe}{Fs} = \frac{Ae \cdot qc}{(Di + Do)\, L \,.fs} = \frac{Ae}{(Di + Do)L \,.\, FR}$$

for Ae = $10.7 cm^2$
Di = 1.375 in
Do = 2 in
FR = 1% (Loose to med. sands, Schmertmann 1971)

We get $\frac{Fe}{Fs} = \frac{39.7}{L}$

FOR VARIOUS LENGTHS OF SAMPLER IMBEDMENT THIS GIVES:

DEPTH OF SAMPLER IMBEDMENT (in)	$\frac{Fe}{Fs}$	Resistance From End Bearing %	Resistance From Friction %
6	2.60	72%	28%
12	1.30	56%	44%
18	0.868	46%	59%
24	0.651	39%	61%

APPENDIX 3

LIQUEFACTION POTENTIAL RELATIONSHIPS

(1) CHRISTIAN & SWIGER (1975)

$$A = \frac{a\,\sigma}{\sigma_o'}$$

where A = stress ratio at some depth
σ = overburden pressure at that depth
σ_o' = effective stress at that depth
a = maximum ground acceleration

for a water table at the surface at the soil, as in the Fraser Delta: $\sigma \approx 2\sigma_o'$ so $A \approx 2a$

for design earthquake of 17 = 7.4, Fig. 4-2-12 predicts maximum ground surface acceleration of 0.16g.

So: A = 2(.16) = .32g

The relation developed by Christian & Swiger (1975) and presented by Byrne (1977) predicts that for A = .32g liquefaction is unlikely to occur in sands with a Relative Density greater than 71% as determined from the Gibbs and Holtz relations. The Gibbs and Holtz relation for Nvs. DR = 71% was plotted in fig. 5-2.

(2) SEED, MURARKI, LYSMER, IDRISS (1976)

$$A = 0.65 \frac{a}{g} \cdot \frac{\sigma_o}{\sigma_o'} \cdot r_d$$

where

A = cyclic stress ratio of some depth causing liquefaction

a = maximum ground acceleration
g = acceleration due to gravity
σ_o = total overburden stress
σ_o' = effective overburden stress

r_d = stress reduction factor

for - water table at the surface
-totaluunit weight of 122 pcf
-a of 0.16g

$$A = .65\left(\frac{0.16g}{g}\right)\frac{122\ (\text{depth}) \cdot rd}{(122-62.4)(\text{depth})}$$

$$A = .21rd$$

Seed and Idriss (1971) produced relations between rd and depth so the stress ratio can be determined with depth.

The stress ratio causing liquefaction can be related empirically to the penetration resistance, so from data presented by Seed, Arango and Chan 1975, the blow count in sands unlikely to liquefy may be determined for the various stress ratios calculated. The blow count given is one corrected to a standard overburden pressure so from it the actual blow count required at each depth may be determined from the relation.

$$CN = 1-1.25 \log \sigma_o' \quad \text{where } N = \frac{N_1}{CN}$$

here CN = correction factor
N = true blow count
N_1 = blow count normalized to standard pressure.

In this way a relationship between the blow count required to reduce the possibility of liquefaction under a particular earthquake, and depth may be developed. This relation is plotted in fig. 5-1.